



Characterization of the radical SAM domain of the Elp3 subunit in yeast and plant Elongator complexes

DISSERTATION

zur Erlangung des akademischen Grades
doctor rerum naturalium (Dr. rer. nat.)

vorgelegt der
Naturwissenschaftlichen Fakultät I - Biowissenschaften
der Martin-Luther-Universität Halle-Wittenberg

von

Osita Fidelis Onuma

geboren am: 16.03.1971 in Nsukka, Nigeria

Gutachter /in

1. Prof. Dr. K. Breunig
2. Prof. Dr. Gary Sawers
3. PD Dr. Antonio Pierik

Halle (Saale), 14. 12. 2011

I DEDICATION

Dedication

This PhD Dissertation is dedicated to the memory of my beloved father, **Late Mazi Fidelis Ofokaja Onuma**. May his soul rest in perfect peace in Jesus name, Amen.

II PUBLICATIONS

Publications

- ◆ **Onuma, O. F, Brüser, T., and Breunig, K. D. (2008).** Characterization of the Radical SAM Domain of the Elongator Complex in Yeast and Plant. *BIOspectrum(Tagungsband)*. Abstract KH 01, Page 72.

Summary

The γ -toxin, the catalytic subunit of the *Kluyveromyces lactis* killer toxin (zymocin), functions as a tRNA endonuclease. Elongator-dependently modified tRNA species containing the 5-methoxycarbonylmethyl-2-thiouridine (mcm⁵s²U), 5-methoxycarbonylmethyluridine (mcm⁵U) and 5-carbamoylmethyluridine (ncm⁵) side chains at the wobble uridine (U₃₄) position are its substrates. The mechanism of side chain formation at the wobble position is poorly understood. To address this issue, this study was initiated on the basis that AtElp3 and ScElp3 protein sequences harbor a domain showing high sequence similarity to the radical SAM enzymes. The characterization of the recombinantly expressed Elp3 subunit of *Saccharomyces cerevisiae* (ScElp3) and its *Arabidopsis thaliana* homologue (AtElp3) yielded the below summarized findings:

- ◆ The yeast and *Arabidopsis* Elp3 proteins bind at least one [4Fe-4S] cluster.
- ◆ The cuboidal [3Fe-4S]⁺¹ cluster binding to AtElp3 was revealed upon reconstitution under anoxic conditions and analysis by EPR.
- ◆ Two cysteine motifs, the AdoMet (CysX₉CysX₂Cys) and a 2nd motif (CysX₁₁CysX₁₂CysX₂₇Cys) are conserved in eukaryotic Elp3 sequences.
- ◆ The exchange of the three cysteine residues of the AdoMet motif to alanine (C₃-A₃, triple mutant) gave a ScElp3 variant which still binds iron, indicating the presence of a 2nd [Fe-S] cluster binding site.
- ◆ Genetic analyses showed that each of the three AdoMet cysteine (C108, C118 and C121) is indispensable for Elongator function unlike the cysteine residues of the putative 2nd [Fe-S] cluster binding motif.
- ◆ ScElp3 cysteine mutated variants were less stable than the wild type protein but could still be incorporated into the yeast Elongator complex *in vivo*, suggesting that loss of function is not due to structural distortion.
- ◆ The redox protein Kti11 probably functions in the maintenance of ScElp3 [4Fe-4S] in the reduced state.

The data demonstrate that AtElp3 and ScElp3 proteins are [Fe-S] cluster-binding proteins and that their radical SAM domains are indispensable for Elongator function. It is proposed that Elongator contributes to tRNA wobble uridine modification by radical chemistry.

IV TABLE OF CONTENTS

Table of contents

Dedication.....	I
Publications.....	II
Summary.....	III
Table of contents.....	IV
Lists of tables	X
List of figures.....	XI
List of abbreviations.....	XV
1.0 INTRODUCTION.....	1
1.1 The radical SAM enzyme superfamily.....	1
1.1.1 Role of [Fe-S] clusters in transcriptional and translational regulation.....	5
1.1.2 Biogenesis and incorporation of [Fe-S] into apoproteins.....	6
1.1.3 Eukaryotic Elp3 proteins possess a putative radical SAM domain.....	9
1.2 Conservation of the Elongator complex in eukaryotes.....	11
1.2.1 Subunits of the Elongator complex.....	12
1.2.2 The Elongator regulatory protein, Kti12.....	15
1.2.3 Functions associated with the Elongator complex.....	16
1.2.4 The <i>elp/tot</i> phenotypes of Elongator mutation.....	18
1.2.5 Zymocin, the <i>Kluyveromyces lactis</i> killer toxin.....	19
1.2.6 Mechanism of action of zymocin.....	20
1.3 Aims of research.....	22
2.0 MATERIALS AND METHODS.....	23
2.1 General methods.....	23
2.1.1 Chemicals, biochemicals and their sources.....	23
2.1.2 Kits and markers.....	23
2.1.3 Enzymes.....	24
2.1.4 Antibodies.....	24
2.1.4.1 Primary antibodies.....	24
2.1.4.2 Secondary antibodies.....	24
2.2 Apparatus and equipment.....	25
2.3 Consumables.....	26
2.4 Buffers and solutions.....	27
2.5 Anaerobic methods.....	31

IV TABLE OF CONTENTS

2.5.1	Anaerobic buffers and solutions.....	31
2.5.2	Anaerobic chamber and gases.....	31
2.6	Microbiological methods.....	32
2.6.1	Bacterial strains and media.....	32
2.6.1.1	Bacterial cloning and protein expression strains.....	32
2.6.1.2	Bacterial growth and culture media.....	33
2.6.1.3	Storage and collection of bacterial strains.....	34
2.7	Oligonucleotides primers.....	34
2.8	Molecular biology methods.....	37
2.8.1	Agarose gel electrophoresis.....	37
2.8.2	Preparation of competent bacterial cells by chemical method.....	37
2.8.2.1	Transformation of competent cells.....	38
2.8.3	Isolation of plasmid DNA.....	38
2.8.3.1	Determination of plasmid DNA concentration.....	38
2.8.3.2	DNA purification from enzymatic reactions.....	39
2.8.3.3	Isolation of DNA from agarose gel.....	39
2.9	Mutagenesis.....	39
2.10	Polymerase chain reaction (PCR).....	40
2.11	DNA sequencing.....	41
2.12	Bacterial and yeast shuttle plasmids.....	42
2.13	Biochemical methods.....	52
2.13.1	Cell culture for bacterial protein expression.....	52
2.13.2	Cell harvest and storage.....	52
2.13.3	Preparation of HiPIP inclusion body from <i>E. coli</i>	52
2.13.4	Purification of His ₆ -tagged fusion proteins.....	53
2.13.5	Purification of Strep-tagged fusion proteins.....	54
2.14	<i>In vitro</i> folding and reconstitution of non-native purified proteins.....	54
2.14.1	Concentration and desalting of reconstituted and dialysed proteins.....	55
2.14.2	Purification of desalted proteins by gel filtration.....	55
2.15	Protein analytical methods.....	55
2.15.1	SDS-polyacrylamide gel electrophoresis (SDS-PAGE).....	55
2.15.2	Western blot analysis.....	56
2.15.3	Determination of protein concentration.....	56
2.16	Yeast strains.....	57

IV TABLE OF CONTENTS

2.16.1	<i>Kluyveromyces lactis</i> strain.....	57
2.16.2	<i>Saccharomyces cerevisiae</i> strains.....	57
2.17	Biophysical methods.....	58
2.17.1	UV-VIS absorption spectroscopy.....	58
2.17.2	Preparation of protein samples for EPR analysis.....	58
2.18	Genetic methods.....	58
2.18.1	Yeast growth media.....	58
2.18.2	Isolation of RNA from DH5 α <i>E. coli</i> cells.....	59
2.18.3	Preparation of competent yeast cells.....	59
2.18.4	Transformation of competent yeast cells.....	59
2.18.5	Extraction of chromosomal DNA from yeast cells.....	60
2.18.6	Protein extraction from yeast cells.....	60
2.19	Disruption of <i>ScELP3</i> gene to generate <i>Ura</i> ⁺ strains.....	61
2.19.1	Integration of <i>ScELP3</i> and mutant fragments into genome of <i>Ura</i> ⁺ strains.....	61
2.19.2	Intracellular expression of γ -toxin in yeast.....	62
2.19.3	Killer-toxin eclipse assay.....	62
2.19.4	Suppression assay.....	63
2.20	Immunological techniques.....	63
2.20.1	Coupling of antibody to Protein A-Sepharose matrix.....	63
2.20.2	Coimmunoprecipitation of ScElp3 proteins.....	64
3.0	RESULTS	65
3.1	Recombinant expression of AtElp3 variants affinity epitope-tagged in <i>E. coli</i>	65
3.1.1	Expression of a full length AtElp3H ₆ protein using the pET vector system.....	65
3.1.2	Attempts to purify AtElp3 and radical SAM domain variants under native conditions on Ni-NTA-agarose matrix.....	66
3.1.2.1	Affinity chromatography of AtElp3H ₆ protein.....	66
3.1.2.2	Expression of radical SAM domain variants as C-terminal His ₆ -tagged fusion proteins.....	67
3.1.2.3	Purification of the radical SAM domain subfragments, AtElp3(76-366)H ₆ and AtElp3(111-366)H ₆	69
3.1.3	Alternative tagging and plasmid coexpression of AtElp3 protein.....	71

IV TABLE OF CONTENTS

3.1.3.1	Expression and purification of a full length Strp-AtElp3-H ₁₀ fusion protein.....	71
3.1.3.2	Coexpression of the Strp-AtElp3H ₁₀ protein with the iron-sulfur cluster (<i>isc</i>) biogenesis plasmid, pRKISC.....	72
3.1.4	Characterization of H ₆ -AtElp3-Strp fusion protein.....	73
3.1.4.1	Solubility analysis of a full length H ₆ -AtElp3-Strp protein.....	73
3.1.4.2	Affinity chromatography of full length H ₆ -AtElp3-Strp protein on Ni-NTA-agarose matrix.....	74
3.1.4.3	Attempts to disrupt the H ₆ -AtElp3-Strp interaction with DnaK.....	75
3.2	Purification of recombinant AtElp3 protein variants from inclusion body preparations.....	77
3.2.1	Purification of H ₆ -AtElp3-Strp protein expressed from the pON-ELO3-3 construct.....	77
3.2.2	Affinity purification of AtElp3H ₆ protein using the pON-ELO3-1 construct.....	78
3.2.2.1	Refolding and reconstitution of denatured AtElp3 protein purified under non-native conditions.....	80
3.2.2.2	Chromatography of reconstituted AtElp3H ₆ protein by gel filtration.....	81
3.3	Biochemical characterization and analyses of wild type AtElp3 proteins.....	82
3.3.1	UV-visible absorption spectroscopic analyses of AtElp3 variants.....	82
3.3.2	EPR spectroscopic characterization of reconstituted AtElp3H ₆ protein.....	83
3.3.3	Mass spectrometric analyses of full length AtElp3H ₆ protein and degradation products.....	84
3.4	Recombinant expression of yeast Elp3 (ScElp3).....	85
3.4.1	Expression of ScElp3H ₆ protein.....	86
3.4.2	Purification of full length ScElp3H ₆ protein on Ni-NTA-agarose matrix.....	87
3.4.3	Expression and affinity chromatography of H ₆ -ScElp3-Strp protein under native conditions on Ni-NTA-agarose.....	89
3.4.4	Attempts to improve folding and solubility of ScElp3.....	91

IV TABLE OF CONTENTS

3.4.5	Affinity chromatography of wild type ScElp3H ₆ protein coexpressed with pGroEL plasmid.....	93
3.5	Non-native purification of ScElp3H ₆ wild type coexpressed with pGroEL from inclusion body preparations.....	95
3.5.1	Purification of reconstituted ScElp3H ₆ protein by gel filtration on Sephadex 200 column.....	96
3.6	Generation of ScElp3 radical SAM cysteine mutated variants by site-directed mutagenesis.....	98
3.6.1	Expression of the radical SAM domain cysteine mutated variants.....	100
3.6.2	Affinity chromatography of ScElp3(C ₃ -A ₃)H ₆ mutated variant coexpressed with pGroEL from inclusion body preparations.....	101
3.6.3	Expression of radical SAM domain cysteine H ₆ -ScElp3-Strp mutated variants.....	102
3.6.4	Affinity purification of radical SAM domain H ₆ -ScElp3p-Strp C ₃ -A ₃ and C ₅ -A ₅ mutated variants under native conditions.....	103
3.7	Characterization and analyses of ScElp3 radical SAM domain mutated variants by biochemical methods.....	106
3.7.1	UV-visible absorption spectroscopic analyses of ScElp3 cysteine mutated variants.....	106
3.7.2	Analysis of reconstituted ScElp3(C ₃ -A ₃)H ₆ cysteine mutated variant by gel filtration.....	107
3.8	Generation and characterization of overexpressed and endogenous ScElp3-c(myc) ₃ mutated variants.....	109
3.8.1	Analyses of overexpressed ScElp3-c(myc) ₃ radical SAM cysteine mutated variants using the γ -toxin assay.....	109
3.8.2	Construction of endogenous ScElp3-c(myc) ₃ radical SAM domain cysteine mutant strains by homologous recombination.....	112
3.8.3	Construction of putative ScElp3-c(myc) ₃ glycine radical mutant strains.....	113
3.9	Influence of radical SAM domain mutants on ochre tRNA ^{Tyr} suppression.....	115
3.10	Role of the radical SAM domain on Elongator complex formation.....	116
3.11	Radioactive incorporation of ⁵⁵ Fe into ScElp3 wild type and mutated proteins.....	118

IV TABLE OF CONTENTS

3.12	Reduction of the iron-sulfur cluster of reconstituted ScElp3H ₆ by Kti11 protein.....	120
4.0	DISCUSSION	122
4.1	Expression and purification of recombinant Elp3 variants.....	123
4.2	Inclusion body preparation as source of AtElp3, ScElp3 and cysteine mutated proteins.....	126
4.3	Evidence for [4Fe-4S] cluster-binding in AtElp3 and ScElp3.....	127
4.4	Influence of cysteine mutations in the radical SAM domain for the structural integrity of the Elongator complex.....	131
4.5	Biological importance of the radical SAM domain for Elongator function.....	132
4.6	Regulation of the radical SAM domain by the Elongator-associated redox protein, Kti11.....	136
5.0	OUTLOOK	140
6.0	REFERENCES	141
7.0	ENCLOSURES	168
	Declaration.....	168
	Acknowledgements.....	169
	Curriculum vitae.....	171

IV LIST OF TABLES

List of Tables

Table 1.0	Some members of the radical SAM enzyme superfamily and their catalytic functions.....	3
Table 2.0	<i>Escherichia coli</i> cloning and expression strains.....	32
Table 2.1	Overview oligonucleotide primers utilized.....	34
Table 2.2	Summary of yeast shuttle plasmids and bacterial fusion protein expression plasmids.....	42
Table 2.3	<i>Kluyveromyces lactis</i> strain utilized.....	57
Table 2.4	<i>Saccharomyces cerevisiae</i> strains used in this study.....	57
Table 3.0	Overview of the different constructs used for the purification of AtElp3 protein and radical SAM domain variants.....	79
Table 3.1	Summary of AtElp3 MALDI/TOF mass spectrometric analyses data.....	85
Table 3.2	Wild type ScElp3 constructs, coexpression plasmids and reagents used for protein expression.....	92
Table 3.3	Summary of MALDI/TOF mass spectrometric analyses data of ScElp3H ₆ coexpressed with <i>E.coli</i> GroEL.....	95
Table 3.4	Summary of purification of the different full length ScElp3 protein and the radical SAM domain cysteine mutated variants.....	105

List of Figures

Figure 1.0 Coordination of [4Fe-4S] and SAM and Subsequent SAM cleavage by radical SAM enzymes.....	2
Figure 1.1 Machineries involved in the biogenesis of eukaryotic Fe-S proteins and their putative evolutionary ancestry.....	8
Figure 1.2 Sequence conservation of two-domain Elp3-related histone acetyltransferases (HATs) and S-adenosylmethionine (SAM) radical enzymes in eukaryotes and archaea.....	10
Figure 1.3 Conservation of the Elongator complex in Yeast and <i>Arabidopsis</i>	12
Figure 1.4 Systematic drawing of Elongator-dependent modification of some tRNA species at the wobble (U ₃₄) position.....	17
Figure 1.5 Phenotypes of Yeast and <i>Arabidopsis</i> <i>elp3Δ</i> mutants.....	19
Figure 3.0 Cloning and solubility analysis of full length AtElp3H ₆ protein expressed in <i>E. coli</i>	66
Figure 3.1 Affinity chromatography of wild type AtElp3H ₆ (67.4 kDa) on Ni-NTA-agarose matrix.....	67
Figure 3.2 Cloning and expression analysis of the radical SAM domain variants, AtELP3(76-366), AtELP3(111-366) in comparison to full length AtElp3H ₆	68
Figure 3.3 Solubility analysis of the radical SAM domain variants, AtElp3(76-366)H ₆ (33.5 kDa) and AtElp3(111-366)H ₆ (29.7 kDa)...	69
Figure 3.4 SDS-PAGE and Western blot analyses of the radical SAM domain variants, AtElp3(76-366)H ₆ (33.5 kDa) and AtElp3(111-366)H ₆ (29.7 kDa) upon affinity purification on Ni-NTA-agarose matrix.....	70
Figure 3.5 Expression and purification of full length Strp-AtElp3-H ₁₀ (69.6 kDa) on Ni-NTA-agarose matrix.....	71
Figure 3.6 Coexpression of Strp-AtElp3-H ₁₀ (69.6 kDa) fusion protein with the <i>isc</i> operon plasmid, pRKISC.....	72
Figure 3.7 Solubility analysis of H ₆ -AtElp3-Strp (69.3 kDa) protein.....	73
Figure 3.8 Purification profile of a full length H ₆ -AtElp3-Strp (69.3 kDa) on Ni-NTA-agarose matrix.....	74

V LIST OF FIGURES

Figure 3.9 Disruption of the interaction between H ₆ -AtElp3-Strp (69.3 kDa) and DnaK.....	76
Figure 3.10 Affinity chromatography of the H ₆ -AtElp3-Strp protein from inclusion bodies generated from the pON-ELO3-3 construct.....	78
Figure 3.11 Affinity purification of the AtElp3H ₆ protein from inclusion bodies generated using the pON-ELO3-1 construct.....	80
Figure 3.12 Chromatography of reconstituted AtElp3H ₆ protein by gel filtration and analyses of eluted fractions.....	81
Figure 3.13 UV-visible spectroscopic analyses of AtElp3 protein.....	82
Figure 3.14 EPR spectrum of [Fe-S] cluster in the reconstituted AtElp3H ₆ protein.....	83
Figure 3.15 MALDI/TOF Mass spectrometric analysis of full AtElp3H ₆ protein and its degradation products.....	84
Figure 3.16 Cloning and expression of wild type ScElp3H ₆ (67.4 kDa) protein from different <i>E. coli</i> BL21(DE3) clones.....	86
Figure 3.17 Solubility analyses of wild type ScElp3H ₆ protein expressed in different <i>E. coli</i> cell fractions at varying temperatures.....	87
Figure 3.18 Analysis of wild type ScElp3H ₆ (67.4 kDa) upon affinity purification on Ni-NTA-agarose matrix.....	88
Figure 3.19 Affinity chromatography of H ₆ -ScElp3-Strp wild type protein on Ni-NTA-agarose matrix and analyses of samples.....	90
Figure 3.20 Analysis of H ₆ -ScElp3-Strp by UV-visible absorption spectroscopic method.....	90
Figure 3.21 Expression of wild type ScElp3 protein using different constructs, osmolytes and coexpression plasmids.....	93
Figure 3.22 Affinity purification of ScElp3H ₆ from pON-ELP3-1 construct coexpressed with pGroEL and supplemented with betaine hydrochloride and NaCl.....	94
Figure 3.23 MALDI/TOF mass spectrometric analysis of purified ScElp3H ₆ protein after coexpression with <i>E. coli</i> GroEL.....	94
Figure 3.24 Affinity chromatography of wild type ScElp3H ₆ coexpressed with GroEL under denaturing conditions on Ni-NTA-agarose.....	96
Figure 3.25 Analysis of wild type ScElp3H ₆ protein samples upon reconstitution and size exclusion chromatography.....	97

V LIST OF FIGURES

Figure 3.26 Gel filtration chromatography and UV-VIS analysis of reconstituted ScElp3H ₆ protein.....	98
Figure 3.27 Schematic representation of the point mutations introduced into the ScElp3 protein.....	99
Figure 3.28 Expression of the radical SAM domain cysteine mutated ScElp3H ₆ proteins in <i>E. coli</i> BL21(DE3) strain.....	100
Figure 3.29 Purification of radical SAM domain triple cysteine ScElp3(C ₃ -A ₃)H ₆ mutated variant coexpressed with GroEL under denaturing conditions on Ni-NTA-agarose.....	101
Figure 3.30 Analysis of reconstituted ScElp3(C ₃ -A ₃)H ₆ mutated protein samples purified by gel filtration.....	102
Figure 3.31 Expression and analysis of H ₆ -ScElp3-Strp (69.5 kDa) radical SAM domain cysteine mutant proteins in <i>E.coli</i> BL21(DE3) strain.....	102
Figure 3.32 Purification and analyses of C ₃ -A ₃ and C ₅ -A ₅ cysteine mutated H ₆ -ScElp3-Strp variants.....	104
Figure 3.33 UV-visible absorption spectroscopic analyses of ScElp3 C ₃ -A ₃ and C ₅ -A ₅ cysteine mutated variants.....	107
Figure 3.34 Gel filtration chromatography of non-native purified and reconstituted ScElp3(C ₃ -A ₃)H ₆ mutated protein.....	108
Figure 3.35 Characterization of the Elongator tRNA modification function by complementation of a yeast <i>elp3Δ</i> strain with C-terminal c-(myc) ₃ -tagged <i>ScELP3</i> and radical SAM domain mutated variants.....	109
Figure 3.36 Characterization of the Elongator tRNA modification function by complementation of a yeast <i>elp3Δ</i> strain with double cysteine mutated variants of the “2 nd putative Fe-S binding motif”.....	111
Figure 3.37 Analyses of generated ScElp3-c(myc) ₃ wild type and cysteine mutant strains by PCR using genomic DNA with ORF-ELP3-SAM-FW and TDH-RV primers.....	112
Figure 3.38 Sequence alignment of ScElp3 with <i>E. coli</i> PFL and AnRR and PCR analyses of generated ScElp3-c(myc) ₃ glyceryl radical mutant strains using genomic DNA with ORF-ELP3-SAM-FW and p424TDH-3myc-RV primers.....	114

V LIST OF FIGURES

Figure 3.39 Wild type <i>ScELP3</i> and double cysteine and glycine mutations confer tRNA suppression in UMY2916 strain.....	116
Figure 3.40 Incorporation of the ScElp3 wild type and radical SAM domain mutants into the Elongator complex by coimmunoprecipitation.....	117
Figure 3.41 Significance of conserved cysteine residues in ScElp3 for the assembly of [Fe-S] cluster(s) on ScElp3.....	119
Figure 3.42 Reduction of the ScElp3H ₆ wild type [4Fe-4S] cluster peak by the Elongator regulatory protein Kti11.....	121
Figure 4.0 Schematic overview of UV-visible spectroscopic data obtained for the wild type and radical SAM domain mutated variants of ScElp3 on [4Fe-4S] binding.....	129
Figure 4.1 Schematic picture of <i>in vivo</i> data on Elongator function from the γ -toxin sensitivity and <i>SUP4</i> assays using the radical SAM domain mutated variants of ScElp3.....	135

V LIST OF ABBREVIATIONS

List of Abbreviations

Abbreviation	Full name
Δ	Deletion
A	Alpha
β	Beta
γ	Gamma
Aa	Amino acid
Acetyl-CoA	Acetyl coenzyme A
AdoMet	S-Adenosylmethionine
Amp	Ampicillin
Amp ^R	Ampicillin resistance
APS	Ammonium persulfate
<i>At</i>	<i>Arabidopsis thaliana</i>
ATP	Adenosine triphosphate
BSA	Bovine serum albumin
cDNA	Complementary DNA
CoA	Coenzyme A
CoIP	Coimmunoprecipitation
Cm	Chloramphenicol
Cm ^R	Chloramphenicol resistance
DNA	Deoxyribonucleic acid
dsDNA	Double stranded deoxyribonucleic acid
DMF	N,N-Dimethylformamide
DTT	1,4-Dithiothreitol
FOA	5-Fluoroorotic acid
EDTA	Ethylenediaminetetraacetic acid
Elp	Elongator protein
EPR	Electron paramagnetic resonance
[Fe-S]	Iron sulfur cluster
H	Hydrogen
H ₂	Hydrogen gas
HA	Hemagglutinin

V LIST OF ABBREVIATIONS

HAP	Histone acetyltransferase associated protein
HAT	Histone acetyltransferase
HiPIP	High-potential iron-sulfur protein
HPLC	High performance liquid chromatography
HRP	Horse radish peroxidase
IPTG	Isopropyl- β -D-thiogalactopyranoside
kDa	Kilo dalton
Kti	Killer toxin insensitive
MOPS	3-(N-morpholino) propanesulfonic acid
MWCO	Molecular weight cut-off
Nitrogen	Nitrogen
N ₂	Nitrogen gas
NaOAc	Sodium acetate
NTP	Nucleoside triphosphate
OD	Optical density
ORF	Open reading frame
PAS	Protein A sepharose
PCI	Phenol:chloroform: <i>isoamylalcohol</i>
PCR	Polymerase chain reaction
<i>Pfu</i>	<i>Pyrococcus furiosus</i>
PMSF	Phenylmethylsulfonyl fluoride
Q4	Quadruple cysteine mutated variant (C ₄ -A ₄)
Q5	Quintuple cysteine mutated variant (C ₅ -A ₅)
RNA	Ribonucleic acid
SAM	S-adenosylmethionine
<i>Sc</i>	<i>Saccharomyces cerevisiae</i>
SDS	Sodium dodecyl sulfate
SDS-PAGE	Sodium dodecyl sulfate polyacrylamide gel electrophoresis
<i>Taq</i>	<i>Thermus aquaticus</i>
TEMED	N,N,N',N'-Tetramethyl-ethylenediamine
Tet	Tetracycline
Tet ^R	Tetracycline resistance
TM	Triple cysteine mutated variant (C ₃ -A ₃)

V LIST OF ABBREVIATIONS

Tris	Tris(hydroxymethyl) aminomethane
tRNA	Transfer ribonucleic acid
UV	Ultraviolet
UV-VIS	UV-visible absorption spectroscopy
v/v	Volume per volume
X-Gal	5-Bromo-4-chloro-3-indolyl- β -D-galactopyranoside
w/v	Weight per volume
WT	Wild type
YNB	Yeast nitrogen base
YPD	Yeast peptone dextrose

1.0 Introduction

Over the past 20 years numerous enzymatic reactions have been observed to proceed via mechanisms involving organic radicals as intermediates. Radical enzymatic reactions, though rare compared to their non-radical counterparts, are increasingly acknowledged to be indispensable to the mainstream of biosynthetic arsenal in the three domains of life and are reserved for most difficult chemical reactions (Banerjee 2003). Radical reactions in enzymology are often linked to redox-active cofactors like flavin (Tittmann *et al.*, 2005; Kay *et al.*, 1999; Guan *et al.*, 2003; Fitzpatrick *et al.*, 2005), pterin (Kappock & Caradonna 1996; Wei *et al.*, 2003), quinone (Fridovich 1997; Erman & Vitello 2002; Bravo *et al.*, 1997), or metallo-cofactors (Frey & Magnusson 2003; Frey 2001; Frey & Booker 2001; Buis & Broderick 2005; Hernández *et al.*, 2007). A significant role of proteins containing iron-sulfur cofactors is the initiation of radical chemistry needed to instigate chemically difficult reactions such as unusual methylation, sulfur insertion, anaerobic oxidation, ring formation, vitamins and cofactor biosynthesis (Sofia *et al.*, 2001). In anaerobes, the radical SAM family of enzymes produces a highly oxidizing 5'-deoxyadenosyl radical which reacts with the substrates resulting in the cleavage of non-activated C-H bonds (Layer *et al.*, 2004). The generation of radical species involves the monoelectronic reduction of S-adenosylmethionine (SAM or AdoMet) through a reduced $[4\text{Fe-4S}]^{+1}$ cluster (Frey & Magnusson 2003).

1.1 The radical SAM enzyme superfamily

In diverse biological systems, enzyme catalysis based on both stable and transient organic radical has been on the increase in recent years (Stubbe & van der Donk 1998; Frey 2001). The radical SAM (AdoMet) enzyme superfamily constitute metalloproteins that use a reduced unconventional $[4\text{Fe-4S}]^{+1}$ cluster bound in a consensus CysX₃CysX₂Cys sequence motif (Sofia *et al.*, 2001), to catalyze the reductive cleavage of S-adenosylmethionine (SAM or AdoMet) to methionine and a 5'-deoxyadenosyl radical species (Frey *et al.*, 2006; Frey & Magnusson 2003). The requirement for a close proximity between the cofactor / cosubstrate SAM and the $[4\text{Fe-4S}]^{+1}$ in all radical SAM enzymes is a prerequisite for cluster coordination and

1 INTRODUCTION

transfer of electron from one to another (Frey & Magnusson 2003). Figure 1.0 illustrates a prevalent reaction steps found in all radical SAM enzymes.

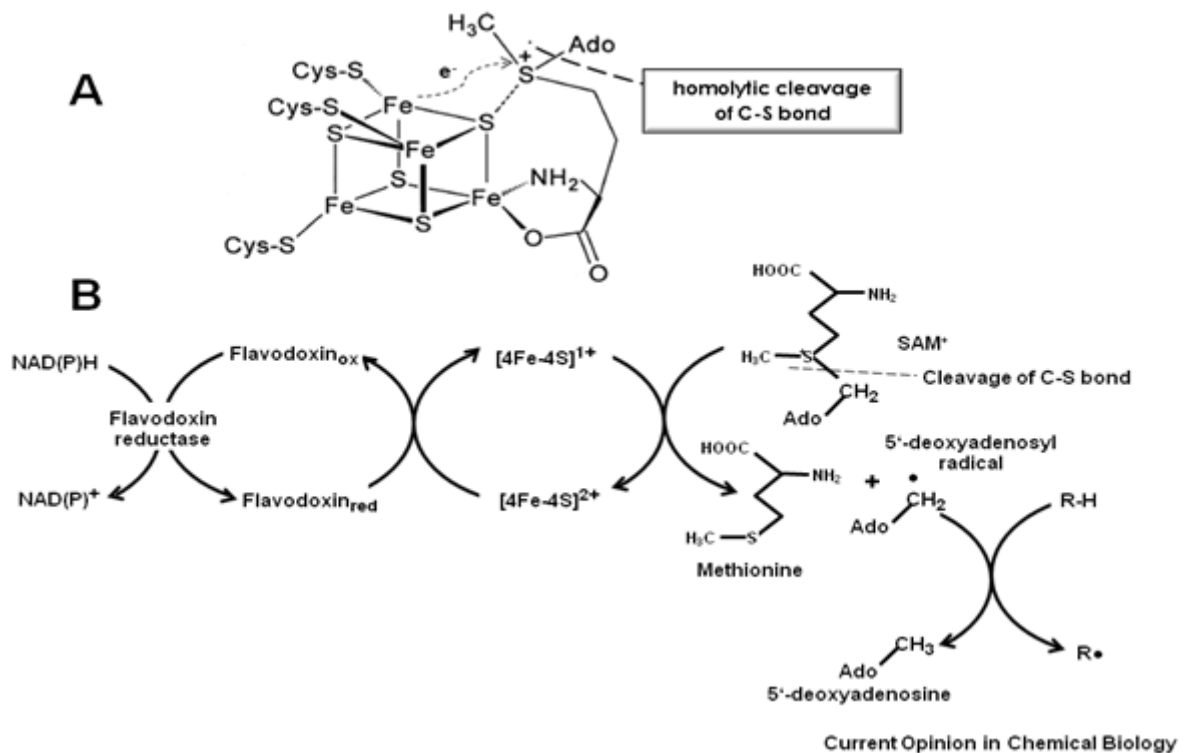


Figure 1.0 | Coordination of [4Fe-4S] and SAM and subsequent SAM cleavage by radical SAM enzymes. (A) The three AdoMet cysteines (CysX₃CysX₂Cys) coordinate 3Fe and the 4th unique Fe is ligated by the α-amino group nitrogen and α-carboxylic oxygen of the methionine moiety. (B) Reaction steps common to all radical SAM enzymes. An initial electron donor (usually flavodoxin in prokaryotes or adrenodoxin / Kti11 in eukaryotes?) reduces the [4Fe-4S] to the +1 state. Next, the reduced [4Fe-4S]⁺¹ then transfers an electron to the sulfonium of SAM resulting in the homolytic cleavage of the C5'-S bond of SAM to liberate methionine and the highly oxidizing 5'-deoxyadenosyl radical. Finally, the 5'-deoxyadenosyl radical abstracts a hydrogen atom from an appropriately placed substrate (R-H) to produce a substrate or protein based radical (R•) (Wagner *et al.*, 1992; Layer *et al.*, 2003, 2005; Sun *et al.*, 1996).

Genome database search has estimated about 3000 putative proteins bearing the CysX₃CysX₂Cys signature motif (Frey *et al.*, 2008). This enzyme superfamily is composed of functionally diverse proteins that are involved in key steps in general metabolism, RNA modification, DNA biosynthesis and repair and biosynthesis of several cofactors, coenzymes, vitamins, antibiotics and herbicides (Sofia *et al.*, 2001; Vey & Drennan, 2011) (Table 1.0). Others have been postulated to participate in various cellular functions and cell-cycle regulation (Sofia *et al.*, 2001; Chin & Cresswell 2001; Ching & Wang 2000).

1 INTRODUCTION

Table 1.0 | Some members of the radical SAM enzyme superfamily and their catalytic functions

Enzyme^a	Catalytic function^b	References
PFL-AE	Glycyl radical formation in pyruvate metabolism	Buis & Broderick 2005; Knappe & Wagner 2001
ANRR-AE (Class III)	Glycyl radical formation in dNTP biosynthesis	Jarrett 2003; Frey & Magnusson 2003
BssD-AE	Glycyl radical formation in toluene metabolism	Krieger <i>et al.</i> , 2001; Qiao & Marsh 2005
GD-AE	Glycyl formation on glycerol dehydratase	O'Brien <i>et al.</i> 2004
BioB	Biotin biosynthesis	Ugulava <i>et al.</i> , 2002; Jarrett 2003; Berkovitch <i>et al.</i> , 2004
LipA	Lipoyl biosynthesis	Miller <i>et al.</i> , 2000
MoaA	Molybdopterin biosynthesis	Hänzelmann & Schindelin 2006; Santamaria-Araujo <i>et al.</i> 2004
MiaB	Thiomethylation of isopentenyl adenosine in tRNA	Pierrel <i>et al.</i> , 2003; Esberg <i>et al.</i> , 1999
RimO	Thiomethylation of Asp-88 on ribosomal protein S12	Lee <i>et al.</i> , 2009; Arragain <i>et al.</i> , 2010
RlmN, Cfr	Methylation of C2 or C8 of adenosine 2503 on 23S rRNA respectively	Toh <i>et al.</i> , 2008; Giessing <i>et al.</i> , 2009; Grove <i>et al.</i> , 2011; Boal <i>et al.</i> , 2011
ThiC	Thiamine biosynthesis	Martinez-Gomez <i>et al.</i> , 2009
ThiH	Thiamine biosynthesis	Kriek <i>et al.</i> , 2007
TYW1	Wybutosine tRNA biosynthesis	Noma <i>et al.</i> , 2006
HydE, HydG	Hydrogenase maturation	Rubach <i>et al.</i> , 2005
HemN	Heme biosynthesis	Layer <i>et al.</i> 2002, 2003, 2005
LAM	Lysine metabolism and β -lysine antibiotics	Frey & Magnusson 2003; Frey <i>et al.</i> , 1998

^aAbbreviations: PFL-AE, pyruvate formate lyase activating enzyme; ANRR-AE, anaerobic ribonucleotide reductase activating enzyme; BssD-AE, gene product D in benzylsuccinate biosynthetic pathway; GD-AE, glycerol dehydratase activating enzyme; BioB, biotin synthase; LipA, lipoic acid synthase; HemN, oxygen-independent coproporphyrinogen III oxidase; LAM, lysine 2,3-aminomutase.

^bAll enzymes contain the AdoMet CysX₃CysX₂Cys signature imperative for their catalytic function.

The 5'-deoxyadenosyl radical, resulting from the reductive cleavage of SAM is highly oxidizing and can directly abstract hydrogen atoms from unactivated C-H bonds in the substrate, prompting the formation of stable substrate radicals, for example in lysine 2,3-aminomutase (LAM), biotin synthase (BioB), oxygen-independent coproporphyrinogen III oxidase (HemN), lipoic acid synthase (LipA), and MiaB (Marsh & Drennan 2001; Frey & Reed 2000). Alternatively, a protein substrate may be involved, generating a catalytic glycy radical. Glycyl radical reactions where protein substrates are involved have never been described for eukaryotes. Such radical SAM enzymes function as activating enzymes and typical examples include anaerobic ribonucleotide reductase activating enzyme (ARNR-AE), pyruvate formate lyase activating enzyme (PFL-AE), glycerol dehydratase activating enzyme (GD-AE) and gene product D in benzylsuccinate biosynthetic pathway (BssD-AE) and the glycyl radicals on such enzymes are relatively stable and can be observed by electron paramagnetic resonance (EPR) spectroscopy (Verfürth *et al.*, 2004; Duboc-Toia *et al.*, 2003; Sun *et al.*, 1996; Wagner *et al.*, 1992; Young *et al.*, 1994; Knappe & Wagner 2001). Till date, radical SAM proteins containing as much as three [Fe-S] clusters have been characterized. Site-directed mutagenesis studies have led to the discovery of other conserved cysteine residues that contribute ligands to a second or a third Fe-S cluster, which may or may not be essential for function (Broach & Jarrett 2006; Cicchillo *et al.*, 2004; Hernández *et al.*, 2007; Urzica *et al.*, 2009; Grove *et al.*, 2008). Apart from the AdoMet [4Fe-4S]⁺¹ cluster involved in the production of the highly reactive 5'-deoxyadenosyl radical, additional Fe-S clusters have been attributed to function like sulfur donor in sulfur insertion reactions, for instance reactions catalyzed by BioB (Broach & Jarrett 2006), LipA (Cicchillo *et al.*, 2004) MiaB (Hernández *et al.*, 2007) and RimO (Lee *et al.*, 2009; Arragain *et al.*, 2010). In these catalytic processes, the enzymes insert sulfur into their substrates using the additional [Fe-S] in a self sacrifice mechanism (Booker *et al.*, 2007). In other radical SAM proteins like MoeA (Hänzelmann & Schindelin 2006; Santamaria-Araujo *et al.*, 2004; Hänzelmann *et al.*, 2004) and HydE (Rubach *et al.*, 2005; Nicolet *et al.*, 2008) the functions of additional [Fe-S] clusters still remain unknown.

1.1.1 Role of [Fe-S] clusters in transcriptional and translation regulation

Several [Fe-S] clusters in Fe-S proteins have been well-characterized in bacteria to play important roles in the transcriptional and translational regulation of gene expression (Kiley & Beinert 2003). Each [Fe-S] cluster senses a different type of environmental stimuli and utilizes a distinct sensing mechanism that may involve cluster conversion, assembly or redox chemistry. The three *Escherichia coli* transcription factors, SoxR, FNR and IscR are typical examples of proteins that utilize [Fe-S] as a key for their regulatory functions. In addition, the tricarboxylic acid cycle (TCA) enzyme, aconitase, plays a role in translational regulation in *Bacillus subtilis* and *E.coli* via the loss of its [Fe-S] cluster, which necessitates its regulatory RNA-binding activity. A common strategy involved in the regulatory functions of Fe-S cluster is that these Fe-S clusters mediate cellular response to specific oxidizing agents like O₂, reactive oxygen species (ROS) and also nitric oxide (NO). SoxR was the first transcription factor shown to possess a Fe-S cluster. It was discovered based on its role in sensing superoxide and NO stress by oxidation of its [2Fe-2S] and thereby stimulating transcriptional expression of SoxS responsible for activating the transcription of various enzymes in the oxidative stress response pathway (Dempfle *et al.*, 2002; Ding & Dempfle 2000). FNR (for fumarate nitrate reduction) protein is a global transcriptional regulator of various *E. coli* genes in response to oxygen limitation. The regulatory function of FNR depends on the integrity of the [4Fe-4S], which is necessary for FNR dimerization (Moore & Kiley 2001), site-specific DNA binding (Khoroshilova *et al.*, 1997; Green *et al.*, 1996) and transcription activation (Ralph *et al.*, 2001). Under aerobic conditions, the DNA-binding dimeric [4Fe-4S]²⁺ active form of FNR is converted to its monomeric [2Fe-2S]²⁺ form to control genes partaking in aerobic and anaerobic respiratory pathways (Kiley & Beinert 2003). The negative feedback repressor, IscR has been demonstrated to regulate both the ISC and SUF systems involved in [Fe-S] cluster biogenesis (Giel *et al.*, 2006; Yeo *et al.*, 2006). IscR can exist in two forms, holo- and apo-IscR. Holo-IscR contains a [2Fe-2S] cluster, which can repress the expression of the *iscRSUA* operon by its binding to the promoter region (Schwartz *et al.*, 2001). Upon impairment or loss of the [2Fe-2S] cluster because of its sensitivity to oxygen, iscR converts to the apo-form and thereafter released from the *isc* promoter, thus causing the expression of the *isc* operon. Apart from

regulating the *isc* operon activity, apo-IscR can also activate the *suf* (*sufABCDSE*) operon by directly binding to the *suf* promoter under oxidative conditions (Giel *et al.*, 2006; Yeo *et al.*, 2006). To effect its regulatory function, IscR continually changes between its holo- and apo-forms due to the sensitivity of the [Fe-S] cluster to oxygen and the feedback control of IscR on [Fe-S] biogenesis. Aconitases catalyze the reversible isomerization of citrate to isocitrate in the tricarboxylic acid and glyoxylate cycles. They are monomeric enzymes containing an [Fe-S] cluster which are interconvertible between the catalytically active [4Fe-4S] forms and the inactive [3Fe-4S] and the apo-enzyme forms (Beinert *et al.*, 1996). The active cytosolic aconitase containing [4Fe-4S] cluster has the same activity with the mitochondrial enzyme, but the apo-form, also known as IRP (iron regulatory protein), binds to specific mRNA to either stabilize the mRNA or inhibit its translation (Beinert *et al.*, 1996). IRPs coordinate translational control under limiting iron levels, since the proportion of aconitase containing an [Fe-S] cluster depends on oxidative stress and/or iron availability (Cairo *et al.*, 2002; Eisenstein 2000). IRPs have been shown to inhibit translation of some mRNAs, for instance ferritin mRNA, by binding to iron-responsive elements (IREs) in the 5' untranslated region (5'UTR) of the transcript or alternatively promoting translation of certain mRNAs, for example transferrin receptor mRNA, by increasing mRNA stability resulting from its binding to IREs in the 3' untranslated region of the transcript (Hentze & Kuhn 1996; Hirling *et al.*, 1994; Rouault & Klausner 1996; Klausner & Rouault 1993).

1.1.2 Biogenesis and incorporation of [Fe-S] into apoproteins

Proteins containing Fe-S clusters are ubiquitous in nature and can be found in anaerobic and aerobic prokaryotes and eukaryotes. Iron-sulfur clusters are one of the most ancient metallocofactors (Hall *et al.*, 1971) and were first discovered in the early 1960s (Hall *et al.*, 1971; Beinert *et al.*, 1997; Rees & Howard 2003). In the biological systems, they function in vast roles like electron transport, possess catalytic and structural roles, are involved in regulation of gene expression and act as sensors for iron and oxygen (Johnson 1998; Flint & Allen 1996; Beinert *et al.*, 1996). The most prevalent forms of Fe-S cluster include [2Fe-2S], [3Fe-4S], and [4Fe-4S], in which the iron ions are tetrahedrally coordinated by thiolate ligands of cysteine residues, with additional coordination to each iron by inorganic sulfur. Iron-sulfur

1 INTRODUCTION

clusters can be spontaneously generated and incorporated into apoproteins *in vitro* (Merchant & Dreyfuss, 1998; Külzer *et al.*, 1998, Ollagnier *et al.*, 1999), but in biological systems, Fe-S biogenesis and incorporation into apoproteins are highly regulated by conserved biosynthetic machineries to prevent toxicity associated with free iron and sulfide and allow delivery at lower intracellular concentrations of these species (Tokumoto *et al.*, 2004; Land & Rouault, 1998). Though simple in structure, [Fe-S] biogenesis requires intricate interplay of a number of proteins that function in three basic steps: formation of elemental sulfur, sulfur and iron cluster assembly, and insertion of cluster into apoproteins.

In bacteria, three separate Fe-S cluster biogenesis systems have been identified; they include the ISC (iron-sulfur cluster), the NIF (nitrogen fixation) and the SUF (Sulfur mobilization) (Zheng *et al.*, 1998; Jacobson *et al.*, 1989; Takahashi & Tokumoto 2002) biosynthetic machineries. In eukaryotes, conserved components of the bacterial ISC assembly machinery are localized in the mitochondria, where they participate in the biogenesis of Fe-S clusters (Mühlenhoff & Lill 2000). The ISC assembly machinery is required for the generation of most cellular Fe-S proteins and thus may perform a general “house-keeping” biosynthetic function (Zheng *et al.* 1998). The NIF biosynthetic machinery was the first Fe-S cluster assembly machinery discovered. It is dedicated to the assembly of the Fe-S cluster of the complex protein, nitrogenase that catalyzes the conversion of N₂ to NH₃ in nitrogen-fixing bacteria (Frazzon & Dean 2002; Rees & Howard 2000). Finally, the SUF was discovered as independent biosynthetic machinery involved in the assemblage of Fe-S clusters used predominantly under iron-limiting or oxidative-stress conditions. The SUF system was presumably inherited from the cyanobacterial ancestor of plastids (Zheng *et al.*, 2001; Takahashi & Tokumoto 2002; Nachin *et al.*, 2003; Outten *et al.*, 2004). Although there seems to be an evolutionary link between the Fe-S protein assembly systems in the organelles (mitochondria and plastids) and the bacterial biosynthetic systems, a newly discovered Fe-S protein biosynthetic machinery which is unique for eukaryotes is the so-called cytosolic iron-sulfur protein assembly (CIA) machinery (Roy *et al.*, 2003). The CIA machinery is composed of various components involved in the maturation of cytosolic and nuclear Fe-S proteins. The eukaryotic machineries necessary for the biogenesis of Fe-S proteins are illustrated in Figure 1.1 (Lill & Mühlenhoff 2006).

1 INTRODUCTION

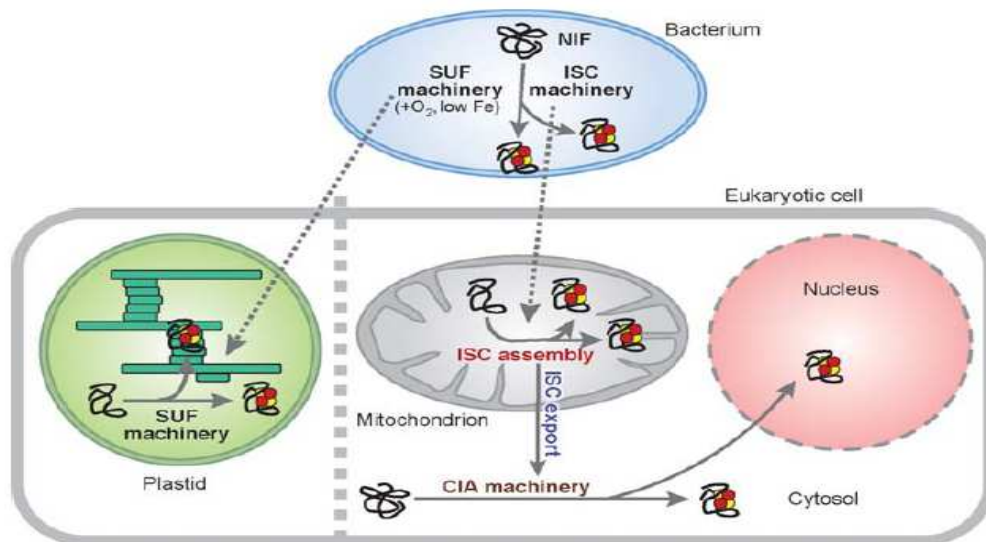


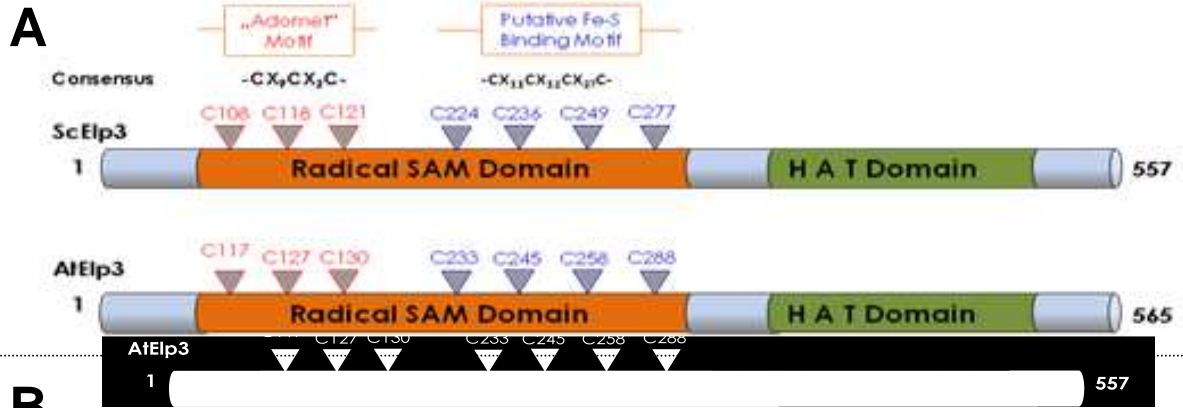
Figure 1.1 | Machineries involved in the biogenesis of eukaryotic Fe-S proteins and their putative evolutionary ancestry. Eukaryotic Fe-S proteins are found in the mitochondria, cytosol and nucleus. The ISC (iron-sulfur cluster) assembly machinery of the mitochondria involved in ‘house-keeping’ Fe-S proteins biosynthesis is predicted to be inherited from α -proteobacteria, the evolutionary ancestor of these organelles. The SUF (sulfur mobilization) machinery of plastids in plants probably evolved via endosymbiosis between the plant cell and a photosynthetic bacterium. The mitochondrial ISC machinery as well as the mitochondrial ISC export system and the cytosolic iron-sulfur protein assembly (CIA) machinery are imperative for the maturation of cytosolic and nuclear Fe-S proteins. These three systems are highly conserved in yeast, humans and plants. The NIF (nitrogen fixation) system is restricted to the assembly of nitrogen in the azototrophic bacteria, *Azotobacter vinelandii*. The red and yellow circles represent Fe-S clusters (Lill & Mühlenhoff 2006).

The current perception of the biogenesis of Fe-S proteins in the eukaryotic model organism, *Saccharomyces cerevisiae*, involved three complex proteinaceous systems known as ISC assembly, ISC export and CIA machineries. The ISC assembly machinery plays a ‘house-keeping’ role and is required for all cellular Fe-S proteins. Alternatively, the ISC export and CIA machineries function in the maturation of cytosolic and nuclear Fe-S proteins. The ISC assembly, ISC export and CIA proteins are highly conserved in eukaryotes and studies in higher organisms confirm similar pathways for the biogenesis of Fe-S proteins in both lower and higher eukaryotes (Lill & Mühlenhoff 2005).

1.1.3 Eukaryotic Elp3 proteins possess a putative radical SAM domain

The Elp3 and its homologues are referred to as the catalytic subunit of the Elongator complex based on the two catalytic domains inherent in their structure. Sequence analysis (Figure 1.2) has shown that Elp3 is a highly conserved member of the GNAT (GCN5-related N-acetyltransferase) protein family, showing the DAB signature (Wittschieben *et al.*, 1999). Mutations affecting the histone acetyltransferase activity of Elp3 HAT domain which acetylates histone H3 and H4 have been reported by Huang *et al.*, (2005) to also affect tRNA modification. The fact that a GNAT domain might be coupled to tRNA modification cannot be neglected, since recent studies illustrated that the protein TmcA utilizes a GNAT domain for transfer of acetyl moiety from acetyl-CoA to the N4 atom of a wobble cytidine of tRNA^{Met} in eubacteria (Chimnaronk *et al.*, 2009). In addition, Elp3 and its homologues show sequence homology to the enzymes of the radical SAM superfamily (Sofia *et al.*, 2001) (Figure 1.0, 1.2, and Table 1.0). The Elp3 radical SAM domain contains in addition to the AdoMet motif (CysX₉CysX₂Cys), a second putative Fe-S cluster binding motif (CysX₁₁CysX₁₂CysX₂₇Cys) (Sofia *et al.*, 2001; Chinenov 2002) conserved in almost all eukaryotes. The Elp3 radical SAM domain of yeast and Arabidopsis show 75% identity on amino acid sequence, whereas the amino acid conservation in the HAT domain is only 66%. Based on the fact that archaeal Elp3 has been shown to bind a [4Fe-4S] cluster and apparently cleaves SAM producing the highly reactive 5-deoxyadenosyl radical (Paraskevopoulou *et al.*, 2006), it could be postulated that eukaryotic Elp3 proteins may be involved in the carbon-radical based chemistry. Although the function of the radical SAM domain has not been thoroughly studied, members of the radical SAM superfamily have been implicated in several RNA modifications (Atta *et al.*, 2009), thus suggesting a possible function of Elp3 radical SAM domain in tRNA modification.

1 INTRODUCTION



B

Sc_Elp3	1	-----MARHGRKPKNTNKKLAPEKERFTCCADITLLELTDSLTSGTTRERINLNG
Hs_Elp3	1	-----MROKRRK-----DLSB-AEILMMLTIGDVIKCLIEAHECG--KIDLNK
At_Elp3	1	MATAVVMNGELRKKQPRFGKGGYQGRGLTPEEARVRAISEIIVSTMIERSHRN--ENVDLNA
Mj_Elp3	1	-----MVIIMPEKAKLMRCIIEIRLLDEYNKGLTDFKRIEQQR
consensus	1*
Sc_Elp3	50	LIIRKYSKKYKLLKQPRLELDIINSIPDOYKRYLLPKLAKPVRTASGIAVVAVMCKPHRCF
Hs_Elp3	41	VKTRTAARKYGLSAQPRLVDTIAAVPEQMRKVLMPKLAKPVRTASGIAVVAVMCKPHRCF
At_Elp3	59	IKTAAARKEYGLARAPKLVEMIAALPDSERETLLPKLRAKPVRTASGIAVVAVMCKPHRCF
Mj_Elp3	39	AECLEIRHRIIGIG-HPSNSEILLOYATEEBKRLIEIRLKKPKVRTSGIAVVAVMCKPHRCF
consensus	61*
Sc_Elp3	110	HIAITGNNICVYCPGGPDSDFEYSTOSYTGYEPTSMRAIRARYDPYECARGRVEQLKOLGH
Hs_Elp3	101	HISITGNNICVYCPGGPDSDFEYSTOSYTGYEPTSMRAIRARYDPYELCARRHRIEQLKOLGH
At_Elp3	119	HIAITGNNICVYCPGGPDSDFEYSTOSYTGYEPTSMRAIRARYNPYVCAARSRIQLKRLGH
Mj_Elp3	98	HG-----KCLFCPPGGVGSVFGDVHQSYPTEPEPALMRGLMFMNDPPLYLCTKARIEQLKGVGH
consensus	121	*.....*
Sc_Elp3	170	SIDKVEYVLMGGTFMFLPKEYREIFIVKLNALSFCENCDIDEALYSQCQLTKCVGITI
Hs_Elp3	161	SVDKVEFVLMGGTFMFLPEEYRDFYFIRNLHDALSCHTSNNIIEAVKYSERSLTKCIGITI
At_Elp3	179	SVDKVEFVLMGGTFMFLPEEYRDFYFIRNLHDALSCHTSANVEAVYSEHSATKCIGMTI
Mj_Elp3	153	PTKTEELIIMGGTFPARDIEYQDFIIRCIIDAMNCGVDASSIEEACKENETAEHRCVALCI
consensus	181	*.....*
Sc_Elp3	230	ETRPDYCQTHLDDMLKYGCTREIGVQSIYEDVARDTNRGHTVRSVCETFAVSKDAGYK
Hs_Elp3	221	ETRPDYCMKRHLSDMLTYGCTREIGVQSVYEDVARDTNRGHTVKAACESFHLAKDSGFK
At_Elp3	239	ETRPDYCLGSHLRQMLTYGCTREIGVQSIYEDVARDTNRGHTVAAVFDCCLAKDAGFK
Mj_Elp3	213	ETRPDYCGEHEINOMLKLGATRVELGVQFTYNEILEFCRNGHTVEDTKATQTLKDSGFK
consensus	241	*.....*
Sc_Elp3	290	VVSHMMPDLPNVGMERDIEQFKEIFENPDFRFDGLKIYPTLVIRGTGLYELWKTGRYKSY
Hs_Elp3	281	VVAHMPDLPNVGLERDIEQFEFFENPDFRFDGLKIYPTLVIRGTGLYELWKTGRYKSY
At_Elp3	299	VVAHMPDLPNVGVERDMESFKEFFESFSFRFDGLKIYPTLVIRGTGLYELWKTGRYRNY
Mj_Elp3	273	VSYHMPGMBPSSIMEVDEKMKFKEIFENPDFKPDVWKIYPCLVIEGTLEYEMWKRGEYKSY
consensus	301	*.....*
Sc_Elp3	350	SANALVDLVARILALVPPWTRIVRVORDIPMPLVTSGVINGNLRELALARMKDLGTTICRD
Hs_Elp3	341	SPSILVELVARILALVPPWTRIVRVORDIPMPLVSGVEHGNLRELALARMKDLGTTICRD
At_Elp3	359	FPECLVDLVARILSIVPPWTRIVRVORDIPMPLVTSGVKGNLRELALARMKDLGTTICRD
Mj_Elp3	333	REPEALEITSYAKSIMEKVVRTSRVORDIATVIVGVKSNLCELVYKMEKHGIKCC
consensus	361*
Sc_Elp3	410	VRTREVGIOEVHKKVCF--DOVELIRRDYVANGGWETFLSYEDPKKIDILIGLLRLRKAISK
Hs_Elp3	401	VRTREVGIOEIHKKVRF--YOVELVRRDYVANGGWETFLSYEDFDLIDILIGLLRLRKCIS
At_Elp3	419	VRTREVGIOEIHKKVRF--EOVELVRRDYVANGGWETFLSYEDFDLIDILIGLLRLRKCIS
Mj_Elp3	393	IRREVGHVMYKKGIMEDIEHRLICREVEYASGGCFHFLSYEDVKNIDILIAFLRLREPY-
consensus	421	*.....*
Sc_Elp3	468	KYTYRKEFTSRTSIVRELHVYGSVVPVH--SRDEKFOHQCFTLLMEEAERIAAEEHGS
Hs_Elp3	458	EEYFRFELCG--VSIVRELHVYGSVVPVH--SRDEKFOHQCFTLLMEEAERIAAEEHGS
At_Elp3	476	KNVTCFELCK--CSVRELHVYGTAVPVH--GRDAKFOHQCFTLLMEEAERIAAEEHGS
Mj_Elp3	452	-KFRKELDNL--TMLVROLHVCGQEKPTKDLKEITWOHCGGRKLEEAERIAAEEFGR
consensus	481*
Sc_Elp3	527	EKISVISGVCVRNYYKGLGYELDGPYMSKRI--
Hs_Elp3	516	GKIAVISGVCIRNYYRKGYRILCGPYMVKMLK
At_Elp3	534	NKIAVISGVCIRHYRKLGYELDGPYMKVHLL
Mj_Elp3	510	KKIIVVSGVREYRKLGYERVGYMCKYLE
consensus	541	*.....*

Radical SAM Domain

HAT Domain

1 INTRODUCTION

Figure 1.2 | Sequence conservation of two-domain Elp3-related histone acetyltransferases (HATs) and S-adenosylmethionine (SAM) radical enzymes in eukaryotes and archaea.

(A) Schematic representation of the domain architecture of the ScElp3 and AtElp3 proteins. The orange region represents the radical SAM domain, while the histone acetyltransferase (HAT) domain is illustrated by the green region. The cysteine residues contributing ligands to putative Fe-S binding in both motifs are shown. The domain architecture is based on the graphical representation of the Pfam family and domain database. (B) Sequences were aligned using ClustalW (Thompson *et al.*, 1994). Only amino acid residues that are identical (black background) or similar (grey background) in all species are shown. The Elp3 eukaryotic sequences are taken from *Saccharomyces cerevisiae* (Sc_Elp3), Human (Hs_Elp3) and *Arabidopsis thaliana* (At_Elp3) as well as from the Archaea, *Methanocaldococcus jannaschii* (Mj_Elp3). The conserved cysteine residues in the 'Adomet' motif (CX₉CX₂C) showing sequence similarity to all radical SAM enzymes (Sofia *et al.*, 2001) that bind Fe-S clusters are marked with red arrows. The other cysteines conserved in a second putative Fe-S cluster-binding motif (CX₁₁CX₁₂CX₂₇C), which may be involved in additional Fe-S cluster(s) binding are designated with green arrows. The blue closed circles mark the region similar to motif I that is characteristic of SAM-dependent methyltransferases (Kagan & Clarke 1994) and this sequence aligns with a GGE motif conserved in radical SAM enzymes and found close to the SAM binding pocket (Nicolet & Drennan 2004; Vey *et al.*, 2008). The conserved D, A and B motifs of GNAT superfamily members are depicted with red bars (Neuwald & Landsman 1997). Open circles depicts residues which are conserved in GNAT superfamily members and when mutated to alanine leads to less than 10% residual HAT activity of recombinant yeast Gcn5 *in vitro* (Kuo *et al.*, 1998). The conserved QXXGXG signature in motif A are critical for acetyl-CoA recognition and binding by known acetyltransferases (Dutnall *et al.*, 1998; Wolf *et al.*, 1998).

1.2 Conservation of the Elongator complex in eukaryotes

The Elongator complex was first discovered at the beginning of 1999 in the laboratory of Svejstrup (Otero *et al.*, 1999) as a multisubunit complex which cofractionated with the chromatin-associated hyperphosphorylated form of the RNA polymerase II in yeast. The Elongator complex is highly conserved in eukaryotes and composed of six subunits encoded by the *ELP1-ELP6* (Elongator protein) genes in yeast (Otero *et al.*, 1999; Fellows *et al.*, 2000; Wittschieben *et al.*, 1999; Winkler *et al.*, 2001). The unstable Elongator complex can be dissociated into two subcomplexes. The core complex is composed of the proteins Elp1 (150 kDa), Elp2 (90 kDa) and Elp3 (60 kDa) (Otero *et al.*, 1999; Winkler *et al.*, 2001). The HAP (HAT associated proteins) complex consisting of Elp4 (50 kDa), Elp5 (35 kDa) and Elp6 (30 kDa) interacts with the core complex to form the holo-Elongator (Winkler *et al.*, 2001; Krogan & Greenblatt 2001; Li *et al.*, 2001). The human

1 INTRODUCTION

homologue of yeast Elp1 is encoded by the *IKAP* gene (Otero *et al.*, 1999; Cohen *et al.*, 1998). Orthologues of the other Elp subunits have also been found in human (Hawkes *et al.*, 2002; Kim *et al.*, 2002), mouse (Collum *et al.*, 2000) and *Arabidopsis* (Nelissen *et al.*, 2005; Mehlgarten *et al.*, 2010) (Figure 1.3). Inactivation of Elongator subunits in yeast, *C. elegans* and *Arabidopsis* results in characteristic pleiotropic phenotypes (Frohloff *et al.*, 2001; Jablonowski *et al.*, 2001, 2004; Krogan & Greenblatt, 2001; Otero *et al.*, 1999; Wittschieben *et al.*, 1999; Fellows *et al.*, 2000; Winkler *et al.*, 2001; Nelissen *et al.*, 2005; Falcone *et al.*, 2007; Chen *et al.*, 2006, 2009; Zhou *et al.*, 2009). In line with the structural and functional similarities of the Elongator complex (Mehlgarten *et al.*, 2010; Chen *et al.*, 2009; Nelissen *et al.*, 2005; 2010; Hawkes *et al.*, 2002) coupled with the pleiotropic phenotypes observed upon deletion of Elongator subunits, Elongator complex has been confirmed to be highly conserved in eukaryotes.

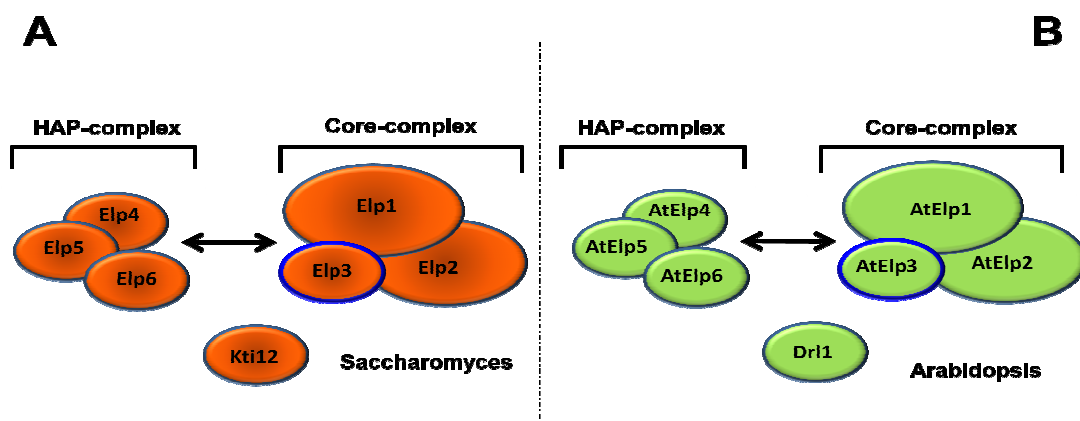


Figure 1.3 | Conservation of the Elongator complex in Yeast and *Arabidopsis*. (A) The yeast Elongator showing the subunits of the HAP- and core-subcomplexes. (B) The *Arabidopsis* Elongator complex also depicting the subunits found in the HAP- and core-subcomplexes. The Elongator associated protein Kti12 (yeast) and Dr11 (*Arabidopsis*) and the subunits of the Elongator complex in both eukaryotes are highly conserved suggesting similar structure and catalytic functions. Elp3 and AtElp3 (blue borders) are the catalytic subunits of the Elongator complex (Mehlgarten 2009; Mehlgarten *et al.*, 2010; Nelissen *et al.*, 2005).

1.2.1 Subunits of the Elongator complex

The Elongator subunits are categorized into two interacting subcomplexes, the HAP complex comprising of the subunits Elp4-Elp6 and the Core subcomplex composed of Elp1-Elp3 (Winkler *et al.*, 2001; Krogan & Greenblatt, 2001; Li *et al.*, 2001). Although the role of the Core subcomplex has been linked to involvement in

transcription elongation in vivo (Otero *et al.*, 1999; Winkler *et al.*, 2001; Svejstrup 2002), the function of the HAP complex is hitherto not known. The *ELP1*, the largest subunit of the Core Elongator subcomplex encodes a protein without discernable motifs (Otero *et al.*, 1999). The *ELP1* is the yeast homologue of *IKBKAP* (I κ B kinase complex-associated protein). The *IKBKAP* gene encodes the scaffold protein IKAP involved in NF- κ B activation that belongs to a five-subunit IKK protein complex (Cohen *et al.*, 1998), although subsequent study (Krappmann *et al.*, 2000) questioned this conclusion, demonstrating that cellular IKK complexes do not harbor IKAP by using various protein-protein interaction and functional assays. Interaction studies in yeast revealed that Elp1 could also act as scaffold protein in the core subcomplex (Frohloff *et al.*, 2003). Elp1 and Elp2 possess a number of WD40 repeats that are capable of folding into one or more β -propeller structures which are imperative as protein-protein interaction platform (Smith *et al.*, 1999). Such WD40 repeats could function as scaffolds for binding of histone substrates to promote acetylation by Elp3 or alternatively binding of tRNA substrates. Interestingly, Gemin5 protein has recently been shown to specifically bind to a small nuclear RNA via a WD40 repeat domains (Lau *et al.*, 2009). Pleiotropic phenotypes are associated with Elp1 mutations in eukaryotes. For instance in human, mutations in IKAP (Slaugenhaupt *et al.*, 2001; Anderson *et al.*, 2001) are responsible for familial dysautonomia (FD; Riley-Day syndrome). Riley-Day syndrome (FD) is a severe recessive neurodegenerative disease of the sensory and autonomous nervous system caused by mutation in *IKBKAP* gene (Slaugenhaupt & Gusella 2002). Pleiotropic phenotypes like chemical and thermal stress in yeast (Otero *et al.*, 1999; Frohloff *et al.*, 2001; Jablonowski *et al.*, 2001; Fichtner & Schaffrath 2002) and growth deficiencies in *Arabidopsis* (Chen *et al.*, 2006; Falcone *et al.*, 2007; Nelissen *et al.*, 2005; Zhou *et al.*, 2009) resulting from Elp1 deletion are also evident.

The *ELP2* gene encodes for a 90 kDa protein containing eight WD40 repeats (Fellows *et al.*, 2000). Elp2 and also Elp1 possess various WD40 repeats that are capable of folding into several β -propeller structures, serving as protein-protein interaction platform (Smith *et al.*, 1999). Interestingly, the human Gemin5 protein was recently shown to specifically bind to a small nuclear RNA via a WD40 repeat domains (Lau *et al.*, 2009). Such WD40 repeats could function as scaffolds for binding of histone H3 and H4 substrates to promote acetylation by Elp3 or

1 INTRODUCTION

alternatively used by Elongator for binding tRNA substrates. Protein-protein interaction studies have also shown the ability of Elp2 to interact with other Elongator subunits and Elongator partner proteins (Fellows *et al.*, 2000; Krogan & Greenblatt 2001; Fichtner *et al.*, 2002a).

The Elp3 is the most conserved subunit of the Elongator complex and shows high sequence conservation from Archaea to human (Wittschieben *et al.*, 1999). All Elp3 homologues contain two characteristic catalytic domains, the HAT (Histone acetyl transferase) and radical SAM domain. The Elp3 HAT domain is highly conserved in all members of the GNAT (GCN5-related N-acetyltransferase) protein family and has been well characterized (Wittschieben *et al.*, 1999, 2000). The HAT activity of recombinant Elp3 has been shown in gel-based assay to be directed towards all four core histones and specifically to lysine-14 of histone H3 and lysine-8 of histone H4 and is essential for Elongator function (Wittschieben *et al.*, 1999; Winkler *et al.*, 2002). The finding that *elp3gcn5* mutant phenotypes could be suppressed by concomitant deletion of the histone deacetylase coding genes, *HDA1* and *HOS2*, further supported the importance of the Elp3 *in vivo* HAT activity, which is necessary for maintaining the balance between transcription-associated histone acetylation and deacetylation (Wittschieben *et al.*, 2000). Gcn5 is the HAT subunit of well-characterized chromatin-remodeling complex SAGA (Grant *et al.*, 1997).

Unlike the HAT domain, the radical SAM domain situated N-terminal in Elp3 has not been well characterized. It possesses significant sequence similarity to the catalytic domain of S-adenosylmethionine (SAM or AdoMet) radical enzymes (Chinenov 2002; Sofia *et al.*, 2001). The radical SAM proteins generate a radical species by reduction cleavage of SAM via an unusual Fe-S cluster (Sofia *et al.*, 2001; Paraskevopoulou *et al.*, 2006). The highly oxidizing 5'-deoxyadenosyl radical reacts with substrates resulting in the activation and cleavage of non-activated C-H bonds (Layer *et al.*, 2004; Frey & Booker 2001; Frey & Magnusson 2003) involved in the catalysis of chemically difficult reactions (Sofia *et al.*, 2001). The existence of the radical SAM domain in eukaryotic Elp3 proteins suggests their possible involvement in carbon-based radical catalysis in the Elongator-dependent mcm⁵ side chain formation at the U₃₄ position in some tRNA species (Huang *et al.*, 2005; Lu *et al.*, 2005; Jablonowski *et al.*, 2006). A typical example of the use of

5'-deoxyadenosyl radical species by a radical SAM enzyme involved in the methylthiolation of tRNA is the MiaB protein in *E.coli* and *Thermotoga maritima* (Pierrel *et al.*, 2002, 2003, 2004; Esberg *et al.*, 1999).

1.2.2 The Elongator regulatory protein, Kti12

The *KTI12* gene encoding the Elongator regulatory protein Kti12 was one of the first genes discovered through a genetic screen to be involved in the zymocin resistance pathway (Butler *et al.*, 1994). Intriguingly, *elp/tot* as well as zymocin resistant phenotypes could be observed upon deletion or overexpression of the *KTI12* gene (Butler *et al.*, 1994; Frohloff *et al.*, 2001; Fichtner *et al.*, 2002a). By using biochemical methods, it was shown that Kti12 is not a structural component of the Elongator complex (Otero *et al.*, 1999; Wittschieben *et al.*, 1999; Fellows *et al.*, 2000; Li *et al.*, 2001; Winkler *et al.*, 2001; Krogan & Greenblatt 2001). Although Kti12 interacts with the Elongator subcomplexes, the assembly or integrity of the Elongator complex is not affected in *KTI12* deletion strain (Frohloff *et al.*, 2001; Fichtner *et al.*, 2002a; Fichtner *et al.*, 2002b). The fact that Kti12 could be found associated with the phosphorylated form of RNA polymerase II (Frohloff *et al.*, 2003) and chromatin (Fellows *et al.*, 2000; Svejstrup 2007; Petrakis *et al.*, 2005), leads to the assumption that Kti12 might be involved with Elongator complex in transcription processes and therefore confirms the view of Kti12 as an Elongator regulatory protein.

Like the Elongator subunits, Kti12 is also important for the mcm⁵ modification at the U₃₄ position in certain tRNA species (Huang *et al.*, 2005). Kti12 protein is highly conserved in eukaryotes. In all its homologues, Kti12 shows high sequence similarity in an N-terminal ATP/GTP binding domain (P-loop) and a potential C-terminal Calmodulin binding domain (CBD) important for its cellular function (Fichtner *et al.*, 2002a; Nelissen *et al.*, 2003). High sequence similarity was recently observed between Kti12 and the phosphoseryl-tRNA^{Sec}-kinase (PSTK) from the archaea *Methanocaldococcus jannaschii* (Sherrer *et al.*, 2008). PSTK is involved in the specific phosphorylation of Ser-tRNA^{Sec} in the 21st amino acid Selenocysteine biosynthetic pathway in eukaryotes and archaea (Carlson *et al.*, 2004). Based on

sequence homology to PSTK, it is postulated that yeast Kti12 may also interact with tRNA substrates and could be a tRNA-dependent kinase (Sherrer *et al.*, 2008).

1.2.3 Functions associated with the Elongator complex

Earlier studies on yeast and human Elongator revealed the six subunit protein complex copurified with hyperphosphorylated RNA polymerase II holoenzyme isolated from chromatin template (Otero *et al.*, 1999; Kim *et al.*, 2002). The HAT activity of yeast and human Elongator has been shown to be directed towards histone H3 (Winkler *et al.*, 2002; Hawkes *et al.*, 2002; Kim *et al.*, 2002). Indeed, it could be postulated that Elongator assists the RNA polymerase II during transcription elongation by its inherent Elp3 HAT activity via histone acetylation and thus influencing chromatin structure remodeling (Kim *et al.*, 2002; Otero *et al.*, 1999; Wittschieben *et al.*, 1999, 2000). In further support of Elongator's role in transcription, RNA and chromatin immunoprecipitation studies revealed that Elongator associates with the nascent RNA emanating from elongating RNA polymerase II along the coding regions of several genes in yeast and human cells (Gilbert *et al.*, 2004; Kouskouti & Talianidis 2005; Close *et al.*, 2006; Metivier *et al.*, 2003; Petrakis *et al.*, 2005). Although Elongator could be found in the nucleus, localization studies confirmed the majority of Elongator to be cytoplasmic in most cell types (Pokholok *et al.*, 2002; Kim *et al.*, 2002; Holmberg *et al.*, 2002) with predicted functions in exocytosis and tRNA modification (Rahl *et al.*, 2005; Huang *et al.*, 2005). Recent studies have shown that the Elongator subunits, Elp1-Elp6 and its regulatory partners, Kti11-Kti13 are indispensable for tRNA modification of 11 tRNA species at the wobble uridine (U₃₄) position in the anticodon loop via formation of 5-methylcarboxymethyl (mcm⁵) or 5-carbamoylmethyl (ncm⁵) side chains (Huang *et al.*, 2005; Lu *et al.*, 2005; Johansson *et al.*, 2008) (Figure 1.4).

Coimmunoprecipitation studies confirmed specific interaction between tRNA^{Glu}_{UUC} and either Elp1 or Elp3 (Huang *et al.*, 2005). Deletion in *ELP3* genes leads to lack of mcm⁵ and ncm⁵ side chains on uridines at the wobble position in these tRNAs. This prompted a study of the mechanism of γ -toxin-induced *elp/tot* phenotypes, which indicated that zymocin may be an RNase which specifically restricts only certain modified, but not unmodified tRNAs (Lu *et al.*, 2005). To support this claim, the

1 INTRODUCTION

methyltransferase Trm9 was observed to specifically methylate U34 in tRNA^{Glu} and tRNA^{Arg}, which is also necessary for the cytotoxicity of zymocin like for the Elongator (Kahlor & Clark 2003; Jablonowski *et al.*, 2006).

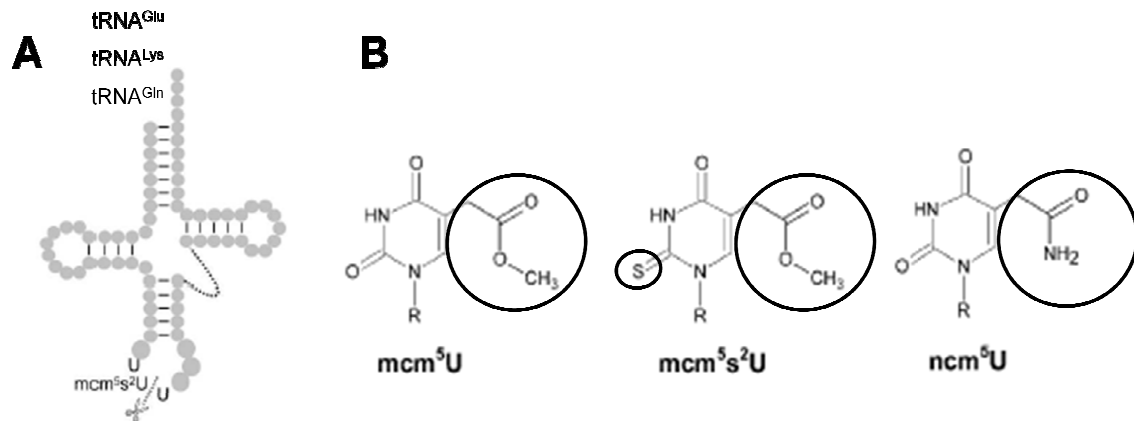


Figure 1.4 | Systematic drawing of Elongator-dependent modification of some tRNA species at the wobble (U₃₄) position. (A) Cleavage of Elongator-dependently modified tRNA substrates (tRNA^{Glu}, tRNA^{Lys} and tRNA^{Gln}) between positions U₃₄-U₃₅ by the *K. lactis* γ toxin. (B) The modified side chains (from left to right) are; 5-methoxycarbonylmethyluridine (mcm⁵U), 5-methoxycarbonylmethyl-2-thiouridine (mcm⁵s²U), 5-carbamoylmethyluridine (ncm⁵U). R represents the ribose sugar. Mcm⁵U and ncm⁵U modifications are Elongator-, Kti11-13- and Trm9-dependent (Huang *et al.*, 2005; Lu *et al.*, 2005).

Recent data also revealed Elongator's role in exocytosis in yeast (Rahl *et al.*, 2005). Exocytosis defects in yeast were linked to *sec2-52* mutation in the essential Sec2, which is a GTP-exchange factor (GEF) for the Rab-GTPase Sec4. Studies in two-hybrid assay could show the direct physical interaction between full length native Elp1 and Sec 2. This interaction is imperative for the correct polarized localization of Sec 2 which is necessary for post-golgi vascular transport (Rahl *et al.*, 2005). Remarkably, in a multi-copy suppressor screen of *elp/tot* phenotypes, two tRNA genes were isolated (Esberg *et al.*, 2006). Overexpression of these tRNA genes together led to the suppression of *elp/tot* phenotypes due to transcriptional defects (Wittschieben *et al.*, 2000) as well as *ELP* mutations on exocytosis (Rahl *et al.*, 2005), indicating that these phenotypes are based on translational dysfunction caused by a tRNA modification defect. Several studies have confirmed the notion that the structure and tRNA modification function of the Elongator complex is conserved in animals, fungi and plants (Huang *et al.*, 2005;

Mehlgarten *et al.*, 2010; Chen *et al.*, 2009). Recent evidences have also connected the Elongator to DNA damage response and gene silencing (Li *et al.*, 2009), RNA interference (Lipardi & Paterson 2009), global DNA demethylation (Okada *et al.*, 2010), acceleration of immune responses (DeFraia *et al.*, 2010) and regulation of auxin related genes (Nelissen *et al.*, 2010). Recent findings in mice have also linked Elp3 to physical interaction and acetylation of α -tubulin in microtubules (Creppe *et al.*, 2009; Solinger *et al.*, 2010) in the context of neuronal migration and development. Additional reports in *Drosophila melanogaster* have demonstrated that Elp3 actively functions in the control of synaptic bouton expansion and sleep (Singh *et al.*, 2010) and also essential for viability, normal development and hematopoiesis (Walker *et al.*, 2011). Several cellular functions have evolved in parallel that differentially utilize the highly conserved Elongator complex. More recently, the Elp1 protein in human, yeast, and *C. elegans* have been reported to exhibit RNA-dependent RNA polymerase activity (Lipardi & Paterson 2009). Two main studies that focused on zymocin resistance in yeast have shown that Elongator could interact with and thus be regulated by the antagonistic action of the Hrr25 kinase and the Sit4 phosphatase (Jablonowski *et al.*, 2004; Mehlgarten *et al.*, 2009). Although arguments support the role of Elongator in tRNA modification / translation, since overexpression of two tRNA species underlies the pleiotropic *elp/tot* phenotypes associated with *ELP* gene inactivation resulting from transcriptional and exocytosis defects (Esberg *et al.*, 2006), the discussion for the elucidation of the major function of Elongator still lingers on.

1.2.4 The *elp/tot* phenotypes of Elongator mutation

Mutations in the *ELP1-ELP6* or the *KTI* (killer toxin insensitive) genes encoding the Elongator subunits and the Kti proteins respectively, lead to characteristic pleiotropic phenotypes referred to as the *elp/tot* phenotypes. The pleiotropic phenotypes may result from delayed transcriptional activation of certain genes (Otero *et al.*, 1999; Wittschieben *et al.*, 1999) or due to slow growth adaption to various growth conditions (Otero *et al.*, 1999; Frohloff *et al.*, 2001; Jablonowski *et al.*, 2001). Other characteristics of these phenotypes are temperature sensitivity, sensitivity to the *Kluyveromyces lactis* killer toxin, to the purine alkaloid, caffeine as well as to the cell wall toxin, calcofluor white (Otero *et al.*, 1999; Frohloff *et al.*, 2001;

1 INTRODUCTION

Jablonowski *et al.*, 2001; Fichtner & Schaffrath 2002). Additionally, the *elp/tot* and *kti* mutants are mildly sensitive to the drug 6-azauracil which inhibits enzymes involved in nucleotide metabolic pathway and show significant delay in the G₁-to-S phase transition (Frohloff *et al.*, 2001; Fichtner & Schaffrath 2002). Pleiotropic phenotypes associated with *Arabidopsis* include defects in cell proliferation and morphology, sensitivity to abscisic acid, drought tolerance, oxidative stress resistance and influence in anthocyanin biosynthesis (Chen *et al.*, 2006; Falcone *et al.*, 2007; Nelissen *et al.*, 2005; Zhou *et al.*, 2009). Yeast and *Arabidopsis elp/tot* phenotypes are illustrated in Figure 1.5.

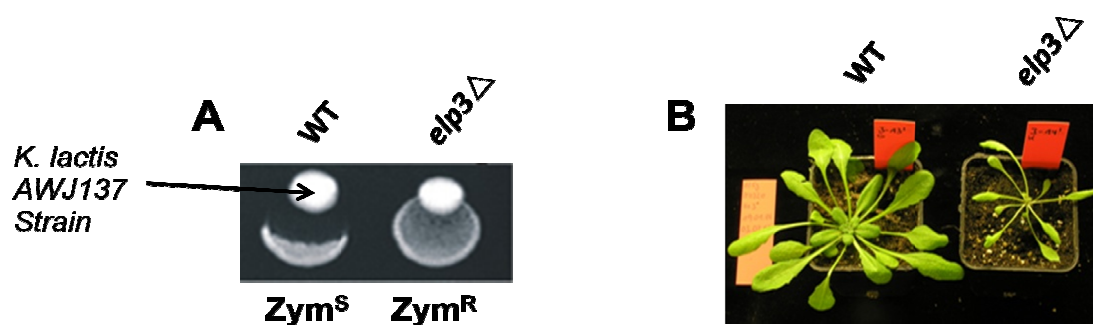


Figure 1.5 | Phenotypes of Yeast and *Arabidopsis elp3Δ* mutants. (A) Eclipse bioassay according to Kishida *et al.*, (1996). *Saccharomyces cerevisiae* wild type strain is sensitive to the *K. lactis* zymocin toxin in comparison to the *elp3Δ* strain showing resistance to zymocin. *S. cerevisiae* sensitive (Zym^S) and resistant (Zym^R) strains were spotted on YPD plates and then treated with the *K. lactis* killer strains (AWJ137). The inhibition of the WT strains is seen as an eclipse around the *K. lactis* killer strain, while the resistant strain can grow in the presence of the *K. lactis* killer strain. (B) The *Arabidopsis* AtElp3 WT and *elp3Δ* phenotypes.

1.2.5 Zymocin, the *Kluyveromyces lactis* killer toxin

Secretion of toxic substances is a common strategy evolved by micro-organisms to gain selective growth advantage over microbial competitors. A typical example is the dairy yeast *Kluyveromyces lactis* that produces a heterotrimeric toxin (zymocin). The lethality of zymocin on sensitive yeast strains like *Saccharomyces cerevisiae* is caused by the induction of G₁ cell cycle arrest (Gunge *et al.*, 1981; Sugisaki *et al.*, 1983; White *et al.*, 1989; Schaffrath & Meinhardt 2005). The heterotrimeric toxin complex consisting of the α (99 kDa), β (30 kDa) and γ (27.5 kDa) subunits is encoded by a linear dsDNA plasmid (Gunge *et al.*, 1981; Stark *et al.*, 1990). In addition, the *K. lactis* killer strain is toxin-insensitive courtesy of

the expression of immunity against the secreted zymocin (Gunge *et al.*, 1981). The cytotoxicity of zymocin resides on the γ -subunit, since its conditional expression from regulatable *GAL* promoters mimics the action of exogenous zymocin (Tokunaga *et al.*, 1989; Butler *et al.*, 1991b). Transport of the γ -toxin into susceptible yeast cells is facilitated by the α - and β -subunits by enhancing cell surface contact and membrane association (Butler *et al.* 1991b; Jablonowski *et al.*, 2001; Zink *et al.*, 2005; Mehlgarten *et al.*, 2004, 2007; Schaffrath & Meinhardt 2005). The *in vitro* exochitinase activity of the α -subunit is imperative for zymocin action (Butler *et al.*, 1991b), while the γ -subunit is biologically inactive upon exogenous application (Tokunaga *et al.*, 1989). Zymocin resistant *Saccharomyces cerevisiae* mutants can be categorized into two groups (Butler *et al.*, 1991a; Butler *et al.*, 1994; Frohloff *et al.*, 2001). Class I resistant mutants are defective in zymocin binding / uptake and thus are protected against exogenous zymocin, but sensitive to intracellular γ -toxin expression. Class II mutants' exhibit toxin-target defects and are resistant to both exogenous zymocin and intracellular γ -toxin.

1.2.6 Mechanism of action of zymocin

The γ -subunit of zymocin was the first eukaryotic toxin discovered that targets tRNAs which are modified in the wobble uridine (U_{34}) position. Initial molecular evidence was unraveled by Huang *et al.*, (2005) showing that the modification of 11 out of 42 tRNA species in yeast, found at the U_{34} position is dependent on the Elongator subunits, Elp1-Elp6 and its regulatory partners, Kti11-Kti13 grouped as class II zymocin-related proteins (Butler *et al.*, 1991a; Butler *et al.*, 1994; Frohloff *et al.*, 2001). The wobble uridine (U_{34}) modifications include mcm^5U (5-methoxycarbonylmethyluridine), mcm^5s^2U (5-methoxycarbonylmethyl-2-thiouridine), ncm^5U (5-carbamoyl-methyluridine), cm^5 (5-carboxymethyluridine), and these U_{34} modification are lacking in Elongator minus cells (Huang *et al.*, 2005) (Figure 1.5), and thus the *elp3 Δ* phenotypes resulting from translational defects are protected against the action of the γ -toxin. The absence of the mcm^5 modification at the wobble position in Elongator mutants prevents the performance of U_{34} -containing suppressors (Huang *et al.*, 2005; Jablonowski *et al.*, 2006), hence the requirement of the mcm^5 side chain for the ochre suppressor tRNA *SUP4* for nonsense read-through

1 INTRODUCTION

of *ade2-1* and *can1-100* alleles. Although the pleiotropic phenotypes associated with *elp/kti* mutants (Otero *et al.*, 1999; Frohloff *et al.*, 2001; Jablonowski *et al.*, 2001) have been attributed to transcription defects, evidence shows that lack of Elongator-dependent modification of U₃₄ may be a consequence of inefficient translation caused by improper codon-anticodon pairing (Agris 1991; Lim 1994; Okumura *et al.*, 1995). The γ -toxin is a tRNA endonuclease that cleaves its preferred substrates (tRNA^{Glu}, tRNA^{Lys} and tRNA^{Gln}) between positions U₃₄ and U₃₅ generating a 2', 3' cyclic phosphate and a 5' hydroxyl group (Huang *et al.*, 2005; Lu *et al.*, 2005). Coimmunoprecipitation experiments also showed that the Core Elongator subunits Elp1 and Elp3 could immunoprecipitate tRNA^{Glu} on of the γ -toxin targets (Lu *et al.*, 2005).

The methyltransferase Trm9, a class II zymocin resistant mutant (Kahlor & Clark 2003; Frohloff *et al.*, 2001), is also involved in the mcm⁵ modification by acting downstream of the Elongator proteins (Kahlor & Clarke 2003; Huang *et al.*, 2005; Jablonowski *et al.*, 2006) and its deletion mutant lacks the methylation on the mcm⁵ side chain. Interestingly, *trm9* Δ cells are protected against intracellular expression of γ -toxin efficiently like in the Elongator mutants lacking mcm⁵ modification at the U₃₄ position (Jablonowski *et al.*, 2006; Lu *et al.*, 2005). This implies that Elongator may influence the toxin function of zymocin by promoting the U₃₄ methylation by Trm9, which supports a scenario where excess levels of Elongator- and Trm9-dependent tRNAs suppress zymocin cytotoxicity (Butler *et al.*, 2004; Lu *et al.*, 2005; Jablonowski *et al.*, 2006). In addition, the overexpression of *TRM9* could revert the suppression due to hypomethylated tRNA and therefore restores the γ -toxin cytotoxicity (Jablonowski *et al.*, 2006).

1.3 Aims of research

The two-domain Elp3 protein is referred to as the catalytic subunit of the Elongator complex. It is the most conserved of all Elongator subunits and possesses enzymatic activity. The HAT domain has been well characterized to be involved in histone acetylation (Winkler *et al.*, 2002; Hawkes *et al.*, 2002; Kim *et al.*, 2002). In addition to the HAT domain, Elp3 also contains the radical SAM domain which shows high sequence similarity to the radical SAM enzyme superfamily (Sofia *et al.*, 2001). The aims of this research are to characterize the radical SAM domain in *Saccharomyces cerevisiae* (ScElp3) and *Arabidopsis thaliana* (AtElp3) proteins and also elucidate the biological importance of the radical SAM domain for the structure and function of the Elongator complex. The long term goal will be to understand the function of AtElp3 in the Elongator complex in *Arabidopsis thaliana*, since no *in vitro* protein purification and characterization studies exist for the plant Elongator.

The characterization of both proteins will involve *in vitro* expression, purification and analyses of the presence of Fe-S cluster(s) and its role for the structure and function of the Elongator complex. With the aid of site-directed mutagenesis in the radical SAM domain, the *in vivo* biological importance for functional and structural integrity of the Elongator complex will be unraveled. Mutation in the conserved putative glycyl radical motif in ScElp3 will also address the possibility of ScElp3 to act as a glycyl radical protein. The role of the Elongator partner protein Kti11 acting as a reductant of the Elongator complex directed towards the radical SAM domain of the ScElp3 protein will be addressed by *in vitro* characterization.

Apart from Trm9 that methylates mcm^5 , mcm^5s^2 , ncm^5 at U_{34} position, no enzyme or protein has been linked to the Elongator- and Kti11-13-dependent catalysis of the mcm^5 and ncm^5 modification at U_{34} of certain tRNA species (Huang *et al.*, 2005). Based on the sequence similarity of the Elp3 proteins with the radical SAM enzyme superfamily, it is worthwhile to predict that Elongator- and Kti11-13-dependent mcm^5 , mcm^5s^2 and ncm^5 modification at the U_{34} of certain tRNAs may follow a radical-based catalytic mechanism of the radical SAM domain of Elp3, same mechanism used by the radical SAM enzyme superfamily for their catalytic activity.

2 MATERIALS AND METHODS

2.0 Materials and methods

2.1 General methods

2.1.1 Chemicals, biochemicals and their sources

All the laboratory chemicals and biochemicals that were used for this research work, but not listed below were purchased from these companies: Sigma-Aldrich, Biomol, Bio-Rad, Boeringer-Ingelheim, New England Biolabs, Fluka, Merck, Roche, ROTH, Sartorius, SERVA, Fermentas, AppliChem, Qiagen and PeQLab. Chemicals and biochemicals as well as their producers and specifications will be provided in the corresponding sections in the text. All reagents, chemicals and biochemicals were of analytical grade. Most of the enzymes used were obtained from Fermentas (St. Leon-Rot).

2.1.2 Kits and markers

1 kb GeneRuler™ DNA Ladder Mix	Fermentas
6X Loading Dye Solution	Fermentas
PageRuler™ Prestained Protein Ladder	Fermentas
DNA Extract Kit (PureExtreme)	Fermentas
MiniElute Gel Extract Kit	Qiagen
Plasmid Midi Kit	Qiagen
MiniElute PCR Purification Kit	Qiagen
MiniElute Reaction Clean up Kit	Qiagen
GeneJet™ Plasmid Miniprep Kit	Fermentas
QuikChange Multi Site-Directed Mutagenesis Kit	Stratagene
DNA Ligation Kit	Fermentas
BigDye Terminator v1.1 Cycle Sequencing Kit	Applied Biosystems
FastStart PCR Master Mix	Roche

2 MATERIALS AND METHODS

2.1.3 Enzymes

The restriction enzymes used for molecular biology analyses and the corresponding buffer systems were obtained from Fermentas or New England Biolabs. Enzymes obtained from other companies are indicated.

Benzonase	Merck
Lysozyme	Sigma
Protease Inhibitor Cocktail Set III	Calbiochem
<i>Taq</i> DNA polymerase	Fermentas
T4 DNA Ligase	Fermentas
<i>Pfu</i> DNA polymerase	Fermentas
Schrimp Alkaline Phosphatase (SAP)	Fermentas

2.1.4 Antibodies

2.1.4.1 Primary antibodies

Specificity	Species		Dilution	Producer
Anti-His ₅	Mouse	Monoclonal	1:3000	Qiagen
Anti-His ₆	Mouse	Monoclonal, H3	1:3000	Santa Cruz
Anti-c-Myc	Mouse	Monoclonal	1:3000	Roche
Anti-c-Myc	Rabbit	Polyclonal, A-14	1:3000	Santa Cruz
Anti-HA	Mouse	Monoclonal, F-7	1:3000	Santa Cruz
Anti-Strep Tag II	Mouse	Monoclonal, 71590	1:3000	Novagen
Anti-DnaK	Rabbit	Polyclonal, AS08 350	1:10000	Acris GmbH
Anti-GroEL	Mouse	Monoclonal, 2E4	1:3000	Acris GmbH

2.1.4.2 Secondary antibodies

Specificity	Species	Dilution	Producer
Anti-mouse-IgG HRP conjugate	Mouse	1:3000	Dianova
Anti-rabbit-IgG HRP conjugate	Rabbit	1:3000	Dianova

2.2 Apparatus and equipment

Centrifuges

Centrifuge 5417R	Eppendorf
Centrifuge 5417C	Eppendorf
Centrifuge 5810R	Eppendorf
Avanti 30 Centrifuge	Beckman Coulter
Averti J-25 Centrifuge	Beckman Coulter

Autoclave, incubator and shaker

Autoclave (Varioklav)	Thermo Scientific
Autoclave (Perfect Plus)	WMF (Germany)
Shaker HT INFORS	Bottmingen
Minishaker (MS2)	Benedikt Heinemann
Shaker, WT12	Biometra
Shaker, Heidolph Polymax 1040	Benedikt Heinemann Labortechnik

Electrophoresis and Western blot apparatus

Gel Electrophoresis Apparatus	
EasyCast Minigel System	Owl Scientific
Mini Trans Blot	BioRad
Protein Minigel Apparatus	BioRad
Western Blot Apparatus	Schleicher /Schuell
Nitrocellulose Membrane, Hybond-C	Amersham Buchlar
Voltage Meter	
Power Pac 200	BioRad
Power Pac 300	BioRad
Power Pack p25	Biometra

Ultrasonicator, Frenchpress, heatblock and waterbath

Ultrasonicator, Bioruptor	Diagenode
Ultrasonic Branson Sonifier 250	Labequip
Thermomixer Compact	Eppendorf
Rotilabo – Block – Heater H250	ROTH

2 MATERIALS AND METHODS

Techne DRI – BLOCK (DB-20)	Schütt Labortechnik
Waterbath, FBC 720	Fisherbrand
Waterbath, Julabo 7A	Schütt Labortechnik
French® Pressure Cell Press	SLM Instruments, Inc.

Spectrophotometer

UV-VIS Spectrophotometer, DU® 640	Beckman Coulters
UV-VIS Spectrophotometer, UVIKON 930	Kontron Instruments

Thermocycler and apparatus for UV-detection / quantification of DNA and RNA

Mastercycler, personal	Eppendorf
Mastercycler, Gradient	Eppendorf
UNO-Thermoblock	Biometra
UV Transilluminator	Syngene
Nanophotometer	IMPLEN

Miscellaneous apparatus

DNA Sequencer	Perkin Elmer
pH Meter, WTW	InoLab
H ₂ O Distillator, USF ^{ELGA} , PURELAB Plus	MTJ
Vacupack Plus	Krups
Vortex	Bender / Hobein AG
Dryer	HERAEUS
Pipettes	Eppendorf
Precision Cells (Cuvettes)	Hellma
ÄKTA FPLC	GE Healthcare
FPLC Gradient GP-250	Pharmacia Biotech

2.3 Consumables

The FPLC matrix used for protein purification (Superdex 200™ High grade, 16/60) was purchased from GE Healthcare (Munich). Ni-NTA-agarose and Ni-NTA-sepharose matrices from Qiagen (Hilden) and GE Healthcare (Munich) respectively were used for purification of His-tagged proteins by gravity flow. Strep-Tactin

2 MATERIALS AND METHODS

sepharose (IBA) was employed for the purification of Strep-tagged proteins. For the concentration of protein-containing fractions, ultrafiltration membranes (Amicon® Ultra-15 YM10) from Millipore (Schwalbach) with MWCO of 30 kDa were used. For dialysis of protein samples, Spectral / Por membranes from Spectrum Laboratories (Canada) were utilized. Desalting of concentrated protein fractions was done using the PD-10 desalting columns (Sephadex G-25) from GE Healthcare (Munich) with MWCO of 5 kDa. For Western blot analyses, nitrocellulose membrane (0.45 µm) obtained from GE Healthcare (Munich) was used. Whatman blotting paper and Filters (12.5 cm Ø) were purchased from Macherey-Nagel (Düren).

2.4 Buffers and solutions

Molecular biology

50X TAE buffer		242 g Tris
		57.1 ml acetic acid
		100 ml 0.5 M Na ₂ EDTA
		add H ₂ O to 1 litre
Plasmid prep. buffer P1		50 mM Tris.HCl, pH 8.0
		10 mM EDTA
Plasmid prep. buffer P2		0.2 M NaOH
		1% SDS
Plasmid prep. buffer P3		2.55 M potassium acetate, pH 4.8
TFBI (100 ml)	1 ml	3 M potassium acetate, C ₂ H ₃ KO ₂
	1.2 g	rubidium chloride
	1 ml	1 M calcium chloride
	966 mg	manganese chloride
	15 ml	100% glycerol
		adjust to pH5.8 with diluted acetic acid and sterile-filter.
TFBII (100 ml):	209 mg	MOPS
	7.5 ml	1 M CaCl ₂
	120 mg	rubidium chloride
	15 ml	100% glycerol
		adjust to pH6.5 with KOH and sterile-filter.

2 MATERIALS AND METHODS

1X TE buffer	10 ml 1 M Tris, pH 8.0 2 ml 0.5 M Na ₂ EDTA, pH 8.0 add H ₂ O to 1 litre autoclave and store at room temperature
PCI (25:24:1) Breaking buffer	phenol: chloroform: isoamylalcohol (25:24:1) 2% Triton X-100 1% SDS 100 mM Tris.HCl, pH8.0 1 mM EDTA, pH8.0
PLAG solution	40% PEG 4000 0.1 M lithium acetate 10 mM Tris.HCl, pH7.5 1 mM EDTA 15% glycerol (v/v)
10X agarose gel sample buffer	Dissolve 25 mg bromophenol blue in 3.3 ml 150 mM Tris pH 7.6 Add 6 ml glycerol and 0.7 ml H ₂ O Store at room temperature.

Protein biochemistry

5X SDS-PAGE sample buffer	0.25 M Tris.HCl, pH8.0 25% glycerol 7.5% SDS 0.25mg/ml bromophenol blue 12.5% v/v β-mercaptoethanol
Separating gel buffer	18.2 g Tris 0.4 g SDS adjust pH to 8.8 and add H ₂ O to 100 ml
Stacking gel buffer	6.1 g Tris 0.4 g SDS adjust pH to 6.8 and add H ₂ O to 100 ml
10X SDS-PAGE running buffer	30.3 g Tris 144.1 g glycine 10 g SDS

2 MATERIALS AND METHODS

	Add H ₂ O to 1 litre
SDS-separating gel (12%) (Two gels)	3.49 ml acrylamide (30%) 2.15 ml H ₂ O 4.14 ml separating gel buffer 50 µl 10% APS 10 µl TEMED
SDS-stacking gel (4%) (Two gels)	0.78 ml acrylamide (30%) 3.49 ml H ₂ O 1.13 ml collecting gel buffer 50 µl 10% APS 10 µl TEMED
Commassie reagent	1.5 g commassie brilliant blue R250 455 ml methanol 80 ml acetic acid add distilled H ₂ O to 1 litre
Destaining solution	300 ml ethanol (96%) 100 ml acetic acid add distilled H ₂ O to 1 litre
Gel dry solution	50 ml ethanol (96%) 5 ml glycerol (100%) add distilled H ₂ O to 250 ml
B60 buffer	50 mM Hepes-KOH, pH 7.3 60 mM potassium acetate 5 mM magnesium acetate 1% Triton X-100 10% glycerol 1 mM NaF 20 mM glycerophosphate 1 mM DTT Complete protease inhibitor cocktail (Roche)
Buffer W	100 mM Tris.HCl, 150 mM NaCl, pH8.0

2 MATERIALS AND METHODS

Western Blot

10X Transfer buffer	144.1 g glycine 30.3 g Tris 20% methanol add distilled H ₂ O to 1 litre
Blocking buffer	5% milk powder in PBST buffer
1X PBS buffer	8 g NaCl 0.2 g KH ₂ PO ₄ 2.72 g Na ₂ HPO ₄ adjust pH to 7.2 - 7.4 and add H ₂ O to 1 litre.
PBST buffer	1X PBS buffer + 0.3% Tween 20

Protein purification

His-tagged fusion proteins

Lysis buffer	50 mM NaH ₂ PO ₄ 300 mM NaCl 10 mM imidazole, pH 8.0
Wash buffer	50 mM NaH ₂ PO ₄ 300 mM NaCl 20 mM imidazole, pH8.0
Elution buffer	50 mM NaH ₂ PO ₄ 300 mM NaCl 250 mM imidazole, pH8.0

For purification of His-tagged fusion proteins from inclusion body preparations under denaturing conditions, all buffers were supplemented with 8M urea.

Strep-tagged fusion proteins

Lysis buffer	100 mM Tris.HCl 150 mM NaCl, pH 8.0
Wash buffer	100 mM Tris.HCl 150 mM NaCl, pH 8.0
Elution buffer	100 mM Tris.HCl 150 mM NaCl 2.5 mM Desthiobiotin, pH 8.0

2 MATERIALS AND METHODS

As recommended by IBA GmbH, 1 mM EDTA was omitted in all three buffers to prevent chelation of the [Fe-S] cluster(s) in native proteins.

2.5 Anaerobic methods

2.5.1 Anaerobic buffers and solutions

All buffers and solutions were prepared using distilled H₂O. For protein purification under strictly anaerobic conditions, buffers were flushed several times with N₂ gas. To remove every trace of O₂, buffers were stirred overnight in an anaerobic chamber under the N₂/H₂-Atmosphere (95% / 5%, v/v). Before the buffers were used for protein purification, they were supplemented with freshly prepared sodium dithionite as reducing agent to a final concentration of 1 mM. The main buffers used were 50 mM Tris.HCl, pH8.0 and 50 mM sodium phosphate buffer, pH8.0. The composition of each buffer will be stated in the respective method section.

2.5.2 Anaerobic chamber and gases

Most of the experiments carried out under strictly anaerobic conditions were done in an anaerobic chamber (Coy Laboratory Products, Ann Arbor, Michigan, USA). The anaerobic chamber is composed of an N₂/H₂ atmosphere (95% / 5%, v/v). Traces of oxygen (O₂) gas were continuously removed via reduction with H₂ in a Palladium catalyst (BASF, Ludwigshafen). In addition, an alkaline solution of pyrogallol was also used as an O₂ indicator. The presence of O₂ can be observed by an irreversible colour change. The pyrogallol solution was changed frequently so as to keep the O₂ concentration in the anaerobic chamber at 0%. Hydrogen-Nitrogen mixture (H₂/N₂, 95:5), N₂ (99.996%), H₂ (99.9995%) and CO (99.997%) were purchased from Messer-Griesheim (Siegen). All the gases and gas mixtures used were of the quality grade 5.0. Apparatus and buffers used in the anaerobic chamber were made O₂-free by subjection to vacuum and N₂/H₂ (95% / 5%, v/v) for three times in an outer chamber before introduction into the anaerobic chamber. Before use, all reagents and apparatus were first equilibrated overnight in the O₂-free atmosphere of the anaerobic chamber.

2 MATERIALS AND METHODS

2.6 Microbiological methods

2.6.1 Bacterial strains and media

2.6.1.1 Bacterial cloning and protein expression strains

The *E.coli* strains used for cloning were DH5 α , XL1 Blue and XL10 Gold. For plasmid amplification and transformation of ligation cocktails, DH5 α (Life Technologies) was mostly used. DH5 α , XL1 Blue and XL10 Gold *E.coli* cloning strains are convenient hosts for initial cloning of target DNA into vectors and for maintaining plasmids since they are *recA*⁻ *endA*⁻. They possess high transformation efficiencies and produce high quality plasmid DNAs. All *E. coli* strains used for cloning and protein expression are listed in Table 2.0

Table 2.0 | *Escherichia coli* cloning and expression strains

Strain	Genotype	Reference
DH5 α	<i>supE44</i> Δ <i>lacU169</i> (Φ 80 <i>dlacZ</i> Δ M15) <i>hsdR17 recA1 endA1 gyrA96 thi-1 relA1</i>	Hanahan 1983
BL21(DE3)	F ⁻ <i>dcm ompT hsdS_B(r_B⁻ m_B⁻) gal λ(DE3)</i>	Studier & Moffatt 1986
XL1 Blue	<i>recA1 endA1 gyrA96 thi-1 hsdR17 supE44</i> <i>relA1 lac [F'proAB lac^fZΔM15 Tn10 (Tet^R)]</i>	Stratagene
MC4100	F ⁻ <i>araD139 Δ(argF-lac)U169 rspL150(Str')</i> <i>relA1 flbB5301 fruA25 deoC1 ptsF25 rbsR</i>	Casadaban 1976
XL10-Gold (Ultracompetent)	Tet ^R Δ (<i>mcrA</i>)183 Δ (<i>mcrCB-hsdSMR-</i> <i>mrr</i>)173 <i>endA1 supE44 thi-1 recA1 gyrA96</i> <i>relA1 lac Hte [F' proAB lac^fZΔM15 Tn 10</i> <i>(Tet^R) Amy Cam^R]</i>	Stratagene
Rosetta™	F ⁻ <i>ompT hsdS_B(r_B⁻ m_B⁻)gal dcm</i> pRARE (Cm ^R)	Novagene

For purposes of protein expression, the BL21(DE3), Rosetta™ (Novagen) and MC4100 were used. The *E. coli* BL21(DE3) host is a lysogen of bacteriophage DE3 and contains a DNA fragment possessing the *lacI* gene, the *lacUV5* promoter and the gene for T7 RNA polymerase (Novy *et al.*, 2001; Studier & Moffatt 1986) inducible by

2 MATERIALS AND METHODS

IPTG. Another advantage of the *E.coli* expression strains is that they lack *lon* and the *ompT* outer membrane proteases that are capable of degrading proteins during purification (Grodberg & Dunn 1988) and also suitable for expression of non-toxin genes. The MC4100 strain lacks the *araD* gene involved in the degradation of L-arabinose and possesses an arabinose sensitive phenotype (Casadaban 1976).

2.6.1.2 Bacterial growth and culture media

The bacterial strains used for this study were grown at 37°C. The composition of the Luria Bertani (LB) medium (Miller 1987) used for bacterial growth and culture preparation is shown below:

Luria Bertani (LB) medium:	1% Tryptone 0.5% Yeast extract 0.5% NaCl
Luria Bertani (LB) agar medium:	LB medium + 2% Agar-agar
SOB medium:	2% Tryptone 0.5% Yeast extract 10 mM NaCl 2.5 mM KCl 10 mM MgCl ₂ 10 mM MgSO ₄

For the selection of bacterial strains containing plasmids with Amp^R, LB medium is supplemented with ampicillin to a final concentration of 100 µg/ml. The ampicillin is added to the LB medium after the medium is autoclaved and allowed to cool to 50°C. Stock solution of ampicillin is prepared by dissolving 100 mg/ml ampicillin in 50% ethanol, sterile-filtered and stored at -20°C. Other antibiotics are added to LB medium to a final concentration as indicated in brackets; chloramphenicol (34 µg/ml); tetracycline (12.5 µg/ml). Chloramphenicol and tetracycline stock solutions like for ampicillin were prepared in 50% ethanol and stored at -20°C until use.

IPTG: Stock solution of 1 M isopropyl β-D-1-thiogalactopyranoside (IPTG) is dissolved in H₂O and sterile-filtered. For induction of bacteria-containing

2 MATERIALS AND METHODS

plasmids, a final concentration of 0.1 mM IPTG is added to the bacterial growth medium

X-Gal: For induction of plasmids containing the *lacZ* gene controlled by the *lac* promoter, 5-bromo-4-chloro-3-indolyl- β -D-galactopyranoside (X-Gal) is added to bacterial agar plates to a final concentration of 40 μ g/ml. X-Gal was dissolved in DMF before addition to media.

2.6.1.3 Storage and collection of bacterial strains

The bacteria strains were stored for longer periods of time as glycerol stocks. Glycerol stocks were prepared by addition of 700 μ l of overnight bacterial culture to 300 μ l of 50% autoclaved glycerol solution to give a final concentration of 15% glycerol (v/v). Glycerol stocks were stored at -80°C until use.

2.7 Oligonucleotide primers

The oligonucleotide primers required for amplification of DNA via PCR, DNA sequencing and mutagenesis reactions were ordered from MWG Biotech (now Operon Biotech). The oligonucleotide primers are listed in Table 2.1

Table 2.1 | Overview of oligonucleotide primers utilized

a) Sequencing primers

Name of primer	Sequence (5' – 3')
ScElp3_Seq1	GACCCGTTTAGAGGCCCAAG
ScElp3_Seq2	GACCCGTTTAGAGGCCCAAG
ScElp3_Seq3	AGAGGACACACCGTTAGGTC
ScElp3_Seq4	CCGATCTTCCCATCGGTGATG
ScElp3_Seq5	TGTTCTGATGGGTGGTACATT
ScElp3_Seq6	AGATTTTCAACCCATCAGTCC
ScElp3_Seq7	CAACAACCAAGGTTAACCGATA
TDH_FW	CTGAAATTATCCCCTACTTGACT
TDH_RV	TGGTTGAACTTTATGATGCACT
CYC_FW	AATATTTGTGTTTATTGTCCAGGTG
CYC_RV	TCAAGCAAGGTTTTTCAGTATAATGTT
MET25_FW	CATAATAACCGAAGTGTCGAAAA

2 MATERIALS AND METHODS

b) Mutagenesis primers

Name of Primer	Sequence (5' – 3')
ScRSAM_Mut1	ACC TGT ATA TGC AAT GTG AGG AGC ACG ATG TGG TTT ACA CAT AAC
ScRSAM_Mut2	CTG GAC CAC CTG GAC AAT AAA CAG CAA TAT TAC CTG TAT ATG CAA TGT G
ScRSAM_Mut3	CTG AAT CTG GAC CAC CTG GAG CAT AAA CAC AAA TAT TAC CTG
ScRSAM_Mut4	CTG AAT CTG GAC CAC CTG GAG CAT AAA CAG CAA TAT TAC CTG
ScRSAM_Mut5	GTA TCG TGA GCA TCC TCT CTC GTT TCA TCG GTA TCA TTA C
ScRSAM_Mut6	GCC TAG TTT CGA TTG TTA TAC CAA CAG CCT TCG TTA AAC TTT GTT GCG
ScRSAM_Mut7	GTC CAA ATG TGT TTG CGT AGC ATA ATC AGG CCT AGT TTC GAT TG
ScRSAM_Mut8	GGA CTG AAC ACC AAT TTC TAA TCT GGT AGC GCC ATA TTT TAA CAT ATC GTC C
ScRSAM_Mut9	TT TAG ACA CAG CAA AAG TTT CAG CAA CAG CC TAA CGG TGT GTC C
ScGlyRadMot	CTT ACA CCA ACA GCA GAA ATA ACA GAA ATT TTC TCT GAA CCA TGC TCT TCC TTG GCG
ScGlyRadMot1	GAT CCA GTT CGA TGT AAC CCA CTC GTG CAC CCA ACT GAT CTT
ScGlyRadMot2	GGA CCG TCT AGT TCA TAT CCT AGT TTA GCA TAG TAA TTT CTT ACA CCA ACA CCA G
ScGlyRadMot3	GGA CCG TCT AGT TCA TAT GCT AGT TTA CCA TAG TAA TTT CTT ACA CCA ACA CCA G

2 MATERIALS AND METHODS

c) Cloning primers for hexahistidine (*His₆*) – fusion proteins

Name of Primer	Sequence (5' – 3')*
At(76-366)_NcoI_FW	T <u>ACCATGGAGCT</u> CGTGGAGATGATTGCT
At(76-366)_XhoI_RV	TACTCGAGCACAAGCTGCTCAGGTGGATAA
At(111-366)_NcoI_FW	AT <u>CCATGGCGAAGCCT</u> CATAGGTG
At(111-366)_XhoI_RV	TACTCGAGCACAAGCTGCTCAGGTGGATAA
ScWT_HindIII_FW	CATAAGCTTATGGCTCGTCATGGAAAAGGC
ScWT_XhoI_RV	CTACTCGAGAATTCTTTTCGACATGTATGGACCG

*The restriction sites used in the PCR cloning primers are underlined. The nucleotides leading to amino-acid substitution in the mutagenesis primers are marked in bold.

d) *Saccharomyces cerevisiae* ELP3 knock-out and PCR amplification primers

Name	Sequence 5' – 3'
KO-ELP3-SAM FW	TTA TTA CCC AAA TTG AAG GCT AAG CCA GTA AGA ACA GCA TCG GGT ATT GCC GAC GGC CAG TGA ATT CCC GG
KO-ELP3-SAM RV	AAA CCT GTA CCC CTA ATG ACT AAA GTT GGA TAG ATT TTC AAC CCA TCA GTA GCT TGG CTG CAG GTC GAC GG
KO-ELP3-G534A-FW-1	GCA CTT TCT GGG TTC AAT GGT AAT GAT ATT GAT GAA GCT ATT CTT TAT TCG CGA CGG CCA GTG AAT TCC C
KO-ELP3-G534A-RV	GGA CCG TCT AGT TCA TAT CCT AGT TTA CCA TAG TAA TTT CTT ACA CCA ACA GCT TGG CTG CAG GTC GAC G
ORF-ELP3-SAM FW	CTA AAG CAA CAA CCA AGG TTA ACC G
ORF-ELP3-SAM-RV	TTC TAG CAA CTA AGT CCA CTA AGG C
TDH_RV	TGGTTGAAC TTTATGATGCACT

2 MATERIALS AND METHODS

e) *Saccharomyces cerevisiae* ELP3-(c-myc)₃ and ELP3 cloning primers

Name	Sequence 5' – 3'
p424TDH-FW	GGGTATCCAAGAAGTGCATCA
p424TDH-3myc-RV	AT <u>CTCGAG</u> CTAGACTCTAGATGATCCGT ^a
p424TDH-Stop-RV	AT <u>CTCGAG</u> CTAAATTCTTTTCGACATGTATG ^a

^aThe restriction sites used in the PCR cloning primers are underlined.

2.8 Molecular biology methods

2.8.1 Agarose gel electrophoresis

Agarose gel electrophoresis was used to check restriction cocktails, plasmid preparations as well as for the preparative isolation of DNA fragments. The gels were prepared from 0.8% agarose (w/v) in 1X TAE buffer and dissolved by heating briefly in a microwave. When the agarose is dissolved, the gel is supplemented with 0.25 µg/ml ethidium bromide. The DNA probe is loaded into gel in 1X sample loading buffer. The 1 kbp GeneRuler Ladder Mix (Fermentas) is used as a length reference marker. The gel was run for 1 hour at 80 volts with 1X TAE buffer. The analysis of the DNA bands is done under a UV lamp. For preparative isolation of DNA fragment, the corresponding band is excised from the gel and purified using the MiniElute Gel Extraction Kit (Qiagen).

2.8.2 Preparation of competent bacterial cells by chemical method

An overnight bacterial culture (1.25 ml) was used to inoculate 250 ml LB or SOB medium to an OD_{600nm} of 0.1. The culture incubated at 37°C until OD_{600nm} of 0.6 - 0.7 was reached. Then the culture was cooled on ice and centrifuged at 4°C for 5 minutes at 3000 rpm. The pellet was resuspended in 0.2 vol (50 ml) of ice-cold TFBI solution followed by incubation on ice for 5 minutes. Afterwards, the culture was centrifuged again at 4°C for 5 minutes at 3000 rpm. The pellet obtained was then resuspended in 0.04 vol (10 ml) of ice-cold TFBII solution, followed by incubation on ice for 30 minutes. Aliquots of 150 µl were frozen in liquid N₂ and stored until use at -80°C.

2.8.2.1 Transformation of competent cells

The competent bacterial cells were incubated on ice with 50-100 ng DNA for about 20 minutes with regular vortexing. Then the cells were heat-shocked for 45 seconds at 37°C and then cooled on ice. This heat shock procedure at 37°C was applied only to DH5α cells. Other *E. coli* strains were heat-shocked for 2 minutes at 42°C. 1 ml LB medium was added to the heat-shocked cells, followed by incubation at 37°C for 1 hour. Centrifugation followed at 7000 rpm for 5 minutes and the cells were then resuspended in 100 µl LB medium and plated on agar plates containing the appropriate antibiotic needed for selection.

2.8.3 Isolation of plasmid DNA

For the preparation of plasmid DNA, the GeneJet (Fermentas) Miniprep kit was used. The plasmid DNA was isolated via alkaline lysis procedure and purified by anion-exchange chromatography according to the specifications of the manufacturer. The plasmid DNA bound to the spin column is eluted with 50 µl elution buffer. Higher quantities of plasmid DNA are isolated with the Qiagen plasmid Midi kit according to the specifications of the manufacturer using 150 ml overnight culture. Elution is done with 500 µl of autoclaved distilled H₂O or 1X TE buffer.

2.8.3.1 Determination of plasmid DNA concentration

Reliable measurement of DNA concentration is important for many applications in molecular biology. DNA quantitation was generally performed by spectrophotometric measurement of the absorption at 260 nm using the Nanophotometer (IMPLEN), or by agarose gel analysis. Only OD_{260nm} values between 0.1 and 1.0 were reliable enough to be used for DNA quantitation. 1 unit of A₂₆₀ in a 1 ml detection path corresponds to 50 µg/ml dsDNA, 33 µg/ml ssDNA, 40 µg/ml RNA and 20-30 µg/ml oligonucleotides. The ratio of A₂₆₀/A₂₈₀ of a DNA probe should be in the range between 1.80-1.95. Higher ratio above 2.0 indicates denatured DNA or RNA contamination, while lower ratio points to protein or phenol contamination.

2 MATERIALS AND METHODS

2.8.3.2 DNA purification from enzymatic reactions

For the purification of DNA from enzymatic reactions, the reactions were stopped by enzyme deactivation at 65°C for 15 minutes, followed by desalting and removal of enzymes used in previous reactions. For this process, the Qiagen MiniElute PCR purification Kit is used following the specification of the manufacturer. The DNA bound on the spin column is eluted with 6-10 µl elution buffer.

2.8.3.3 Isolation of DNA from agarose gel

Extraction of DNA up to 4 kbp from agarose gel was done with the aid of the MiniElute Gel Extraction Kit (Qiagen). For DNA fragments larger than 4 kbp, the DNA Extraction Kit (PureExtreme) from Fermentas was utilized. The elution of DNA from the spin columns was done using 10-20 µl of the elution buffer as specified by the manufacturers.

2.9 Mutagenesis

The QuikChange multi site-directed mutagenesis kit (Stratagene) was used for mutagenesis experiments. For codon or exchange of amino acids in the ScE1p3 protein, mutagenesis primers (Table 2.1b) were designed in such a way that a change in one or more nucleotides resulted in the required amino acid substitution. The methodology involves the usage of thermal cycling procedure to achieve multiple rounds of mutant strand synthesis. Components of the thermal cycling reaction include 100 ng of supercoiled dsDNA template, two synthetic oligonucleotide primers (7,6 pmol each) containing the desired mutations, dNTP mix and the kit-provided enzyme blend featuring the high fidelity *PfuTurbo* DNA polymerase. The reaction cocktail was properly mixed and centrifuged shortly. The mutagenesis reaction was done in a thermocycler using the following conditions:

1. 95°C for 1 minute (Initial denaturation)
2. 95°C for 1 minute (Denaturation)
3. 55°C for 1 minute (Primer annealing)
4. 65°C for 2 minutes / kb plasmid (Primer extension)

2 MATERIALS AND METHODS

5. Repeat steps 2-4 for 30 cycles
6. Hold at 10°C

After cooling of the thermal cycling reaction product, it was treated with 1 µl of the restriction endonuclease *DpnI* for 1 hour at 37°C. The *DpnI* endonuclease (target sequence: 5'-Gm⁶ATC-3') is specific for hemimethylated and methylated DNA (Nelson & McClelland 1992) and was used to digest the parental DNA template. DNAs isolated from almost all *E. coli* strains are dam methylated and hence susceptible to *DpnI* digestion. After *DpnI* digestion, 1.5 µl of the reaction mix was then transformed into XL-10 Gold Ultracompetent cells (Stratagene), where the mutant closed circle ssDNA is converted into duplex form *in vivo*. The plasmid was isolated from transformants and the mutation confirmed by plasmid DNA sequencing using sequencing primers (Table 2.1a). Average efficiency for obtaining mutated products was always greater than 50%

2.10 Polymerase chain reaction (PCR)

For high-fidelity PCR amplification of plasmid or genomic DNA, the *Pfu* DNA polymerase (Lundberg *et al.*, 1991) was used. In a 50 µl reaction mixture, 50-100 ng of DNA was added to a PCR tube containing 200 µM dNTPs, 1X polymerase buffer (with MgSO₄), 0.4 µM upstream and downstream primers respectively and 1.25 units of *Pfu* DNA polymerase. The PCR cocktail was mixed thoroughly and amplified using the following conditions:

1. 95°C for 4 minutes (Initial denaturation)
2. 95°C for 30 seconds (Denaturation)
3. 58°C for 30 seconds (Primer annealing)
4. 72°C for 2 minutes (Primer extension)
5. Repeat steps 2-4 for 35 cycles
6. 72°C for 10 minutes
7. Hold at 10°C

The amplified PCR product was analyzed using a preparative agarose gel electrophoresis and the amplified fragments excised if necessary and purified using

2 MATERIALS AND METHODS

the MiniElute Gel extraction Kit (Qiagen). Colony PCR was often used to confirm successful cloning experiments. Oligonucleotide primers (0.4 μ M each) were designed to hybridize upstream and downstream of the cloned fragment. For such error-prone PCR analysis, the FastStart PCR Master Mix (Roche) was basically used in a 20 μ l reaction mix featuring a tiny resuspended colony. After PCR amplification, the PCR products were analyzed by agarose gel electrophoresis to check for colonies bearing the corresponding PCR fragment. The colonies exhibiting positive signals were inoculated in growth medium and the cultures then used for plasmid isolation and DNA sequencing

2.11 DNA sequencing

The sequencing was done according to the dideoxy chain termination method (Sanger *et al.*, 1977) and the analyses of the results were performed using the chromas software obtained from <http://www.technelysium.com.au/chromas14x.html>. The sequencing of plasmid DNA or PCR products was carried out using the BigDye Terminator v1.1 Cycle Sequencing Kit (Applied Biosystems). The sequencing reaction in 20 μ l cocktail was composed of 2 μ l of 10X BigDye Buffer, 2 μ l of BigDye Termination Mix, 1.6 μ l down- and upstream primers (2 μ M each) and 100-200 ng DNA. The DNA sequencing was then performed in a Mastercycler (Eppendorf) with the following cycling conditions:

1. 95°C for 1 minutes (Initial denaturation)
2. 95°C for 30 seconds (Denaturation)
3. 50°C for 15 seconds (Primer annealing)
4. 60°C for 4 minutes (Primer extension)
5. Repeat steps 2-4 for 30 cycles
6. Hold at 10°C

At the end of the sequencing reaction, the probes were purified and precipitated. For purification and precipitation of the sequencing cocktails, the 20 μ l probes were made up to 100 μ l with autoclaved distilled H₂O and supplemented with 10% 3 M NaOAc, pH 4.8 and 3 vol (300 μ l) ice-cold 96% ethanol. The mixture was then centrifuged at 4°C for 20 minutes at 14000 rpm. Afterwards, the pellet was resuspended and

2 MATERIALS AND METHODS

washed 2X with 3 vol (300 µl) 70% ethanol. At the end, the pellet was dried and forwarded for sequencing at the sequencing unit of the Institute for Biology (Genetics section) at the Martin-Luther-University, Halle-Wittenberg.

2.12 Bacterial and yeast shuttle plasmids

The plasmids used for the intracellular expression of wild type and truncated forms of AtElp3 as well as the wild type and mutant versions of ScElp3 and yeast shuttle plasmids used for characterization studies in yeast are illustrated in Table 2.2.

Table 2.2 | Summary of yeast shuttle plasmids and bacterial fusion protein expression plasmids

Plasmid	Description	Reference
pET-21b	Amp ^R , C-term. His ₆	Novagen
pET-52b	Amp ^R , C-term. His ₆ , N-term. Strep	Novagen
pASK-43	Amp ^R , N-term. His ₆ , C-term. Strep	IBA
pBAD-TatB	Amp ^R , <i>E. coli</i> TATB ligated with pBAD	Invitrogen; AG Brüser
pGroEL	Cm ^R	Aguilar-Netz
pRKISC	Tet ^R	Nakamura <i>et al.</i> , 1999
pEAG80	<i>K.lactis</i> multicopy plasmid with <i>KIGAL80</i> , <i>ADH1</i> promoter, Amp ^R , <i>URA3</i>	Wrackmeyer 2005
pAIV	pEAG80 x <i>EcoRI</i> and relegation of 6098bp fragment. Amp ^R , <i>URA3</i> , and <i>ADH1</i> promoter, <i>TEF</i> terminator.	Wrackmeyer 2005
pAIV2	Ligation of pAIV x <i>Sall</i> with <i>AtELP3</i> -PCR fragment (1,7kbp), generated from <i>Pfu</i> -PCR on RAFL08-11-J12 with <i>Sall</i> restriction site amplified with primers cDNAfw and cDNA2re, Amp ^R	Mehlgarten <i>et al.</i> , 2010
YDp-KIU	Amp ^R pUC9Q derivative, <i>K. lactis</i> <i>URA3</i>	Jablonowski <i>et al.</i> , 2001a
pCR-2.1-TOPO	Amp ^R Kan ^R f1ori <i>plac lacZα</i> pMB1ori	Invitrogen
pFF7	pCR-2.1-TOPO derivative plus blunt end PCR ORF from <i>ELP3</i> , Amp ^R	Frohloff 2005
pLF16	YCplac111 (<i>ARS1/CEN4/LEU2</i> , Amp) carrying <i>GAL1::k1ORF4</i> (γ -toxin gene)	Fichtner 2000

2 MATERIALS AND METHODS

YCplac111	YCp cloning vector, <i>ARS1/CEN4/LEU2</i> , Amp ^R , pMB1ori	Gietz & Sugino 1988
pJET12	<i>ELP1-HA::YCplac111</i> , <i>ARS1/CEN4/LEU2</i> , Amp ^R ,	Täubert 2007
pCM24	KTI12-(myc) ₃ ::YCplac33, <i>ARS1/CEN4/URA3</i> , Amp ^R ,	Mehlgarten 2009
p424TDH	Amp ^R <i>ARS1/CEN4 TRP1 CYC1 ter TDH3</i> promoter	Mumberg <i>et al.</i> , 1995
p416-MET25	Amp ^R <i>ARS1/CEN4 URA3 CYC1 ter MET25</i> promoter	Mumberg <i>et al.</i> , 1994
pBluescript II SK(+)	Amp ^R , <i>lacZ'</i> , pUC ori, f1 ori, <i>lac</i> promoter	Stratagene
pBSK- <i>ELP3TM</i>	Ligation of pBluescript II SK(+) <i>EcoRI/SalI</i> restriction fragment with pON15 x <i>EcoRI/SalI</i> fragment	This study
pON-ELO3-1	<i>AtELP3</i> ORF from pAIV2 x <i>SalI</i> in pET-21b x <i>SalI</i> (C-term. His ₆ , Amp)	This study
pON-ELO3-2	<i>AtELP3</i> ORF from pAIV2 x <i>SalI</i> in pET-52b x <i>SalI</i> (N-term. Strp, C-term. His ₁₀ , Amp)	This study
pON-ELO3-3	pON-ELO3-1 x <i>SalI/XhoI</i> ligated with pASK-43 x <i>SalI</i> (N-term. His ₆ , C-term. Strp, Amp)	This study
pON-ELP3-1	<i>ELP3</i> ORF amplified by <i>Pfu</i> -PCR using pFF7 as template. Ligation of PCR fragment x <i>HindIII/XhoI</i> with pET-21b x <i>HindIII/XhoI</i>	This study
pON-ELP3-2	pON-ELP3-1 x <i>SalI/XhoI</i> religated with pASK-43 x <i>XhoI</i> (N-term. His ₆ , C-term. Strp, Amp ^R)	This study
pON1	pON-ELO3-1 with truncated <i>AtELP3</i> allele (76-366) amplified from pAIV2 using primers, <i>At(76-366)_NcoI_FW</i> and <i>At(76-366)_XhoI_RV</i> . Restricted with <i>NcoI/XhoI</i> and ligated to pBAD x <i>NcoI/XhoI</i> fragment	This study

2 MATERIALS AND METHODS

pON2	pON-ELP3-1 with truncated <i>AtELP3</i> allele (111-366) amplified from pAIV2 using primers, At(111-366)_ <i>NcoI</i> _FW and At(111-366)_ <i>XhoI</i> _RV. Restricted with <i>NcoI/XhoI</i> and ligated to pBAD x <i>NcoI/XhoI</i> fragment	This study
pON3	pON-ELP3-1 with <i>ELP3</i> allele (C108A) mutated with ScRSAM_Mut1 and ScRSAM_Mut5 primers	This study
pON4	pON-ELP3-1 with <i>ELP3</i> allele (C118A) mutated with ScRSAM_Mut2 and ScRSAM_Mut5 primers	This study
pON5	pON-ELP3-1 with <i>ELP3</i> allele (C121A) mutated with ScRSAM_Mut3 and ScRSAM_Mut5 primers	This study
pON6	pON-ELP3-1 with <i>ELP3</i> allele (C224A) mutated with ScRSAM_Mut5 and ScRSAM_Mut6 primers	This study
pON7	pON-ELP3-1 with <i>ELP3</i> allele (C236A) mutated with ScRSAM_Mut5 and ScRSAM_Mut7 primers	This study
pON8	pON-ELP3-1 with <i>ELP3</i> allele (C249A) mutated with ScRSAM_Mut5 and ScRSAM_Mut8 primers	This study
pON9	pON-ELP3-1 with <i>ELP3</i> allele (C277A) mutated with ScRSAM_Mut5 and ScRSAM_Mut9 primers	This study
pON10	pON-ELP3-1 with <i>ELP3</i> allele (C108A, C118A) mutated with ScRSAM_Mut2 and ScRSAM_Mut5 primers using pON3 as template	This study
pON11	pON-ELP3-1 with <i>ELP3</i> allele (C108A, C121A) mutated with ScRSAM_Mut3 and ScRSAM_Mut5 primers using pON3 as template	This study
pON12	pON-ELP3-1 with <i>ELP3</i> allele (C118A, This study	This study

2 MATERIALS AND METHODS

	C121A) mutated with ScRSAM_Mut3 and ScRSAM_Mut5 primers using pON4 as template	
pON13	pON-ELP3-1 with <i>ELP3</i> allele (C108A, C224A) mutated with ScRSAM_Mut5 and ScRSAM_Mut6 primers using pON3 as template	This study
pON14	pON-ELP3-1 with <i>ELP3</i> allele (C224A, C236A) mutated with ScRSAM_Mut5 and ScRSAM_Mut7 primers using pON6 as template	This study
pON14a	pON-ELP3-1 with <i>ELP3</i> allele (C224A, C249A) mutated with ScRSAM_Mut5 and ScRSAM_Mut8 primers using pON6 as template	This study
pON14b	pON-ELP3-1 with <i>ELP3</i> allele (C224A, C277A) mutated with ScRSAM_Mut5 and ScRSAM_Mut9 primers using pON6 as template	This study
pON14c	pON-ELP3-1 with <i>ELP3</i> allele (C236A, C249A) mutated with ScRSAM_Mut5 and ScRSAM_Mut8 primers using pON7 as template	This study
pON14d	pON-ELP3-1 with <i>ELP3</i> allele (C236A, C277A) mutated with ScRSAM_Mut5 and ScRSAM_Mut9 primers using pON7 as template	This study
pON14e	pON-ELP3-1 with <i>ELP3</i> allele (C249A, C277) mutated with ScRSAM_Mut5 and ScRSAM_Mut9 primers using pON8 as template	This study
pON15	pON-ELP3-1 with <i>ELP3</i> allele (C108A, C118A, C121A) mutated with ScRSAM_Mut4 and ScRSAM_Mut5 primers using pON3 as template	This study
pON16	pON-ELP3-1 with <i>ELP3</i> allele (C108A, C118A, C121A) mutated with ScRSAM_Mut4 and ScRSAM_Mut5 primers using pON3 as template	This study

2 MATERIALS AND METHODS

	C118A, C121A, C224A) mutated with ScRSAM_Mut5 and ScRSAM_Mut6 primers using pON15 as template	
pON17	pON-ELP3-1 with <i>elp3</i> allele (C108A, C118A, C121A, C224A, C236A) mutated with ScRSAM_Mut5 and ScRSAM_Mut7 primers using pON16 as template	This study
pON18	pON3 restricted with <i>XhoI/SalI</i> and religated with pASK-43 x <i>XhoI</i>	This study
pON19	pON4 restricted with <i>XhoI/SalI</i> and religated with pASK-43 x <i>XhoI</i>	This study
pON20	pON5 restricted with <i>XhoI/SalI</i> and religated with pASK-43 x <i>XhoI</i>	This study
pON21	pON6 restricted with <i>XhoI/SalI</i> and religated with pASK-43 x <i>XhoI</i>	This study
pON22	pON7 restricted with <i>XhoI/SalI</i> and religated with pASK-43 x <i>XhoI</i>	This study
pON23	pON10 restricted with <i>XhoI/SalI</i> and religated with pASK-43 x <i>XhoI</i>	This study
pON24	pON11 restricted with <i>XhoI/SalI</i> and religated with pASK-43 x <i>XhoI</i>	This study
pON25	pON12 restricted with <i>XhoI/SalI</i> and religated with pASK-43 x <i>XhoI</i>	This study
pON26	pON13 restricted with <i>XhoI/SalI</i> and religated with pASK-43 x <i>XhoI</i>	This study
pON27	pON14 restricted with <i>XhoI/SalI</i> and religated with pASK-43 x <i>XhoI</i>	This study
pON28	pON15 restricted with <i>XhoI/SalI</i> and religated with pASK-43 x <i>XhoI</i>	This study
pON29	pON16 restricted with <i>XhoI/SalI</i> and religated with pASK-43 x <i>XhoI</i>	This study
pON30	pON17 restricted with <i>XhoI/SalI</i> and religated with pASK-43 x <i>XhoI</i>	This study
pON31	pON-ELP3-1 with <i>ELP3</i> allele (G534A) mutated with ScGlyRadMot and ScRSAM_Mut5 primers	This study

2 MATERIALS AND METHODS

pON32	pON31 restricted with <i>XhoI/SalI</i> and religated with pASK-43 x <i>XhoI</i>	This study
pON33	p424TDH x <i>XhoI</i> ligated with WT <i>ELP3</i> fragment generated by <i>XhoI/SalI</i> restriction of pON-ELP3-1 resulting in WT <i>ScELP3</i> without stop codon	This study
pON34	Ligation of pON33 x <i>EcoNI/XhoI</i> with <i>EcoNI/XhoI</i> restricted <i>ScELP3-Pfu</i> -PCR fragment amplified from FF3t using p424TDH-FW and p424TDH-3myc-RV primers to generate myc-tagged WT <i>ELP3-c(myc)₃</i>	This study
pON35	Ligation of pON33 x <i>EcoNI/XhoI</i> with <i>EcoNI/XhoI</i> restricted <i>ScELP3-Pfu</i> -PCR fragment amplified from FF3t using p424TDH-FW and p424TDH-Stop-RV primers to generate untagged WT <i>ELP3</i>	This study
pON36	pON34 with <i>ELP3-c(myc)₃-C108A</i> allele generated by pON34 x <i>NheI/NdeI</i> and ligated with pON3 x <i>NheI/NdeI</i> fragment	This study
pON37	pON34 with <i>ELP3-c(myc)₃-C118A</i> allele generated by pON34 x <i>NheI/NdeI</i> and ligated with pON4 x <i>NheI/NdeI</i> fragment	This study
pON38	pON34 with <i>ELP3-c(myc)₃-C224A</i> allele generated by pON34 x <i>NheI/NdeI</i> and ligated with pON6 x <i>NheI/NdeI</i> fragment	This study
pON39	pON34 with <i>ELP3-c(myc)₃-C236A</i> allele generated by pON34 x <i>NheI/NdeI</i> and ligated with pON7 x <i>NheI/NdeI</i> fragment	This study
pON40	pON34 with <i>ELP3-c(myc)₃-C249A</i> allele generated by pON34 x <i>NheI/NdeI</i> and ligated with pON8 x <i>NheI/NdeI</i> fragment	This study
pON41	pON34 with <i>ELP3-c(myc)₃-C277A</i> allele generated by pON34 x <i>NheI/NdeI</i> and ligated with pON9 x <i>NheI/NdeI</i> fragment	This study
pON42	pON34 with <i>ELP3-c(myc)₃-C108A-C118A</i>	This study

2 MATERIALS AND METHODS

	allele generated by pON34 x <i>NheI/NdeI</i> and ligated with pON10 x <i>NheI/NdeI</i> fragment	
pON43	pON34 with <i>ELP3-c(myc)₃-C108A-C118A-C121A</i> allele generated by pON34 x <i>NheI/NdeI</i> and ligated with pON15 x <i>NheI/NdeI</i> fragment	This study
pON44	pON34 with <i>ELP3-c(myc)₃-C108A-C118A-C121A-C224A</i> allele generated by pON34 x <i>NheI/NdeI</i> and ligated with pON16 x <i>NheI/NdeI</i> fragment	This study
pON45	pON34 with <i>ELP3-c(myc)₃-C108A-C118A-C121A-C224A-C236A</i> allele generated by pON34 x <i>NheI/NdeI</i> and ligated with pON17 x <i>NheI/NdeI</i> fragment	This study
pON46	pON34 with <i>ELP3-c(myc)₃-G534A</i> allele mutated using ScGlyRadMot and ScGlyRadMot1 primers with pON34 as template	This study
pON46a	pON34 with <i>ELP3-c(myc)₃-G542A</i> allele mutated using ScGlyRadMot1 and ScGlyRadMot2 primers with pON34 as template	This study
pON46b	pON34 with <i>ELP3-c(myc)₃-G545A</i> allele mutated using ScGlyRadMot1 and ScGlyRadMot3 primers with pON34 as template	This study
pON47	pON35 with <i>ELP3-G534A</i> allele mutated using ScGlyRadMot and ScGlyRadMot1 primers with pON35 as template	This study
pON48	pON35 with <i>ELP3-C108A</i> allele generated by ligation of pON35 x <i>NheI/NdeI</i> and pON3 x <i>NheI/NdeI</i> fragments	This study
pON49	pON35 with <i>ELP3-C118A</i> allele generated by ligation of pON35 x <i>NheI/NdeI</i> and pON4 x <i>NheI/NdeI</i> fragments	This study

2 MATERIALS AND METHODS

pON50	pON35 with <i>ELP3-C121A</i> allele generated by ligation of pON35 x <i>NheI/NdeI</i> and pON5 x <i>NheI/NdeI</i> fragments	This study
pON51	pON35 with <i>ELP3-C108A-C118A</i> allele generated by ligation of pON35 x <i>NheI/NdeI</i> and pON10 x <i>NheI/NdeI</i> fragments	This study
pON52	pON35 with <i>ELP3-C108A-C118A-C121A</i> allele generated by ligation of pON35 x <i>NheI/NdeI</i> and pON15 x <i>NheI/NdeI</i> fragments	This study
pON53	Ligation of pBluescript II SK(+) x <i>EcoRI/SalI</i> with <i>ELP3</i> fragment (1431bp) generated by <i>EcoRI/SalI</i> restriction of pON15	This study
pON54	Ligation of pBluescript II SK(+) x <i>EcoRI/SalI</i> with <i>ELP3</i> fragment (1431bp) generated by <i>EcoRI/SalI</i> restriction of pON16	This study
pON55	Ligation of pBluescript II SK(+) x <i>EcoRI/SalI</i> with <i>ELP3</i> fragment (1431bp) generated by <i>EcoRI/SalI</i> restriction of pON17	This study
pON56	P416-MET25 x <i>XhoI</i> ligated with <i>ELP3</i> fragment generated by <i>XhoI/SalI</i> restriction of pON-ELP3-1 resulting to <i>ScELP3</i> WT without stop codon	This study
pON57	Ligation of pON56 x <i>EcoNI/XhoI</i> with <i>ScELP3-Pfu-PCR</i> x <i>EcoNI/XhoI</i> restricted fragment amplified from FF3t using p424TDH-FW and p424TDH-3myc-RV primers to generate WT <i>ELP3-c(myc)₃</i>	This study
pON58	Ligation of pON56 x <i>EcoNI/XhoI</i> with <i>ScELP3-Pfu-PCR</i> x <i>EcoNI/XhoI</i> fragment amplified from FF3t using p424TDH-FW and p424TDH-Stop-RV primers	This study

2 MATERIALS AND METHODS

	to generate WT <i>ELP3</i> with stop codon	
pON59	pON57 with <i>ELP3-c(myc)₃-C108A</i> allele generated by pON57 x <i>NheI/EcoNI</i> and ligated with pON3 x <i>NheI/EcoNI</i> fragment	This study
pON60	pON57 with <i>ELP3-c(myc)₃-C224A</i> allele generated by pON57 x <i>NheI/EcoNI</i> and ligated with pON6 x <i>NheI/EcoNI</i> fragment	This study
pON61	pON57 with <i>ELP3-c(myc)₃-C236A</i> allele generated by pON57 x <i>NheI/EcoNI</i> and ligated with pON7 x <i>NheI/EcoNI</i> fragment	This study
pON62	pON57 with <i>ELP3-c(myc)₃-C224A-C236A</i> allele generated by pON57 x <i>NheI/EcoNI</i> and ligated with pON14 x <i>NheI/EcoNI</i> fragment	This study
pON63	pON57 with <i>ELP3-c(myc)₃-C108A-C118A-C121A</i> allele generated by pON57 x <i>NheI/EcoNI</i> and ligated with pON15 x <i>NheI/EcoNI</i> fragment	This study
pON64	pON58 with <i>ELP3-C108A</i> allele generated by pON58 x <i>NheI/EcoNI</i> and ligated with pON3 x <i>NheI/EcoNI</i> fragment	This study
pON65	pON58 with <i>ELP3-C224A</i> allele generated by pON58 x <i>NheI/EcoNI</i> and ligated with pON6 x <i>NheI/EcoNI</i> fragment	This study
pON66	pON58 with <i>ELP3-C224A-C236A</i> allele generated by pON58 x <i>NheI/EcoNI</i> and ligated with pON14 x <i>NheI/EcoNI</i> fragment	This study
pON67	pON58 with <i>ELP3-C108A-C118A-C121A</i> allele generated by pON58 x <i>NheI/EcoNI</i> and ligated with pON15 x <i>NheI/EcoNI</i> fragment	This study
pON68	pON-ELP3-1 with <i>ELP3</i> allele (G534A) mutated using ScGlyRadMot and ScGlyRadMot1 primers	This study
pON69	pON68 restricted with <i>XhoI/SaI</i> and religated with pASK-43 x <i>XhoI</i>	This study

2 MATERIALS AND METHODS

pON70	pON34 with <i>ELP3-c(myc)₃-C224A-C236A</i> allele generated by pON34 x <i>NheI/NdeI</i> and ligated with pON14 x <i>NheI/NdeI</i> fragment	This study
pON70a	pON34 with <i>ELP3-c(myc)₃-C224A-C249A</i> allele generated by pON34 x <i>NheI/NdeI</i> and ligated with pON14a x <i>NheI/NdeI</i> fragment	This study
pON70b	pON34 with <i>ELP3-c(myc)₃-C224A-C277A</i> allele generated by pON34 x <i>NheI/NdeI</i> and ligated with pON14b x <i>NheI/NdeI</i> fragment	This study
pON70c	pON34 with <i>ELP3-c(myc)₃-C236A-C249A</i> allele generated by pON34 x <i>NheI/NdeI</i> and ligated with pON14c x <i>NheI/NdeI</i> fragment	This study
pON70d	pON34 with <i>ELP3-c(myc)₃-C236A-C277A</i> allele generated by pON34 x <i>NheI/NdeI</i> and ligated with pON14d x <i>NheI/NdeI</i> fragment	This study
pON70e	pON34 with <i>ELP3-c(myc)₃-C249A-C277A</i> allele generated by pON34 x <i>NheI/NdeI</i> and ligated with pON14e x <i>NheI/NdeI</i> fragment	This study

The correct orientation of each insert was confirmed by restriction with appropriate enzyme and transformed into *E. coli* expression strains. The plasmids of the ScElp3 radical SAM mutated variants are listed in Table 2.2. All the above cloned fragments were confirmed by sequencing using an appropriate sequencing primer(s) listed in Table 2.1a.

2.13 Biochemical methods

2.13.1 Cell culture for bacterial protein expression

For the optimization of expression conditions, 50 ml LB medium containing appropriate antibiotic was inoculated with 1 ml overnight culture. The protein expression was conducted at 16°C, 25°C, 30°C and 37°C after induction at OD_{600nm} of 0.7 with 0-4 mM IPTG. For expression from the pASK-43 vectors, cultures were induced with 2 ng/ml anhydrotetracycline. At 2 hours interval, 1 ml aliquots were taken and centrifuged and the pellet stored at -20°C. The pellets were resuspended in 20 µl 5X sample buffer and 80 µl lysis buffer. The samples were incubated in an ultrasonic bath for 5 minutes on ice to shear the chromosomal DNA into small pieces and heated to 95°C for 10 minutes prior to SDS-PAGE. To enhance protein solubility, different growth temperatures, chaperones and osmolytes that substantially increase protein solubility (De Marco *et al.*, 2005) were used. Osmolytes such as betaine hydrochloride, benzyl alcohol and NaCl were added 30 minutes prior to induction to a final concentration of 5 mM, 10 mM and 0.5 M respectively.

2.13.2 Cell harvest and storage

For large-scale production of bacterial cells, 1 to 5 liter culture flasks were used. The LB medium was always supplemented with the appropriate antibiotics and inoculated with 3-5% overnight culture and incubated at 37°C, 170 rpm until an OD_{600nm} of 0.6-0.7 was attained. Protein expression was induced for 3 hours with either 0.1 mM IPTG or 2 ng/ml anhydrotetracycline depending on expression plasmid. Cells were harvested by centrifugation at 10000 rpm for 20 minutes at 4°C. The cell pellets were then stored at -20°C until needed.

2.13.3 Preparation of HiPIP inclusion body from *E. coli*

The preparation of HiPIP inclusion bodies from *E. coli* was conducted according to a modified method of Brüser *et al.*, (2003). 1-3 liters *E. coli* BL21(DE3) culture co-transformed with / without pGroEL plasmid in LB-Amp-Cm was grown at 37°C with high aeration (>220 rpm shaker) until OD_{600nm} of 1.0 is achieved. Induction is

2 MATERIALS AND METHODS

followed with 0.1 mM IPTG for 3 hours. Then cells were harvested by centrifugation at 8000 rpm for 15 minutes at 4°C. Cells were washed in 1/20 culture volume with cold buffer W followed by centrifugation for 20 minutes at 8000 rpm at 4°C. Cell pellet was resuspended in 30 ml of buffer W and supplemented with 0.1 mg/ml lysozyme and DNase I. The cell suspension was disrupted by 2X passage through French press (>20000 psi cell pressure). The disrupted cells were centrifuged at 15000 rpm for 20 minutes at 4°C. The supernatant was set aside for eventual SDS-PAGE and Western blot analyses. The pellet was further washed with 30ml buffer W followed by centrifugation at 15000 rpm for 20 minutes at 4°C. Thereafter, pellet was resuspended in 20 ml cold 50 mM Tris.HCl, pH8.0 containing 2 mM DTT and 8 M urea. Incubation was conducted at room temperature for 1 hour with continuous stirring. Centrifugation followed at 17000 rpm for 30 minutes at 4°C. The clear supernatant represents soluble inclusion bodies and was then stored in aliquots at -20°C until needed.

2.13.4 Purification of His₆-tagged fusion proteins

Cell pellet from 100 ml cell culture was resuspended in 2 ml lysis buffer for His₆-tagged fusion proteins and supplemented with 0.1 mg/ml lysozyme, complete protease inhibitor cocktail (Roche), 1 mg/ml lysozyme and DNase I followed by incubation on ice for 30 minutes. The cells were then disrupted by ultrasonication (5X @10 seconds intervals). After centrifugation at 4000 rpm at 4°C for 10 minutes, the supernatant was loaded on 500 µl Ni-NTA-agarose matrix (1 column volume, CV) equilibrated with 2CV using lysis buffer. The matrix was incubated on a shaker for 1 hour at 4°C to allow for effective binding of fusion proteins to matrix. Afterwards, the flow through was collected and the matrix washed 6X with 1CV of wash buffer for His₆-tagged fusion proteins. The bound proteins were eluted 6X with 0.5CV of elution buffer for His₆-tagged fusion proteins. For the purification of His₆-tagged fusion proteins under denaturing conditions, inclusion body preparations were utilized. The same procedures were used like for native purification of His₆-tagged fusion proteins, but all buffers were supplemented with 8 M urea. All samples recovered after affinity purification were analyzed by SDS-PAGE and Western blotting. For 1 litre cultures and above, 5 ml Ni-NTA-agarose matrix was used for purification of His-tagged fusion proteins.

2.13.5 Purification of Strep-tagged fusion proteins

Cell pellet obtained from 100 ml culture was resuspended in 2 ml lysis buffer. The resuspended cell was then supplemented with 0.1 mg/ml lysozyme, complete protease inhibitor cocktail (Roche), benzonase and DNase I, followed by 30 minutes incubation on ice. Cells are then disrupted at 5X @10seconds interval. The cell suspension was centrifuged at 4000 rpm for 10 minutes at 4°C. The resulting supernatant was loaded on 500 µl Strep-Tactin sepharose matrix (1CV) which has been equilibrated with 2CV of lysis buffer for Strep-tagged proteins and incubated on a shaker for 1 hour at 4°C to allow for binding of Strep-tagged fusion proteins. Flow through was collected and the matrix was washed 6X with 1CV of wash buffer. Bound proteins were thereafter eluted using 0.5CV of elution buffer. The purification probes were then analyzed by SDS-PAGE and Western blotting. For more than 1 liter cultures, 5 ml of the Strep-Tactin sepharose matrix was utilized.

2.14 *In vitro* folding and reconstitution of non-native purified proteins

The [Fe-S] clusters of most holoproteins could be reconstituted from the apoprotein forms by the use of various refolding procedures (Merchant & Dreyfuss 1998; Külzer *et al.*, 1998; Ollagnier *et al.*, 1999). The Elp3 proteins purified from inclusion body preparations under denaturing conditions were reconstituted *in vitro* using the method of Brüser *et al.*, (2003). All buffers used were flushed with N₂ gas and the process was conducted in an anaerobic chamber. For *in vitro* refolding and reconstitution experiments, 2-5 mg denatured protein obtained by affinity chromatography was initially diluted with 8 ml 50 mM Tris.HCl, pH8.0 containing 2 mM DTT and 8 M urea, followed by addition of 5 ml 50 mM Tris.HCl buffer containing 0.7 mM Ammonium Fe (III) citrate and 2 mM DTT. After 5 minutes incubation, 1 ml 50 mM Tris.HCl supplemented with 20 mM Li₂S and 2 mM DTT was added and the sample further incubated for 20 minutes. The refolded protein samples were dialysed overnight against 3 liter dialysis buffer (50 mM Tris.HCl, pH8.0, 150 mM NaCl).

2 MATERIALS AND METHODS

2.14.1 Concentration and desalting of reconstituted and dialysed proteins

The reconstituted and dialyzed protein samples were concentrated using the Amicon Ultra-4 membrane. In order to eliminate residual excess Fe and S salts used during the *in vitro* refolding and reconstitution of protein, the protein samples were desalted with 10 ml column volume (CV) of PD10 Sephadex G25 column (GE Healthcare). Before desalting, the column was first equilibrated 3X with 1CV dialysis buffer. 2.5 ml of concentrated protein samples were loaded on the desalting column. After all protein solution has adsorbed on the column, the protein was eluted using 3.5 ml dialysis buffer. The desalted protein samples were then subjected to size exclusion chromatography.

2.14.2 Purification of desalted proteins by gel filtration

The concentrated and desalted protein probes were further purified on a Superdex 200™ high grade gel filtration column (16/60) from GE Healthcare. The gel filtration column was equilibrated with 120 ml lysis buffer (50 mM Tris.HCl, pH8.0, 150 mM NaCl) flushed with N₂ gas and stored overnight in an anaerobic chamber and supplemented with freshly prepared 1 mM sodium dithionite before use in order to reduce residual O₂. After the protein probes were applied to the column, the proteins were eluted with the same buffer. The protein fraction eluted as a single peak exactly at 40 ml retention volume (peak maximum) corresponding to the AtElp3 molecular weight of 67.4 kDa. The fractions were collected in anaerobic bottles, incubated on ice and stored at 4°C until use.

2.15 Protein analytical methods

2.15.1 SDS-polyacrylamide gel electrophoresis (SDS-PAGE)

To determine the molecular weight and purity of Elp3 proteins, protein blots were prepared using polyacrylamide gel electrophoresis (PAGE) and proteins were separated under denaturing condition (Laemmli 1970). The gel electrophoresis was done using the BioRad Electrophoresis apparatus (Mini Protean II). The gels (80 mm

2 MATERIALS AND METHODS

x 65 mm x 0.75 mm) were prepared as described in section 2.4. Before protein samples were applied to the gel, they were diluted with 20% 5X sample loading buffer and heated at 95°C for 10 minutes. 10-20 µl protein probes were loaded and the SDS-PAGE ran with 1X SDS-PAGE buffer at a constant voltage of 100 volts. For protein molecular weight references, the PageRuler™ prestained protein ladder (#SM0671) from Fermentas was utilized. Thereafter, protein bands on gels were stained with the coomassie staining dye and further destained using destaining solution.

2.15.2 Western blot analysis

For Western blot analysis of proteins using specific antibodies, protein probes were ran on SDS-PAGE. The proteins on the gel were transferred to a nitrocellulose membrane using a Mini Trans Blot apparatus (Bio-Rad). The nitrocellulose membrane was first soaked in transfer buffer for 10 minutes. The Mini Trans Blot apparatus was setup to transfer gel on the nitrocellulose membrane in transfer buffer. A “transfer sandwich” was placed in a container, and then a Whatman paper, before the gel was placed on the Whatman paper. The nitrocellulose membrane was dropped on top of the gel. The blotting of the gel to the nitrocellulose membrane was done at a constant voltage of 100 volts for 1 hour. The membrane was blocked for 1 hour at room temperature and then overnight with the blocking buffer containing 1:3000 dilution of the primary antibody. The membrane was washed 3X @ 10 minutes with 1X PBST, before incubation with secondary antibody (1:3000 dilution) for 2 hours at 4°C. Then the membrane was washed again 3X 10 minutes with 1X PBST, followed by detection using the ECL reagent (GE Healthcare). Thereafter, the membrane was exposed to an x-ray film between 15 seconds to 5 minutes.

2.15.3 Determination of protein concentration

The determination of protein concentration of samples was done using Bradford (1976) method, utilizing the Protein Assay Dye reagent (Bio-Rad). The protein concentration of the probes was determined using a BSA standard curve generated with 1-20 µg protein.

2 MATERIALS AND METHODS

2.16 Yeast strains

The yeast strains used in this study are listed in Tables 2.3 and 2.4.

2.16.1 *Kluyveromyces lactis* strain

Table 2.3 | *Kluyveromyces lactis* strain utilized

Strain	Genotype	Reference / Source
AWJ137	<i>MATa, Leu2, trp1, [k1⁺ k2⁺]</i>	Kämper <i>et al.</i> , 1991

2.16.2 *Saccharomyces cerevisiae* strains

Table 2.4 | *Saccharomyces cerevisiae* strains used in this study

Strain	Genotype	Reference / Source
FY1679-08A	<i>MATa ura3-52 leu2Δ1 trp1-Δ63 his3-Δ200 GAL</i>	Euroscarf
FFY3t	Like FY1679-08A, but <i>ELP3-(c-myc)₃::SpHIS5</i>	Frohloff <i>et al.</i> , 2001
CMY307	Like FY1679-08A, but <i>elp3Δ::natNT2</i>	Mehlgarten <i>et al.</i> , 2010
UMY2916	<i>MATa SUP4, Leu2-3,112, trp1-1, can1-100 ura3-1, ade2-1, his3-11,15, elp3Δ::KanMX4</i>	Huang <i>et al.</i> , 2005
ONY1	Like FFY3t, but <i>elp3Δ::KIURA3</i>	This study
ONY2	Like ONY1, but <i>ELP3-(c-myc)₃::SpHIS5</i>	This study
ONY3	Like ONY1, but <i>ELP3-(c-myc)₃-C108A::SpHIS5</i>	This study
ONY4	Like ONY1, but <i>ELP3-(c-myc)₃-C118A::SpHIS5</i>	This study
ONY5	Like ONY1, but <i>ELP3-(c-myc)₃-C121A::SpHIS5</i>	This study
ONY6	Like ONY1, but <i>ELP3-(c-myc)₃-C224A::SpHIS5</i>	This study
ONY7	Like ONY1, but <i>ELP3-(c-myc)₃-C224A-C236A::SpHIS5</i>	This study
ONY8	Like ONY1, but <i>ELP3-(c-myc)₃-C224A-C249A::SpHIS5</i>	This study
ONY9	Like ONY1, but <i>ELP3-(c-myc)₃-C224A-C277A::SpHIS5</i>	This study
ONY10	Like ONY1, but <i>ELP3-(c-myc)₃-C236A-C277A::SpHIS5</i>	This study
ONY11	Like ONY1, but <i>ELP3-(c-myc)₃-C108A-C118A-</i>	This study

2 MATERIALS AND METHODS

<i>C121A::SpHIS5</i>		
ONY12	Like ONY1, but <i>ELP3</i> -(c-myc) ₃ - <i>C108A-C118A-C121A-C224A-C236A::SpHIS5</i>	This study
ONY-G1	Like FFY3t, but <i>elp3Δ::KIURA3</i>	This study
ONY-G2	Like ONY-G1, but <i>ELP3</i> -(c-myc) ₃ :: <i>SpHIS5</i>	This study
ONY-G3	Like ONY-G1, but <i>ELP3</i> -(c-myc) ₃ - <i>G542A::SpHIS5</i>	This study
ONY-G4	Like ONY-G1, but <i>ELP3</i> -(c-myc) ₃ - <i>G545A::SpHIS5</i>	This study

2.17 Biophysical methods

2.17.1 UV-VIS absorption spectroscopy

UV-visible absorption spectra were recorded by scanning the wavelength of protein probes from 260 nm to 700 nm with a UVIKON 930 spectrophotometer (Kontron Instruments). The elution buffer or dialysis buffer was always used as a baseline control.

2.17.2 Preparation of protein samples for EPR analysis

The EPR tube is composed of extremely high quality Quartz glass (99.99%) with an inner diameter of 3 mm and thickness of 0.5 mm. The protein probes were prepared under anaerobic condition in an anaerobic chamber under N₂/H₂ (95%/5%) atmosphere. The protein probes were introduced into the EPR tube with the aid of a long tiny pipette, in such a way as to prevent the introduction of air bubbles into the protein probes. The protein samples were frozen in liquid N₂ and stored at -80°C before dispatch for EPR analysis at the group of Prof. Peter Kroneck at the University of Konstanz.

2.18 Genetic methods

2.18.1 Yeast growth media

Yeast strains were grown in rich media containing 2% peptone, 1% yeast extract and 2% dextrose (YPD) or 2% galactose (YPG) or on synthetic complex (SC) medium according to the method of Sherman (1991).

2 MATERIALS AND METHODS

2.18.2 Isolation of RNA from DH5 α *E. coli* cells

The RNA needed for the preparation of yeast competent cells was produced using *E. coli* DH5 α cells. Overnight culture (500 μ l) was used to inoculate 1 liter freshly prepared SOB medium and the culture was grown overnight for 12 hours. The cells were harvested by centrifugation for 10 minutes at 5000 rpm. The cell pellet was resuspended in 30 ml plasmid prep. buffer P1. Then 30 ml of buffer P2 was added and the suspension was mixed by inversion. Again 30 ml of buffer P3 was added. The suspension was centrifuged for 45 minutes at 10000 rpm at 4°C. The supernatant was filtered. The filtered supernatant was further supplemented with 1 volume of Isopropanol and centrifuged at 10000 rpm for 45 minutes at 4°C. The pellet obtained was washed 2X with 70% ethanol and dried on air. The dried RNA pellet was resuspended in 1X TE buffer to a final concentration of 10 mg/ml. Aliquots of 250 μ l were made and stored at -20°C until use.

2.18.3 Preparation of competent yeast cells

The preparation of competent yeast cells was based on the method of Akada *et al.* (2000). Overnight culture was made in either YPD or YNB medium. The overnight culture (2 ml) was used to inoculate 50 ml freshly prepared YPD or YNB medium. The culture was allowed to grow until an OD_{600nm} of 0.8 (2.1×10^7 / ml) was reached. The culture was then centrifuged for 5 minutes at 4000 rpm at 4°C. The pellet obtained was resuspended in 2 ml PLAG solution and supplemented with 250 μ l RNA (10 mg/ml). Aliquots of 200 μ l of the competent cells were incubated for 1 hour at -20°C before freezing at -80°C until use.

2.18.4 Transformation of competent yeast cells

For the transformation of plasmids DNA or restriction DNA fragments, 1-5 μ g DNA was added to the frozen competent yeast cells. The cells were then agitated in a shaker at 37°C for 3 minutes. Thereafter, the cells were incubated at 42°C for 2 hours. The cell suspension was plated on YNB plates to select for the transformed plasmid. For fragment integration into the yeast genome, fragment-transformed yeast competent cells were plated on YPD plates and incubated overnight at 30°C.

2 MATERIALS AND METHODS

The YPD plate was then replica-plated next day on YNB plate to select for transformants with integrated fragment.

2.18.5 Extraction of chromosomal DNA from yeast cells

The extraction of chromosomal DNA from yeast cells was based on the methods of Davis *et al.*, (1980) and Ausubel *et al.*, (1998). 5-10 ml overnight culture was centrifuged for 5 minutes at 4000 rpm at room temperature. The pellet was washed with 500 µl distilled H₂O and introduced into a 1.5 ml Eppendorf tube. The cells were again centrifuged at 14000 rpm for 1 minute and the supernatant disposed. The pellet was resuspended in 200 µl breaking buffer. 0.3 g glass beads (~200 µl volume) and then 200 µl PCI solution were added. The cell suspension was strongly vortexed for 4 minutes. Then 400 µl autoclaved distilled H₂O was added and the suspension centrifuged at 14000 rpm for 5 minutes. The aqueous-phase supernatant was collected in a new tube containing 1 ml ice-cold 96% ethanol and then properly mixed by inversion before centrifugation at 14000 rpm for 5 minutes at room temperature. The pellet obtained was dried on air and resuspended in 200-400µl 1X TE buffer.

2.18.6 Protein extraction from yeast cells

The extraction of protein from yeast cells was done according to the methods of Zachariae *et al.*, (1996) and Ausubel *et al.*, (1998). Overnight yeast cultures (5 ml) were used to inoculate 50 ml of an appropriate yeast medium. The cultures were then allow to grow for about 4 hours at 30°C to attain the logarithmic growth phase (OD_{600nm} of 1-2). The cells were then harvested by centrifugation at 4000 rpm at 4°C for 5 minutes. Cell pellet was resuspended in 400 µl B60 buffer and 300 µl glass beads (Ø 0.4-0.6 mm) was then added (Klekamp & Weil 1982). The cells were then disrupted by vigorous vortexing 3X at 4 minutes interval. Between each vortexing, the cells were placed on ice for 5 minutes. After cell disruption, cell debris was removed by centrifugation at 14000 rpm at 4°C for 5 minutes and the supernatant transferred to a new tube. The supernatant was again centrifuged at 14000 rpm for 20 minutes at 4°C and the supernatant obtained were used for subsequent protein analyses.

2.19 Disruption of *ScELP3* gene to generate *Ura*⁺ strains

The disruption of the *ELP3* gene in *Saccharomyces cerevisiae* strain, FFY3t (Frohloff 2001), using *K. lactisURA3* as selectable marker was done by PCR-based targeting procedure developed by Wach *et al.*, (1997). The *KIURA3* gene was amplified from the YDp-KIU plasmid (Jablonowski *et al.*, 2001a) with the aid of the *ELP3* knock-out primers (Table 2.1d). The knock-out primers for the PCR amplification of the *KIURA3* cassette were flanked with the relevant *ELP3* sequences. The PCR amplification of the *KIURA3* gene was done in 3 fractions of 100 µl each. The PCR products were pooled and analyzed on 0.8% agarose gel to confirm the *KIURA3* gene product of ~1.5 kbp. The *KIURA3* cassette was precipitated using the routine procedure of DNA precipitation. The precipitated *KIURA3* cassette was resuspended in 30 µl H₂O and transformed into competent yeast FFY3t cells (Frohloff *et al.*, 2001). The transformation cocktail was plated on YNB plates containing mixture of all amino acids but lacking L-uracil, to select colonies (*Ura*⁺) that have integrated the *KIURA3* cassette into their genomes. The knock-out of the *ELP3* gene to generate the ONY1 and ONY-G1 yeast *elp3Δ* strains was confirmed by a) Western blotting, b) Killer-toxin eclipse assay and c) PCR method using specific primers (Table 2.1).

2.19.1 Integration of *ScELP3* and mutant fragments into genome of *Ura*⁺ strains

The successful construction of the ONY1 and ONY-G1 yeast strains by a one-step PCR targeting of the *ScELP3* gene (Wach *et al.*, 1997) with the *URA3* cassette was confirmed by three independent analyses. In the next step competent ONY1 and ONY-G1 cells were prepared. In order to analyze Elongator function, the *URA3* gene was disrupted by homologous recombination using *ScELP3* wild type and mutant fragments obtained by restriction of 5 µg of the respective plasmids (Table 2.2) with *NcoI* and *NheI*. The restriction cocktails obtained from the *ScELP3* wild type and radical SAM mutant variants were transformed into competent ONY1 yeast cells and the glycine mutant restriction cocktails into competent ONY-G1 yeast cells. The transformation cocktails were plated on YPD plates and incubated overnight at 30°C and then replica-plated on YNB agar plates containing fluoro-orotic-acid (FOA) and

2 MATERIALS AND METHODS

mixture of amino acids including L-uracil. The untransformed ONY1/ONY-G1 cells were used as negative controls. FOA allows for selection of uracil auxotrophic strains due to its toxicity towards uracil prototrophs (Boeke *et al.*, 1984; Francois *et al.*, 2004). The plates were then incubated for 3-5 days at 30°C. The transformants obtained were tested using a) Colony PCR analysis b) Killer-toxin eclipse assay and c) Western blotting to confirm the replacement of the *KIURA3 ORF* by the *ScELP3* WT or mutant variant fragments.

2.19.2 Intracellular expression of γ -toxin in yeast

For the testing of yeast strains using the endotoxin assay, the pLF16 plasmid (Fichtner 2000) was transformed into the generated yeast strains. The pLF16 plasmid contains the γ -toxin *ORF* under the control of the *GAL1* promoter. The expression of γ -toxin can be repressed in the presence of glucose and induced in galactose. Cell suspensions of *ScELP3*WT and mutant yeast strains generated were prepared and serially diluted from the same OD_{600nm} values and spotted on YNB plates lacking L-leucine for γ -toxin selection, but containing either glucose or galactose and incubated for 3 days at 30°C.

2.19.3 Killer-toxin eclipse assay

The killer-toxin eclipse assay as described by Kishida *et al.*, (1996), was used to analyze the effect of the exogenous *Kluyveromyces lactis* killer-toxin on *S. cerevisiae* strains and to test for biological functionality of Elongator. Single colonies were picked and resuspended in 200 μ l autoclaved distilled H₂O. The OD_{600nm} of the resuspended cells were diluted to 1.0, and then further serially diluted. Then 5 μ l of cell suspension was spotted on YPD plates. On drying of the cell suspension, the *K. lactis* killer toxin-producing strain (AWJ137) was then spotted on the periphery of the dried cell suspension. The plates were then incubated overnight at 30°C. Appearance of an eclipse zone of growth inhibition on the periphery of the *S. cerevisiae* strains indicated sensitivity, while absence of eclipse zone of growth inhibition signifies resistance to the *K. lactis* toxin, zymocin.

2.19.4 Suppression assay

The investigation of the effect of the radical SAM domain alleles on tRNA suppression was done using the *can1* system (Huang *et al.*, 2005). The *S. cerevisiae* UMY2916 strain contains the ochre allele, *CAN1-100*. *CAN1* gene codes for an arginine permease and its mutation leads to resistance to the cytotoxic arginine analog canavanine. The efficiency of an ochre suppressor tRNA to decode the *can1-100* (UAA) codon can be assayed on SC plates lacking arginine but containing 6µg/ml canavanine (SC-Arg+Can). Suppression of the ochre mutation *can1-100* by the tRNA^{Tyr} suppressor gene *SUP4* was then scored by canavanine sensitivity / resistance on SC-Arg+Can plates.

2.20 Immunological techniques

2.20.1 Coupling of antibody to Protein A-Sepharose matrix

Cross-linking of antibody to Protein A-Sepharose (PAS), preparation of yeast cell extracts and co-immunoprecipitation were performed as previously described (Zachariae *et al.*, 1996; Frohloff *et al.*, 2001). A 15 ml falcon tube was used for the suspension of 200 µl of PAS in 2 ml of glycine-OH-buffer (1.45 M glycine; 3 M NaCl, pH8.9 adjusted with NaOH). The sample was incubated at room temperature for 1 hour on a shaker. Thereafter, 100 µg (500 µl) anti-α-hemagglutinin (HA) mouse monoclonal IgG antibody from Santa Cruz Biotechnology (Heidelberg) was added to the tube and incubation was continued at 4°C for 1hour. 10 ml 0.2 M Na-borate buffer, pH9.0 was added to the falcon tube and then centrifuged for 1 minute at 1000 rpm and the supernatant carefully removed. This washing step was repeated twice. Then 10 ml 0.2 M Na-borate, pH9.0 supplemented with 20 mM dimethylpimelimidate was added and the sample was incubated further for 30 minutes on a shaker at room temperature. Then the falcon tube was centrifuged for 2 minutes at 1000 rpm and the PAS coupled anti-HA antibody was washed twice with 10 ml 0.2 M ethanolamine, pH8.0. The PAS coupled anti-HA antibody was then incubated in 10 ml 0.2 M ethanolamine, pH8.0 for 2 hours at room temperature on a shaker. Next, the falcon tube was centrifuged for 2 minutes at 1000 rpm and the PAS coupled anti-HA antibody was then blocked in 2 ml BSA (5 mg / ml) for 30 minutes at

2 MATERIALS AND METHODS

room temperature. Finally, the falcon tube was centrifuged for 2 minutes at 1000 rpm and the supernatant was carefully removed. The PAS coupled anti-HA antibody was then resuspended in 1X PBS buffer, pH7.2 and stored at 4°C.

2.20.2 Coimmunoprecipitation of ScElp3 proteins

Yeast raw extracts obtained upon ScElp3 protein expression were added to 50-100 µl PAS-coupled α-HA primary antibody and mixed together. The mixture was then incubated on a shaker for 90 minutes at 4°C. Thereafter, the mixture was centrifuged at 1000 rpm at 4°C for 1 minute and the supernatant discarded. The PAS-coupled α-HA antibody pellet was washed with 1 ml B60 buffer and centrifuged at 1000 rpm for 1 minute at 4°C. The supernatant was discarded and the wash step was repeated 3X. The PAS-coupled antibody pellet was then resuspended in 50-100 µl SDS buffer (10% SDS) and incubated at room temperature for 10 minutes. The suspension was centrifuged through a PCR-filter pipette. The supernatant was analyzed by SDS-PAGE and Western blotting.

3 RESULTS

3.0 Results

The yeast ScElp3 and its *Arabidopsis* homologue, AtElp3 are the catalytic subunits of the yeast and plant Elongator. They are the most conserved of all Elongator subunits and their radical SAM domain show high sequence similarity to the radical SAM enzyme superfamily (Sofia *et al.*, 2001). The radical SAM domain of the archaeal *Methanocaldococcus jannaschii* Elp3 protein was shown to bind and cleave SAM (Paraskevopoulou *et al.*, 2006), hence the need to study the importance of this domain for Elp3 and its role for Elongator function in eukaryotes. Both Elp3 proteins were recombinantly expressed in *Escherichia coli* in order to obtain sufficient protein for *in vitro* analyses. The aim was to characterize the putative radical SAM domains of the eukaryotic ScElp3 and AtElp3 proteins structurally and functionally.

3.1 Recombinant expression of AtElp3 variants affinity epitope-tagged in *E. coli*

3.1.1 Expression of a full length AtElp3H₆ protein using the pET vector system

In order to characterize the putative radical SAM domain of *Arabidopsis thaliana* AtElp3, the catalytic subunit of the Elongator complex, full length AtElp3H₆ protein was recombinantly expressed in *Escherichia coli* as a C-terminal His₆-tagged fusion protein using the pET-21b vector (Novagen). The AtELP3 ORF from plasmid pAIV2 (Mehlgarten *et al.*, 2010) was excised as a *SalI* fragment and cloned into the *SalI* site to obtain the expression plasmid pON-ELO3-1 (Figure 3.0A).

The pON-ELO3-1 plasmid was subsequently transformed into the *E. coli* expression strain BL21(DE3). Gene expression under the control of the T7lac promoter was induced with IPTG. Cells were lysed by sonication and AtElp3H₆ was analyzed in the soluble and pellet fractions by Western blotting using anti-His₆ antibody (Figure 3.0B). Only approximately 10% of the protein was recovered in the soluble fraction whereas 90% was detected in the pellet fraction indicating inclusion body formation (Figure 3.0B). In addition to a band migrating at the position of the full

3 RESULTS

length AtElp3H₆ (67.4 kDa), several smaller peptides were detected, which presumably represent degradation products.

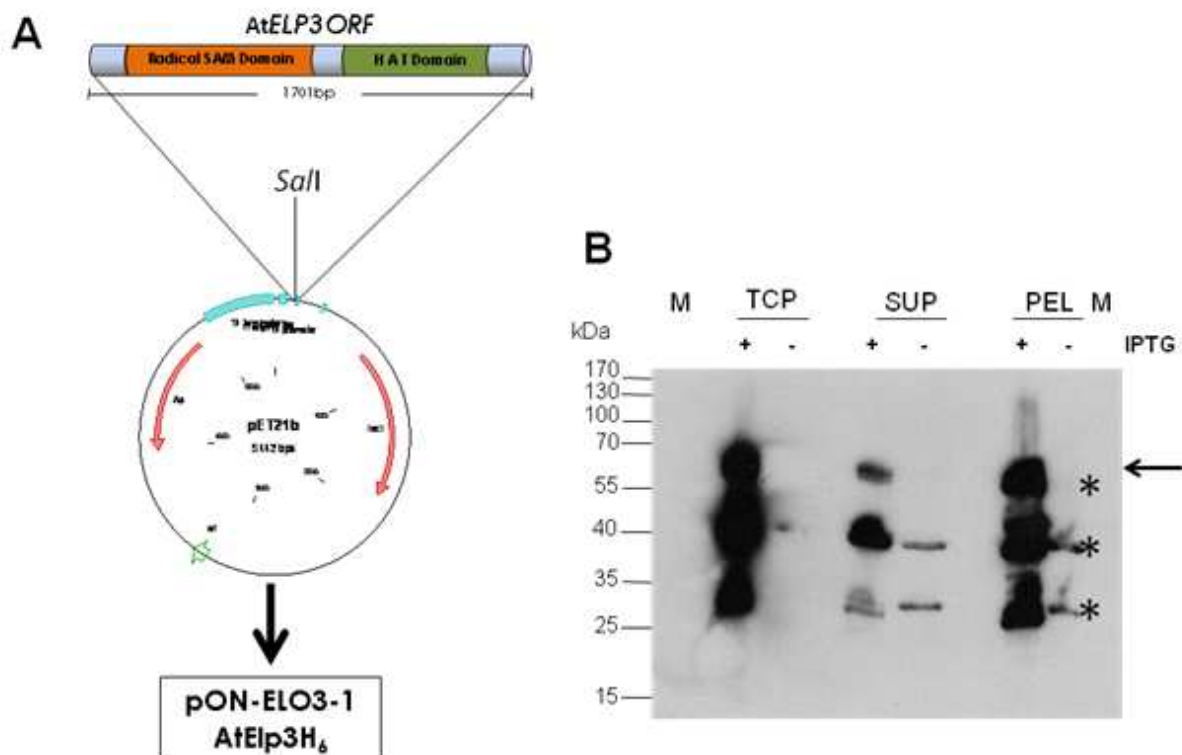


Figure 3.0 | Cloning and solubility analysis of full length AtElp3H₆ protein expressed in *E. coli*. (A) Construction of pON-ELO3-1. The full length AtELP3 ORF was inserted into the SalI site of the pET-21b vector to generate pON-ELO3-1, which expresses the C-terminal His₆-tagged AtElp3 wild type fusion protein AtElp3H₆. (B) Solubility profile of AtElp3H₆. Protein expression was induced with IPTG and detected by Western blotting using α -His₆-antibody. Equal amount of samples were analyzed on 12% SDS-PAGE. Full length AtElp3H₆ (67.4 kDa) protein is designated by an arrow (←) and asterisks (*) indicate degradation products (65, 40 and 30 kDa). +/- indicates expression with / without IPTG. TCP, total cell protein; SUP, supernatant; and PEL, pellet fractions. M denotes the molecular weight markers.

3.1.2 Attempts to purify AtElp3 and radical SAM domain variants under native conditions on Ni-NTA-agarose matrix

3.1.2.1 Affinity chromatography of AtElp3H₆ protein

The *E. coli* expression strain, BL21(DE3) containing the plasmid pON-ELO3-1 was used for affinity purification of AtElp3H₆ with Ni-NTA-agarose under native conditions as described in the materials and methods section. From the soluble fraction, only low binding efficiency was observed. The full length protein was primarily detected in

3 RESULTS

the flow through and hence could not be enriched by affinity purification whereas the 40 kDa degradation product could be bound to the matrix (Figure 3.1). In total, from 1 liter culture only 1.26 mg AtElp3H₆ protein was obtained after purification (Table 3.0). Therefore, expression of subfragments encompassing the radical SAM domain only was considered.

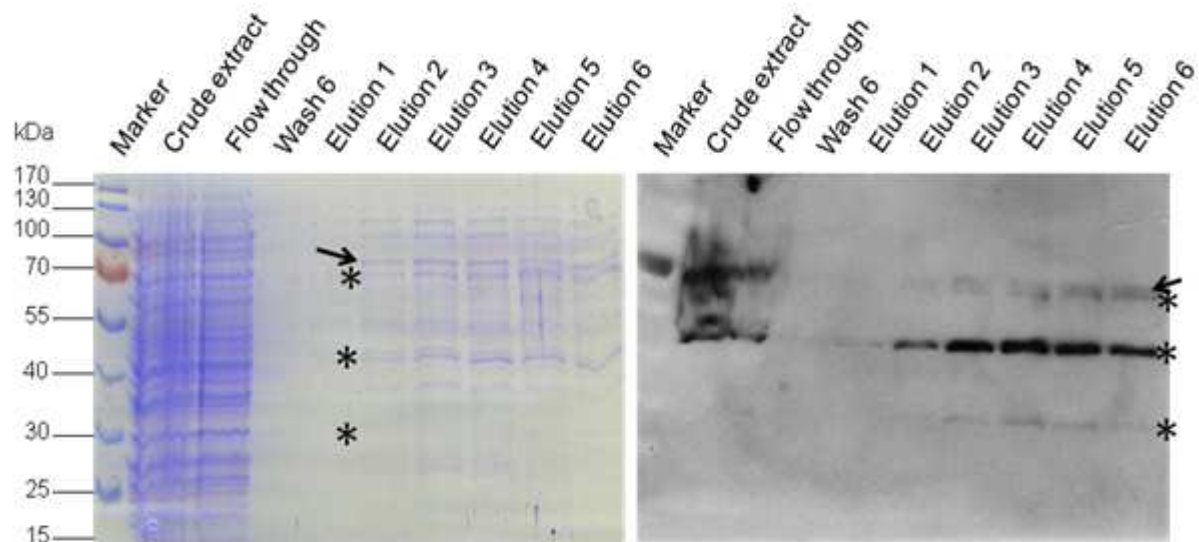


Figure 3.1 | Affinity chromatography of wild type AtElp3H₆ (67.4 kDa) on Ni-NTA-agarose matrix. Staining of samples on 12% SDS-PAGE by Coomassie (left) and Western blotting using α -His₆ antibody (right). Equal volumes of samples were analyzed. The full length AtElp3H₆ protein (67.4 kDa) is designated with an arrow (\rightarrow) and the degradation products (65, 40 and 30 kDa) are marked with asterisks (*).

3.1.2.2 Expression of radical SAM domain variants as C-terminal His₆-tagged fusion proteins

Since the solubility problem observed upon expression of the wild type AtElp3H₆ protein might be due to very high expression levels in the pET-21b system (Figure 3.0), the pBAD vector was used to express subfragments of AtElp3. Protein expression using pBAD makes use of the araC promoter (P_{araC}), which can be sensitively controlled by L-arabinose in the growth medium (Guzman *et al.*, 1995). Two different fragments containing the radical SAM domain with distinct truncations of the N-terminus were chosen for expression studies. Amplification of two radical SAM domain fragments, AtElp3(76-366)H₆ and AtElp3(111-366)H₆ was achieved by PCR using two sets of primers; At(76-366)_NcoI_FW and At(76-366)_XhoI_RV; At(111-366)_NcoI_FW and At(111-366)_XhoI_RV and the pAIV2 plasmid as

3 RESULTS

template. The PCR fragments were cloned into the pBAD vector utilizing the *Nco*I and *Xho*I restriction sites (Figure 3.2A). The resulting constructs, pON1 and pON2 were then transformed into the *E. coli* strain MC4100. 0.1% L-arabinose was added to induce expression of the radical SAM domain variants as C-terminal His₆-tagged fusion proteins. The soluble fraction is shown in Figure 3.2B. In comparison to a control plasmid expressing the *E. coli* TatB protein using the pBAD vector (Lane 3), lower levels of the tagged AtElp3 fragments were obtained. The yield of AtElp3(111-366)H₆ appeared slightly higher than that of AtElp3(76-366)H₆ and the full length AtElp3H₆ in the pET vector (Figure 3.2B).

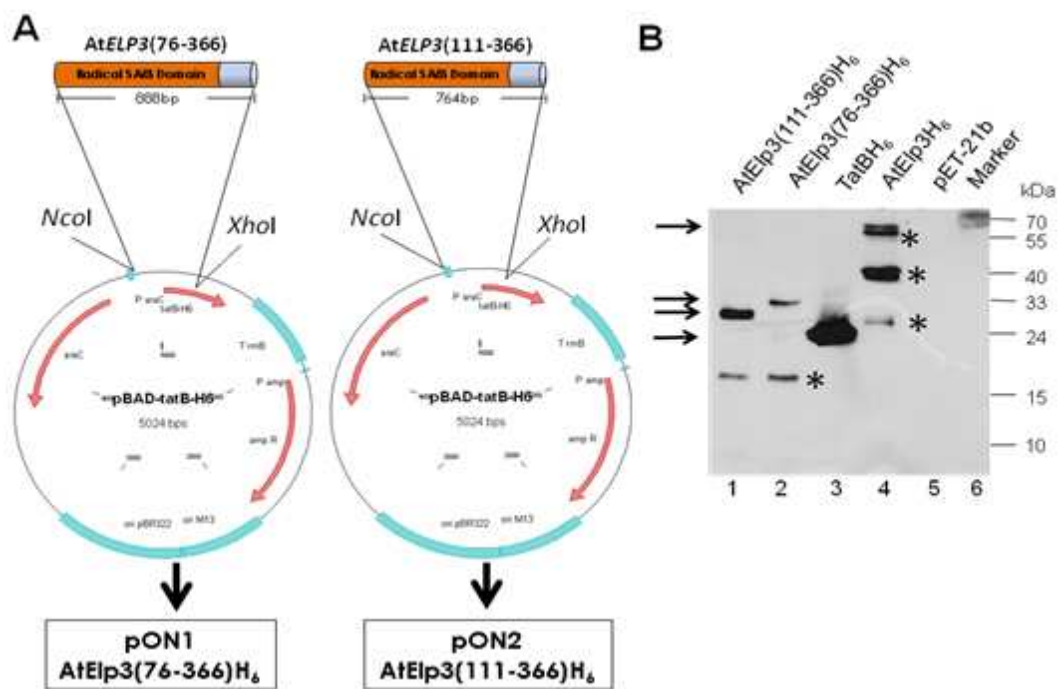


Figure 3.2 | Cloning and expression analysis of the radical SAM domain variants, AtELP3(76-366), AtELP3(111-366) in comparison to full length AtElp3H₆. (A) AtELP3(76-366) and AtELP3(111-366) were cloned into the *Nco*I / *Xho*I site via replacement of the *TatB* ORF to generate the pON1 and pON2 constructs, which express the AtElp3(76-366)H₆ and AtElp3(111-366)H₆ peptides respectively, as C-terminal His₆-tagged fusion proteins. (B) Analysis of protein expression of wild type AtElp3H₆ (67.4 kDa) and the radical SAM domain variants, AtElp3(76-366)H₆ (33.5 kDa) and AtElp3(111-366)H₆ (29.7 kDa) by Western blotting using α-His₆-antibody, after induction of protein expression with IPTG (pON-ELO3-1, lane 4) and L-arabinose (pON1, lane 1 and pON2, lane 2), respectively. Supernatant protein fractions (50 μg) were loaded on 12% SDS-PAGE. The TatBH₆ protein (~20 kDa, lane 3) and empty vector, pET-21b (lane 5) serve as positive and negative controls. The arrows (→) indicate the expected sizes of full length proteins, degradation products are designated with asterisks (*).

3 RESULTS

To test the solubility profile of the two radical SAM domain variants, the crude extract and the insoluble pellet fractions of the *E. coli* strain MC4100, expressing each sub-fragment were analyzed. As shown in Figure 3.3, about equal amounts of the full length AtElp3(76-366)H₆ (Figure 3.3A) and AtElp3(111-366)H₆ (Figure 3.3B) proteins could be detected in the soluble and the pellet fractions. Also degradation products of the same molecular weight (20 kDa) were observed from both radical SAM domain variants (Figure 3.3). In conclusion, there is a slight improvement in the solubility of the radical SAM domain variants in comparison with the full length AtElp3 protein (Figure 3.0 and Figure 3.3).

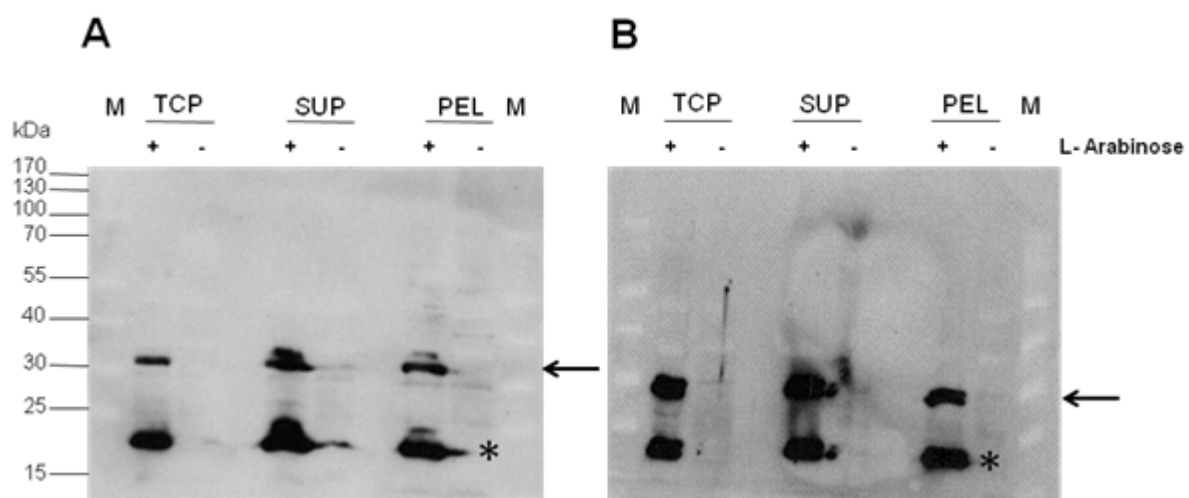


Figure 3.3 | Solubility analysis of the radical SAM domain variants, AtElp3(76-366)H₆ (33.5 kDa) and AtElp3(111-366)H₆ (29.7 kDa). The radical SAM variants, (A) AtElp3(76-366)H₆ and (B) AtElp3(111-366)H₆ were analysed for their solubility by Western blotting. The same degradation products of both radical SAM domain variants (20 kDa) were detected. 50 µg of soluble protein as well as equal amounts of TCP and PEL fractions were analyzed on 12% SDS-PAGE. +/- denotes expression with / without 0.1% L-arabinose respectively. TCP, total cell protein; SUP, supernatant; PEL, pellet. The size of full length proteins 33.5 and 29.7 kDa are indicated with arrows and the degradation products with asterisks (*). M designates marker in kDa. Proteins were detected by Western blotting with α-His₆-antibody.

3.1.2.3 Purification of the radical SAM domain subfragments, AtElp3(76-366)H₆ and AtElp3(111-366)H₆

To purify the radical SAM domain variants, the *E. coli* MC4100 strain containing the respective expression plasmids, pON1 expressing AtElp3(76-366)H₆ and pON2 expressing AtElp3(111-366)H₆ were used for affinity purification on Ni-NTA-agarose

3 RESULTS

(Section 3.1.2.1). As observed for the wild type AtElp3H₆ protein (Section 3.1.2.1, Figure 3.1), the two radical SAM domain variants also could not bind effectively to the Ni-NTA-agarose matrix. Both proteins could be detected in the flow through fractions by Western blotting (Figure 3.4B and 3.4D). In the elution fractions only 1.8 mg and 1.1 mg of the radical SAM domain variants, AtElp3(76-366)H₆ and AtElp3(111-366)H₆ were recovered from 212 mg and 227 mg total protein, respectively (Table 3.0). Thus, neither the wild type AtElp3H₆ nor two radical SAM domain variants could be effectively purified on Ni-NTA-agarose matrix due to their low binding efficiency. In summary, the expression constructs used for the purification of wild type AtElp3H₆ (pON-ELO3-1), the radical SAM domain variants, AtElp3(76-366)H₆ (pON1) and AtElp3(111-366)H₆ (pON2) are not ideal for the production of sufficient amount of proteins needed for further studies. To characterize the radical SAM domain milligram amounts of protein would be needed.

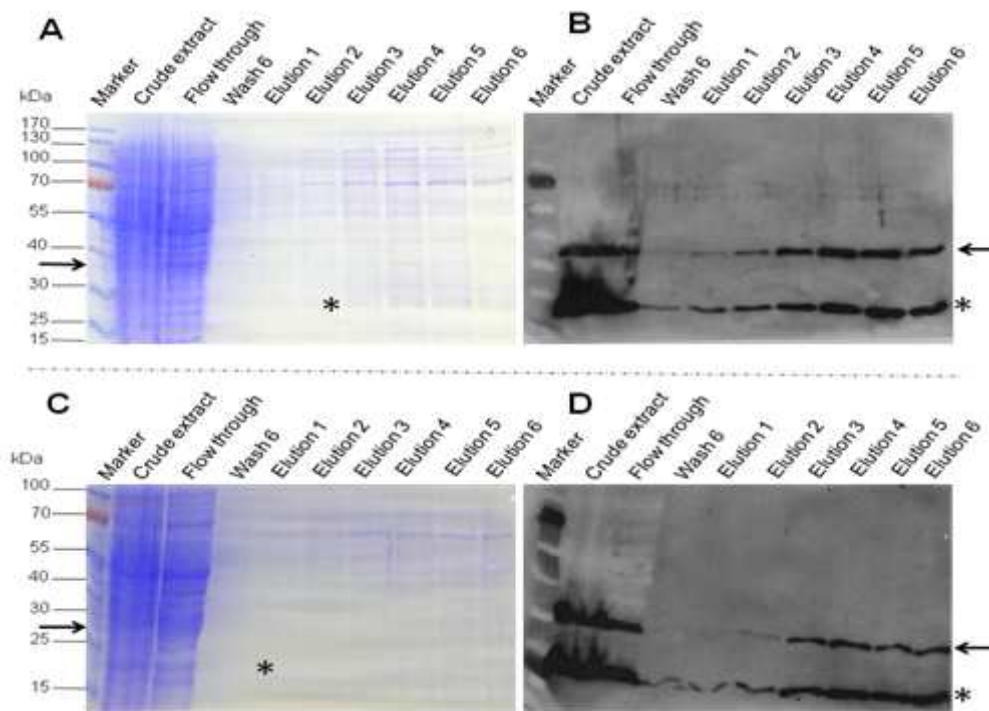


Figure 3.4 | SDS-PAGE and Western blot analyses of the radical SAM domain variants, AtElp3(76-366)H₆ (33.5 kDa) and AtElp3(111-366)H₆ (29.7 kDa) upon affinity purification on Ni-NTA-agarose matrix. (A) Analysis of AtElp3(76-366)H₆ purification probes on 12% SDS-PAGE stained with Coomassie reagent. (B) Detection of AtElp3(76-366)H₆ protein by Western blot using α -His₆ antibody. (C) SDS-PAGE analysis of AtElp3(111-366)H₆ purification samples and (D) Western blot analysis of AtElp3(111-366)H₆ protein using α -His₆ antibody. Equal volumes of samples were analyzed. The position of full length radical SAM domain variant proteins (33.5 kDa and 29.7 kDa), respectively are indicated by arrows (\rightarrow) and the degradation products (20 kDa) are marked with asterisks (*)

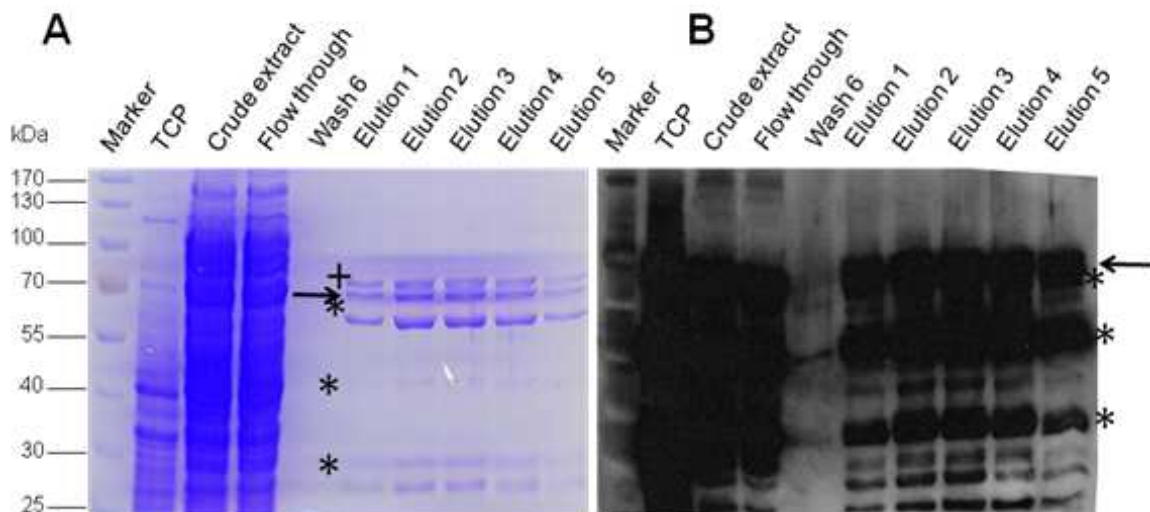
3 RESULTS

3.1.3 Alternative tagging and plasmid coexpression of AtElp3 protein

3.1.3.1 Expression and purification of a full length Strp-AtElp3-H₁₀ fusion protein

In an attempt to increase the binding efficiency of the AtElp3 protein, the *AtELP3* ORF was cloned into the pET-52b plasmid (Novagen) to generate a double tagged AtElp3 protein. The resulting plasmid, pON-ELO3-2 should give AtElp3 as an N-terminal Strep- and C-terminal His₁₀-tagged fusion protein. Again most of the Strp-AtElp3-H₁₀ full length protein was detected in the inclusion body fraction (data not shown). To test whether alternative tagging enhances binding and purification properties of AtElp3 protein, Strep-Tactin affinity chromatography was performed with the soluble protein.

The Strp-AtElp3-H₁₀ protein could not be purified on this column due to low binding affinity (data not shown), and hence no protein enrichment could be achieved. Upon chromatography of the soluble Strp-AtElp3-H₁₀ fraction on Ni-NTA-agarose column, increased protein yield was noticed by Coomassie staining (Figure 3.5A). A total of 2.4 mg protein was recovered from 1 liter culture (Table 3.0). Nevertheless, high amounts of Strp-AtElp3-H₁₀ protein in the flow through indicated inefficient binding to Ni-NTA-agarose. Additional proteins coeluted with the full length Strp-AtElp3-H₁₀ protein (Figure 3.5A). Some of these are probably the same degradation products that were observed with the AtElp3H₆ protein using the pON-ELO3-1 expression construct (Section 3.1.2.1; Figure 3.1).



3 RESULTS

Figure 3.5 | Expression and purification of full length Strp-AtElp3-H₁₀ (69.6 kDa) on Ni-NTA-agarose matrix. (A) SDS-PAGE analysis of Strp-AtElp3-H₁₀ purified on Ni-NTA-agarose stained with Coomassie reagent. (B) Detection of purified Strp-AtElp3-H₁₀ protein by Western blot using α -His₆ antibody. 20 μ l of 2.5 ml elution fractions were analyzed. The position of full length Strp-AtElp3-H₁₀ is depicted with arrow (\rightarrow), the degradation products (65, 40 and 30 kDa) are marked with asterisks (*). An additional bigger protein coeluting with the Strp-AtElp3-H₁₀ protein is marked (+). TCP represents total cell protein.

3.1.3.2 Coexpression of the Strp-AtElp3H₁₀ protein with the iron-sulfur cluster (*isc*) biogenesis plasmid, pRKISC

Based on the high sequence similarities of members of the radical SAM enzyme superfamily and the radical SAM domain of the Elongator subunit, Elp3 (Sofia *et al.*, 2001), Elp3 proteins may be regarded as putative Fe-S cluster binding proteins. To check if there would be a possible increase in soluble protein yield when Fe-S cluster assembly was supported, the pON-ELO3-2 plasmid was coexpressed with a plasmid containing the *isc* operon, pRKISC. In *E. coli*, the iron-sulfur cluster (*isc*) operon, *ORF1-ORF2-iscS-iscU-iscA-hscB-hscA-fdx-ORF3* encodes enzymes that are imperative in the assembly of [Fe-S] clusters (Takahashi & Nakamura 1999). Coexpression of ferredoxin (Fd) with the *isc* operon has been shown (Nakamura *et al.*, 1999) to tremendously increase the production of holoFd. Upon coexpression of full length Strp-AtElp3-H₁₀ protein with the pRKISC plasmid, a significant increase in the yield was observed when compared to the Strp-AtElp3-H₁₀ protein expressed without the *isc* operon plasmid (Figure 3.6), although most of the Strp-AtElp3-H₁₀ protein was still found in the inclusion body fraction.

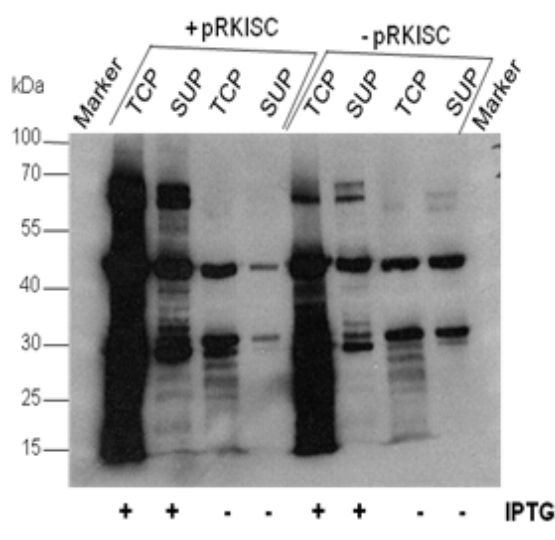


Figure 3.6 | Coexpression of Strp-AtElp3-H₁₀ (69.6 kDa) fusion protein with the *isc* operon plasmid, pRKISC. Western blot analysis of overexpressed Strp-AtElp3-H₁₀ fusion protein using α -His₆ antibody. Equal amount of samples was analyzed on 12% SDS-PAGE. Increased Strp-AtElp3-H₁₀ protein yield was observed upon coexpression with pRKISC compared to Strp-AtElp3-H₁₀ protein expression without pRKISC plasmid. Cells were induced with 0.4 mM IPTG. TCP, total cell protein; SUP, supernatant. +/-, induction with / without IPTG

3 RESULTS

3.1.4 Characterization of H₆-AtElp3-Strp fusion protein

3.1.4.1 Solubility analysis of a full length H₆-AtElp3-Strp protein

The low amounts of proteins obtained upon Ni-NTA-agarose affinity purification indicated very low binding efficiency of the C-terminally tagged AtElp3 protein. Therefore an attempt to increase the binding efficiency of the wild type AtElp3 protein by N-terminal His₆-tag was considered. In frame cloning of the AtElp3 into the pASK-IBA-43 produced an N-terminal His₆- and a C-terminal Strep-tagged AtElp3 fusion protein H₆-AtElp3-Strp. Protein expression in the plasmid is controlled by the Tet promoter (p_{Tet}) which is inducible by anhydrotetracycline. For the analyses of the expression and solubility profile of the H₆-AtElp3-Strp, the pON-ELO3-3 expression plasmid was transformed into the *E. coli* expression strains BL21(DE3) and Rosetta™ (Figure 3.7). Like all constructs used for the expression of wild type AtElp3 fusion protein (Table 3.0), the pON-ELO3-3 expression construct also revealed that approximately 90% of the H₆-AtElp3-Strp protein was found in the total cell protein (TCP) fraction (Figure 3.7). Only about 10% of the protein was detected in the soluble fraction. Nevertheless, the 10% soluble fraction of the H₆-AtElp3-Strp protein was used for affinity chromatography on Ni-NTA-agarose column.

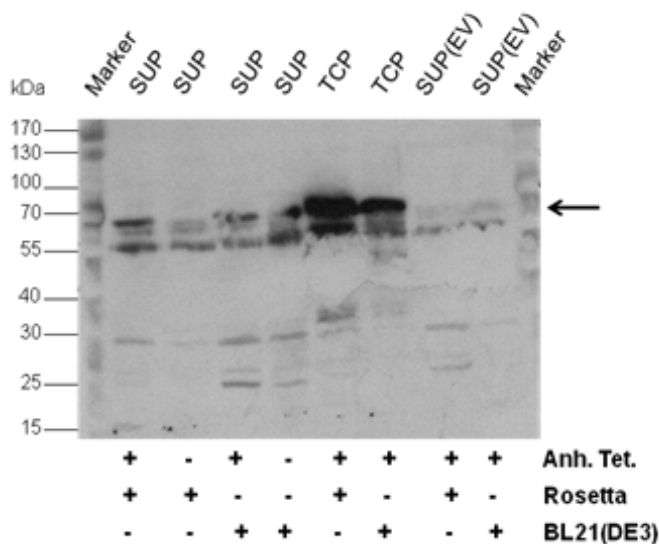
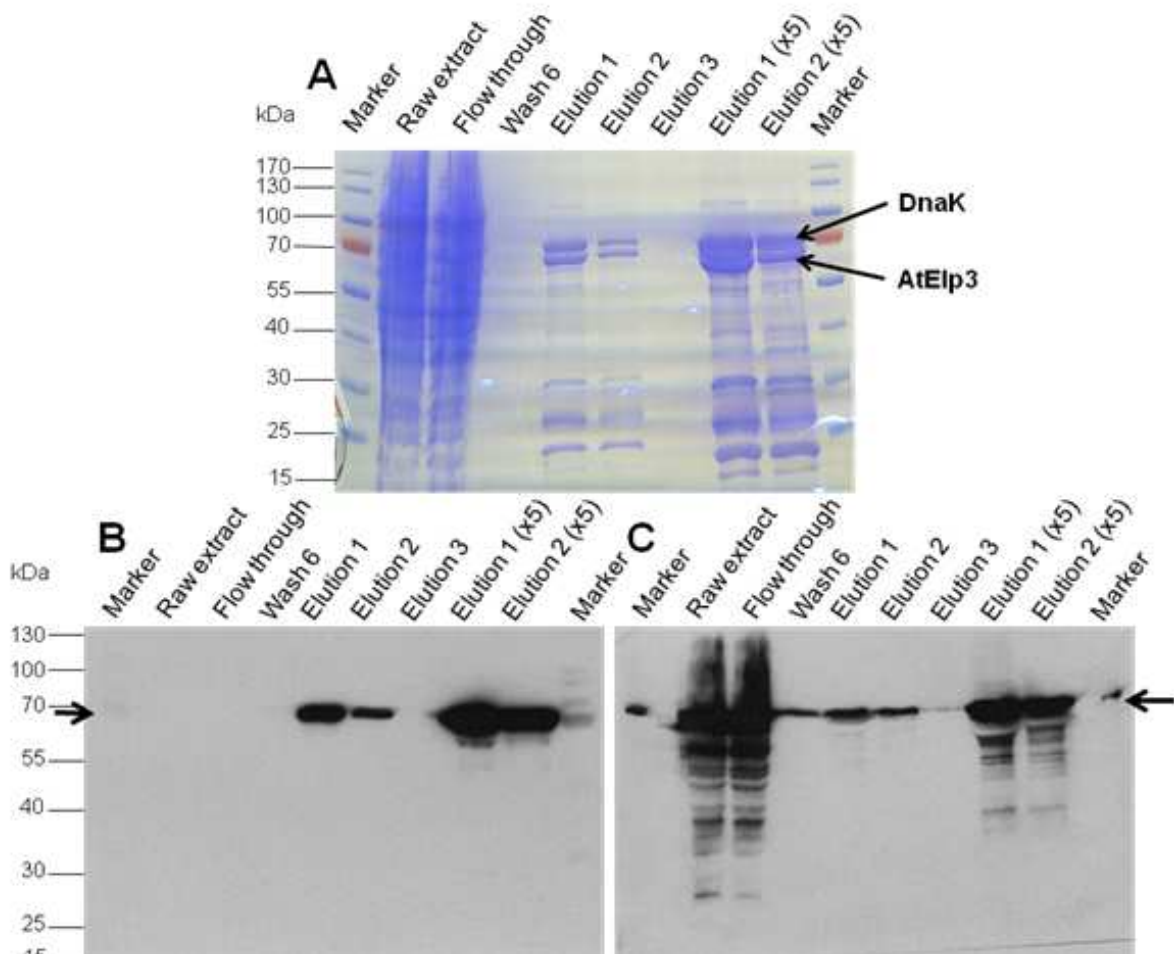


Figure 3.7 | Solubility analysis of H₆-AtElp3-Strp (69.3 kDa) protein. Western blot analysis of H₆-AtElp3-Strp protein using α -His₆ antibody. Equal amount of induced and uninduced supernatant and TCP fractions was analyzed on 12% SDS-PAGE. Arrow indicates full length H₆-AtElp3-Strp protein. TCP, total cell protein; SUP, supernatant; EV, empty vector (pASK-43). *E. coli* BL21(DE3) and Rosetta™ strains were used for protein expression. +/-, induction / without induction with anhydrotetracycline (anh. Tet.).

3 RESULTS

3.1.4.2. Affinity chromatography of full length H₆-AtElp3-Strp protein on Ni-NTA-agarose matrix

To purify the full length H₆-AtElp3-Strp fusion protein on Ni-NTA-agarose column, the *E. coli* BL21(DE3) strain containing the pON-ELO3-3 plasmid was used for protein expression in a 2 liter culture at 37°C. The soluble cell extract was loaded on Ni-NTA-agarose matrix and bound proteins were eluted using imidazole containing buffer. As shown in Figure 3.8, no trace of protein was seen in the flow through fraction indicating high binding efficiency of the protein to the matrix. A total of 4.6 mg purified protein was recovered in the eluate fractions. The H₆-AtElp3-Strp fusion protein eluted in a sharp peak and was detected in only two fractions. The protein coeluting with the H₆-AtElp3-Strp protein was identified as the heat shock protein, DnaK (Hsp70), using α -DnaK antibody (Figure 3.8C). These results were promising but due to interaction of H₆-AtElp3-Strp with the heat shock protein DnaK, further measures were needed to dissociate the two proteins.



3 RESULTS

Figure 3.8 | Purification profile of a full length H₆-AtElp3-Strp (69.3 kDa) on Ni-NTA-agarose matrix. (A) Analysis of H₆-AtElp3-Strp eluted samples on 12% SDS-PAGE after purification on Ni-NTA-agarose matrix. The gel was stained with Coomassie reagent. Arrows show full length H₆-AtElp3-Strp and DnaK proteins. (B) Detection of H₆-AtElp3-Strp protein by Western blotting using α -His₆ antibody. (C) Western blot analysis of H₆-AtElp3-Strp protein using α -DnaK antibody, confirming co-elution of the DnaK (70 kDa) chaperone. 20 μ l of 2.5 ml elution fractions were analyzed. The eluates 1 and 2 were concentrated 5 folds (5X) with Amicon Ultra-4 membrane.

3.1.4.3 Attempts to disrupt the H₆-AtElp3-Strp interaction with DnaK

Members of the Hsp70 protein family including *E. coli* DnaK function as molecular chaperones to mediate protein folding, protein assembly / disassembly, protein translocation and repair of unfolded proteins damaged as a result of environmental stresses (Bukau *et al.*, 2006; Bukau & Horwich 1998). For the disruption of the interaction between H₆-AtElp3-Strp full length protein and DnaK, 700 mM NaCl (WB₇₀₀) or the non-hydrolysable ATP analogue (500 μ M ATP γ S) which is a substrate of DnaK was used in the wash buffer. After binding of H₆-AtElp3-Strp protein, the Ni-NTA-agarose column was washed 6X with wash buffer containing 300 mM NaCl (WB₃₀₀). Afterwards, the column was further washed twice using WB₇₀₀ buffer and lastly again twice with WB₃₀₀. Trace amounts of H₆-AtElp3-Strp protein were lost after 2X wash with WB₇₀₀ buffer (Lane, Wash700) but DnaK remained associated with H₆-AtElp3-Strp and was coeluted with imidazole (Figure 3.9A).

Likewise, when the matrix was washed with 500 μ M ATP γ S (Figure 3.9B), the interaction between wild type H₆-AtElp3-Strp protein and DnaK (Hsp70) could not be disrupted. Therefore, other methods would be needed for the purification of the AtElp3 protein required for the characterization studies. Another option that was considered for the disruption of H₆-AtElp3-Strp and DnaK was affinity chromatography of H₆-AtElp3-Strp protein on Strep-Tactin matrix employing its C-terminal epitope tag.

3 RESULTS

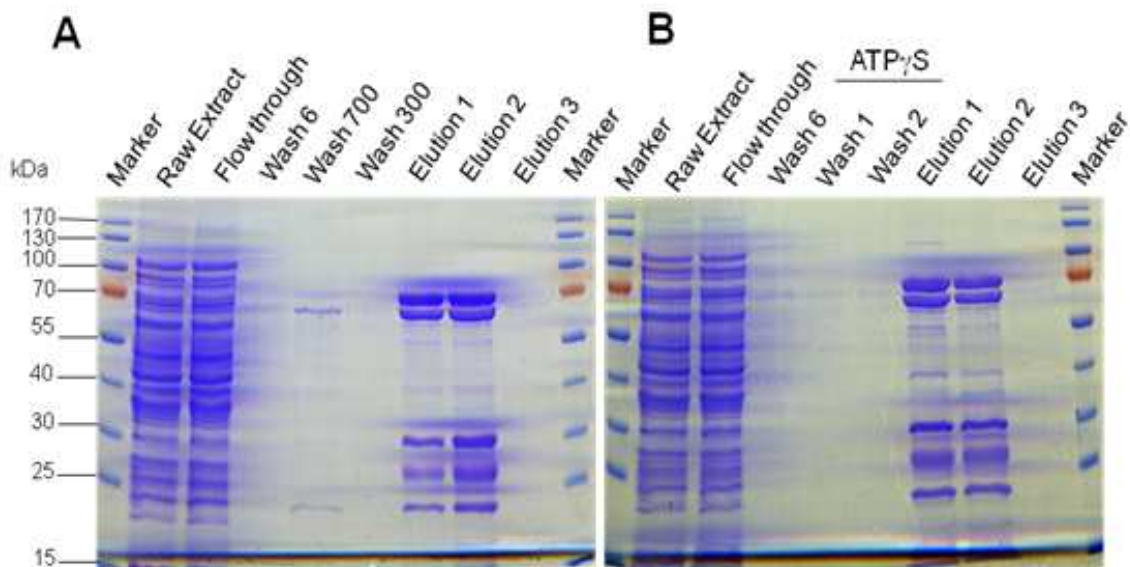


Figure 3.9 | Disruption of the interaction between H₆-AtElp3-Strp (69.3 kDa) and DnaK. (A) Attempt to disrupt the protein-protein interaction using high salt concentration in the Wash buffer. (B) Use of ATP γ S to disrupt the interaction between H₆-AtElp3-Strp and DnaK proteins. 20 μ l of 2.5 ml elution samples was analyzed on 12% SDS-PAGE.

A second affinity purification step made use of the C-terminal Strep epitope tag on the H₆-AtElp3-Strp protein. The eluates from the first purification step (Section 3.1.4.2; Figure 3.8A) were pooled, concentrated 4-fold and loaded on a Strep-Tactin matrix. The matrix was washed and bound proteins were eluted with elution buffer containing 2.5 mM desthiobiotin. The result (data not shown) indicated that trace amounts of H₆-AtElp3-Strp protein could be bound and eluted from the Strep-Tactin matrix, but almost all the Ni-NTA-agarose purified H₆-AtElp3-Strp protein loaded on the Strep-Tactin matrix was collected in the flow through. This may be an indication that the H₆-AtElp3-Strp protein either loses its Strep epitope tag or binds poorly to the Strep-Tactin column. Therefore, the C-terminal Strep epitope-tag of H₆-AtElp3-Strp is apparently not accessible for binding and hence cannot be used for the disruption of H₆-AtElp3-Strp from DnaK and protein enrichment by purification on Strep-Tactin column.

3 RESULTS

3.2 Purification of recombinant AtElp3 protein variants from inclusion body preparations

Several trials have been made to increase the binding properties and yield of AtElp3 protein in solution. However, no significant improvement has been achieved. Although high amount of the H₆-AtElp3-Strp protein could be recovered after purification using the pON-ELO3-3 construct on Ni-NTA-agarose matrix (Figure 3.8), its interaction with the heat shock protein DnaK could not be disrupted (Figure 3.9). In all cases, over 90% of the AtElp3 protein formed inclusion bodies. Therefore purification under denaturing conditions from solubilized inclusion body preparations was considered.

3.2.1. Purification of H₆-AtElp3-Strp protein expressed from the pON-ELO3-3 construct

An *E. coli* strain BL21(DE3) expressing H₆-AtElp3-Strp from the pON-ELO3-3 construct was harvested, the cells were disrupted and soluble crude extract was separated from the inclusion body pellet fraction by centrifugation at 17000 rpm for 30 minutes at 4°C. The inclusion body pellet was then solubilized using solubilization buffer containing 8 M urea and 2 mM DTT. The soluble fraction recovered after a further centrifugation step at 25000 rpm is referred to as the inclusion body fraction. Approximately 50 mg inclusion body preparation was recovered from a liter culture upon solubilization in 20 ml solubilization buffer. The inclusion body preparation was loaded on Ni-NTA-agarose column and the elution of bound H₆-AtElp3-Strp protein was achieved under denaturing conditions using elution buffer containing 8 M urea supplemented with 250 mM imidazole. The yield of H₆-AtElp3-Strp protein obtained after purification was very low. Low amounts of H₆-AtElp3-Strp protein could be attributed to loss of the N-terminal His₆ tag since only full length AtElp3 protein could be purified using this construct (Figure 3.10). High levels of H₆-AtElp3-Strp protein degradation products (30, 40, 65 kDa) could indeed be observed on SDS-PAGE in the crude extract, but their purification was impossible due to loss of N-terminal His₆-tag. Only a total of 100 µg H₆-AtElp3-Strp protein was obtained from 50 mg protein after purification on Ni-NTA-agarose under denaturing conditions. The low

3 RESULTS

yield of H₆-AtElp3-Strp upon purification from inclusion bodies may be attributed to poor binding of the N-terminal His₆-tag of H₆-AtElp3-Strp on Ni-NTA-agarose matrix.

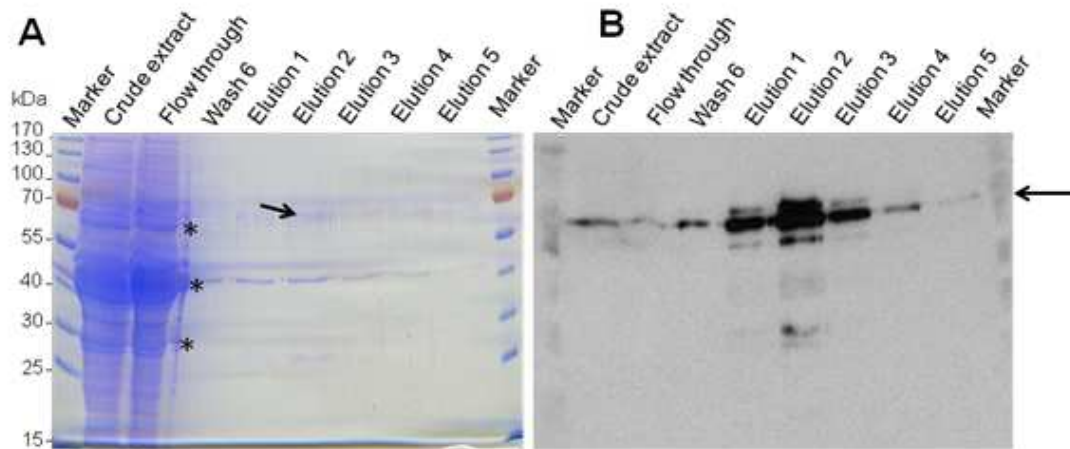


Figure 3.10 | Affinity chromatography of the H₆-AtElp3-Strp protein from inclusion bodies generated from the pON-ELO3-3 construct. (A) Analysis of H₆-AtElp3-Strp samples obtained upon purification on Ni-NTA-agarose on 12% SDS-PAGE and samples were visualized by Commassie staining. (B) Western blot analysis of the non-native H₆-AtElp3-Strp probes using α -His₆ antibody. 20 μ l fraction from each 2.5 ml elution sample was analyzed. The position of full length H₆-AtElp3-Strp protein is indicated by an arrow and the degradation products (30, 40 and 65 kDa) are marked with asterisk (*).

To check if AtElp3H₆ protein could be enriched upon affinity purification from inclusion body preparation under denaturing conditions, the accessibility of a C-terminal His₆-tag for binding on Ni-NTA-agarose was tested. Inclusion bodies prepared from *E. coli* BL21(DE3) cells expressing AtElp3H₆ from the pON-ELO3-1 construct, analogous to the pON-ELO3-3 construct (Section 3.2.1), were used for affinity purification.

3.2.2 Affinity purification of AtElp3H₆ protein using the pON-ELO3-1 construct

Upon overexpression of AtElp3 as a C-terminal His₆-tagged fusion protein from *E. coli* BL21(DE3) carrying the pON-ELO3-1 expression construct, a total of 50 mg of AtElp3H₆ inclusion body preparation was obtained per liter culture, after dissolution of the AtElp3H₆ inclusion body pellet in lysis buffer containing 8 M urea as described in section 3.2.1. For the purification of the AtElp3H₆ protein, the inclusion body sample was applied on a Ni-NTA-agarose matrix. All buffers used were supplemented with 8 M urea. Under denaturing conditions, the AtElp3H₆ protein binds efficiently to the

3 RESULTS

Ni-NTA-agarose and could be purified in a purification step. The full length AtElp3H₆ protein and three major degradation products of 65, 40 and 30 kDa were observed upon analysis of the elution fractions (Figure 3.11). The truncation of AtElp3H₆ protein occurred at the N-terminus, since the Western blot revealed that the C-terminal His₆-tag on these degradation products was retained. A total of 12 mg AtElp3H₆ protein was recovered after affinity purification from 50 mg inclusion bodies (Table 3.0). This protein was reconstituted and used for further analyses. The summary of the various constructs used for the purification of full length AtElp3 protein and the radical SAM domain variants is illustrated in Table 3.0.

Table 3.0 | Overview of the different constructs used for purification of the full length AtElp3 protein and radical SAM domain variants

Protein variant	Expression plasmid	Purification matrix / condition	[§]Total protein loaded [mg]	[∅]Yield after purification [mg]	Estimated amount of purified protein [%]
AtElp3-H₆	pON-ELO3-1	Ni-NTA-agarose Native	148	1.3	0.9
AtElp3-H₆	pON-ELO3-1	Ni-NTA-agarose non-native	50	12	24.0
Strp-AtElp3-H₁₀	pON-ELO3-2	Ni-NTA-agarose Native	128	2.4	1.9
H₆-AtElp3-Strp	pON-ELO3-3	Ni-NTA-agarose Native	324	2.3	0.7
H₆-AtElp3-Strp	pON-ELO3-3	Ni-NTA-agarose non-native	50	0.1	0.2
AtElp3(76-366)H₆	pON1	Ni-NTA-agarose Native	212	1.8	0.9
AtElp3(111-366)H₆	pON2	Ni-NTA-agarose native	227	1.1	0.5

[§]- Crude extract protein from 1 liter culture loaded on matrix

[∅]- Total amount of protein recovered after purification determined by Bradford (1976) method

3 RESULTS

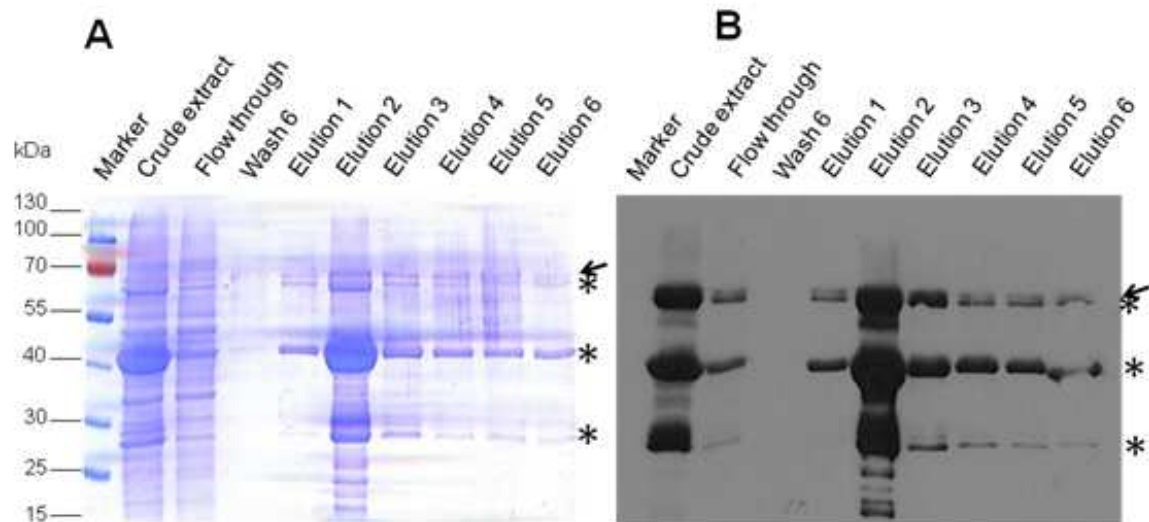


Figure 3.11 | Affinity purification of the AtElp3H₆ protein from inclusion bodies generated using the pON-ELO3-1 construct. (A) Affinity purification of AtElp3H₆ from inclusion bodies under denaturing conditions by Ni-NTA chromatography. Samples were separated on 12% SDS-PAGE and visualized by Commassie staining. (B) Western blot analysis of the denatured AtElp3H₆ samples using α -His₆ antibody. 20 μ l fraction from each 2.5 ml elution sample was analyzed. The full length AtElp3H₆ protein is designated by an arrow and the degradation products (65, 40 and 30 kDa) are marked with asterisks (*)

3.2.2.1 Refolding and reconstitution of denatured AtElp3 protein purified under non-native conditions

Iron-sulfur clusters with substantial inherent stability in anaerobic solutions have been spontaneously generated *in vitro* from iron III and sulfide salts, in the presence of organic thiolate compounds (Beinert *et al.*, 1997; Rao & Holm 2004). To try to reconstitute the hypothetical [Fe-S] cluster in AtElp3 protein, about 2-5 mg AtElp3H₆ protein purified under denaturing conditions on Ni-NTA-agarose matrix was diluted with Tris.HCl buffer, pH8.0 containing ammonium iron (III) citrate and 2 mM DTT to a urea concentration of 2 M. The protein sample was then incubated with Tris.HCl buffer, pH8.0 supplemented with 20 mM Li₂S and 2 mM DTT for 20 minutes. At the end of the reconstitution step, the AtElp3H₆ protein sample was dialysed overnight at 4°C against buffer W (50 mM Tris.HCl, pH8.0; 150 mM NaCl). Upon centrifugation of the dialyzed protein sample at 20000 rpm for 30 minutes, approximately 75% of AtElp3H₆ protein was usually recovered in the supernatant fraction after [Fe-S] cluster reconstitution. Sometimes the AtElp3H₆ protein aggregated and pelleted after centrifugation at 14000 rpm indicating the absence of proper reconstitution. To

3 RESULTS

remove residual aggregates and excess iron and sulfur salts, the reconstituted AtElp3H₆ protein was further purified by gel filtration.

3.2.2.2 Chromatography of reconstituted AtElp3H₆ protein by gel filtration

The reconstituted AtElp3H₆ protein was loaded on a Superdex 200 column equilibrated with buffer W (50 mM Tris.HCl, pH8.0; 150 mM NaCl). A major and a minor protein peak were eluted (Figure 3.12A). The AtElp3H₆ protein and its degradation products were only detected in the major peak in fractions 8-12 (Peak A) at a retention volume of 10 ml. These fractions were pooled, concentrated and analyzed by SDS-PAGE and Western blot (Figure 3.12B, C). The reconstituted and gel-filtration purified AtElp3H₆ protein was then used for characterization studies.

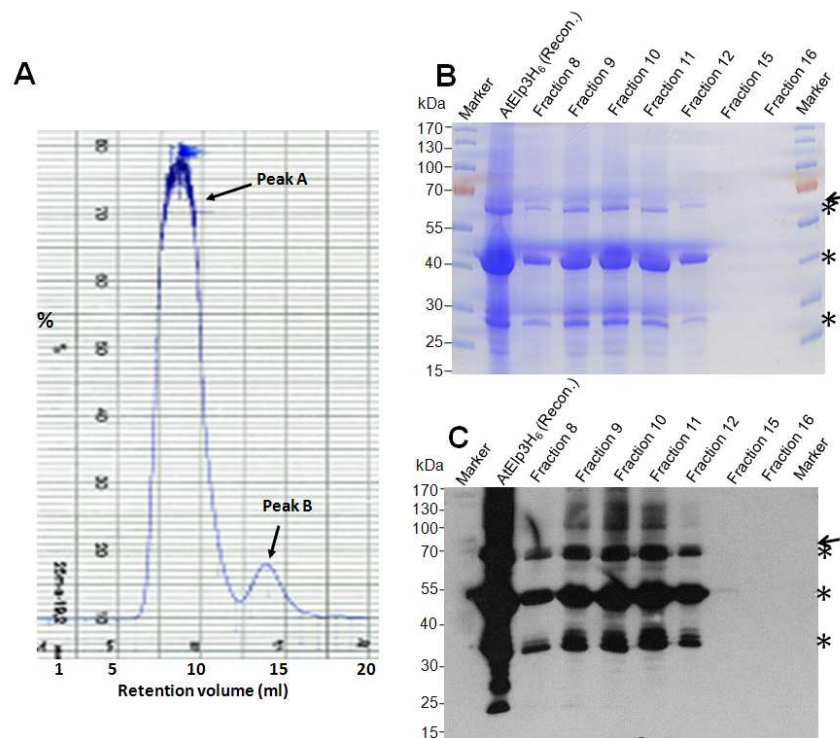


Figure 3.12 | Chromatography of reconstituted AtElp3H₆ protein by gel filtration and analyses of eluted fractions. (A) Elution profile of AtElp3H₆ protein purified by gel filtration on Superdex 200. The reconstituted AtElp3H₆ protein eluted as a major peak (Peak A) at a retention volume of 10 ml. A minor peak without AtElp3H₆ was also eluted (Peak B) at a retention time of 14 ml. (B) Analysis of reconstituted and purified AtElp3H₆ probes on 12% SDS-PAGE stained with Coomassie reagent. (C) Western blot analysis of reconstituted and purified AtElp3H₆ samples detected with α-His₆ antibody. 20 μl fraction from each 2 ml elution sample was analyzed. The position of full length AtElp3H₆ protein is designated by an arrow and degradation products are marked with asterisks (*).

3 RESULTS

3.3 Biochemical characterization and analyses of wild type AtElp3 proteins

3.3.1 UV-visible absorption spectroscopic analyses of AtElp3 variants

First attempts to characterize the AtElp3 protein were made with the isolated H₆-AtElp3-Strp protein samples (Section 3.1.4.2, Figure 3.8A), which were subjected to UV-visible absorption spectroscopic analysis. Scanning the eluates in the UV-VIS range (260-700 nm) gave a broad peak with a long tail at 420 nm (Figure 3.13A). Additionally, the AtElp3H₆ variant purified under non-native conditions from inclusion bodies, reconstituted and purified by gel-filtration (Section 3.2.2.2, Figure 3.12B) was also analyzed by UV-visible spectroscopy (Figure 3.13B). Similar result was obtained like for the H₆-AtElp3-Strp protein, but with an additional broad peak at about 615 nm. The broad peaks observed at 420 nm in both cases are hallmarks for [4Fe-4S] cluster-containing proteins and could be reduced in the presence of sodium dithionite (Figure 3.13A). This is a hint that both variants of the AtElp3 (H₆-AtElp3-Strp and AtElp3H₆) protein are [Fe-S] cofactor-containing proteins.

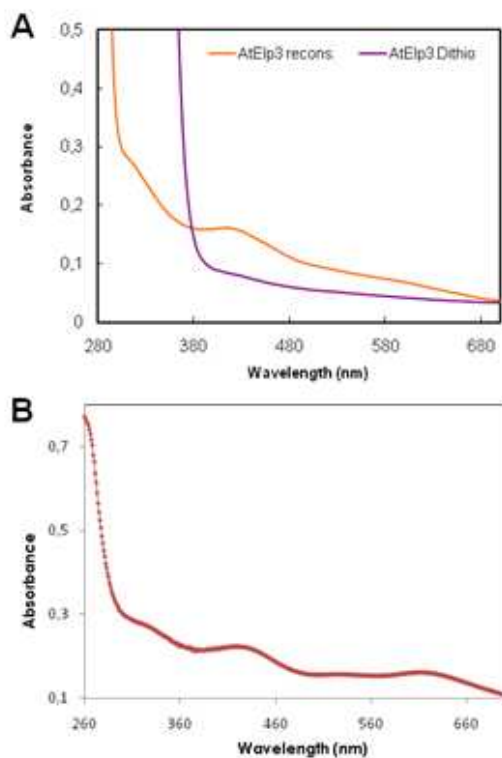


Figure 3.13 | UV-visible spectroscopic analyses of AtElp3 protein. (A) UV-visible absorption spectrum of full length H₆-AtElp3-Strp protein purified on Ni-NTA-agarose under native conditions (Figure 3.8A). The absorbance ratio A_{400}/A_{280} is given as 0.1. The broad peak at 420 nm disappeared upon reduction with 2 mM sodium dithionite, confirming H₆-AtElp3-Strp protein as an [Fe-S] binding protein. (B) UV-visible absorption spectrum of non-native purified and reconstituted AtElp3H₆ protein. The AtElp3H₆ protein was purified by affinity and size exclusion chromatography and its [Fe-S] cluster(s) reconstituted using Fe³⁺ and S²⁻ salts. The concentration of AtElp3H₆ protein used for the UV-VIS analysis was 0.39 mg/ml, with absorbance ratio A_{400}/A_{280} of 0.5

3 RESULTS

3.3.2 EPR spectroscopic characterization of reconstituted AtElp3H₆ protein

Based on the ferromagnetic properties of iron-sulfur clusters, different types of [Fe-S] clusters can be characterized using electron paramagnetic resonance (EPR) spectroscopic method. To further characterize the [Fe-S] cofactor bound by the reconstituted AtElp3H₆ protein, the reconstituted protein sample was reduced with sodium dithionite and subjected to further analysis by EPR. This involves exchange of the gas phase of the protein sample with N₂. The protein was then frozen at -70°C to allow its gradual oxidation (autooxidation) under the influence of a magnetic field. The EPR result obtained on analysis of the AtElp3H₆ protein sample at 30 K is shown in Figure 3.14. The spectrum contains a cuboidal signal with a g-value of 2.015 that is characteristic of [3Fe-4S]⁺¹ cluster similar to that observed in *Desulfovibrio gigas* Ferredoxin II (Moreno *et al.*, 1994), pyruvate formate-lyase activating enzyme (Broderick *et al.*, 2000) and the enzyme aconitase (Kent *et al.*, 1985). The EPR Experiment was carried out in the laboratory of Prof. Peter Kroneck at the University of Konstanz.

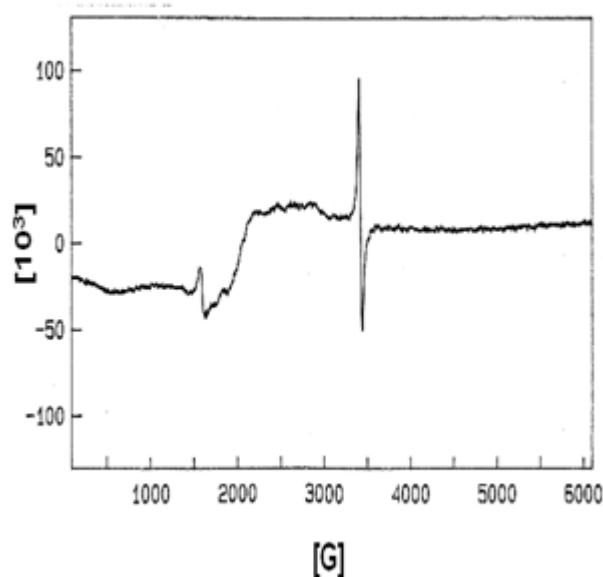


Figure 3.14 | EPR spectrum of [Fe-S] cluster in the reconstituted AtElp3H₆ protein. The EPR spectrum of AtElp3H₆ protein (50 μM) was measured after autooxidation (under N₂ at -70°C for 20 minutes). The EPR Spectrum was recorded under the following conditions: 30 K; Microwave Power, 2 mW; Microwave Frequency, 9.654 GHz; Center field, 3100 G, Sweep Width, 6000 G; Resolution, 1024 points; Number of Scans, 4. The sharp peak seen at g value of 2.015 represents a [3Fe-4S]⁺¹ cluster

3 RESULTS

3.3.3 Mass spectrometric analyses of full length AtElp3H₆ protein and degradation products

Purified AtElp3H₆ protein was always associated with formation of degradation products (Figure 3.11; 3.12). To confirm the full length AtElp3H₆ and to characterize the degradation products, the respective fragments were excised from a 12% SDS-PAGE gel and restricted by tryptic peptide cleavage followed by MALDI/TOF MS analyses. The results confirmed the AtElp3 full length sequence of the top band since the peptide containing the initial methionine residue of AtElp3H₆ was observed. Also peptides that show 100% identity to the AtElp3H₆ protein sequence were also seen in the degradation products (Figure 3.15; Table 3.1).

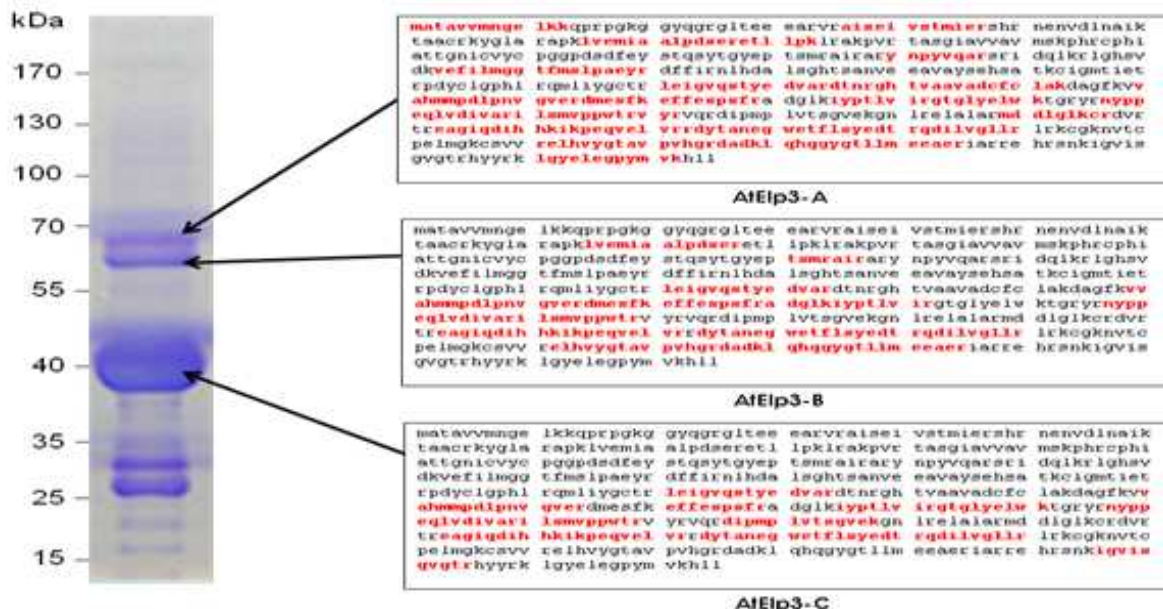


Figure 3.15 | MALDI/TOF Mass spectrometric analysis of full AtElp3H₆ protein and its degradation products. The full length AtElp3H₆ protein (67.4 kDa) is denoted as AtElp3-A and its degradation products of 65 kDa depicted as AtElp3-B and 40 kDa illustrated as AtElp3-C. The matched peptides are shown in red. Sequence cleavage of the analyzed probes (AtElp3-A, AtElp3-B and AtElp3-C) was carried out with trypsin which cuts C-terminal side of KR unless next residue is P. Also refer to Figure 3.1.

The MALDI/TOF Mass spectrometric data confirmed the result obtained upon Western blotting of purified AtElp3H₆ protein (Figure 3.11). The two major degradation products, AtElp3-B (65 kDa) and AtElp3-C (40 kDa) resulted from N-terminal truncation of the full length AtElp3H₆ protein, AtElp3-A (67.4 kDa) (Figure 3.15), since the C-terminal His₆-tags on the degradation products were still

3 RESULTS

observed. The matched sequences after trypsin cleavage are designated in red. The difference between the two degradation products of AtElp3H₆ is the site of cleavage. The AtElp3-B fragment was cleaved close to the N-terminus and still contains all the conserved cysteine residues in the radical SAM domain. The AtElp3-C fragment was cleaved around the middle of the AtElp3H₆ protein and it lacks the first 6 conserved cysteine residues of the radical SAM domain.

The summary of the results obtained on analyses of the full length AtElp3H₆ protein, and its degradation products by MALDI/TOF mass spectrometric method is shown in Table 3.1.

Table 3.1 | Summary of AtElp3 MALDI/TOF Mass spectrometric analyses data

Sample	Match to	Score	Mol. Wt (kDa)	pI	Sequence coverage (%)
AtElp3-A	AtElp3	87	63,7	8,92	49
AtElp3-B	AtElp3	48	63,7	8.92	34
AtElp3-C	AtElp3	885	63,7	8.92	26

3.4 Recombinant expression of yeast Elp3 (ScElp3)

In order to address the functional significance of the radical SAM domain, further studies were considered using the ScElp3 protein. Previous studies were conducted using the AtElp3 protein. This was based on the fact that the Elp3 project was financed in a plant-related initiative. Elongator mutant phenotypes have been well characterized in the yeast *Saccharomyces cerevisiae* (Frohloff *et al.*, 2001; Jablonowski *et al.*, 2001; Fichtner & Schaffrath 2002; Huang *et al.*, 2005) and thus would allow for easy monitoring of the consequences of mutations in the radical SAM domain. Based on the high sequence similarity of AtElp3 and ScElp3, equivalent exchanges of conserved amino acid residues could be made on the ScElp3 protein. For the production of ScElp3 protein required for *in vitro* characterization studies, the *ScELP3 ORF* was cloned into pET-21b plasmid and the ScElp3 expressed in *E. coli* BL21(DE3) as a C-terminal His₆ fusion protein (ScElp3H₆).

3 RESULTS

3.4.1 Expression of ScElp3H₆ protein

The *ScELP3* ORF was amplified from the pFF7 template by PCR using *Pfu* DNA polymerase. The PCR product obtained was then cloned into the *Sal*I site of the pET-21b (Novagene) plasmid. The resulting expression vector pON-ELP3-1 (Figure 3.16A) generated was sequenced to exclude additional mutation in the *ScELP3* ORF during PCR amplification. The pON-ELP3-1 plasmid was transformed into *E. coli* BL21(DE3) strain and used for protein expression. Single colonies of the BL21(DE3) *E. coli* strain carrying the pON-ELP3-1 plasmid were used for the expression of wild type ScElp3H₆ as C-terminal His₆-tagged fusion protein, after induction with 0.1 mM IPTG at 37°C in 20 ml cultures. Upon protein expression, the total cell protein (TCP) fractions were analyzed by Western blotting (Figure 3.16B).

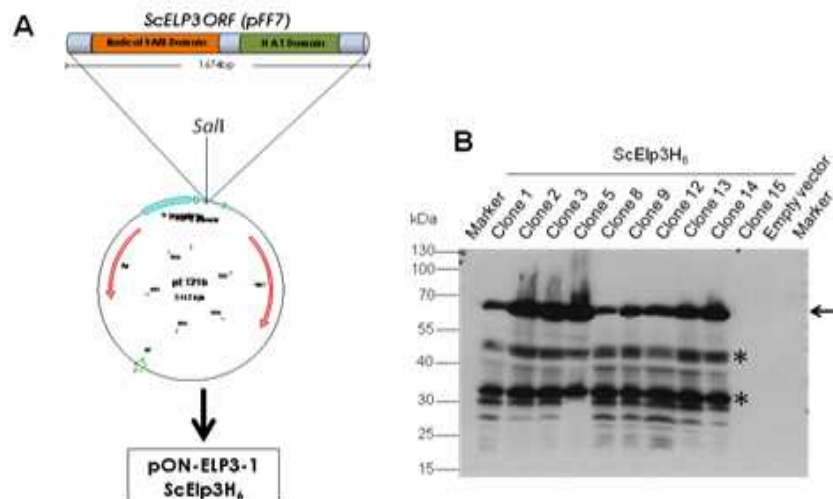


Figure 3.16 | Cloning and expression of wild type ScElp3H₆ (67.4 kDa) protein from different *E. coli* BL21(DE3) clones. (A) The cloning of full length *ScELP3* ORF obtained from pFF7 by PCR amplification into the *Sal*I site of the pET-21b vector, generating a *ScELP3* expression construct, pON-ELP3-1. The pON-ELP3-1 plasmid expresses a C-terminal His₆-tagged ScElp3 wild type fusion protein, ScElp3H₆. (B) Western blot analysis of the expression profile of ScElp3H₆ protein from different *E. coli* clones using α -His₆ antibody. Full length ScElp3H₆ (67.4 kDa) protein is indicated by an arrow (\leftarrow) and the two major degradation products are designated with asterisk (*). The OD_{600nm} from the culture of each clone was normalized and equal amount of the total cell protein (TCP) samples was analyzed. Empty vector is the pET-21b plasmid without insert.

The result confirmed that the wild type ScElp3H₆ protein could be expressed as a C-terminal His₆-tagged fusion protein in almost all the clones tested (Figure 3.16B). Higher yield of ScElp3H₆ full length was observed in comparison to AtElp3H₆ protein (Figure 3.1). Apart from the full length ScElp3H₆ protein (67.4 kDa), two prominent

3 RESULTS

degradation products were observed (45 kDa and 35 kDa). The degradation products were the result of truncation of the full length ScElp3H₆ protein at the N-terminus, since both degradation products retained the His₆-tag and thus could be seen upon Western blotting using α -His₆ antibody.

To study the effect of temperature on the solubility of ScElp3H₆ protein, *E. coli* cells expressing ScElp3H₆ were induced with 0.1 mM IPTG at different temperatures and cells were harvested and disrupted by ultrasonication. Subsequently, different fractions of the *E. coli* cells were analyzed on SDS-PAGE and by Western blotting (Figure 3.17). The result showed that ScElp3H₆ protein was detected mostly in the insoluble inclusion body fraction, as was also observed for AtElp3H₆ (Figure 3.0). The highest amount of the ScElp3H₆ protein was expressed at 37°C (Figure 3.17).

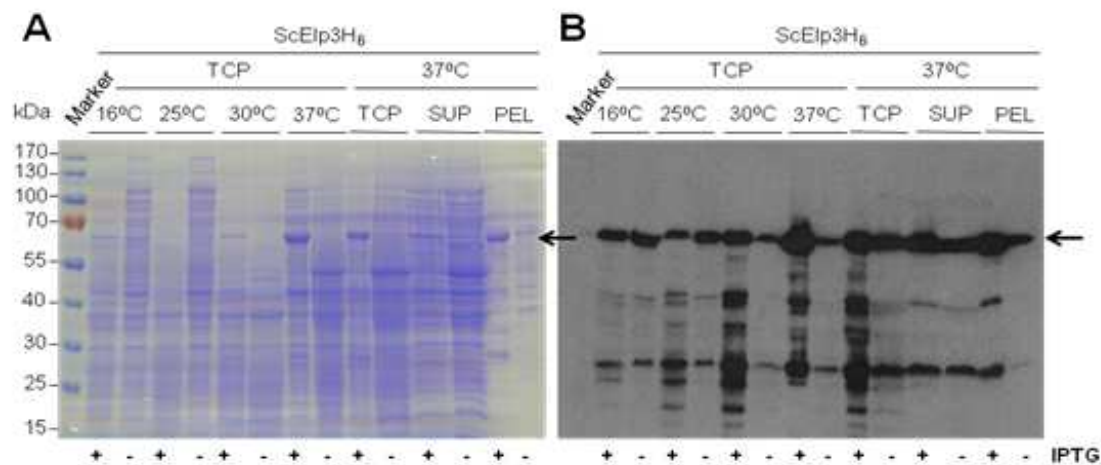


Figure 3.17 | Solubility analyses of wild type ScElp3H₆ protein expressed in different *E. coli* cell fractions at varying temperatures. (A) Analysis of wild type ScElp3H₆ protein in different *E. coli* cell fractions on SDS-PAGE stained with Coomassie reagent (B) Western blot detection of ScElp3H₆ using α -His₆-antibody. Full length ScElp3H₆ (67.4 kDa) protein is designated by an arrow (\leftarrow). 50 μ g soluble protein (SUP) and equal amount of OD₆₀₀ units of total cell protein (TCP) and pellet (PEL) fractions were analyzed on 12% SDS-PAGE. +/- indicates induced / non-induced with IPTG.

3.4.2 Purification of full length ScElp3H₆ protein on Ni-NTA-agarose matrix

Although most of the wild type ScElp3H₆ protein was expressed as inclusion bodies, about 10% of the ScElp3H₆ protein could be recovered in the soluble cell extract fraction (Figure 3.17). This fraction of ScElp3H₆ protein was subjected to Ni-NTA chromatography. One liter of *E. coli* BL21(DE3) strain transformed with pON-ELP3-1 plasmid was used for ScElp3H₆ protein expression at 37°C upon induction with 0.1 mM IPTG. Cells were harvested and disrupted by ultrasonication and soluble cell

3 RESULTS

extract fraction recovered after centrifugation was loaded on Ni-NTA-agarose column. After the wash steps, the proteins bound on the matrix were eluted using Elution buffer containing imidazole. The samples obtained after affinity purification of ScElp3H₆ on Ni-NTA-agarose matrix were then analyzed on SDS-PAGE and by Western blotting (Figure 3.18).

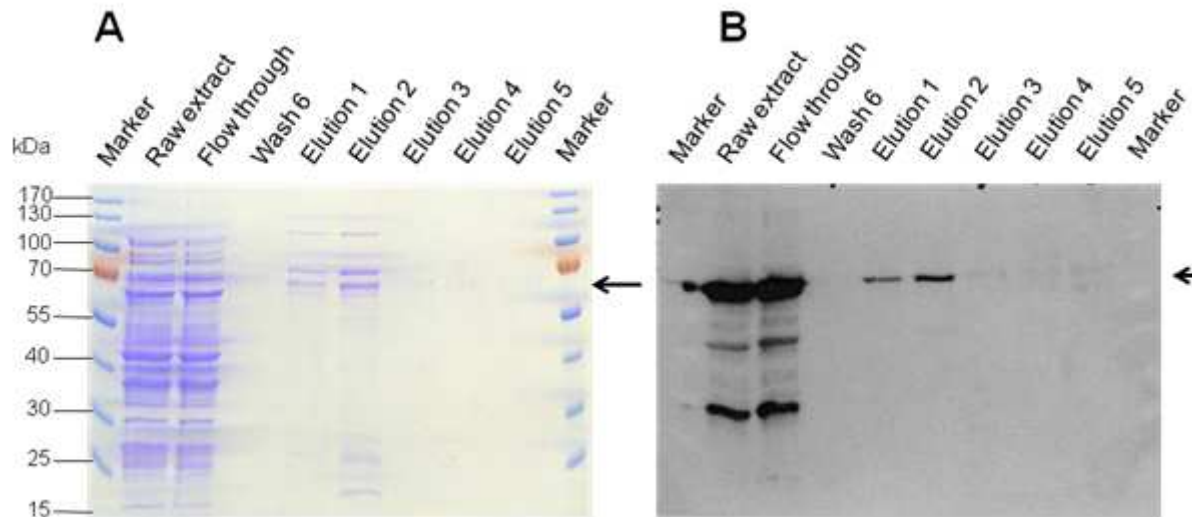


Figure 3.18 | Analysis of wild type ScElp3H₆ (67.4 kDa) upon affinity purification on Ni-NTA-agarose matrix. (A) Analysis of samples after affinity purification of ScElp3H₆ on 12% SDS-PAGE and gel stained with Coomassie reagent. (B) Detection of ScElp3H₆ protein by Western blotting using α -His₆ antibody. 20 μ l sample from 2.5 ml elution fractions was analyzed. The full length ScElp3H₆ protein (67.4 kDa) is designated with an arrow (\leftarrow).

The result indicates that the ScElp3H₆ protein was almost completely in the flow through fraction. Similar result was achieved upon affinity chromatography of AtElp3H₆ protein (Figure 3.1). Only a small amount (650 μ g) of ScElp3H₆ was recovered after affinity purification under native conditions (Figure 3.18). The low binding efficiency of the C-terminally tagged ScElp3H₆ protein on Ni-NTA-agarose is similar to the finding with AtElp3H₆ protein (Figure 3.1). Thus, the C-terminus of Elp3H₆ proteins is probably not accessible under native conditions and hence is not ideal for use for affinity purification of ScElp3H₆. Alternative tagging of the ScElp3 protein was considered for use in further expression and purification experiments to produce enough amounts of ScElp3H₆ protein required for characterization studies. Based on the fact that the C-terminal His₆-tag is not ideal for purification of ScElp3H₆ protein, alternative tagging of the ScElp3 protein was considered. The wild type ScELP3 ORF was excised using *SalI/XhoI* from the pON-ELP3-1 construct and

3 RESULTS

cloned into the *SaI* site of pASK-IBA-43, as already described for AtElp3 in section 3.1.4. The resulting plasmid pON-ELP3-2 expresses the wild type H₆-ScElp3-Strp as an N-terminal His₆- and C-terminal Strep-tagged fusion protein. The primary amino acid sequence of the H₆-ScElp3-Strp encodes a 610 aa H₆-ScElp3-Strp wild type fusion protein, with an approximate molecular weight of 69.5 kDa.

3.4.3 Expression and affinity chromatography of H₆-ScElp3-Strp protein under native conditions on Ni-NTA-agarose

The purification of the wild type H₆-ScElp3-Strp under native condition on the Ni-NTA-agarose column was carried out using 1 liter culture from the expression of the pON-ELP3-2 construct in *E. coli* BL21(DE3) strain. After protein expression, the cells were harvested; disrupted and soluble cell extract recovered after centrifugation was then loaded on Ni-NTA-agarose matrix. The proteins bound to the matrix were eluted using 0.5 column volume of elution buffer containing imidazole. The wild type H₆-ScElp3-Strp protein bound to the Ni-NTA-agarose could be eluted in a sharp peak, although most of the wild type H₆-ScElp3-Strp protein was present in the inclusion body fraction (Figure 3.19). Also small amount of the H₆-ScElp3-Strp protein could be found in the flow through indicating low binding efficiency on Ni-NTA-agarose matrix. The wild type H₆-ScElp3-Strp protein like the H₆-AtElp3-Strp protein (Figure 3.8) interacts strongly with DnaK (data not shown), as confirmed by the use of α -DnaK antibody (Figure 3.8C). The molecular chaperone, DnaK may function in the stabilization of H₆-ScElp3-Strp protein by binding to its hydrophobic regions to prevent protease attack and / or irregular 3-dimensional folding.

The sum of 4.9 mg protein was eluted upon purification of wild type H₆-ScElp3-Strp protein on Ni-NTA-agarose matrix (Figure 3.19). The purified full length H₆-ScElp3-Strp protein still contains C-terminal degradation products and contaminating impurities. Attempts to remove these by-products by affinity chromatography using the Strep-tag on the C-terminus were not successful. Similar result was obtained for H₆-AtElp3-Strp protein (data not shown).

3 RESULTS

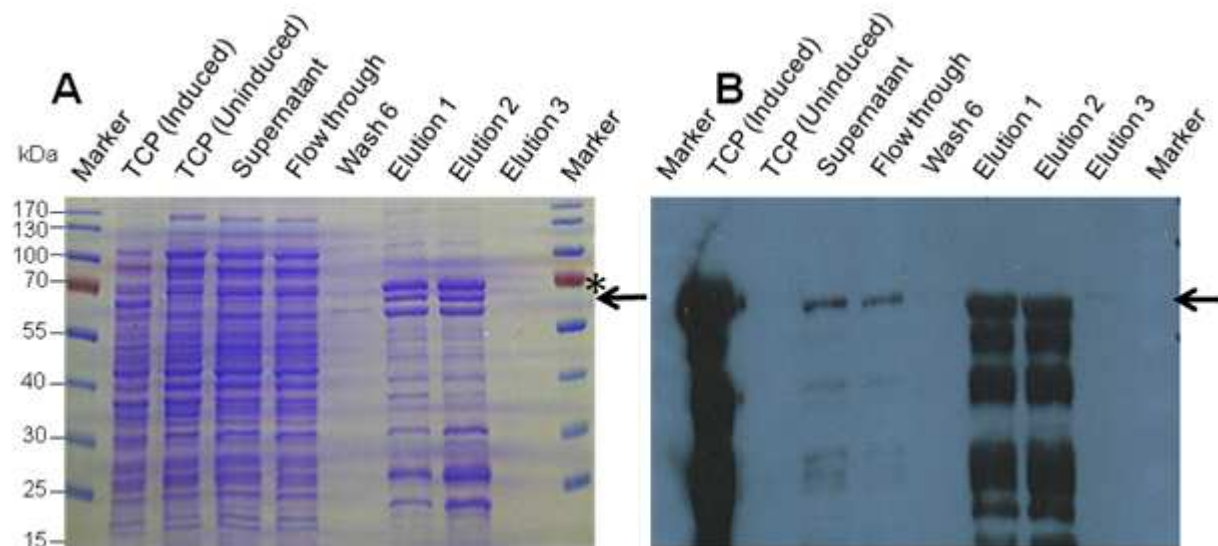


Figure 3.19 | Affinity chromatography of H₆-ScElp3-Strp wild type protein on Ni-NTA-agarose matrix and analyses of samples. (A) Analysis of H₆-ScElp3-Strp protein samples after affinity chromatography on 12% SDS-PAGE. (B) Detection of purified H₆-ScElp3-Strp protein by Western blot using α -His₆ antibody. Arrow indicates the full length H₆-ScElp3-Strp protein and asterisk (*) depicts DnaK confirmed with α -DnaK antibody (data not shown). TCP, total cell protein. 20 μ l sample from the 2.5 ml elution fractions was analyzed.

The elution fractions 1 and 2 of H₆-ScElp3-Strp were pooled and analysed by UV-visible absorption spectroscopy (Figure 3.20) via scanning in the UV-VIS range. The UV-visible absorption spectrum of the H₆-ScElp3-Strp eluates indicated the presence of [4Fe-4S] cluster, which is a hallmark of all radical SAM AdoMet proteins (Sofia *et al.*, 2001). The broad peak observed at 420 nm was reduced in the presence of sodium dithionite.

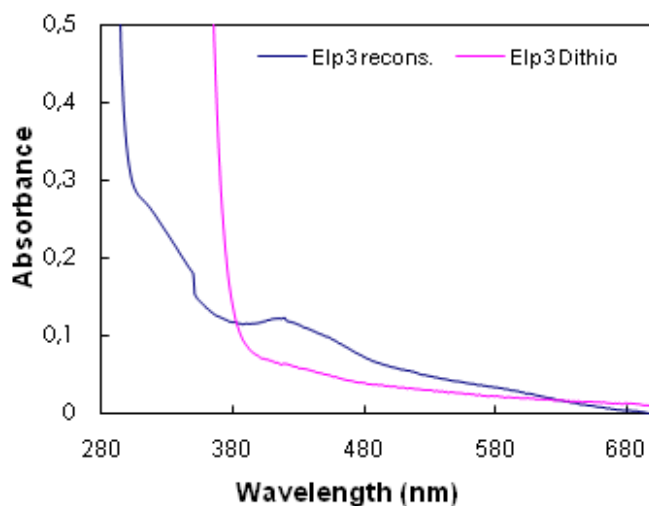


Figure 3.20 | Analysis of H₆-ScElp3-Strp by UV-visible absorption spectroscopic method. UV-visible absorption spectrum of wild type H₆-ScElp3-Strp purified under native conditions on Ni-NTA-agarose with an absorbance ratio A_{400}/A_{280} 0.1. The broad peak at 420 nm characteristic of [4Fe-4S] disappeared upon reduction with 2 mM sodium dithionite, confirming H₆-ScElp3-Strp as an [Fe-S] containing protein.

3 RESULTS

To produce and purify high amounts of ScElp3 protein without contaminating impurities that is needed for characterization studies, other expression constructs and reagents would be required. To achieve this goal, attempts were made to increase ScElp3 protein yield by employing different ScElp3 expression constructs, coexpression plasmids and osmolytes.

3.4.4 Attempts to improve folding and solubility of ScElp3

Native folding of aggregation-prone recombinant proteins could be enhanced by the use of osmolytes, plasmid- or benzyl alcohol-overexpressed molecular chaperones (De Marco *et al.*, 2005). To improve native folding of wild type ScElp3 protein, different constructs, coexpression plasmids and osmolytes were utilized (Table 3.2). For protein expression in 100 ml cultures, induction of *E. coli* BL21(DE3) strains carrying the pON-ELP3-1 plasmid, expressing the ScElp3H₆ protein was achieved using 0.1 mM IPTG. Likewise, *E. coli* strain containing the pON-ELP3-2 construct, expressing H₆-ScElp3-Strp protein was induced with 20 µg anhydrotetracycline. The osmolytes utilized for ScElp3 protein expression were added 30 minutes prior to induction. The ScElp3 protein variants were expressed at 20°C for 3 hours. The different ScElp3 constructs, coexpression plasmids and osmolytes used to improve the ScElp3 protein yield are illustrated in Table 3.2. After ScElp3 protein expression using constructs in Table 3.2, soluble cell extracts recovered after cell disruption and centrifugation were analyzed by Western blotting using α-His₆ antibody (Figure 3.21). The results revealed varying ScElp3 protein expression profiles upon analysis of 50 µg of soluble cell extracts using probes 1-24 (Table 3.2). The highest yield of soluble ScElp3 protein was observed in probes 9-12 (Figure 3.20; boxed in red). Therefore, increased yield of soluble ScElp3 protein can be achieved using the pON-ELP3-1 construct when coexpressed with the *E. coli* GroEL plasmid (pGroEL) and supplemented with osmolytes. The best osmolytes that resulted to increased ScElp3 soluble protein yield were betaine hydrochloride and NaCl, if added prior to induction of protein expression (Table 3.2; Probe 11). The subsequent step was the large scale expression and affinity purification of the soluble ScElp3H₆ protein using *E. coli* cells transformed with the pON-ELP3-1 construct, coexpressing the pGroEL plasmid and supplemented with betaine hydrochloride and NaCl.

3 RESULTS

Table 3.2 | Wild type ScElp3 constructs, coexpression plasmids and reagents used for protein expression

Probe	ScElp3 expression construct	Coexpression plasmid	Osmolytes
1	pON-ELP3-1 ^d	-	-
2	pON-ELP3-1	-	BA ^a + NaCl
3	pON-ELP3-1	-	Betaine HCl ^b + NaCl ^c
4	pON-ELP3-1	-	BA + Betaine HCl + NaCl
5	pON-ELP3-2 ^e	-	-
6	pON-ELP3-2	-	BA + NaCl
7	pON-ELP3-2	-	Betaine HCl + NaCl
8	pON-ELP3-2	-	BA + Betaine HCl + NaCl
9	pON-ELP3-1	pGroEL ^f	-
10	pON-ELP3-1	pGroEL	BA + NaCl
11	pON-ELP3-1	pGroEL	Betaine HCl + NaCl
12	pON-ELP3-1	pGroEL	BA + Betaine HCl + NaCl
13	pON-ELP3-2	pGroEL	-
14	pON-ELP3-2	pGroEL	BA + NaCl
15	pON-ELP3-2	pGroEL	Betaine HCl + NaCl
16	pON-ELP3-2	pGroEL	BA + Betaine HCl + NaCl
17	pON-ELP3-1	pRKISC ^g	-
18	pON-ELP3-1	pRKISC	BA + NaCl
19	pON-ELP3-1	pRKISC	Betaine HCl + NaCl
20	pON-ELP3-1	pRKISC	BA + Betaine HCl + NaCl
21	pON-ELP3-1	pRKISC + pGroEL	-
22	pON-ELP3-1	pRKISC + pGroEL	BA + NaCl
23	pON-ELP3-1	pRKISC + pGroEL	Betaine HCl + NaCl
24	pON-ELP3-1	pRKISC + pGroEL	BA + Betaine HCl + NaCl

Osmolytes: ^aBA, benzyl alcohol; ^bBetaine HCl, betaine hydrochloride; ^cNaCl, sodium chloride; Plasmids: ^dpON-ELP3-1, ScElp3H₆ expression plasmid; ^epON-ELP3-2, H₆-ScElp3-Strp expression plasmid; ^fpGroEL, *E. coli* GroEL expression plasmid; ^gpRKISC, iron-sulfur cluster (*isc*) operon plasmid.

3 RESULTS

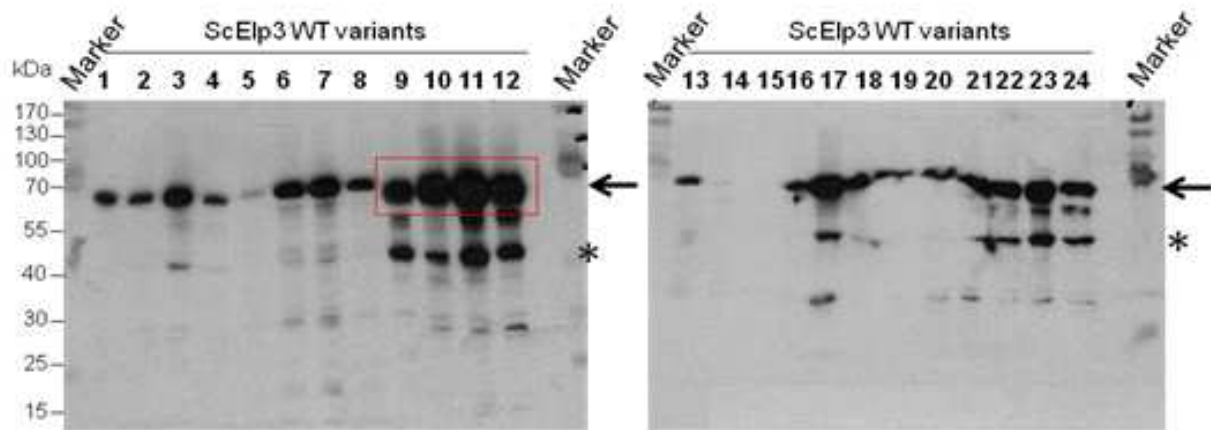


Figure 3.21 | Expression of wild type ScElp3 protein using different constructs, osmolytes and coexpression plasmids. The expressed ScElp3 protein variants were detected by Western blotting using α -His₆ antibody. In each case 50 μ g soluble cell extract sample was analyzed. The full length ScElp3 protein is designated with an arrow (\leftarrow) and the position of the degradation products (40 kDa) is designated by asterisk (*). The different wild type ScElp3 protein expression constructs (Probes 1-24), coexpression plasmids and osmolytes are summarized on Table 3.2. The most soluble ScElp3 protein yield was observed with coexpression of pON-ELP3-1 construct (ScElp3H₆) with pGroEL and supplemented with betaine hydrochloride and NaCl (boxed in red).

3.4.5 Affinity chromatography of wild type ScElp3H₆ protein coexpressed with pGroEL plasmid

For large scale protein expression and affinity chromatography of soluble ScElp3 protein, *E. coli* BL21(DE3) strain expressing the pON-ELP3-1 construct and coexpressing the GroEL was used (Table 3.2; Probe 11) in 1 liter culture as already described (Section 3.4.4). Prior to induction of ScElp3H₆ expression, betaine hydrochloride and NaCl were added to the culture medium. Cells were harvested after protein expression and disrupted. The soluble cell extract recovered upon centrifugation was loaded on Ni-NTA-agarose matrix. The column was then washed and the bound proteins were eluted using elution buffer containing imidazole. The eluted proteins were subjected to analyses by SDS-PAGE and Western blotting (Figure 3.22). The bulk of ScElp3H₆ protein bound to the affinity matrix was eluted in a sharp peak consisting of two eluate fractions amounting to a total of 8 mg protein. Despite the high yield of soluble ScElp3H₆ protein upon affinity chromatography on Ni-NTA-agarose matrix, ScElp3H₆ co-eluted tightly bound to the coexpressed *E. coli* GroEL protein. Attempts to disrupt interaction of both proteins using either ATP γ S or high NaCl concentration were unsuccessful (data not shown).

3 RESULTS

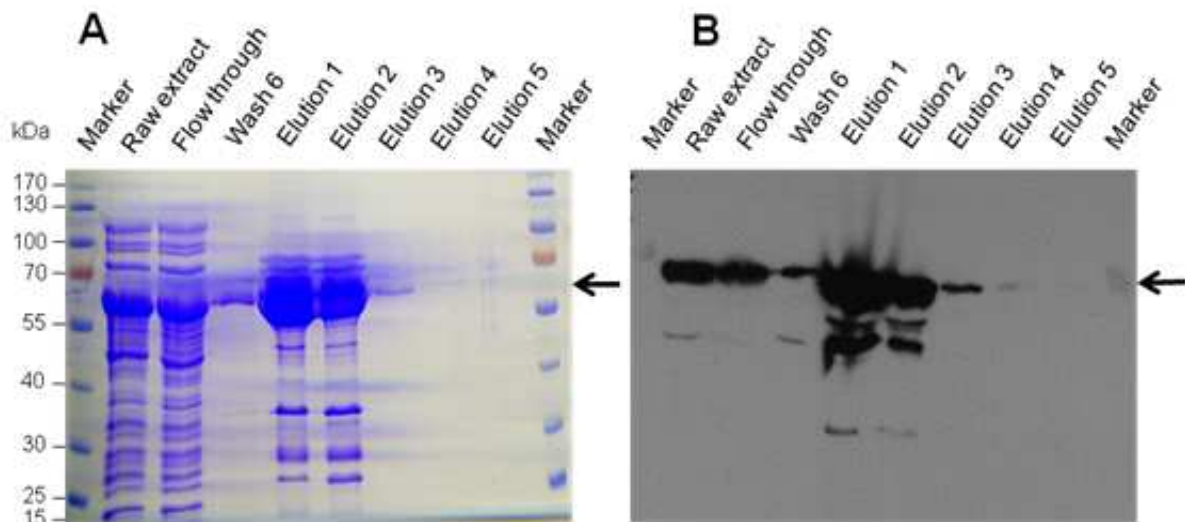


Figure 3.22 | Affinity purification of ScElp3H₆ protein from pON-ELP3-1 construct coexpressed with pGroEL and supplemented with betaine hydrochloride and NaCl. (A) Analysis of ScElp3H₆ affinity purified samples by SDS-PAGE and gel stained with Commassie reagent. (B) Detection of purified ScElp3H₆ samples by Western blotting using α -His₆ antibody. 20 μ l sample from 2.5 ml elution fractions was analyzed. The full length ScElp3H₆ protein tightly bound to the *E. coli* GroEL is designated with an arrow (\leftarrow).

The elution fractions obtained after native purification of ScElp3H₆ protein coexpressed with *E. coli* GroEL (Figure 3.22) were analyzed by mass spectrometry. To confirm if only full length ScElp3H₆ was purified or rather coeluted with *E. coli* GroEL, the interacting bands were excised from gel and further analyzed by MALDI/TOF mass spectrometry upon tryptic digestion. The mass of the digested fragments were then analyzed using MALDI/TOF mass spectrometry. The result confirmed both full length ScElp3H₆ and *E. coli* GroEL proteins (Figure 3.23). The summary of the result is shown in Table 3.3. The ScElp3H₆ and GroEL bands were afterwards confirmed by Western blot using α -His₆-tagged (Figure 3.22) and α -GroEL (data not shown) antibodies respectively.

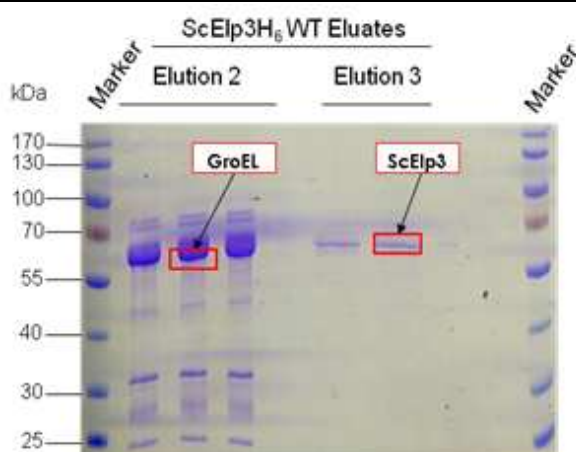


Figure 3.23 | MALDI/TOF mass spectrometric analysis of purified ScElp3H₆ protein after coexpression with *E. coli* GroEL. The fragments excised are boxed in red. The 60 kDa (GroEL) and 67.4 kDa (ScElp3H₆) bands were first digested using trypsin and then analyzed by MALDI/TOF mass spectrometry. The elution fractions 2 and 3 (Figure 3.22) were separated again on 12% SDS-PAGE in order to excise the GroEL (lower) ScElp3H₆ (upper) bands used for the MALDI/TOF mass spectrometric analysis.

3 RESULTS

Table 3.3 | Summary of MALDI/TOF Mass spectrometric analysis data of ScElp3H₆ coexpressed with *E.coli* GroEL

Probe	Match to	Score	Mol. Wt (kDa)	pI	Sequence coverage (%)
ScElp3	S61980	79	63.6	9.1	24
GroEL	CH60_ECO57	1895	57.2	4.85	58

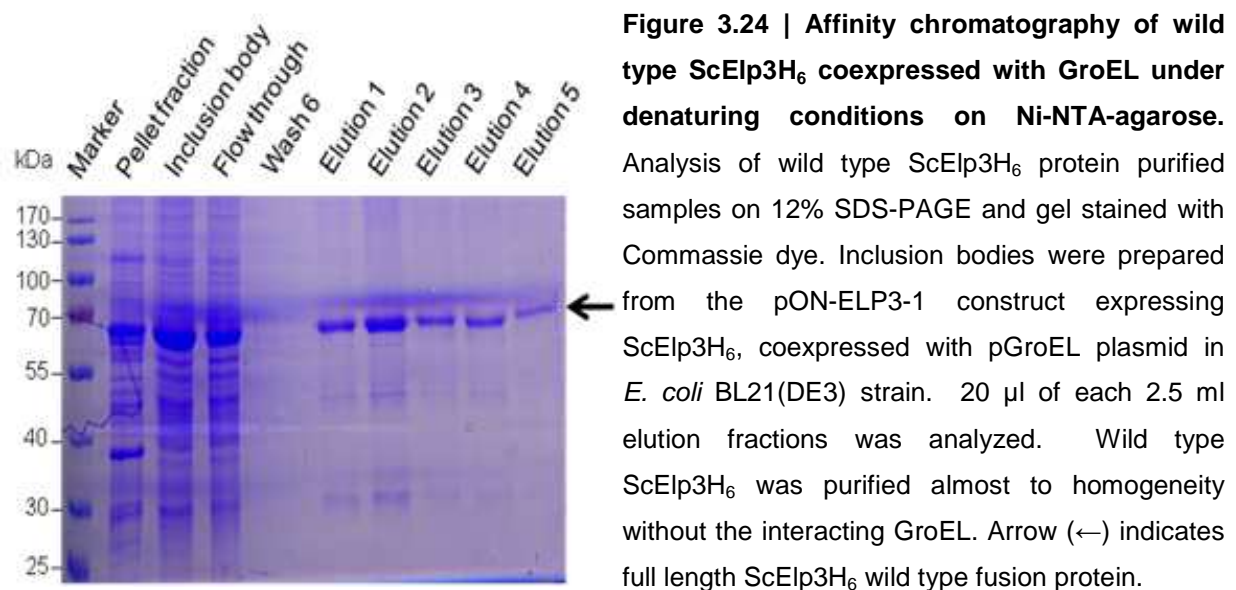
The fact that ScElp3 protein could also be detected in the flow through fraction indicates that the binding capacity of the Ni-NTA-agarose matrix may have been completely utilized. Although coexpression of ScElp3H₆ using the *E. coli* pGroEL plasmid in the presence of betaine hydrochloride and NaCl increased the yield of ScElp3H₆ protein, attempts were made to recover the ScElp3H₆ from inclusion body fraction after coexpression with the pGroEL plasmid and check if the interaction of both proteins would be disrupted under denaturing conditions.

3.5 Non-native purification of ScElp3H₆ wild type coexpressed with pGroEL from inclusion body preparations

Since the disruption of the ScElp3H₆ protein interaction with GroEL was not successful under native conditions, it was necessary to purify ScElp3H₆ protein coexpressed with GroEL under denaturing conditions from inclusion body preparations. The ScElp3 inclusion bodies were prepared from the pON-ELP3-1 construct coexpressed with pGroEL in BL21(DE3) *E. coli* strain using 1 liter culture as already described (Section 3.2.1; Table 3.2). A total of 41 mg wild type ScElp3H₆ inclusion bodies were loaded on Ni-NTA-agarose matrix. All buffers used were supplemented with 8 M urea. Bound ScElp3H₆ fusion protein was eluted and analyzed. The results indicated that the ScElp3H₆ protein could be purified almost to homogeneity (Figure 3.24). Although some ScElp3H₆ protein was in the flow through fraction, significant amounts were eluted from the column. A total of 6.6 mg purified ScElp3H₆ was recovered. Higher yields could be obtained using this purification strategy, in comparison with purification of the ScElp3H₆ without coexpression of GroEL under native conditions (Section 3.4.2; Figure 3.18). The denatured and purified ScElp3H₆ eluates were pooled and concentrated using Amicon Ultra-4 membrane. The denatured, purified and concentrated ScElp3H₆ protein was thereafter reconstituted with iron (III) and sulfide salts in the presence of DTT as

3 RESULTS

already described for AtElp3H₆ protein (Section 3.2.2.1). The reconstituted ScElp3H₆ protein was further purified by gel filtration.



3.5.1 Purification of reconstituted ScElp3H₆ protein by gel filtration on Sephadex 200 column

The reconstituted ScElp3H₆ wild type protein which was affinity purified under non-native conditions from inclusion body generated from pON-ELP3-1 construct coexpressed using pGroEL plasmid (Section 3.5), was further purified under anaerobic conditions by gel filtration on Sephadex 200 column. A total of 1.3 mg reconstituted ScElp3H₆ wild type (WT) protein was loaded on Sephadex 200 column equilibrated with buffer W (50 mM Tris.HCl, pH8.0; 150 mM NaCl). The reconstituted ScElp3H₆ fusion protein eluted as a single peak at 40 ml retention volume (Figure 3.25). A total of 0.98 mg reconstituted ScElp3H₆ wild type protein was recovered. The eluted fractions were then analyzed on SDS-PAGE and by Western blotting using α-His₆ antibody as illustrated in Figure 3.25.

3 RESULTS

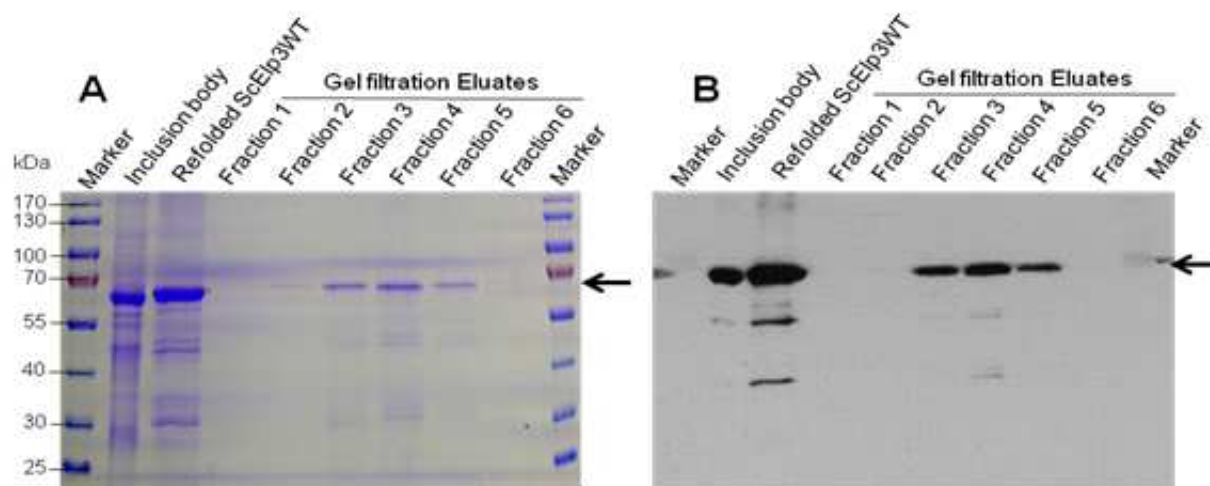


Figure 3.25 | Analyses of wild type ScElp3H₆ protein samples upon reconstitution and size exclusion chromatography. (A) Analysis of purified samples on 12% SDS-PAGE and gel stained with Coomassie dye. (B) Detection of reconstituted and gel filtration-purified ScElp3H₆ protein samples using α -His₆ antibody. 20 μ l of each 2 ml eluted samples was analyzed. Full length wild type (WT) ScElp3H₆ is depicted with arrow (\leftarrow)

The purification of the wild type ScElp3H₆ protein by gel filtration after reconstitution of its [Fe-S] cluster was necessary to discard excess iron (III) and sulfur salts and other impurities which could not be removed by affinity purification on Ni-NTA-agarose (Figure 3.24). The ScElp3H₆ protein recovered in the eluate fractions upon purification by gel filtration amounted to 0.98 mg. Similar result like for H₆-ScElp3-Strp protein (Figure 3.20) was obtained when the gel filtration fractions of ScElp3H₆ were pooled and subjected to UV-VIS spectroscopic analysis (Figure 3.26A). An additional peak at 615 nm was also noticed. The results illustrate that both ScElp3 variants could be referred to as [Fe-S] containing proteins as indicated by their inherent [4Fe-4S] cluster binding status. Upon chromatography of ScElp3H₆ protein by gel filtration after reconstitution of its [Fe-S] cluster(s), a single ScElp3H₆ protein peak as confirmed by SDS-PAGE and Western blotting (Figure 3.25) was eluted at 40 ml retention volume (Figure 3.26B). The binding of [4Fe-4S] cluster by the ScElp3H₆ protein was also evident by the UV-VIS peak at 420 nm eluting concurrently with the protein peak (Figure 3.26B). The minor peak eluting at 20 ml retention volume may be an aggregated ScElp3H₆ protein without bound [Fe-S] cluster(s).

3 RESULTS

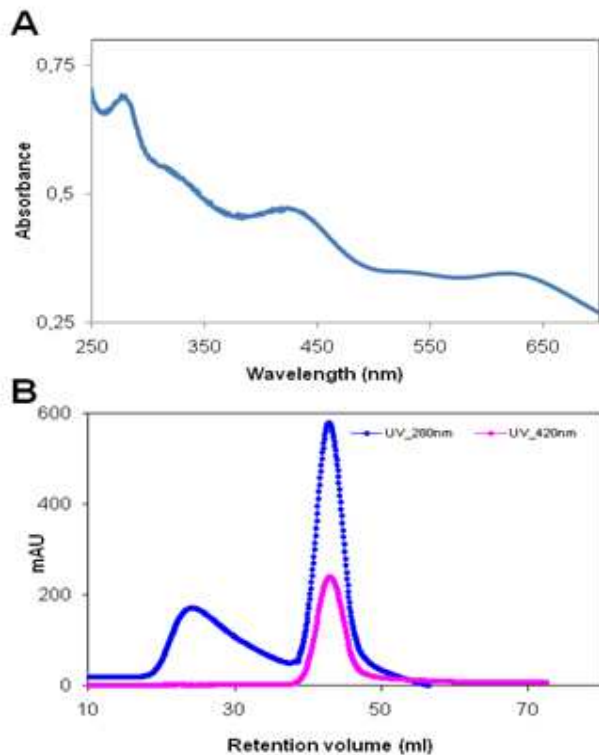


Figure 3.26 | Gel filtration chromatography and UV-VIS analysis of reconstituted ScElp3H₆ protein. (A) UV-visible absorption spectrum of reconstituted ScElp3H₆ protein purified from inclusion bodies. The spectrum was recorded with 0.43 mg/ml protein and the absorbance ratio A_{400}/A_{280} of 0.67 was obtained and the broad peak at 420 nm was also observed. (B) Gel filtration profile of ScElp3H₆ wild type protein eluting at 40 ml retention volume bound to its [Fe-S] cluster(s), evident by UV-VIS peak at 420 nm. The absorbance ratio A_{400}/A_{280} of 0.41 was recorded. The minor peak at 20 ml retention volume may be an unreconstituted and aggregated ScElp3H₆ protein.

To study the role of the radical SAM domain for Elongator function, mutants of the conserved cysteine residues of the radical SAM domain were generated. The cysteine mutants would be needed to elucidate the biological importance of the radical SAM domain using *in vitro*, *in vivo* co-immunoprecipitation, genetic and ⁵⁵Fe radioactive binding methods.

3.6 Generation of ScElp3 radical SAM cysteine mutated variants by site-directed mutagenesis

Different independent experimental methods indicated the presence of [Fe-S] cluster(s) in the AtElp3 and ScElp3 proteins. To determine if the binding of [Fe-S] cluster(s) by ScElp3 is important for its biological functions, cysteine residues in the putative [Fe-S] cluster binding AdoMet motif CX₉CX₂C (Sofia *et al.*, 2001; Figure 3.27) were substituted with alanine. In addition, conserved cysteine residues (-CX₁₁CX₁₂CX₂₇C-) in the radical SAM domain, that may also act as [Fe-S] binding ligands were mutated. The substitution mutations were introduced by site-directed mutagenesis using the Stratagene multi-site directed mutagenesis kit and the wild type ScElp3H₆ expression plasmid, pON-ELP3-1 as template. The mutagenesis primers used (Table 2.1b) and the expression constructs of all the radical SAM

3 RESULTS

domain mutants generated have been summarized (Table 2.2) in the materials and method section. The incorporation of each mutation was confirmed by sequencing using the sequencing primers listed in Table 2.1a. The mutations introduced into the ScElp3 protein are schematically represented in Figure 3.27. The radical SAM domain mutant plasmids were transformed into the *E. coli* BL21(DE3) strain and used for the expression of mutant ScElp3 proteins.

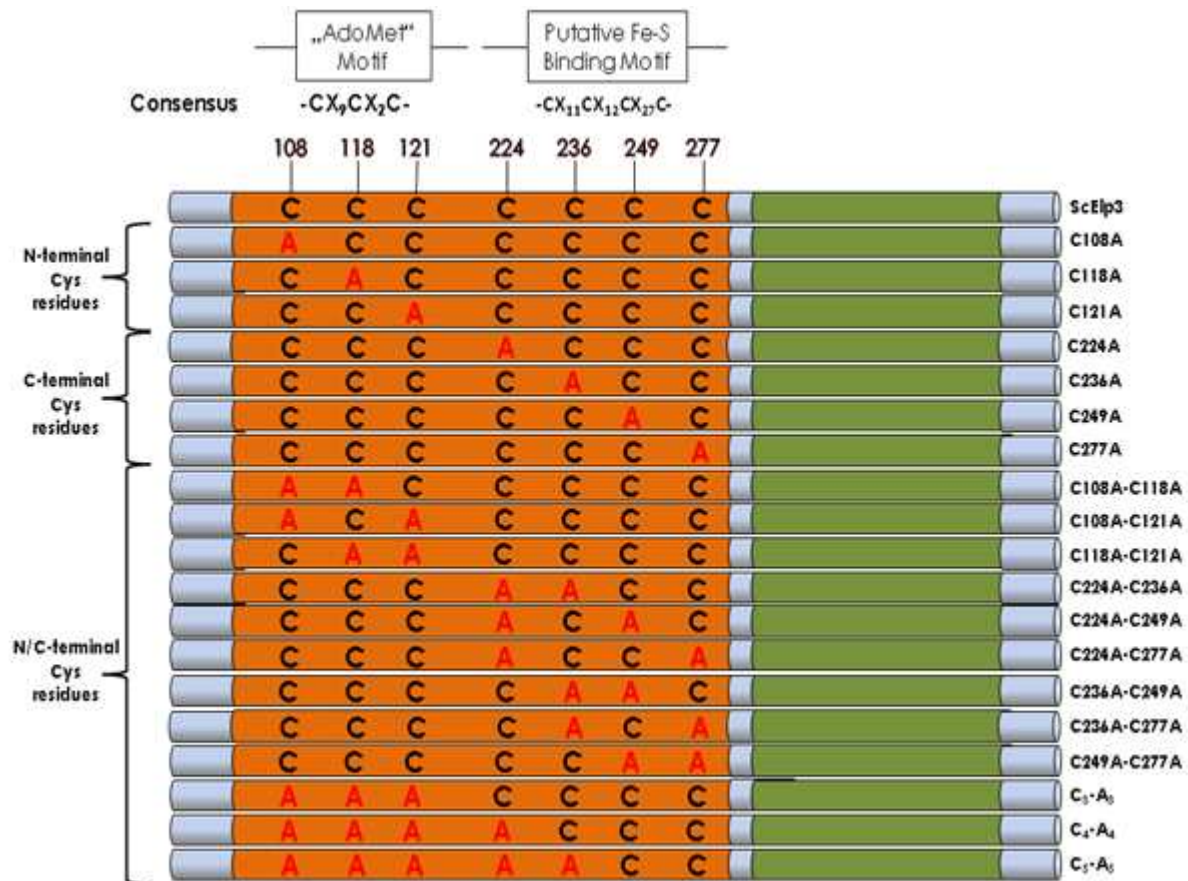


Figure 3.27 | Schematic representation of the point mutations introduced into the ScElp3 protein. The figure depicts a schematic representation of the ScElp3 protein and the seven conserved cysteine residues. The mutations generated are colored in red. The AdoMet motif shows considerable sequence similarity to the radical SAM enzyme superfamily (Sofia *et al.*, 2001). The conserved cysteine residues in the putative Fe-S cluster binding motif may be involved in the binding of an additional [Fe-S] in ScElp3 and its homologues. C₃-A₃ (triple), C108A-C118A-C121A; C₄-A₄ (Quadruple) C108A-C118A-C121A-C224A and C₅-A₅ (Quintuple), C108A-C118A-C121A-C224A-C236A cysteine mutated variants. The orange region denotes the radical SAM domain and the green region designates the HAT domain in ScElp3. SAM denotes S-adenosyl methionine; HAT, histone acetyltransferase

3 RESULTS

3.6.1 Expression of the radical SAM domain cysteine mutated variants

The radical SAM domain mutant constructs used for protein expression have been summarized (Table 2.2, Figure 3.27). Each mutant construct was transformed into the BL21(DE3) *E. coli* strain and used for protein expression. The expression of the radical SAM domain ScElp3H₆ cysteine mutated variants as C-terminal His₆-tagged fusion proteins was carried out as described for the ScElp3H₆ wild type protein (Section 3.4). The results obtained after expression indicated that all radical SAM domain mutated variants could be expressed as C-terminal His₆-tagged fusion proteins in the crude cell extract (Figure 3.28). Nevertheless, like the wild type protein, all the cysteine mutated variants were expressed mostly in the insoluble inclusion body fractions (data not shown).

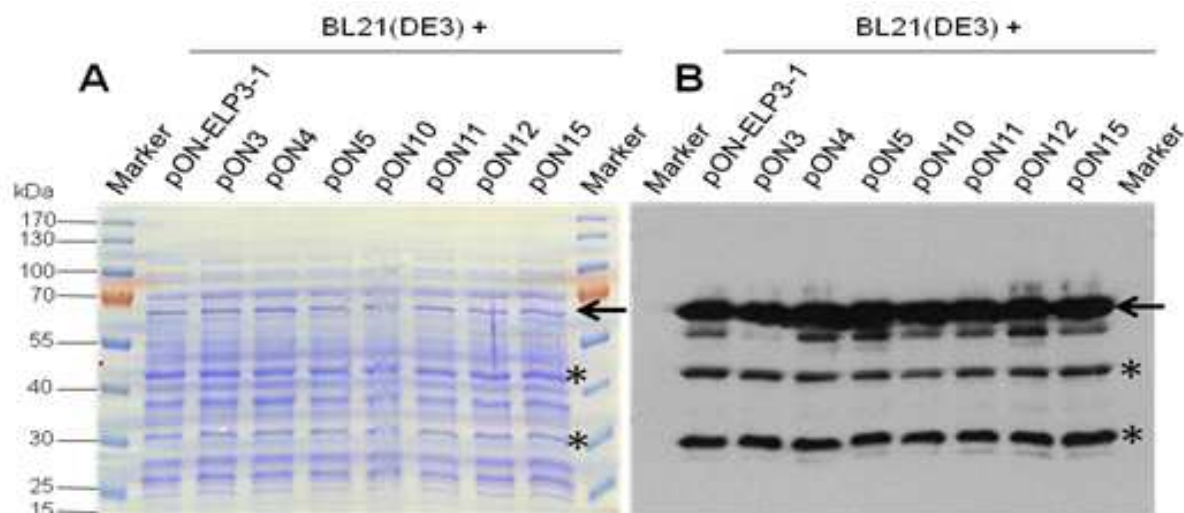


Figure 3.28 | Expression of the radical SAM domain cysteine mutated ScElp3H₆ proteins in *E. coli* BL21(DE3) strain. (A) Analysis of *E. coli* crude cell extract of ScElp3H₆ mutated proteins on 12% SDS-PAGE and visualization done using the Coomassie reagent. (B) Detection of ScElp3H₆ mutated proteins by Western blotting using α -His₆-tagged antibody. The arrow shows full length ScElp3H₆ proteins and the degradation products of 30 and 40 kDa are designated with asterisks (*). 50 μ g crude cell extract of each mutant protein was analyzed. pON-ELP3-1, wild type; pON3, C108A; pON4, C118A; pON5, C121A; pON10, C108A-C118A; pON11, C108A-C121A; pON12, C118A-C121A; pON15, C108A-C118A-C121A, are constructs expressing ScElp3H₆ wild type and radical SAM domain cysteine mutated proteins respectively (Table 2.2; Figure 3.27).

The triple cysteine ScElp3 mutant (ScElp3C₃-A₃) lacking the AdoMet motif (Figure 3.27) was chosen for further analysis.

3 RESULTS

3.6.2 Affinity chromatography of ScElp3(C₃-A₃)H₆ mutated variant coexpressed with pGroEL from inclusion body preparations

The ScElp3(C₃-A₃)H₆ radical SAM domain cysteine mutated variant was purified from inclusion bodies obtained from the pON15 construct expressing the ScElp3(C₃-A₃)H₆ mutated variant after coexpression with the pGroEL plasmid in the *E. coli* BL21(DE3) strain as described for the ScElp3H₆ wild type protein (Section 3.5). A total of 40 mg ScElp3(C₃-A₃)H₆ inclusion bodies recovered from 1 liter culture were loaded on Ni-NTA-agarose matrix equilibrated with lysis buffer containing 8 M urea. Afterwards, the column was washed and bound proteins were eluted and analysed by SDS-PAGE and Western blotting. Like the wild type ScElp3H₆ protein, the ScElp3(C₃-A₃)H₆ cysteine mutant variant could also be purified almost to homogeneity in one purification step by affinity chromatography on Ni-NTA-agarose (Figure 3.29).

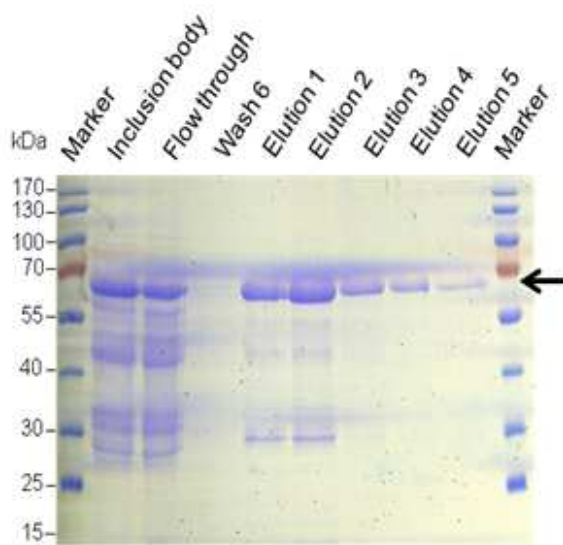


Figure 3.29 | Purification of radical SAM domain ScElp3(C₃-A₃)H₆ cysteine mutated variant coexpressed with GroEL under denaturing conditions on Ni-NTA-agarose. Analysis of radical SAM domain triple cysteine mutated variant ScElp3H₆ purified samples on 12% SDS-PAGE and gel stained with Commassie dye. Inclusion body was prepared from *E. coli* BL21(DE3) strain expressing the pON-15 (ScElp3(C₃-A₃)H₆) cysteine mutant construct, coexpressed with the pGroEL plasmid. 20 µl of each 2.5 ml eluate was analyzed. Arrow (←) indicates full length ScElp3(C₃-A₃)H₆ cysteine mutant protein.

A total of 9.1 mg purified full length ScElp3(C₃-A₃)H₆ cysteine mutated protein was recovered after purification under denaturing conditions. The elution fractions of the ScElp3(C₃-A₃)H₆ cysteine mutated protein were pooled and subjected to [Fe-S] cluster reconstitution, as described for the wild type AtElp3H₆ protein (Section 3.2.2.1). The reconstituted ScElp3(C₃-A₃)H₆ cysteine mutated protein was then purified by gel filtration (Figure 3.30). A total of 2.6 mg reconstituted ScElp3(C₃-A₃)H₆ cysteine mutant protein was recovered from 3.4 mg affinity purified ScElp3(C₃-A₃)H₆ protein.

3 RESULTS

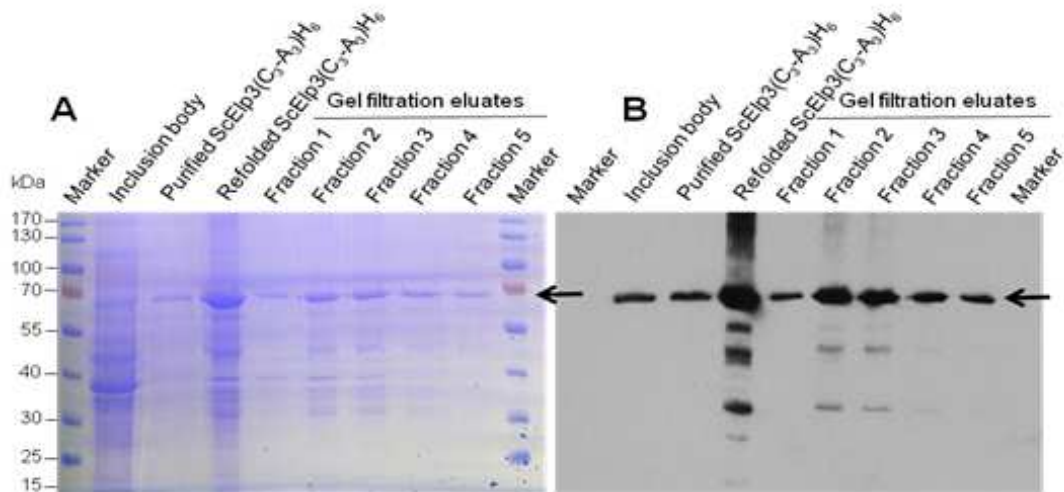
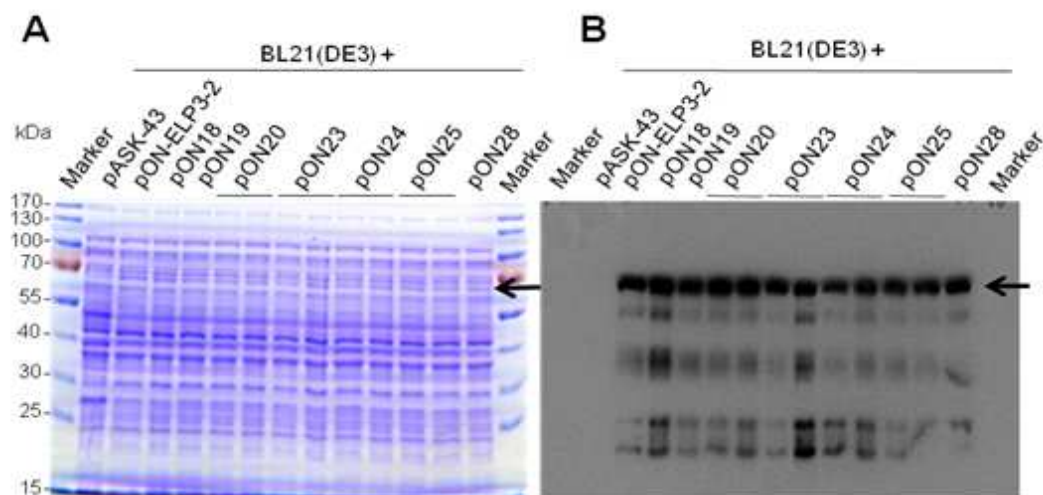


Figure 3.30 | Analyses of reconstituted ScElp3(C₃-A₃)H₆ mutated protein samples purified by gel filtration. (A) Analysis of purified probes on 12% SDS-PAGE and gel visualized with Coomassie dye. (B) Detection of purified ScElp3(C₃-A₃)H₆ cysteine mutated protein samples using α -His₆ antibody. 20 μ l of each 2 ml eluted samples was analyzed. Full length ScElp3(C₃-A₃)H₆ cysteine mutant protein is depicted with arrow (\leftarrow).

3.6.3 Expression of radical SAM domain cysteine H₆-ScElp3-Strp mutated variants

The H₆-ScElp3-Strp radical SAM domain mutated variants were expressed under native conditions, as already illustrated for the wild type protein in section 3.4.3. This involved the transformation of the respective radical SAM domain cysteine mutant expression plasmid (Table 2.2) into *E. coli* BL21(DE3) strain followed by subsequent expression upon induction with anhydrotetracycline. The result upon analysis of the crude cell extract of the mutated proteins indicated equal protein expression levels for the respective radical SAM domain mutated H₆-ScElp3-Strp variants in comparison to the wild type protein (Figure 3.31).



3 RESULTS

Figure 3.31 | Expression and analysis of H₆-ScElp3-Strp (69.5 kDa) radical SAM domain cysteine mutated proteins in *E.coli* BL21(DE3) strain. (A) Analysis of H₆-ScElp3-Strp proteins on 12% SDS-PAGE and gel visualized with Commassie reagent. (B) Western blot detection of H₆-ScElp3-Strp mutated proteins using α -His₆ antibody. Arrow indicates the full length H₆-ScElp3-Strp protein. 50 μ g crude cell extract samples were analyzed. pON-ELP3-2, wild type; pON18, C108A; pON19, C118A; pON20, C121A; pON23, C108A-C118A; pON24, C108A-C121A; pON25, C118A-C121A; and pON28, C108A-C118A-C121A, are expression constructs expressing H₆-ScElp3-Strp wild type and radical SAM domain cysteine mutated proteins respectively. The radical SAM mutated variants have been illustrated in Figure 3.27 and Table 2.2

For further analyses and characterization studies, the triple and quintuple cysteine mutated variants were considered for one-step affinity chromatography on Ni-NTA-agarose matrix under native conditions.

3.6.4 Affinity purification of radical SAM domain H₆-ScElp3p-Strp C₃-A₃ and C₅-A₅ mutated variants under native conditions

The expression and purification of the C₃-A₃ and C₅-A₅ cysteine mutated H₆-ScElp3-Strp variants under native condition on the Ni-NTA-agarose column was implemented using *E.coli* BL21(DE3) transformed with the pON28 and pON30 constructs (Table 2.2) that express the C₃-A₃ and C₅-A₅ cysteine H₆-ScElp3-Strp mutant proteins respectively. The mutated protein expression and affinity purification were executed like for the wild type H₆-ScElp3-Strp protein as extensively documented in section 3.4.3. The N-terminal His₆-tag on both mutated H₆-ScElp3-Strp variants was accessible for binding to the Ni-NTA-agarose matrix, although traces of the mutated proteins could be detected in the flow through fraction, as evident from the results upon SDS-PAGE and Western blot analyses (Figure 3.32). About 2.8 mg and 2.6 mg purified H₆-ScElp3-Strp C₃-A₃ and C₅-A₅ cysteine mutated proteins were recovered per liter culture after purification. It was also observed that both full length cysteine mutated H₆-ScElp3-Strp proteins could be eluted in two elution fractions and like the wild type protein; they also interact strongly with *E. coli* DnaK. The elution fractions from both cysteine mutated variants were pooled and used for further characterization studies. An overview of the purification of wild type ScElp3 and the radical SAM domain cysteine mutated variants using different expression constructs has been summarized in Table 3.4.

3 RESULTS

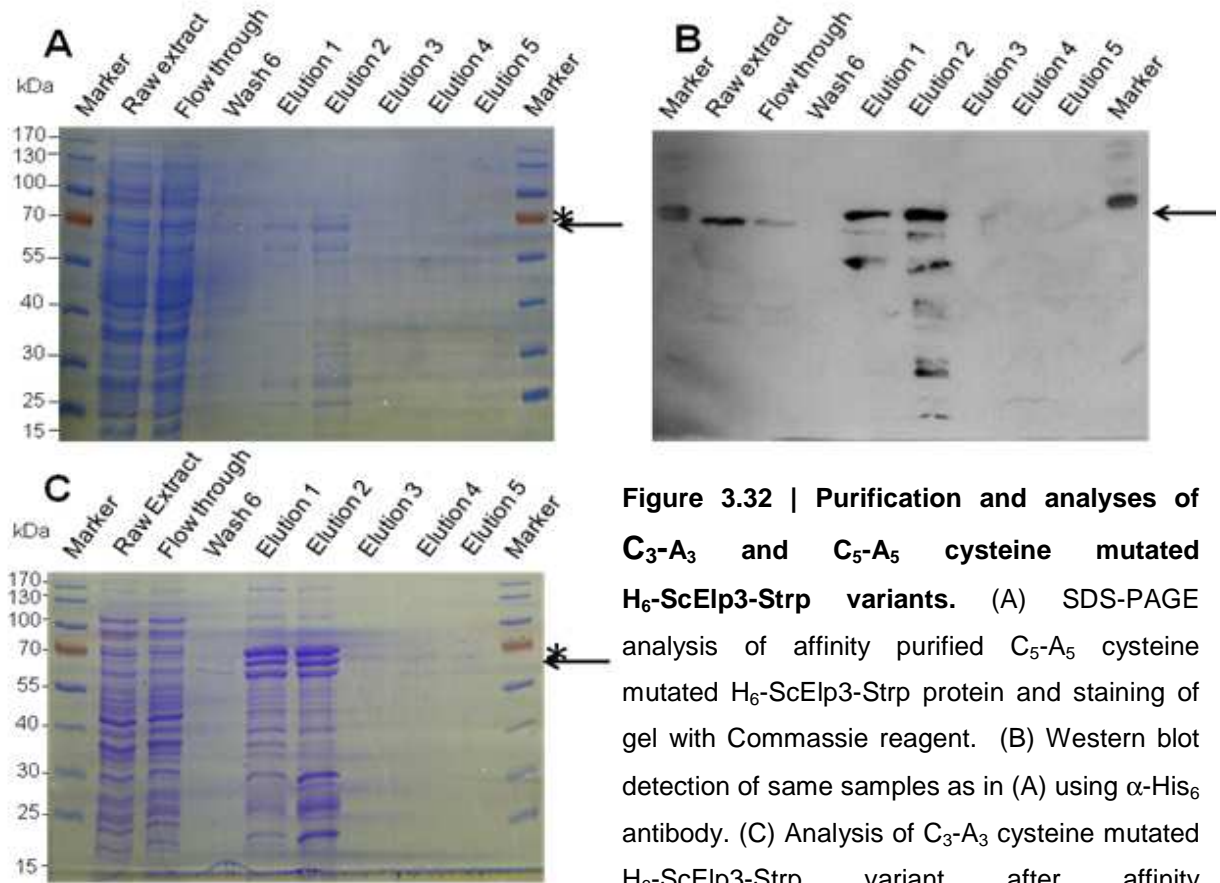


Figure 3.32 | Purification and analyses of C₃-A₃ and C₅-A₅ cysteine mutated H₆-ScElp3-Strp variants. (A) SDS-PAGE analysis of affinity purified C₅-A₅ cysteine mutated H₆-ScElp3-Strp protein and staining of gel with Coomassie reagent. (B) Western blot detection of same samples as in (A) using α-His₆ antibody. (C) Analysis of C₃-A₃ cysteine mutated H₆-ScElp3-Strp variant after affinity chromatography on Ni-NTA-agarose under native conditions. 20 μl of 2.5 ml eluted samples were analyzed on 12% SDS-PAGE. Full length mutant proteins are indicated with arrow (←), while DnaK is depicted with asterisk (*).

3 RESULTS

Table 3.4 | Summary of purification of the different full length ScElp3 protein and the radical SAM domain cysteine mutated variants

Protein variant	Expression plasmid	Purification matrix / condition	Total protein loaded [mg]	Yield after purification [mg]	Estimated amount of purified protein [%]
ScElp3-H ₆	pON-ELP3-1	Ni-NTA-agarose Native	131	0.7	0.5
ScElp3-H ₆	pON-ELP3-1	Ni-NTA-agarose non-native	35	4.0	11.4
ScElp3-H ₆	pON-ELP3-1, pGroEL	Ni-NTA-agarose Native	270	8.0	3.0
ScElp3-H ₆	pON-ELP3-1, pGroEL	Ni-NTA-agarose Non-native	41	6.6	16.1
ScElp3-H ₆	pON-ELP3-1, pGroEL	Sephadex 200 Native	1.3	1.0	76.9
H ₆ -ScElp3-Strp	pON-ELP3-2	Ni-NTA-agarose Native	213	4.9	2.3
H ₆ -ScElp3-Strp	pON-ELP3-2	Strep-Tactin native	4.9	0.1	2.0
H ₆ -ScElp3-Strp Triple mutated (C ₃ -A ₃)	pON28	Ni-NTA-agarose Native	231	2.8	1.2
H ₆ -ScElp3-Strp Triple mutated (C ₃ -A ₃)	pON15, pGroEL	Ni-NTA-agarose non-native	40	9.1	22.8
H ₆ -ScElp3-Strp Triple mutated (C ₃ -A ₃)	pON15, pGroEL	Sephadex 200 Native	3.4	2.6	76.5
H ₆ -ScElp3-Strp Quintuple mutated (C ₅ -A ₅)	pON30	Ni-NTA-agarose Native	150	2.6	1.7

3 RESULTS

In order to characterize the C₃-A₃ and C₅-A₅ cysteine mutated ScElp3 proteins, mutated proteins purified under native (Section 3.6.4) and non-native (Section 3.6.2) conditions were utilized. Reconstitution of ScElp3(C₃-A₃)H₆ mutated protein purified under denaturing conditions was carried out using iron (III) and sulfide salts as described in section 3.2.2.1. The reconstituted ScElp3H₆ triple mutated protein was also purified by gel filtration (Section 3.6.2) and then used for *in vitro* characterization studies.

3.7 Characterization and analyses of ScElp3 radical SAM domain mutated variants by biochemical methods

3.7.1 UV-visible absorption spectroscopic analyses of ScElp3 cysteine mutated variants

Upon purification of H₆-ScElp3-Strp C₃-A₃ (Section 3.6.4; Figure 3.32C) and C₅-A₅ (Section 3.6.4; Figure 3.32A, B) cysteine mutated variants by affinity chromatography on Ni-NTA-agarose, the eluted fractions were subjected to UV-visible spectroscopic analyses as illustrated in Figure 3.33A and 3.33C. The reconstituted ScElp3(C₃-A₃)H₆ mutated variants purified under non-native conditions from inclusion body preparation (Section 3.6.2; Figure 3.30) also showed similar result (Figure 3.33B) with the natively purified H₆-ScElp3-Strp C₃-A₃ mutated variant (Figure 3.33A), but with an additional peak at approximately 615 nm. The peak at 615 nm represents a [2Fe-2S] cluster presumably arising from [4Fe-4S] degradation. The broad peak at 420 nm observed upon UV-VIS analysis of the reconstituted ScElp3(C₃-A₃)H₆ mutant variant could be reduced with sodium dithionite (Figure 3.33B, inset). In both natively purified ScElp3 radical SAM mutated variants, the UV-VIS results showing broad peaks at 420 nm indicative of a [4Fe-4S] cluster are similar to that observed in the wild type ScElp3 protein (Figure 3.20, 3.33A,C). Presumably, the H₆-ScElp3-Strp C₃-A₃ and C₅-A₅ cysteine mutated variants are still able to bind [4Fe-4S] cofactor. Similar results were recorded for ScElp3(C-A)H₆ (single) and ScElp3(C₂-A₂)H₆ (double) cysteine mutated variants (Data not shown).

3 RESULTS

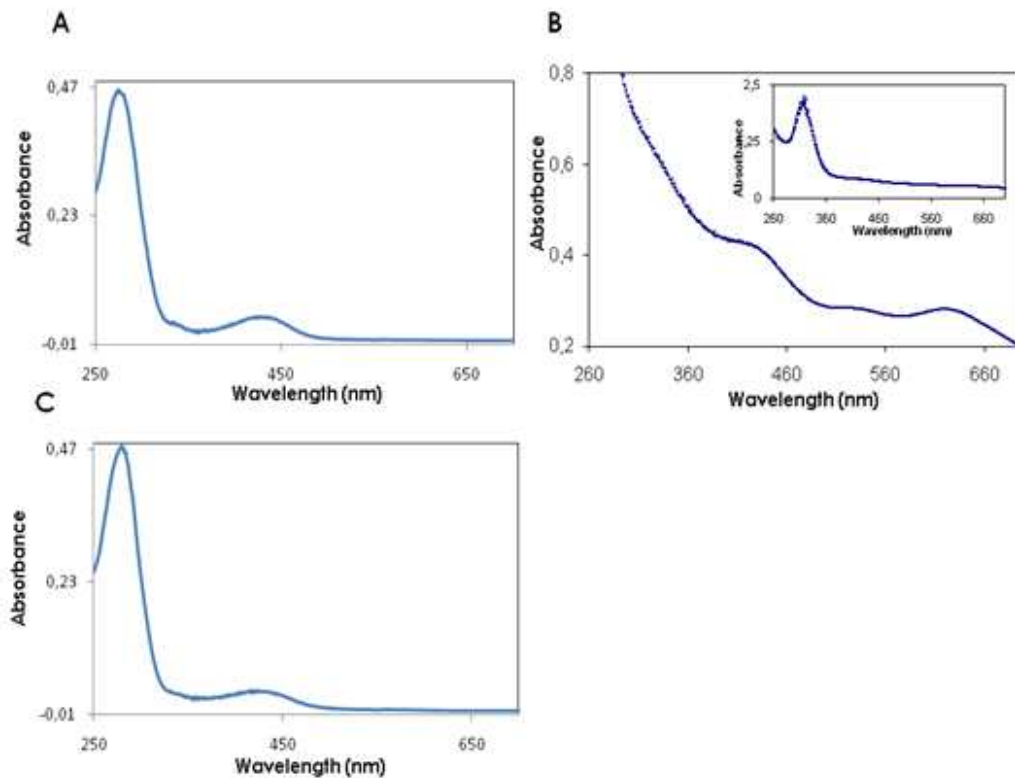


Figure 3.33 | UV-visible absorption spectroscopic analyses of ScElp3 C₃-A₃ and C₅-A₅ cysteine mutated variants. (A) UV-visible absorption spectrum of C₃-A₃ mutated H₆-ScElp3-Strp protein purified under native conditions on Ni-NTA-agarose with 1.3 mg/ml protein and absorbance ratio A_{400}/A_{280} of 0.1. (B) UV-visible absorption spectrum of ScElp3(C₃-A₃)H₆ mutated variant using 0.45 mg/ml reconstituted protein with absorbance ratio A_{400}/A_{280} of 0.47. The broad peak at 420 nm characteristic of [4Fe-4S] disappeared upon reduction with 2 mM sodium dithionite, confirming ScElp3 C₃-A₃ mutated as an [Fe-S] containing protein (Figure 3.34B, inset). An additional feature is observed at 615 nm. (C) UV-visible absorption spectrum of C₅-A₅ mutated H₆-ScElp3-Strp protein purified under native conditions on Ni-NTA-agarose with 1.1 mg/ml protein and absorbance ratio A_{400}/A_{280} of 0.1.

3.7.2 Analysis of reconstituted ScElp3(C₃-A₃)H₆ cysteine mutated variant by gel filtration

The [Fe-S] cofactor of the ScElp3(C₃-A₃)H₆ cysteine mutated variant purified under non-native conditions was reconstituted with Fe³⁺ and S²⁻ salts under anaerobic conditions. Upon further purification by gel filtration to remove excess iron and sulfur salts, a single peak ScElp3(C₃-A₃)H₆ cysteine mutated protein eluting at 40 ml retention volume was confirmed by Western blot (Section 3.6.2; Figure 3.30). The evidence of bound [Fe-S] was observed by the UV-VIS peak at 420 nm co-eluting with the protein peak at the same retention volume (Figure 3.34A). The brown color

3 RESULTS

characteristic of radical SAM enzymes was also observed for the ScElp3(C₃-A₃)H₆ cysteine mutated protein eluates (Figure 3.34B). This is a hint that the eluting protein is still an [Fe-S] containing protein. A minor peak without ScElp3(C₃-A₃)H₆ cysteine mutated protein also eluted at 60 ml retention volume.

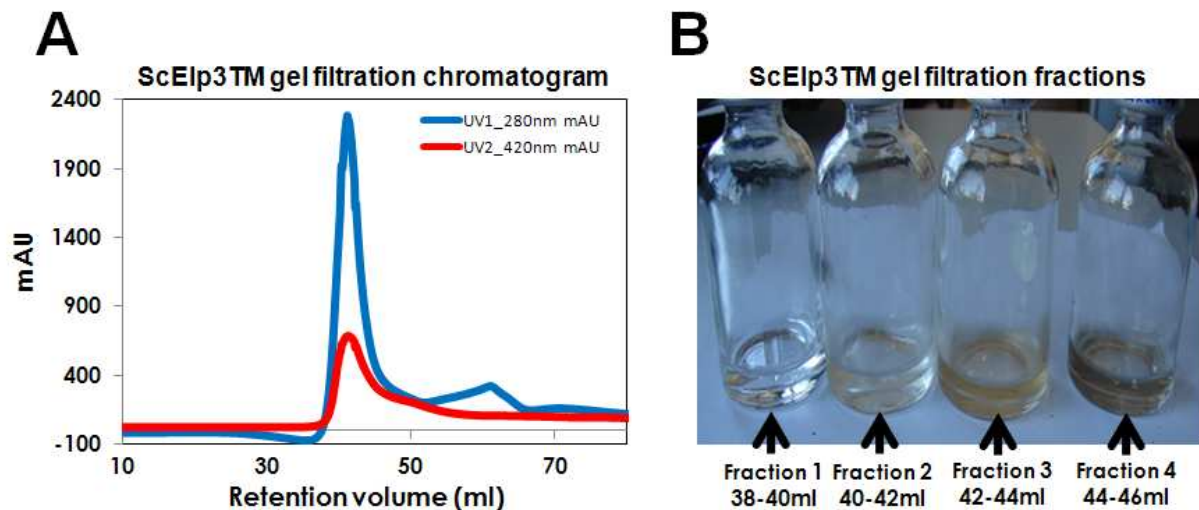


Figure 3.34 | Gel filtration chromatography of non-native purified and reconstituted ScElp3(C₃-A₃)H₆ mutated protein. A) Gel filtration profile of ScElp3(C₃-A₃)H₆ mutated variant eluting at 40 ml retention volume bound to [Fe-S], evident by peak at 420 nm. The absorbance ratio A_{400}/A_{280} is 0.3. B) The color of the fractions eluting as a single peak at about 40 ml elution volume was brown (fraction 2, 3 and 4). This could be a hint that the ScElp3(C₃-A₃)H₆ cysteine mutant protein still binds [Fe-S] cluster.

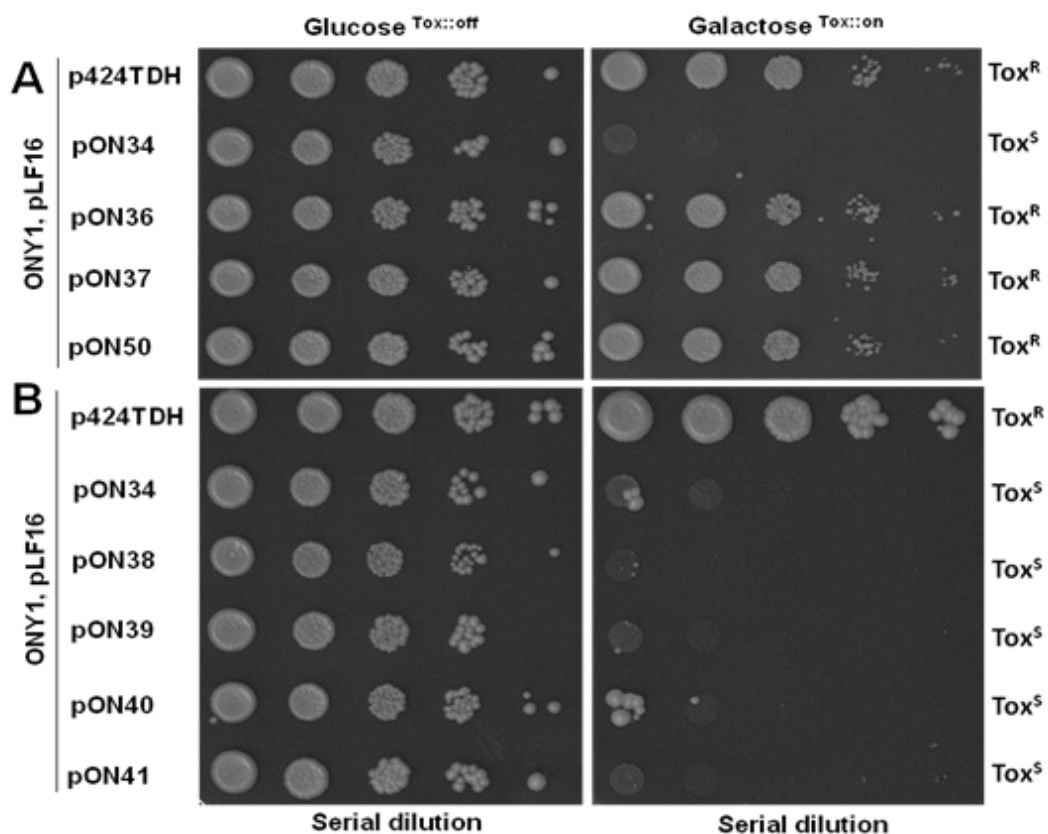
The *in vitro* data of the ScElp3 wild type and radical SAM cysteine mutated proteins have implicated [Fe-S] cluster binding. These data could not be used to distinguish the ScElp3 wild type from the cysteine mutated variants. To confirm the importance of conserved cysteines that may act as ligands for [Fe-S] cluster binding or conserved glycine residues of the putative glycine radical motif for Elongator function, genetic characterization of ScElp3 wild type and mutant phenotypes was carried out in *Saccharomyces cerevisiae* by either overexpressing the ScElp3 protein variants under the control of the strong constitutive p424TDH3 promoter or by expressing them endogenously under the native promoter.

3 RESULTS

3.8 Generation and characterization of overexpressed and endogenous ScElp3-c(myc)₃ mutated variants

3.8.1 Analyses of overexpressed ScElp3-c(myc)₃ radical SAM cysteine mutated variants using the γ -toxin assay

The analyses of the overexpressed wild type ScElp3 and radical SAM domain cysteine mutated variants were carried out using the γ -toxin sensitivity assay (Frohloff *et al.*, 2001). The ONY1 (*elp3 Δ*) yeast strain transformed with the γ -toxin plasmid pLF16 (Jablonowski *et al.*, 2006) expressing the γ -toxin subunit of the *Kluyveromyces lactis* zymocin under the *GAL1* promoter, was cotransformed with either the *TDH3* promoter-controlled (c-myc)₃-tagged wild type *ScELP3* plasmid or the respective (c-myc)₃-tagged radical SAM domain mutated variants (Table 2.2) or empty p424TDH3 vector. The yeast transformants containing both plasmids in each case were grown on 2% (w/v) glucose YNB medium under selective conditions and then spotted on glucose and galactose YNB agar plates in 10-fold serial dilutions. The effect of the γ -toxin expression was observed on the galactose plates after 3 days incubation at 30°C (Figure 3.35).



3 RESULTS

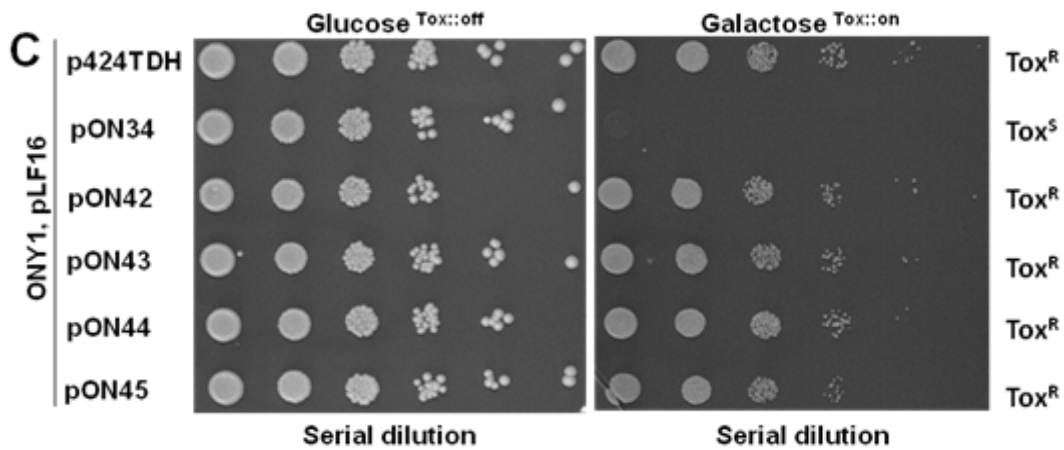


Figure 3.35 | Characterization of the Elongator tRNA modification function by complementation of a yeast *elp3Δ* strain with C-terminal c-(myc)₃-tagged *ScELP3* and radical SAM domain mutated variants. (A) The *elp3Δ* strain (ONY1) was transformed with plasmids containing *ELP3*-(c-myc)₃ (pON34), C108A-(c-myc)₃ allele (pON36), C118A-(c-myc)₃ allele (pON37) and C121A allele (pON50). (B) The *elp3Δ* strain (ONY1) was transformed with plasmids containing *ELP3*-(c-myc)₃ (pON34), C224A-(c-myc)₃ allele (pON38), C236A-(c-myc)₃ allele (pON39), C249A-(c-myc)₃ allele (pON40) and C277A-(c-myc)₃ allele (pON41). (C) The *elp3Δ* strain (ONY1) was transformed with plasmids containing *ELP3*-(c-myc)₃ (pON34), C108A-C118A-(c-myc)₃ double mutant allele (pON42), C108A-C118A-C121A-(c-myc)₃ triple mutant allele (pON43), C108A-C118A-C121A-C224A-(c-myc)₃ quadruple mutant allele (pON44) and C108A-C118A-C121A-C224A-C236A-(c-myc)₃ quintuple mutant allele (pON45). The γ -toxin was expressed from the pLF16 plasmid in the presence of galactose. Growth on galactose signifies γ -toxin resistance (Tox^R) and no growth indicates γ -toxin sensitivity (Tox^S) and was monitored after 3 days incubation at 30°C.

The results illustrated for the overexpressed c-myc tagged wild type *ScELP3* and radical SAM domain mutant gene products (Figure 3.35) show the importance of the radical SAM domain for the Elongator-dependent tRNA modification at the wobble uridine position. The cysteine residues of the AdoMet motif, C108, C118 and C121, single or in combination, are important for Elongator-dependent tRNA modification, since they were unable to complement the yeast ONY1 (*elp3Δ*) strain. On the contrary, the *ScElp3*-(c-myc)₃ mutant plasmids expressing the C224A, C236A, C249A and C277A variants were able to complement the ONY1 (*elp3Δ*) yeast strain and possess no phenotype just like yeast transformant expressing the wild type *ScELP3*-(c-myc)₃. Apparently, mutation of the cysteine residues C224, C236, C249 and C277, considered as part of a 2nd putative [Fe-S] cluster binding motif, CX₁₁CX₁₂CX₂₇C does not affect the Elongator-dependent tRNA modification function.

3 RESULTS

Therefore, double cysteine mutated variants in the 2nd putative [Fe-S] cluster binding motif were generated and analysed by the γ -toxin assay for their importance in the Elongator-dependent tRNA modification (Figure 3.36). The results indicated that all double mutant alleles were also able to complement the yeast ONY1 (*elp3 Δ*) strain and show no *elp/tot* phenotype. Since the loss of ScElp3-(c-myc)₃ mutant plasmids could lead to resistant phenotypes, the γ -toxin assay was considered to be performed in yeast strains expressing endogenous wild type and mutant variant ScElp3-(c-myc)₃ proteins under their native promoters.

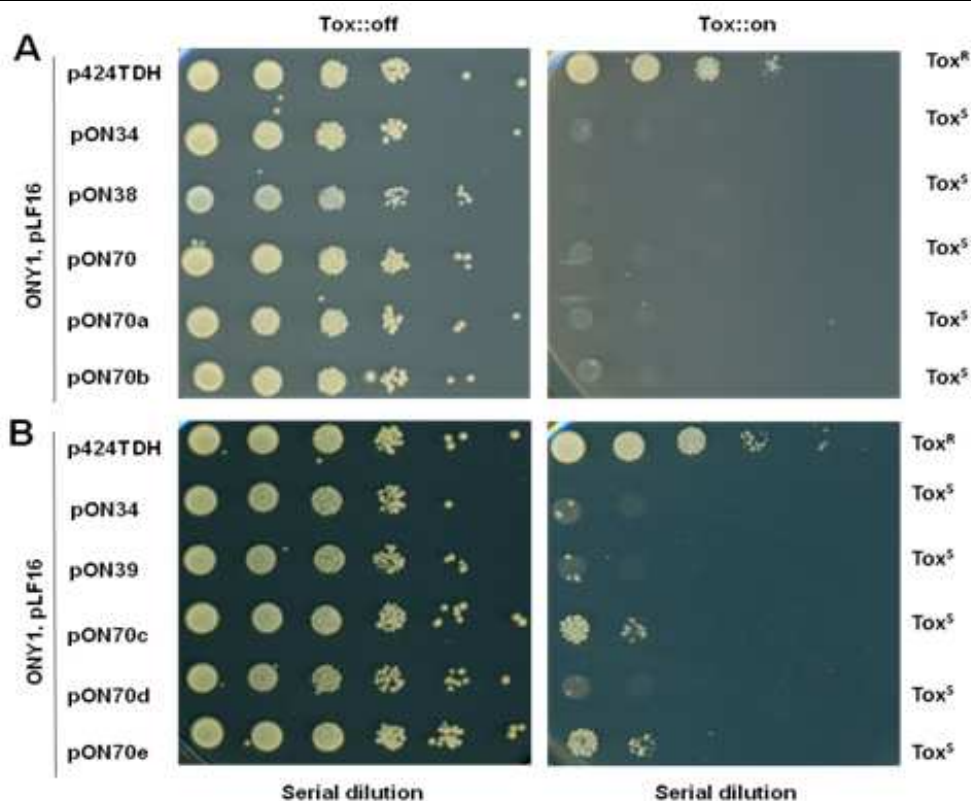
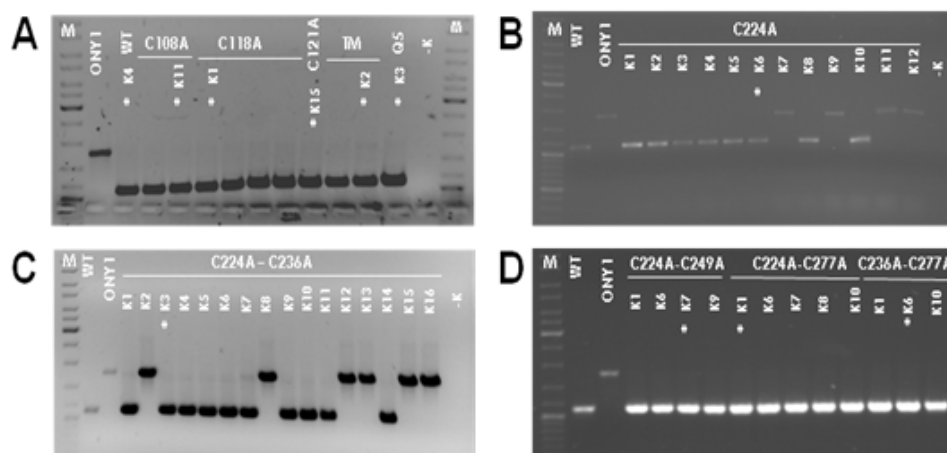


Figure 3.36 | Characterization of the Elongator tRNA modification function by complementation of a yeast *elp3 Δ* strain with double cysteine mutated variants of the “2nd putative Fe-S binding motif”. A) The *elp3 Δ* strain (ONY1) was transformed with plasmids containing *ELP3* (pON34), C224A allele (pON38), C224A-C236A allele (pON70), C224A-C249A allele (pON70a), and the C224A-C277A allele (pON70b). B) The transformation of the *elp3 Δ* strain (ONY1) was done with plasmids containing the wild type *ELP3* (pON34), C236A allele (pON39), C236A-C249A allele (pON70c), C236A-C277A allele (pON70d), C249A-C277A allele (pON70e) and the vector control (p424TDH) in each case. The γ -toxin was expressed using the pLF16 plasmid in the presence of galactose. Growth on galactose indicates γ -toxin resistance (Tox^R) and no growth signifies γ -toxin sensitivity (Tox^S) and was observed after 3 days incubation at 30°C.

3 RESULTS

3.8.2 Construction of endogenous ScElp3-c(myc)₃ radical SAM domain cysteine mutant strains by homologous recombination

For the generation of the ScElp3-c(myc)₃ radical SAM domain cysteine mutant strains, an *elp3Δ::KIURA3* strain was first constructed. The *KIURA3* cassette was amplified by PCR from the YDp-KIU plasmid (Jablonowski *et al.*, 2001a) using KO-ELP3-SAM-FW and KO-ELP3-SAM-RV primers (Table 2.1d). The PCR product was subsequently transformed into the *Saccharomyces cerevisiae* FFY3t strain (Frohloff *et al.*, 2001) for disruption of ScElp3-c(myc)₃ *ORF*. The transformants were selected on plates for uracil prototrophy. The *elp3Δ::KIURA3* (ONY1) strain produced was confirmed using the eclipse bioassay (Kishida *et al.*, 1996) and PCR analysis employing ORF-ELP3-SAM-FW and TDH-RV primers (Table 2.1d). To generate the endogenous ScElp3-c(myc)₃ wild type and radical SAM domain cysteine mutated variants, appropriate mutant plasmids (Table 2.2) were restricted using *NcoI* / *NheI* and then transformed into the ONY1 strain. The transformants were plated on YPD plate and incubated overnight at 30°C. Selection of transformants was performed by replica-plating on synthetic medium containing FOA and incubated for 3 days at 30°C. Genomic DNA isolated from transformants was then verified for integration of the ScElp3 cysteine mutant fragments by PCR using ORF-ELP3-SAM-FW and TDH-RV primers. Subsequently, the PCR products were sequenced to confirm the respective mutations. Strains lacking the *KIURA3* cassette as a result of its replacement with ScElp3 cysteine mutant fragments showed specific DNA fingerprints upon PCR amplification compared to the ONY1 strain. The PCR analyses of various ScElp3 cysteine mutant strains (Table 2.4) using isolated genomic DNA as template are shown in Figure 3.37.



3 RESULTS

Figure 3.37 | Analyses of generated ScElp3-c(myc)₃ wild type and cysteine mutant strains by PCR using genomic DNA with ORF-ELP3-SAM-FW and TDH-RV primers. A) Strains generated upon transformation of *elp3Δ* (ONY1) strain with pON-ELP3-1 (WT, wild type), pON3 (C108A), pON4 (C118A), pON5 (C121A), pON15 (TM, C₃-A₃), pON17 (Q5, C₅-A₅) plasmids restricted with *NcoI/NheI*. B) C224A mutant strains generated by transformation of ONY1 strains with pON6 (C224A) plasmid restricted with *NcoI/NheI*. C) C224A-C236A double cysteine mutant strains generated upon transformation of ONY1 strain with pON14 (C224A-C236A) plasmid restricted with *NcoI/NheI*. D) Double cysteine mutant strains generated upon transformation of ONY1 strain using pON14a (C224A-C249A), pON14b (C224A-C277A), pON14d (C236A-C277A) plasmids restricted with *NcoI/NheI*. Transformants marked with asterisk (*) showing ScElp3WT DNA fingerprint were used for further analyses. K, control without DNA.

The biological functionality of the Elongator containing ScElp3 radical SAM domain mutated variants were tested by killer eclipse bioassay (Kishida *et al.*, 1996).

3.8.3 Construction of putative ScElp3-c(myc)₃ glycine radical mutant strains

The *E. coli* anaerobic ribonucleotide reductase and pyruvate formate-lyase (PFL) have been classified as enzymes that require a stable glycy radical for activity under strictly anaerobic conditions (Sun *et al.*, 1993; Knappe & Wagner 2001). The organic radicals are oxygen-sensitive, and exposure of the radical-containing enzyme to air leads to truncation of anaerobic ribonucleotide reductase at Gly-681 (King & Reichard 1995) and PFL at Gly-734 (Wagner *et al.*, 1992). There is amino acid sequence similarity between the C-terminus of ScElp3 and a stretch of about ten C-terminal residues comprising glycine 681 in the anaerobic ribonucleotide reductase (AnRR) (Sun *et al.*, 1993) or the sequence surrounding glycine 734 at the active site of the glycy radical enzyme pyruvate formate-lyase (Wagner *et al.*, 1992). The ScElp3-c(myc)₃ glycine mutant strains (G542A and G545A) were constructed analogously to the endogenous ScElp3-c(myc)₃ radical SAM domain mutants (Section 3.8.2). The essence of this strain construction was to verify the importance of the glycine residues for the biological functionality of the Elongator complex. A new *elp3Δ* strain (ONY-G1) was necessary for the construction of the glycine mutant strains since its *KIURA3* cassette must encompass the glycine residues to be mutated. The *KIURA3* cassette was amplified by PCR with YDp-KIU plasmid (Jablonowski *et al.*, 2001a) as template using KO-ELP3-G534A-FW-1 and

3 RESULTS

KO-ELP3-G534A-RV primers (Table 2.1d). The PCR product was subsequently transformed into the *S. cerevisiae* FFY3t strain (Frohloff *et al.*, 2001), for disruption of ScElp3-c(myc)₃ ORF. The *elp3Δ::KIURA3* (ONY-G1) strain produced was confirmed and used for the generation of the ScElp3(G542A)-c(myc)₃ and the ScElp3(G545A)-c(myc)₃ glycine mutant strains after restriction of the respective plasmids (Table 2.2) using *SalI/PciI* and then transformed into the ONY-G1 strain. The transformants were analyzed as stated in section 3.8.2, and then verified by PCR using ORF-ELP3-SAM-FW and p424TDH-3myc-RV primers. The PCR analyses of the endogenous ScElp3 glycine mutant strains (Table 2.4) using isolated genomic DNA are shown in Figure 3.38. The endogenously generated ScElp3-c(myc)₃ cysteine and glycine mutant strains were sequenced and further analyzed using the γ -toxin assay. The results confirmed that the cysteines (C108, C118 and C121) are important for Elongator function (data not shown). In contrast, cysteines (C224, C236, C249 and C277) of the 2nd putative Fe-S binding motif and the glycines (G542 and G545) are not significant (data not shown) for the Elongator-dependent modification of certain tRNA species (Huang *et al.*, 2005, 2008; Lu *et al.*, 2005) at the U₃₄ position.

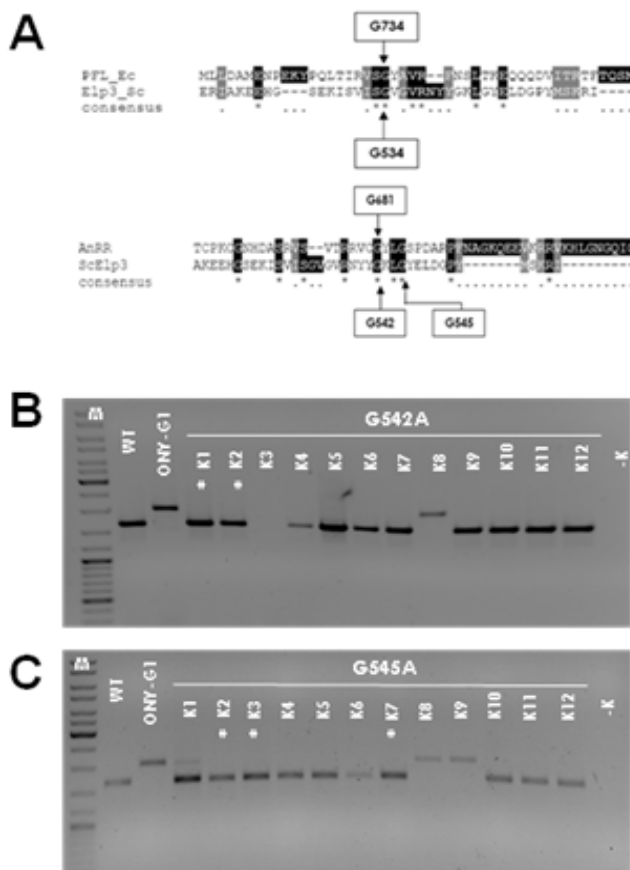


Figure 3.38 | Sequence alignment of ScElp3 with *E. coli* PFL and AnRR and PCR analyses of generated ScElp3-c(myc)₃ glycine mutant strains using genomic DNA with ORF-ELP3-SAM-FW and p424TDH-3myc-RV primers. The C-terminus of ScElp3 was aligned with that of pyruvate formate lyase (PFL) and anaerobic ribonucleotide reductase (AnRR) (A). Yeast strains generated upon transformation of *elp3Δ* (ONY-G1) strain with wild type pON-ELP3-1 and the ScElp3(G542A)-c(myc)₃ pON46a plasmids restricted with *SalI/PciI* (B) or transformed using the ScElp3(G545A)-c(myc)₃ pON46b plasmid restricted also with *SalI/PciI* (C). The ScElp3-c(myc)₃ glycine mutant strains marked with asterisk (*) showing ScElp3 wild type DNA fingerprints were used for further analyses. K, control without DNA.

3 RESULTS

The results from the γ -toxin assay obtained by using overexpression plasmids of ScElp3-c(myc)₃ mutants (Section 3.8.1) correlated with those gotten from endogenously expressed ScElp3-c(myc)₃ mutated variants (data not shown). To support the results obtained from the γ -toxin assay, the tRNA suppression assay was performed.

3.9 Influence of radical SAM domain mutants on ochre tRNA^{Tyr} suppression

To study the role of the radical SAM domain cysteine and the putative glycine mutations for Elongator function, the Elongator tRNA suppression assay was performed. Elongator modification of certain tRNA species at the anticodon wobble uridine (U₃₄) position is a prerequisite for the suppression of nonsense mutations by the tRNA suppressor *SUP4* (Huang *et al.*, 2005). The *SUP4* gene encodes a tRNA^{Tyr} nonsense suppressor that supports readthrough of ochre mutations for example, in *ade2-1* and *can1-100* alleles (Huang *et al.*, 2005). The *CAN1* gene encodes an arginine permease, which results in cell death on medium without arginine but containing the cytotoxic arginine analog canavanine (Hopper *et al.*, 1980). Suppression of the ochre nonsense codon in *can1-100* leads to the same phenotype, but was dependent on U₃₄ Elongator-mediated modification. The *elp3Δ* strain (UMY2916) containing the *SUP4* gene was transformed with *ELP3* wild type, cysteine or glycine mutant plasmids (Table 2.2) and growth was monitored on medium lacking arginine but containing canavanine. The result revealed that the single cysteine C108A, (C118A and C121A, data not shown) mutants of the AdoMet cluster was able to antisuppress *SUP4* and led to canavanine resistance (Can^R) (Figure 3.39). In contrast, the wild type Sc*ELP3* and single (data not shown) or double cysteines of a 2nd putative [Fe-S] cluster binding motif as well as glycine mutant alleles tested promoted *can1-100* suppression by *SUP4* and conferred canavanine sensitivity (Can^S).

3 RESULTS

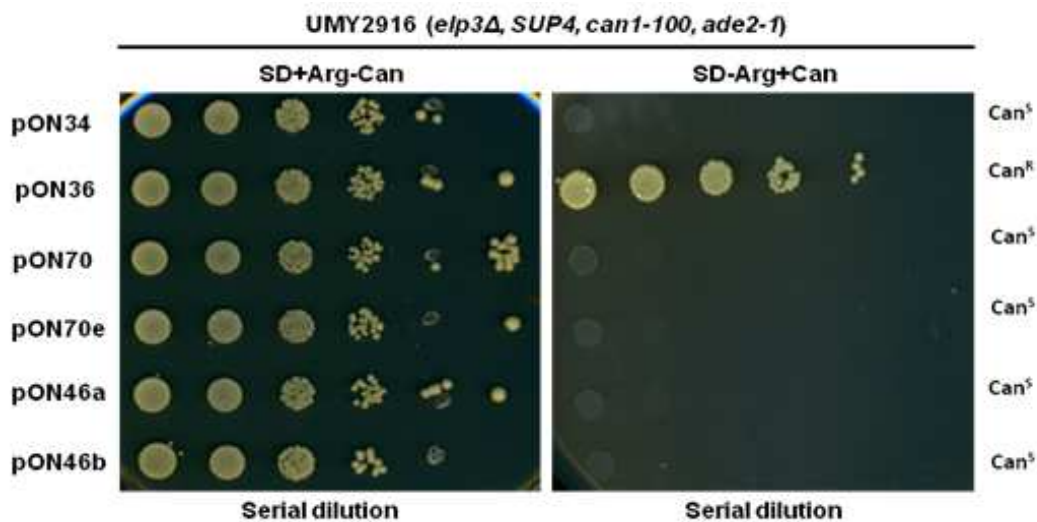


Figure 3.39 | Wild type *ScELP3* and double cysteine and glycine mutations confer tRNA suppression in UMY2916 strain. The yeast strain UMY2916 (*elp3Δ, SUP4, can1-100, ade2-1*) was transformed with plasmids containing *ELP3*-(c-myc)₃ (pON34), C108A-(c-myc)₃ allele (pON36), C224A-C236A-(c-myc)₃ allele (pON70), C249A-C277A-(c-myc)₃ allele (pON70e), G542A-(c-myc)₃ allele (pON46a) and G545A allele (pON46b). The *can1-100* readthrough by *SUP4* was assayed by spotting UMY2916 transformants on SD medium containing arginine (SD+Arg-Can), or lacking arginine but containing the toxic arginine analog canavanine (SD-Arg+Can). *Can1-100* readthrough is depicted by canavanine sensitivity (Can^S) and canavanine resistance corresponds to antisuppression of *SUP4*.

The result of the tRNA suppression assay confirmed all 3 cysteine residues of the AdoMet motif (C108, C118 and C121) to be significant while the cysteine (single or double) residues of a “2nd putative [Fe-S] binding motif” and the conserved glycine residues of the putative glycy radical motif are not important for Elongator-dependent tRNA modification function.

3.10 Role of the radical SAM domain on Elongator complex formation

The six subunit Elongator complex was first copurified with the elongating form of RNA polymerase II (Otero *et al.* 1999; Wittschieben *et al.*, 1999; Wittschieben *et al.*, 2000; Fellows *et al.*, 2000). To analyze the potential role of the radical SAM domain *in vivo*, the interactions between the *ScElp3* cysteine mutants and *Elp1* subunit as well as the Elongator partner protein *Kti12* was tested using coimmunoprecipitation technique (Frohloff *et al.*, 2001; Fichtner *et al.*, 2002a). The yeast *elp3Δ* (CMY307) transformed with *Elp1*-HA (pJET12) and *Kti12*-c(myc)₃ expressing plasmid (pCM24) were further cotransformed with the wild type *Elp3*-c(myc)₃ (pON34), single mutant allele C108A-c(myc)₃ (pON36), C₃-A₃ mutant allele C108A-C118A-C121A-c(myc)₃

3 RESULTS

(pON43), C₄-A₄ mutant allele C108A-C118A-C121A-C224A-c(myc)₃ (pON44) and C₅-A₅ mutant allele C108A-C118A-C121A-C224A-C236A-c(myc)₃ (pON45) expressing plasmids respectively. Total proteins extracted from yeast cells expressing Elp3 wild type and the respective radical SAM domain mutated variants were used for the coimmunoprecipitation analyses. Equal amounts of protein extracts were loaded on Protein A Sepharose (PAS) matrix coupled with polyclonal α-HA antibody.

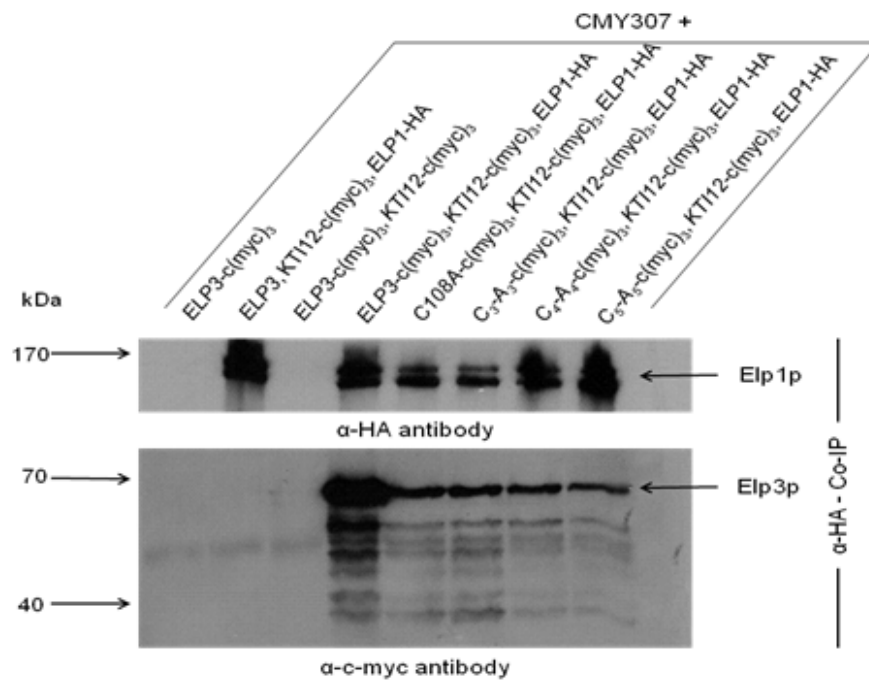


Figure 3.40 | Incorporation of the ScElp3 wild type and radical SAM domain mutated variants into the Elongator complex by coimmunoprecipitation. Equal amounts of total protein extracts from the yeast strain, CMY307 expressing the indicated combinations of untagged Elp3 wild type (*ELP3*), c-(myc)₃-tagged Elp3 wild type *ELP3*-c(myc)₃, and the c-(myc)₃-tagged radical SAM domain single (C108A), triple (C₃-A₃), quadruple (C₄-A₄), quintuple (C₅-A₅) cysteine mutated variants, HA-tagged Elp1 (*ELP1*-HA) and c-(myc)₃-tagged Kti12 (*KTI12*-c(myc)₃) were subjected to immune precipitation utilizing the α-HA antibody. Afterwards, the precipitates were probed separately with α-c-myc (Rabbit) or α-HA (mouse) antibody to detect Elp3 wild type, radical SAM domain mutated variants or Elp1 respectively. The different proteins with their corresponding molecular weights are depicted with arrow (←).

The Elp1-HA immune precipitated proteins were then analyzed for the presence of wild type ScElp3 and cysteine mutated proteins by Western blotting using specific antibodies. The results revealed that the wild type ScElp3 and all radical SAM domain cysteine mutant variants analyzed were able to interact with the Elongator subunit Elp1 (Figure 3.40). In other words, the radical SAM domain cysteine mutated

3 RESULTS

variants could still be incorporated into the Elongator complex, although at lower concentrations in comparison to the wild type ScElp3 protein. The reduced amounts of the ScElp3 radical SAM cysteine mutant proteins observed on ColP may be due to impaired formation of [Fe-S] clusters in the radical SAM cysteine mutated variants resulting in apoproteins that are susceptible to proteolytic degradation. In contrast, no significant protein reduction in the functional ScElp3(C224A-C236A; Figures 3.36 & 3.39) double cysteine mutated variant was observed compared to ScElp3 wild type upon interaction studies with Elp1 protein (Zabel unpublished), suggesting that the structural changes due to the double cysteine substitutions did not affect protein stability compared to the AdoMet cysteine mutated variants. However, no potential Kti12 interactions with ScElp3WT and cysteine mutated variants were observed by ColP because Kti12-c(Myc)₃ was not expressed at detectable levels (Figure 3.40).

3.11 Radioactive incorporation of ⁵⁵Fe into ScElp3 wild type and mutated proteins

Different independent biochemical experiments have shown evidence of [Fe-S] cluster(s) binding in the AtElp3 and ScElp3 proteins. To investigate the consequences of the cysteine mutations in the ScElp3 with respect to the binding of [Fe-S] cluster(s) on ScElp3, the incorporation of radioactive iron (⁵⁵Fe) into ScElp3 protein was monitored *in vivo* according to the method of Kispal *et al.* (1999). The ⁵⁵Fe binding experiments were conducted by Drs. Antonio Pierik and Daili Aguilar-Netz in the laboratory of Prof. Roland Lill at the Philipps-University of Marburg. ScElp3 wild type and mutant strains expressing c-(myc)₃-tagged protein variants under the control of their respective endogenous promoters (Table 2.4) were grown in iron-poor minimal medium containing glucose. After radiolabeling with ⁵⁵Fe, endogenous c-(myc)₃-tagged ScElp3 proteins were immunoprecipitated from cell extracts with anti-myc antibody and the associated radioactivity was quantified by scintillation counting. The radioactivity associated with the myc-beads is tantamount to the degree of incorporation of [⁵⁵Fe-S] clusters into ScElp3-(myc)₃ variants (Figure 3.41). The ⁵⁵Fe associated with the C108A, C₃-A₃ (C108A-C118A-C121A) and C₅-A₅ (C108A-C118A-C121A-C224A-C236A) cysteine mutated variants show reduced [Fe-S] cluster incorporation to background level (Figure 3.41A). The result

3 RESULTS

indicates that a single cysteine mutation in the AdoMet binding motif is sufficient to cause loss of [Fe-S] cluster(s) incorporation into ScElp3 protein.

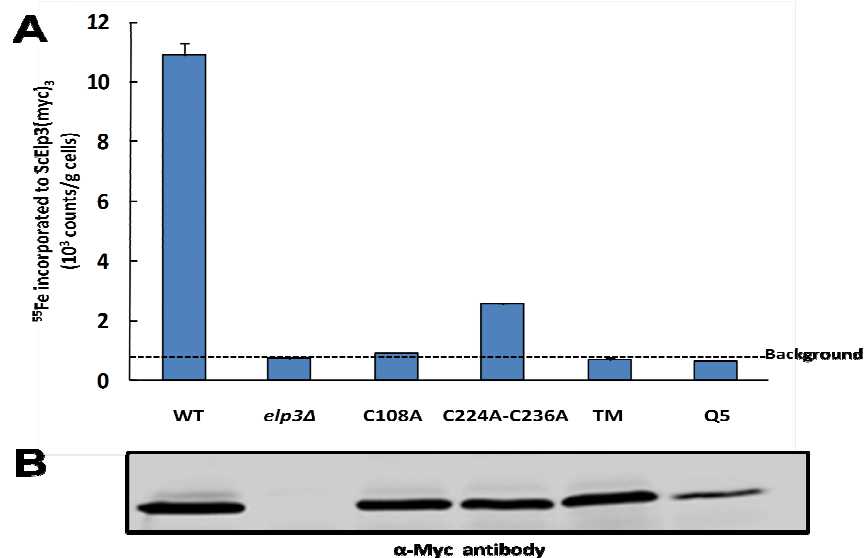


Figure 3.41 | Significance of conserved cysteine residues in ScElp3 for the incorporation of [⁵⁵Fe-S] cluster(s) into ScElp3. (A) Yeast cells expressing c-(myc)₃ tagged ScElp3 wild type and cysteine mutated variants (Section 3.8.2; Figure 3.37) under their endogenous promoters were grown in SC medium for 24 h and in iron-poor medium supplemented with glucose for 16 h. Radiolabeling with ⁵⁵Fe was carried out for 4 h by Antonio Pierik at University of Marburg. Endogenous wild type and mutated ScElp3 proteins were immunoprecipitated from cell extracts using anti-myc antibody. The radioactivity associated with ScElp3 variants was quantified by scintillation counting. The radioactivity levels were corrected for the slight variations in ScElp3 protein levels which were determined by Western blotting (B) and quantitative densitometry.

The slight variations in ScElp3 protein levels were used to normalize the ⁵⁵Fe incorporation results (Figure 3.41B). Double cysteine substitution (C224A-C236A) in a 2nd putative [Fe-S] cluster binding motif resulted in a decrease of the ⁵⁵Fe incorporation to ~76% of the wild type level. The result revealed that in the double C224-C236A mutated protein, a 2nd putative [Fe-S] cluster was lost and only the [Fe-S] cluster of the AdoMet motif could be inserted. In summary, the data suggest the binding of [Fe-S] cluster to a 2nd putative [Fe-S] cluster binding motif, although in the absence of [Fe-S] cluster binding to this motif, [Fe-S] cluster could still be inserted into the AdoMet motif. Taken together, the wild type ScElp3 protein most likely incorporates two [Fe-S] utilizing two conserved binding motifs.

3 RESULTS

3.12 Reduction of the iron-sulfur cluster of reconstituted ScElp3H₆ by Kti11 protein

The Elongator regulatory proteins Kti11 and Kti13 support the Elongator tRNA modification functions in *Saccharomyces cerevisiae*. Apart from a combined loss of Elongator and Kti13, *kti11Δkti13Δ* double inactivation can result to synthetic lethality, suggesting that in addition to their Elongator-dependent roles, Kti13 and Kti11 might share an Elongator-independent role that is imperative for cell viability (Zabel *et al.*, 2008). The immune precipitate of Kti11 contains Elp2 and Elp5 subunits of the Elongator complex and Kti11 has also been reported to participate not only in Elongator-dependent tRNA modification, but also in diphthamide biosynthesis (Bär *et al.*, 2008; Huang *et al.*, 2008). Recent study has implicated Kti11 to be a redox protein which could be reversibly reduced by chemical reductants (Proudfoot *et al.*, 2008). To check if oxidized and reconstituted wild type ScElp3 protein could be reduced by Kti11, different molar concentrations of reduced Kti11 protein expressed and affinity purified from *E. coli* cell extracts were titrated against the wild type ScElp3 protein. Before titration of Kti11 against the wild type ScElp3 protein, the reduced Kti11 was exchanged with buffer W (50 mM Tris.HCl, pH8.0, 150 mM NaCl), to remove traces of sodium dithionite in the reduced Kti11 protein solution.

The results demonstrated gradual reduction and/or disappearance of the [4Fe-4S] clusters UV-VIS peak observed in the oxidized and reconstituted wild type ScElp3H₆ with increasing Kti11 concentration (Figure 3.42A) when compared to the buffer control (Figure 3.42B). The buffer control leads to dilution of ScElp3 protein but does not have any effect on the UV-visible peak at 420 nm. The disappearance of the broad peak at 420 nm observed in Elp3 proteins could also occur upon reduction of wild type ScElp3 with the strong reducing agent, sodium dithionite under anaerobic conditions.

3 RESULTS

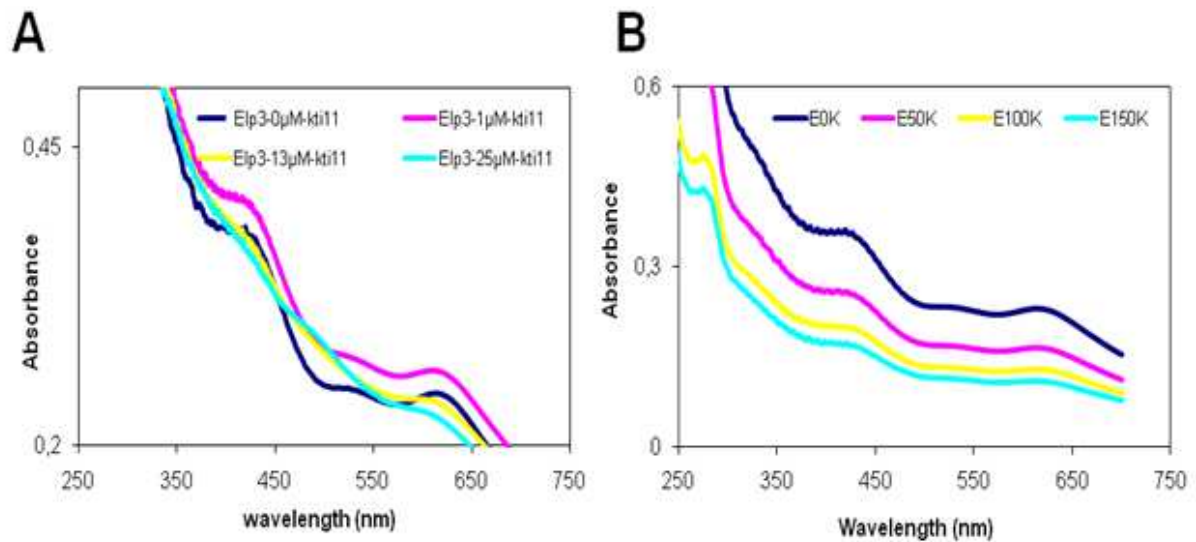


Figure 3.42 | Reduction of the ScElp3H₆ wild type [4Fe-4S] cluster peak by the Elongator regulatory protein Kti11. Titration of Kti11 protein against wild type ScElp3H₆ purified from pON-ELP3-1, coexpressed with pGroEL. (A) UV-visible absorption spectra of ScElp3H₆ upon titration with different molar concentrations of reduced Kti11 protein. The recombinant Kti11 protein was affinity purified from *E. coli* extracts and reduced with 2 mM sodium dithionite. The reduced Kti11 was then exchange with buffer W via a PD-10 gel filtration column (GE Healthcare). (B) UV-visible spectra of ScElp3H₆ protein upon titration with different volumes of buffer W (50 mM Tris.HCl, pH8.0; 150 mM NaCl) was recorded as Kti11 control

4 DISCUSSION

4.0 Discussion

The characterization of the radical SAM domains of Elp3 of the yeast, *Saccharomyces cerevisiae* and that of the plant homologue from *Arabidopsis thaliana* were the focus of this research work. S-adenosyl-L-methionine (SAM or AdoMet) functions as substrates in several enzyme-catalyzed reactions. It provides not only methyl groups in various biological methylation reactions, but serves also as building block in the biosynthesis of the polyamines (spermidine and spermine), nicotianamine, phytosiderophores and the gaseous plant hormone ethylene (Roje 2006). AdoMet is also the source of the catalytic 5'-deoxyadenosyl and 3-amino-3-carboxypropyl radicals (Wang & Frey 2007; Atta *et al.*, 2010; Zhang *et al.*, 2010; Zhu *et al.*, 2011), generated as reaction intermediates by enzymes of the radical SAM superfamily. The radical SAM domain of the archaeal Elp3 was recently shown to bind and cleave SAM (Paraskevopoulou *et al.*, 2006), thereby producing the 5'-deoxyadenosyl radical involved in the catalytic action of most radical SAM enzymes (Frey *et al.*, 2008).

Apart from the *ELP3* gene, no homologues of the other *ELP* genes were detected in the archaea *Methanocaldococcus jannaschii*. The role of the radical SAM domain for Elongator function has not been addressed in eukaryotes. It is thus unknown whether the evolutionarily conserved Elp3 protein exhibits the same function in eukaryotes as in *M. jannaschii*. Elp3 is the only protein that contains a radical SAM as well as a HAT domain in the protein database. The HAT domain of Elp3 is highly conserved among members of the GNAT (GCN5-related N-acetyltransferase) protein family. *In vitro*, it is able to acetylate all four core histones, with a preference for the acetylation of lysine-14 and lysine-8 of histones H3 and H4 (Wittschieben *et al.*, 1999, 2000; Winkler *et al.*, 2002). Elongator has been postulated to assist the RNA polymerase II during transcription elongation by its inherent Elp3 HAT activity directed towards histone acetylation and thus influencing chromatin structure remodeling (Kim *et al.*, 2002; Otero *et al.*, 1999). Mutations inactivating the histone acetyltransferase activity of Elp3 HAT domain have been reported by Huang *et al.*, (2005) to also influence tRNA modification. To study the influence of the radical SAM domain for the functional and structural integrity of the yeast and plant Elongator, conserved cysteine residues contributing ligands to [Fe-S] cluster(s) binding were

4 DISCUSSION

substituted for alanine. Recombinant proteins expressed in *E. coli* were used for the *in vitro* characterization studies. In addition, the biological importance of the conserved cysteine residues was dissected *in vivo*.

4.1 Expression and purification of recombinant Elp3 variants

Most Fe-S cluster-containing proteins, like the radical SAM proteins, tend to be exquisitely sensitive to oxygen (Imlay 2006) and their Fe-S clusters play important roles in determining the three-dimensional structures. Upon heterologous overexpression, such proteins often assemble into inclusion bodies, especially when Fe-S cluster incorporation lags well behind production of the polypeptide scaffold (Grove *et al.*, 2008). The AtElp3 full length and truncation variant proteins were no exception. All AtElp3 full length and truncated protein variants were mostly detected in the inclusion body fraction (Section 3.1). Only about 10% of the AtElp3 full length protein could be detected in the soluble fraction (Section 3.1.1). The truncated variants of AtElp3 protein, AtElp3(76-366) and AtElp3(111-366) were found in equal amounts in the inclusion body and in the soluble fractions (Section 3.1.2.2). Upon affinity purification of the full length AtElp3 and the truncated variants, only very low protein amounts were recovered (Section 3.1.2.1; 3.1.2.3). The low amounts of protein recovered in all cases may be linked to very low binding affinity of the AtElp3 full length and truncated variant proteins on the Ni-NTA-agarose matrix. Low binding of tagged proteins without cofactors to affinity matrices may also result from inaccessibility of the tag for purification. To check possible increase of AtElp3 full length protein yield, coexpression with the *E. coli* iron-sulfur cluster (*isc*) operon (Nakamura *et al.*, 1999; Takahashi & Nakamura, 1999) was carried out. A significant increase in the yield of full length AtElp3 was observed upon coexpression with the pRKISC plasmid (Section 3.1.3.2). Similar results were reported for holo-lipoate synthase (Kriek *et al.*, 2003; Cicchillo *et al.*, 2004), ThiC (Chatterjee *et al.*, 2008) and ferredoxin (Nakamura *et al.*, 1999) with an increased yield of three to four folds. Nevertheless, no influence on the protein solubility was observed, since almost 90% of AtElp3 protein was still found in the inclusion body fraction.

Contrarily, the N-terminal His₆-tagged full length AtElp3 could be highly enriched upon purification on affinity matrix, although only about 10% AtElp3 full length protein

4 DISCUSSION

was expressed in the soluble fraction (Section 3.1.4). In this case, the full length AtElp3 was tightly bound to the molecular chaperone, DnaK. Although high amounts of the full length AtElp3 protein could be obtained by affinity purification, all efforts made to disrupt its interaction with DnaK were unsuccessful (Section 3.1.4.3; Figure 3.9). Inclusion bodies, highly concentrated bodies of misfolded and aggregated non-native proteins, are often associated with molecular chaperones and proteases (Georgiou & Valax 1996; Tomoyasu *et al.*, 2001). The molecular chaperone DnaK most likely binds to the hydrophobic regions of full length AtElp3 when purified under native conditions. This might be necessary for its protection from protease cleavage. The wild type AtElp3 interacting with DnaK is also isolated bound to its [Fe-S] cluster (Section 3.1.4.2; Figure 3.8; Figure 3.13A).

Similar to the AtElp3 full length protein, the wild type ScElp3 and the cysteine mutated variants were found mostly in the inclusion body fraction (Section 3.4.1; 3.4.4; 3.6.1), although a small amount of protein was obtained in the soluble fraction. Again affinity purification of the ScElp3 wild type protein (Section 3.4.2) resulted in the recovery of very little protein, which may probably be due to the inaccessibility of the C-terminal His₆-tag for binding. No significant increase of ScElp3 wild type protein yield was observed upon coexpression with the *isc* operon, pRKISC, when compared to coexpression with the wild type AtElp3 protein (Section 3.1.3.2). Attempts to increase ScElp3H₆ wild type protein yield was achieved by protein coexpression with the *E.coli* GroEL plasmid and supplementation with osmolytes like betaine hydrochloride and NaCl (Section 3.4.4; Table 3.2). Although high yield of wild type ScElp3H₆ was recovered, the shortcoming associated with this process is the inability to disrupt the interaction between GroEL and ScElp3 proteins (Section 3.4.5; Figure 3.22). The N-terminal His₆-tagged ScElp3 wild type, triple (C₃-A₃) and quintuple (C₅-A₅) cysteine mutated proteins could be purified by affinity chromatography (Section 3.4.3; Section 3.6.4) with high protein yield. Like the H₆-AtElp3-Strp protein, the wild type H₆-ScElp3-Strp and both cysteine mutated variants also coeluted with the molecular chaperone, DnaK and could not be disrupted. The molecular chaperones most probably play the role of protecting the Elp3 variants against aggregation and degradation by proteases, since they are recombinantly expressed under native conditions without other partners of the Elongator complex.

4 DISCUSSION

The N-terminal His₆-tagged Elp3 wild type and cysteine mutated proteins affinity-purified under native conditions were used for UV-visible spectroscopic characterization. The UV-visible absorption spectra of the wild type AtElp3, ScElp3 and both cysteine mutated variants indicated the presence of a [4Fe-4S] cluster (Section 3.3.1, Figure 3.13; Section 3.5.1, Figure 3.25; Section 3.7, Figure 3.33).

In summary, the C-termini of Elp3 proteins are not accessible for affinity purification under native conditions. Only the C-termini of Elp3 proteins could be used for purification on affinity matrices under denaturing conditions. In contrast, the N-termini of Elp3 proteins could be used for affinity purification under native conditions, but the purified Elp3 proteins were always associated with molecular chaperones like DnaK or GroEL. Chaperones like DnaK have been reported to assist in the folding of newly synthesized polypeptides (Fink 1999). The N-terminal tags on Elp3 are lost under non-native conditions and thus not available for use in affinity purification.

With the results gathered from the mass spectrometric analysis of the AtElp3 degradation products (Section 3.3.3; Figure 3.15), the approximate region of protease cleavage on the primary architecture of the AtElp3 protein could be determined. The first protease cleavage point giving rise to the 65 kDa AtElp3 fragment is situated just before the radical SAM domain upstream of the tryptic peptide leucine (L₇₅) to arginine (R₈₇) residue. The protease restriction point generating the 40 kDa AtElp3 fragment is located almost at the end of the radical SAM domain upstream of the leucine (L₂₆₁) residue. The protease cleavage sites in AtElp3 protein in both cases are located upstream of a leucine residue as observed by MALDI-TOF MS analysis upon tryptic digestion of AtElp3 (Section 3.3.3; Figure 1.2, Figure 3.15). This suggests that the radical SAM and the GNAT domains are separated by a proteolysis sensitive linker region.

4 DISCUSSION

4.2 Inclusion body preparation as source of AtElp3, ScElp3 and cysteine mutated proteins

Upon inclusion body solubilization under denaturing conditions using 8 M urea, very high protein yield could be recovered after purification by affinity chromatography on Ni-NTA-agarose matrix (Section 3.2.2, Figure 3.11; Section 3.5, Figure 3.24; Section 3.6.2, Figure 3.29). The high protein yield obtained upon non-native purification of wild type AtElp3H₆ and ScElp3H₆ protein as well as the ScElp3(C₃-A₃)H₆ (triple) and ScElp3(C₅-A₅)H₆ (quintuple) cysteine mutated variants could be attributed to accessibility and high binding affinity of the C-terminal His₆-tag on the respective protein and hence they could be purified almost to homogeneity in one purification step. No interactions of Elp3 proteins with molecular chaperones were observed after purification under denaturing conditions. Reconstitution of Elp3 protein variants were implemented by incubation with Fe³⁺ and S²⁻ salts under anaerobic conditions in the presence of DTT and subsequent removal of excess salts was achieved by size exclusion chromatography. No spectroscopic difference was recorded after Elp3 protein reconstitution in the presence or absence of SAM. Therefore, most Elp3 protein reconstitution experiments were carried out in the presence of SAM. Upon dialysis and centrifugation at high speed, only successfully reconstituted Elp3 proteins remain in solution, while aggregated and non-reconstituted proteins are precipitated and discarded. Reconstituted AtElp3 was used for UV-visible spectroscopic (Figure 3.13B) and EPR (Figure 3.14) analyses. The ScElp3 wild type and C₃-A₃ (triple) cysteine mutated proteins were used for UV-visible spectroscopic analysis (Figures 3.26A & 3.33B). The ScElp3 wild type was also titrated against different concentrations of Kti11 protein purified from *E. coli* cell extract (Figure 3.42A). The 3-dimensional structures of the reconstituted and gel-filtration purified Elp3 proteins were not determined and hence it would be difficult to ascertain if Elp3 proteins bind [Fe-S] cluster(s) in their native or rather non-native confirmations. Therefore, the fact that these reconstituted Elp3 proteins bound to [Fe-S] cluster(s) may also exist in different oligomeric forms or aggregates could be possible. It would also be difficult to determine if the [Fe-S] cluster(s) are present in native or non-native forms. The only *in vitro* evidence for the presence of a second [Fe-S] cluster binding in ScElp3C₃-A₃ (triple) cysteine mutated variant was obtained in reconstitution experiments after affinity purification from inclusion bodies,

4 DISCUSSION

reconstitution and analyses of the refolded ScElp3C₃-A₃ cysteine mutated protein. The ScElp3C₅-A₅ (quintuple) cysteine mutated variant could not be purified by gel filtration based on its low stability probably resulting from massive structural changes due to the C₅-A₅ substitutions.

4.3 Evidence for [4Fe-4S] cluster-binding in AtElp3 and ScElp3

The proteins belonging to the radical SAM enzyme superfamily utilize a [4Fe-4S] cluster and S-adenosylmethionine for radical chemistry. Recent genome database analyses have implicated about 3000 proteins possessing the CysX₃CysX₂Cys AdoMet signature (Sofia *et al.*, 2001; Frey *et al.*, 2008, Table 1.0). Six additional amino acid residues occur between the first two cysteines of the AdoMet motif in eukaryotic Elp3 (CysX₉CysX₂Cys) in comparison to the canonical AdoMet sequence motif occurring in all radical SAM enzymes. However, comparison between crystal structures of radical SAM enzymes indicated that additional amino acid insertion between the first two conserved cysteines can be accommodated in the loop without disrupting cluster formation (Layer *et al.*, 2005). The *Salmonella enterica* ThiC and the archaeal Elp3 proteins which contain an additional amino acid residue (CysX₄CysX₂Cys), have been implicated in the binding of a [4Fe-4S] cluster and cleavage of SAM to generate 5'-deoxyadenosyl radical through a similar sulfur-carbon cleavage mechanism (Martinez-Gomez & Downs 2008; Chatterjee *et al.*, 2008; Paraskevopoulou *et al.*, 2006) monitored in the radical SAM enzyme superfamily. This suggests a reasonable flexibility in the loop between the first two cysteines contributing ligands to [4Fe-4S] cluster and thus the potential enzymes encompassed in the AdoMet superfamily may be more diverse than previously envisaged.

Evidence for the presence of [4Fe-4S] cluster(s) in wild types AtElp3 (Figure 3.13), wild type ScElp3 (Figure 3.20), ScElp3C₃-A₃ (triple) and ScElp3C₅-A₅ (quintuple) cysteine mutated variants (Figure 3.33) was observed upon UV-visible spectrophotometric analyses. Similar results were recorded for ScElp3C-A (single (data not shown)), ScElp3C₂-A₂ (double (data not shown)). The wild type AtElp3 reconstituted in the absence of SAM exhibited a nearly isotropic and cuboidal EPR signal with a g-value of 2.015 characteristic of [3Fe-4S]⁺¹ cluster (Section 3.3.2;

4 DISCUSSION

Figure 3.14). Similar cluster has also been detected in the enzyme aconitase (Kent *et al.*, 1985), *Desulfovibrio gigas* ferredoxin II (Moreno *et al.*, 1994), pyruvate formate-lyase activating enzyme (Broderick *et al.*, 2000), and recently the antiviral protein viperin (Duschene & Broderick 2010). The observed $[3\text{Fe-4S}]^{+1}$ may be the consequence of a controlled oxidation and interconversion of $[4\text{Fe-4S}]^{+1}$ to $[3\text{Fe-4S}]^{+1}$ resulting in the depletion of the “unique” iron atom in the cluster (Kennedy *et al.*, 1984; Tamarit *et al.*, 1999; Liu & Gräslund 2000; Ollagnier *et al.*, 1999; Krebs *et al.*, 2000; Broderick *et al.*, 2000; Duin *et al.*, 1997; Petrovich *et al.*, 1992). The $[4\text{Fe-4S}]$ cluster of AtElp3 protein confirmed by EPR may be utilized for the generation of the highly reactive 5'-deoxyadenosyl radical required for activation of C-H bonds as reported for substrates of the radical SAM enzyme superfamily (Wang & Frey 2007).

The UV-visible spectroscopic analyses of single cysteine archaeal Elp3 and Dph2 (involved in diphthamide biosynthesis) mutated proteins also confirmed that two cysteine residues are still able to coordinate $[4\text{Fe-4S}]$ clusters (Paraskevopoulou *et al.*, 2006; Zhu *et al.*, 2011). The additional feature observed at approximately 615 nm upon UV-VIS analyses of reconstituted wild type AtElp3 (Figure 3.13B), wild type ScElp3 (Figure 3.26A) and ScElp3C₃-A₃ (triple) cysteine mutated variant (Figure 3.33B) probably indicates the presence of $[2\text{Fe-2S}]$ clusters (Ugulava *et al.*, 2003; Duschene & Broderick 2010) resulting from $[4\text{Fe-4S}]$ cluster decomposition. The brown color associated with the ScElp3C₃-A₃ cysteine mutated variant (Figure 3.34B) is also common to members of the radical SAM enzyme superfamily (Duschene & Broderick 2010). Disappearance of the $[4\text{Fe-4S}]$ cluster peak observed at 420 nm upon dithionite reduction, characteristic of all radical SAM enzymes (Sofia *et al.*, 2001; Booker *et al.*, 2007; Frey *et al.*, 2008; Duschene *et al.*, 2009; Booker & Grove 2010; Marsh *et al.*, 2010) is also observed for wild type AtElp3, ScElp3 and ScElp3C₃-A₃ (triple) cysteine mutated variants (Figures 3.13A, 3.20 & 3.33A) respectively. The two conserved cysteines (C249 and C277) present in the ScElp3C₅-A₅ (quintuple) cysteine mutated variant (Figure 3.27) might still be sufficient to bind $[\text{Fe-S}]$ cluster and thus contribute to its UV-VIS properties (Figure 3.33).

Although the three conserved cysteine residues of the AdoMet motif (CysX₉CysX₂Cys) in ScElp3, analogous to the (CysX₄CysX₂Cys) motif found in the

4 DISCUSSION

archaeal Elp3 (Paraskevopoulou *et al.*, 2006), have been substituted for alanine (Figure 3.27), the ScElp3C₃-A₃ (triple) cysteine mutated variant appears to still bind a [4Fe-4S] cluster (Figure 3.33A), which is dithionite reducible (Figure 3.33B). In contrast, double mutations of AdoMet domain cysteines (C96S-C101S, C96S-C104S, C101S-C104S) in archaeal Elp3 have been demonstrated to completely abrogate iron-sulfur cluster binding (Paraskevopoulou *et al.*, 2006). ScElp3 still binds [Fe-S] cluster irrespective of multiple cysteine mutations (Figure 3.27). This led to the postulation of a second putative [Fe-S] cluster binding motif (CysX₁₁CysX₁₂CysX₂₇Cys) at the C-terminus of ScElp3 protein (Figure 3.27) conserved in almost all eukaryotic Elp3 proteins. The summary of the [Fe-S] cluster binding in the ScElp3 mutated variants upon UV-visible spectroscopic analyses is shown in Figure 4.0. In contrast, a recent report (Urzica *et al.*, 2009) demonstrated that recombinant yeast Nar1 wild type and cysteine mutated proteins purified from *E. coli* extracts do not contain native [Fe-S] clusters. It could also be possible that ScElp3 wild type, ScElp3C₃-A₃ (triple) and ScElp3C₅-A₅ (quintuple) cysteine mutated variants purified from *E. coli* extracts also do not contain native [Fe-S] clusters. Therefore, it would be imperative to confirm these data by isolating functional ScElp3 wild type and cysteine mutated proteins from their native environment, namely the yeast cytosol.

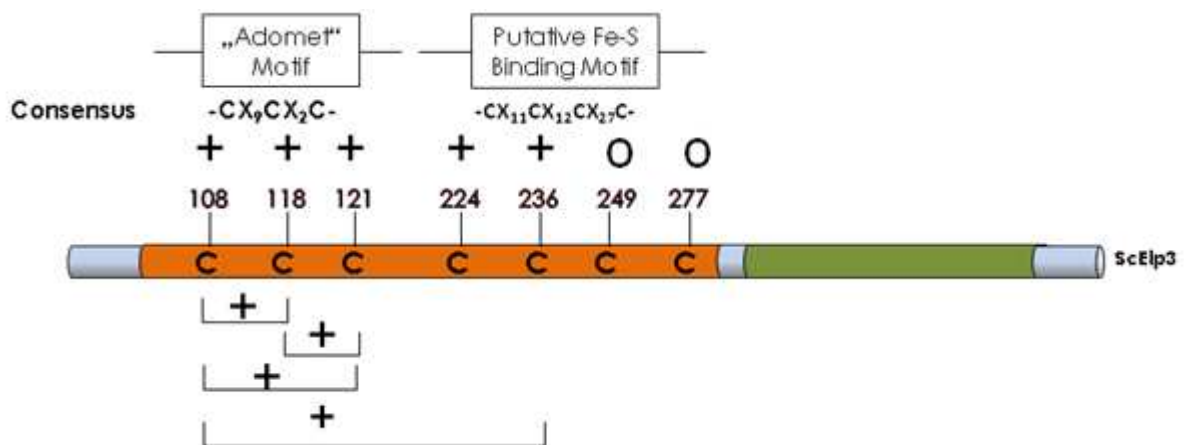


Figure 4.0 | Schematic overview of UV-Visible spectroscopic data obtained for the wild type and radical SAM domain mutated variants of ScElp3 on [4Fe-4S] binding. The positions of the conserved cysteines constituting ligands to the AdoMet and the 2nd putative Fe-S cluster binding motif are shown. The radical SAM domain is depicted in orange and the HAT domain in green. Abbreviations: +, depicts [4Fe-4S] binding similar to that of the wild type; O, indicate mutated variants where the UV-VIS spectra were not determined. Refer to figures 3.13, 3.20, 3.26, 3.33 and 3.34A.

4 DISCUSSION

Evidence that ScElp3 may also bind two [4Fe-4S] clusters was obtained from yeast cells producing ScElp3 mutated protein by direct binding of [⁵⁵Fe-S] cluster *in vivo*. A complete loss of radioactive ⁵⁵Fe incorporation was recorded for the C-A single (C108A), C₃-A₃ triple (C108A-C118A-C121A) and C₅-A₅ quintuple (C108A-C118A-C121A-C224A-C236A) ScElp3 mutated variants. In contrast, the incorporation of ⁵⁵Fe into a double cysteine substitution ScElp3(C224A-C236A) mutated protein of a 2nd putative [Fe-S] cluster binding motif, resulted in a decrease to ~76% of the wild type level (Section 3.11; Figure 3.41). The reduced ⁵⁵Fe binding in the ScElp3 double cysteine (C224A-C236A) mutated variant may be attributed to changes in its native structure resulting from the cysteine to alanine substitutions of the amino acid residues at positions 224 and 236 on the ScElp3 protein. However, in the absence of the AdoMet [Fe-S] binding, there is no [Fe-S] binding to ScElp3. Thus, if any additional Fe binding occurs, the binding of [Fe-S] cluster to the AdoMet motif is a prerequisite for the biogenesis and insertion of the 2nd putative [Fe-S] cluster. Similar findings have been reported for the Nar1 protein involved in cytosolic [Fe-S] cluster assembly (Urzica *et al.*, 2009). The data suggest the binding of an [Fe-S] cluster to a 2nd putative [Fe-S] cluster binding motif, although in its absence, [Fe-S] cluster could still be inserted into the AdoMet motif (Figures 3.27 & 3.41).

Additional evidence for the presence of two [Fe-S] clusters in ScElp3 was gathered from the size exclusion chromatography of the ScElp3 wild type and C₃-A₃ (triple) cysteine mutated variants (Figure 3.26B, Figure 3.34A). The ScElp3 protein fractions eluted simultaneously with the UV-visible peak at 420 nm that signifies [Fe-S] cluster binding. The brown colour associated with the eluates of ScElp3C₃-A₃ (triple) cysteine mutated variant also suggests [Fe-S] cluster binding (Figure 3.34B). Together, the *in vitro* UV-visible spectroscopic and *in vivo* ⁵⁵Fe binding data support the hypothesis that the ScElp3 protein binds two [Fe-S] clusters.

Recently, numerous iron-sulfur cluster binding proteins containing more than one [Fe-S] cluster have been characterized. Typical examples include biotin synthase, lipoyl synthase, MiaB, Nar1 and the formylglycyl-radical generating protein AtsB (Broach & Jarrett 2006; Cicchillo *et al.*, 2004; Hernández *et al.*, 2007; Urzica *et al.*, 2009; Grove *et al.*, 2008). These proteins contain additional cysteine residues contributing ligands to [Fe-S] cluster(s) binding in conserved motifs different

4 DISCUSSION

from the canonical CysX₃CysX₂Cys signature sequence of the enzyme radical SAM superfamily. Several radical SAM enzymes that incorporate two [Fe-S] clusters have been implicated mostly in sulfur insertion reactions, where the second [Fe-S] serves as the source of the sulfur moiety in a self-sacrificial reaction mechanism (Booker *et al.*, 2007). The radical SAM enzyme, MoaA involved in molybdenum cofactor biosynthesis also contains two [Fe-S] clusters (Santamaria-Araujo *et al.* 2004; Hänzelmann & Schindelin 2006). Although the second [4Fe-4S] cluster in MoaA is not involved in any sulfur insertion reaction, it has been proposed to be important for GTP substrate binding and functions only as cofactor in MoaA enzymatic reaction (Hänzelmann & Schindelin, 2006). Unlike in MoaA, the 2nd putative [4Fe-4S] cluster of eukaryotic Elp3 proteins does not play any significant role in Elongator-dependent tRNA modification. The Elp3 proteins coordinate two [Fe-S] clusters, although only the AdoMet [Fe-S] cluster is important for Elongator function.

4.4 Influence of cysteine mutations in the radical SAM domain for the structural integrity of the Elongator complex

The interactions between the subunits of the Elongator complex and its regulatory partner Kti12 have been studied by coimmunoprecipitation (Frohloff *et al.*, 2001, 2003; Fichtner *et al.*, 2002a; Greenwood *et al.*, 2009). Although, AtElp3 is not able to complement yeast *elp3Δ* phenotype, interaction studies by coimmunoprecipitation indicated that AtElp3 could be assembled in a plant-yeast hybrid Elongator complex (Wrackmeyer 2007; Mehlgarten 2009; Mehlgarten *et al.*, 2010). Coimmunoprecipitation studies showed that the cysteine substitutions in the radical SAM domain in ScElp3 protein did not influence the interaction of the ScElp3 cysteine mutated variants with the Elongator subunit Elp1 (Section 3.10; Figure 3.40). Like the ScElp3 wild type protein, the cysteine mutated proteins were able to interact with the Elp1 subunit of the Elongator complex, but highly unstable compared to the wild type. However, the functional ScElp3C224A-C236A double cysteine mutated protein could also be incorporated into the Elongator complex, but exhibited comparable stability like the wild type (Zabel unpublished). Low protein amounts were observed between the interactions of the radical SAM AdoMet cysteine mutated variants and the Elp1 subunit of the Elongator complex compared to the ScElp3 wild type. This may be due to immense structural changes as a

4 DISCUSSION

consequence of damage/loss of [Fe-S] cluster resulting from the substitution of cysteine to alanine, thus making the mutated proteins unstable. Greenwood *et al.*, (2009) recently reported the yeast radical SAM domain to be only important for the structural integrity of the Elongator complex based on the unstable nature of the AdoMet cysteine mutated proteins.

Considering the fact that ScElp3 exhibits high sequence similarity with the radical SAM enzyme superfamily and binds [4Fe-4S] clusters, it could be postulated that the radical SAM domain of ScElp3 may function following a radical-based catalytic mechanism analogous to enzymes of the radical SAM superfamily (Sofia *et al.*, 2001; Frey *et al.*, 2008). Although the functions of the radical SAM domain have not been thoroughly studied, members of the radical SAM superfamily have been implicated in several RNA modifications (Atta *et al.*, 2009), thus suggesting a possible function of Elp3 radical SAM domain in a radical-mediated tRNA modification.

4.5 Biological importance of the radical SAM domain for Elongator function

Deletions of the six genes *ELP1-ELP6* coding for the subunits of the Elongator complex or the Elongator-associated Kti protein coding genes result in the characteristic *elp/tot* phenotypes. Although the pleiotropic phenotypes of yeast Elongator deletion mutants have previously been reported to be as a result of transcriptional defects (Otero *et al.*, 1999; Wittschieben *et al.*, 1999), recent findings suggested that phenotypes of *elp1-elp6* and *kti11-kti14* mutants may be a consequence of less efficient translation and/or mistranslation caused by lack of mcm^5 , mcm^5s^2 and ncm^5 side chains at the wobble position of 11 out of 42 tRNA species in yeast (Huang *et al.*, 2005, 2008; Lu *et al.*, 2005). A defective Elongator complex in *Arabidopsis* is also associated with pleiotropic phenotypes, such as defects in cell proliferation and morphology, sensitivity to abscisic acid, oxidative stress resistance, drought tolerance and influence in anthocyanin biosynthesis (Nelissen *et al.*, 2005; Chen *et al.*, 2006; Falcone *et al.*, 2007; Zhou *et al.*, 2009).

Modifications of nucleosides at positions 34 and 37 in the anticodon region of tRNA species are frequent phenomena and their function has been primarily attributed to

4 DISCUSSION

the decoding process in mRNA (Agris 1991; Lim 1994). This entails involvement in reading frame maintenance and/or restriction or improvement of codon-anticodon interactions. The presence of mcm^5 or ncm^5 groups at U_{34} restricts pairing of A-/G- ending codons and their absence has been suggested to likely cause a general reduction in the efficiency of translation (Lim 1994; Yokoyama & Nishimura 1995). It is assumed that the Kti11-Kti14 proteins regulate Elongator in the modification of uridine at the wobble position and that the activity of the Elongator complex modulates translational efficiency, since overexpression of two specific tRNA genes (Esberg *et al.*, 2006) led to the suppression of *elp/tot* phenotypes resulting from exocytosis (Rahl *et al.*, 2005) and transcriptional defects (Wittschieben *et al.*, 2000). This is an indication that these phenotypes emanate due to translational dysfunction caused by a tRNA modification defect.

To elucidate the biological role of the radical SAM domain for Elongator function, single or multiple substitutions of the conserved cysteine residues contributing ligands to [Fe-S] cluster binding in ScElp3 protein were constructed in the p424TDH plasmid and subsequently transformed into yeast cells carrying an *elp3* deletion. The *elp3Δ* mutant yeast cells were then subjected to phenotypic characterization. It could be shown that the expression of the single C108A, C118A and C121A *elp3* alleles were not able to complement the *elp3Δ* phenotype and hence non-functional (Section 3.8.1; Figure 3.35A). The same results were reported concurrently by Greenwood *et al.*, (2009). They were able to show by γ -toxin assay that all single *elp3* mutants, where the important cysteine residues of the AdoMet binding motif were mutated, appeared to be resistant indicating the importance of all three cysteine (C108, C118 and C121A) residues for Elongator function. This is an indication of the absence of the side chains at the wobble uridine (U_{34}) in the Elongator-dependently modified tRNA species (Huang *et al.*, 2005; Lu *et al.*, 2005). Apparently, the AdoMet cysteine residues involved in [4Fe-4S] cluster formation are also important for the function of the yeast Elongator complex. In contrast, the single *elp3* cysteine mutant alleles contributing ligands to a 2nd putative [Fe-S] cluster binding motif (C224A, C236A, C249A and C277A) when expressed in *elp3Δ* yeast strain were able to restore the γ -toxin sensitivity of the ScElp3 wild type (Section 3.8.1, Figure 3.27, Figure 3.35B). Upon overexpression of different combinations of double cysteine *elp3* mutant alleles

4 DISCUSSION

of a 2nd putative [Fe-S] cluster binding motif (Figure 3.27) in an *elp3Δ* deletion mutant (Section 3.8.1; Figure 3.36) or endogenously under their native promoter (data not shown), Elongator function could still be restored. This suggests that single or combined conserved cysteine mutations of a 2nd putative [Fe-S] binding motif do not affect Elongator function under the tested conditions for tRNA modification and hence the mutants are all functional.

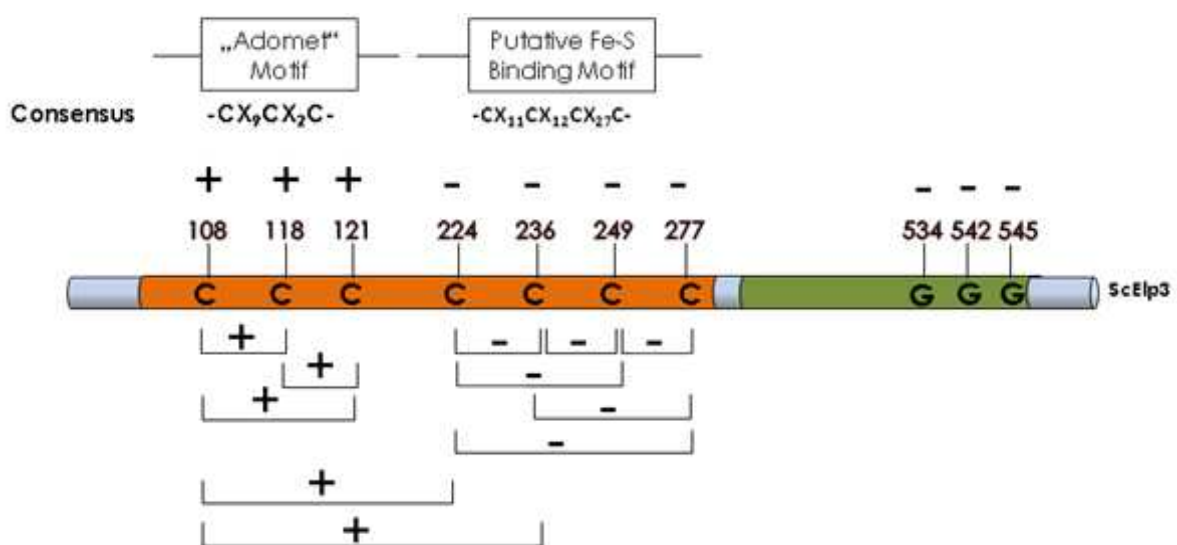
In analogy to the results obtained from the γ -toxin sensitivity assay using ScElp3 double cysteine mutant alleles of a 2nd putative [Fe-S] cluster binding motif (Figure 3.36), expression of two putative glycine radical *elp3* mutant alleles (G542A and G545A) (Figure 3.27; data not shown), could still restore Elongator function in the γ -toxin assay, suggesting that these glycine residues are not essential for Elongator function. The results accumulated from the γ -toxin assay were further supported by the *can1-100* tRNA^{Tyr} suppression by *SUP4* (Huang *et al.*, 2005; Figure 3.39).

Taken together, the conserved cysteine thiolates of the AdoMet motif are important while the conserved cysteines of the 2nd putative [Fe-S] binding motif and the conserved glycine residues are dispensable for tRNA modification. However, conserved cysteine residues acting as ligands for a second [Fe-S] cluster binding in radical SAM enzymes such as MoeA (Hänzelmann *et al.*, 2006), MiaB (Hernández *et al.*, 2007), and the *E. coli* biotin synthase (Ugulava *et al.*, 2002) and lipoyl synthase (Cicchillo *et al.*, 2004) have been reported to play essential roles for enzyme activity. In contrast, the recently characterized radical SAM enzyme HydE involved in iron-only hydrogenase maturation in *Thermotoga maritima* (*TmHydE*) contains two [Fe-S] clusters, a [4Fe-4S] cluster bound to the canonical CysX₃CysX₂Cys AdoMet motif and a second [2Fe-2S] cluster (Rubach *et al.*, 2005; Nicolet *et al.*, 2008). The cysteine residues contributing ligands to the latter [Fe-S] cluster are dispensable for hydrogenase maturation, although they are not conserved in all *hydE* gene sequences (Böck *et al.*, 2006). The *TmHydE* structure obtained when crystals were grown in the presence of dithiothreitol illustrated the ligation of a [2Fe-2S] cluster at the protein surface to Cys³¹¹, Cys³¹⁹, Cys³²² and a water molecule, 20Å away from the conserved 4Fe-4S] cluster. The respective positions of *TmHydE* [2Fe-2S] and

4 DISCUSSION

the second [4Fe-4S] cluster in MoaA are almost equivalent (Hänzelmann & Schindelin 2004). The position of the *TmHydE* [2Fe-2S] cluster and its composition is intriguing. Although only the cysteine thiolates of the AdoMet [4Fe-4S] cluster in ScElp3 are important for the maintenance of Elongator function, the cysteine ligands of the 2nd [Fe-S] binding motif bind a [Fe-S] cluster. The significance of the 2nd [Fe-S] cluster is unknown. It may probably play a role in the kinetics of Elongator-dependent tRNA modification reactions. The results of the mutated conserved cysteine and glycine residues for Elongator function upon γ -toxin and *SUP4* assays are summarized in Figure 4.1.

The conserved cysteines of the 2nd putative [Fe-S] binding and glycines of the putative glycine radical motifs respectively may be significant in other functions apart from Elongator-dependent tRNA modification. The conserved glycine residues are part of motif B in GNAT superfamily members (Neuwald & Landsman 1997) and their mutation to alanine in recombinant yeast Gcn5 does not lead to reduction of *in vitro* HAT activity (Kuo *et al.*, 1998). Nevertheless, mutations affecting the histone acetyltransferase activity of Elp3 HAT domain which acetylates histone H3 and H4 have been reported by Huang *et al.*, (2005) to also affect tRNA modification. Recent studies illustrated that the protein TmcA in eubacteria transfers an acetyl moiety from acetyl-CoA to the N4 atom of a wobble cytidine of tRNA^{Met} (Chimnarongk *et al.*, 2009), thus suggesting a possible coupling of the GNAT domain to tRNA modification.



4 DISCUSSION

Figure 4.1 | Schematic picture of *in vivo* data on Elongator function from the γ -toxin sensitivity and *SUP4* assays using the radical SAM domain mutated variants of ScElp3. The positions of the conserved cysteines constituting ligands to the AdoMet and a 2nd putative Fe-S cluster binding motif and the conserved glycine residues are indicated. Abbreviations: +, resistant phenotype indicates importance for Elongator function similar to *elp3 Δ* strain; -, sensitive phenotype depicting dispensability for Elongator function similar to that of the wild type. See also Section 3.8, Figures 3.35 & 3.36; Section 3.9; Figure 3.39.

4.6 Regulation of the radical SAM domain by the Elongator-associated redox protein, Kti11

The yeast Elongator partner proteins Kti11 and Kti13 are important for Elongator tRNA modification (Huang *et al.*, 2005). Immune precipitates of Kti11 were shown to contain Elp2 and Elp5 subunits of the Elongator complex (Bär *et al.*, 2008). The *kti11 Δ kti13 Δ* double deletion causes lethality, suggesting that apart from their Elongator-dependent roles, Kti13 and Kti11 might share an Elongator-independent role essential for cell viability (Zabel *et al.*, 2008). Kti11 (alias Dph3) is not only important for Elongator function, but is also one of five yeast proteins (Dph1-Dph5) involved in the biosynthesis of diphthamide (Moehring *et al.*, 1980; Mattheakis *et al.*, 1992; Schultz *et al.*, 1998; Liu *et al.*, 2004). Interestingly, diphthamide biosynthesis is also dependent on radical chemistry, with the radical SAM protein Dph2 effecting radical generation. Diphthamide, a unique post-translationally modified histidine residue of translation elongation factor 2 (eEF-2), which is conserved in all eukaryotes and archaeobacteria, functions as the target for diphtheria toxin (Collier 2001). Diphtheria toxin specifically mediates the transfer of ADP-ribose moiety from NAD⁺ to diphthamide on eEF2, leading to eEF2 inactivation, disruption of protein synthesis and subsequent cell death.

Cryo-electron microscopic reconstruction of the yeast ribosome-eEF2 complex illustrated that the tip of domain IV of eEF2, suggested as an anticodon mimicry domain, is in close proximity to the tRNA found in the ribosomal P-site (Spahn *et al.*, 2004). Based on this finding, the eEF2 was proposed to be vital in the stabilization of codon-anticodon pairing during translocation and thus preventing a -1 frameshift. Other studies have implicated eEF2 in the involvement of accurate ribosomal protein synthesis by enhancing the translocation of tRNAs and the

4 DISCUSSION

movement of the mRNA during translation elongation (Gomez-Lorenzo *et al.*, 2000; Ortiz *et al.*, 2006). The initial step in diphthamide biosynthesis is catalyzed by Dph1-Dph4 and entails the transfer of the 3-amino-3-carboxypropyl group (ACP) from AdoMet to the C-2 position of the imidazole ring of the target histidine residues in eEF2. The second step catalyzed by Dph5 involves the trimethylation of the amino group to form the intermediate diphthine. The last step is the ATP-dependent amidation of the carboxyl group of diphthine catalyzed by an unidentified enzyme. In archaea, Dph2 is a homodimeric radical SAM enzyme that binds [4Fe-4S] cluster and cleaves S-adenosylmethionine (Zhang *et al.*, 2010; Zhu *et al.*, 2011). In contrast to the radical SAM enzymes, Dph2 reductively cleaves SAM to generate a non-canonical 3-amino-3-carboxypropyl radical (ACP), instead of a 5'-deoxyadenosyl radical produced by Elp3 from *Methanocaldococcus jannaschii* (Paraskevopoulou *et al.*, 2006). Previous study suggested that an ACP radical is responsible for the addition to or abstraction of hydrogen atom from the imidazole ring of the target histidine residue (His 699 in yeast eEF2) resulting in a C-C bond formation (Zhang *et al.*, 2010), and subsequent formation of diphthamide in the presence of other *DPH* gene products. Nevertheless, the details of the reaction mechanism are still unknown.

The yeast Kti11/Dph3 has recently been reported to bind iron or zinc and can be reversibly reduced by the rubredoxin reductase NorW and exhibits rubredoxin-like electron carrier activity *in vitro* (Proudfoot *et al.*, 2008; Zabel unpublished). The Dph3 and Dph4 proteins have been proposed to be essential for the maintenance of [4Fe-4S] cluster in a reduced state (Zhang *et al.*, 2010) and this was corroborated by the observation that Kti11/Dph3 is a redox active protein that can bind iron (Proudfoot *et al.*, 2008). Alternatively, Kti11/Dph3 and Dph4 may be required for proper biogenesis and insertion of [4Fe-4S] clusters into apoproteins. The Fe-S cluster assembly pathways in prokaryotes and the mitochondria of eukaryotes are known to comprise the J-domain-containing co-chaperones like the bacterial HscB and yeast Jac1 (Johnson *et al.*, 2005; Lill & Mühlhoff 2008), which are similar to Dph4 (Liu *et al.*, 2004). The Elongator partner protein Kti12 carries a kinase-related P-loop motif and preferentially binds GTP. It has also recently been proposed to be involved in the modulation of Elp1 phosphorylation status (Fichtner *et al.*, 2002a; Nelissen *et al.*, 2003; Mehlgarten *et al.*, 2009). Based on the high sequence

4 DISCUSSION

similarity observed between the yeast Kti12 and the archaeal phosphoseryl-tRNA^{Sec}-kinase (PSTK) from *Methanocaldococcus jannaschii*, Kti12 has been proposed to also presumably interact with tRNA substrates and could function as a tRNA-dependent kinase (Sherrer *et al.*, 2008). The radical SAM proteins Elp3 and Dph2 bind and cleave SAM and thus function via radical chemistry (Paraskevopoulou *et al.*, 2006; Zhu *et al.*, 2011). The tRNA and diphthamide modification pathways most likely share functional similarities.

The redox potential of Kti11/Dph3 was determined using xanthine oxidase and indigo carmine as controls and was found to be 6 mV (Proudfoot *et al.*, 2008), which is similar to the redox potential of rubredoxins (-57 to 6 mV) (Moura *et al.*, 1979; Sieker *et al.*, 1994). To test the reducing effect of Kti11/Dph3 on [4Fe-4S] clusters of ScElp3, increasing concentrations of reduced Kti11/Dph3 protein were titrated against reconstituted ScElp3 wild type protein. The result illustrated reduction of ScElp3[4Fe-S4] cluster peak at 420 nm upon incubation of increasing concentration of reduced Kti11/Dph3 with the reconstituted ScElp3 protein (Section 3.12; Figure 3.42). Indeed, the redox potentials for the [4Fe-4S]^{2+/1+} couples of the radical SAM enzymes have been estimated to be in the range of about -450 mV (Hinckley & Frey 2006; Ugulava *et al.*, 2001) and thus thermodynamically inaccessible for reduction by physiological reductants like ferredoxins. Studies conducted by Daley and Holm (2001, 2003) demonstrated that the redox potentials of [4Fe-4S] clusters and the sulfonium cations were such that electron transfer from the former to the latter was favorable thermodynamically. However, investigations on the radical SAM enzyme, lysine-2,3-aminomutase (LAM) that catalyzes the interconversion of L-lysine and L-β-lysine by a free radical mechanism have revealed increase in the [4Fe-4S]^{2+/1+} reduction potential within the range of physiological reductants in the presence of AdoMet (Hinckley & Frey 2006). Wang and Frey (2008) also reported that the contributions of AdoMet and lysine binding to LAM prompted the reduction of the energy barrier for AdoMet cleavage from 32 kcal mol⁻¹ to 9 kcal mol⁻¹. Additionally, transfer of electron from the [4Fe-4S]¹⁺ cluster to the sulfonium of AdoMet converts the pentacoordinate iron of the [4Fe-4S]¹⁺ to the favorable hexacoordinate iron in the [4Fe-4S]²⁺ in LAM and this has been proposed to ease inner-sphere electron transfer (Wang & Frey 2007). Investigation by Jarrett and co-workers has indeed shown that biotin synthase binds AdoMet and its

4 DISCUSSION

substrate desthiobiotin in an ordered manner and thus resulting to increased affinity for AdoMet of more than 20-fold in the presence of substrate (Ugulava *et al.*, 2003).

Taken together, Kti11/Dph3 may facilitate the maintenance of [4Fe-4S] clusters in ScElp3 and Dph2 in the reduced state and subsequent generation of 5'-deoxyadenosyl or 3-amino-3-carboxypropyl radicals, thus playing active roles in Elongator-dependent tRNA modification and diphthamide biosynthesis respectively (Huang *et al.*, 2005; Zhang *et al.*, 2010; Zhu *et al.*, 2011). Most likely, interaction of Kti11 (Dph3) with ScElp3[4Fe-4S] bound to AdoMet and its tRNA substrate and other components of the reaction would increase the redox potential of AdoMet and facilitate single electron transfer from Kti11/Dph3 via ScElp3[4Fe-4S] to the latter. Transition of the [4Fe-4S]²⁺ to the [4Fe-4S]⁺¹ in members of the radical SAM enzyme superfamily by transfer of a single electron is important for the production of the highly oxidizing 5'-deoxyadenosyl radical involved in the catalytic activity of this group of enzymes (Frey & Magnusson 2003; Frey *et al.*, 2008). Thus Kti11/Dph3 protein may exert its regulatory function on Elongator by the reduction of [4Fe-4S] cluster in Elp3 and thus causing subsequent generation of radical species indispensable for the activation of the 5' C-H bond on U₃₄ and formation of the Elongator-dependent mcm⁵, mcm⁵s² and ncm⁵ side chains. The confirmation of electron transfer from Kti11 to AdoMet bound to ScElp3[4Fe-4S] may represent the first report of such mechanism in eukaryotes. Our data, in consistency with those of the *Methanocaldococcus jannaschii* archaeal Elp3 (Paraskevopoulou *et al.*, 2006) and other enzymes of the radical SAM superfamily (Sofia *et al.*, 2001; Frey *et al.*, 2008), support the hypothesis that radical SAM domain of eukaryotic Elp3 proteins may most likely catalyze the radical-based enzymatic reaction mechanism of the Elongator-dependent tRNA modification at the wobble uridine position. In contrast, the ScElp3 radical SAM domain may not only be important for its stability as previously reported (Greenwood *et al.*, 2009).

5.0 Outlook

The dissection of the radical SAM domain of the yeast and plant Elp3 subunit of the Elongator demonstrated that AtElp3 and ScElp3 are [4Fe-4S] binding proteins and also illustrated the importance of this domain for Elongator-dependent tRNA modification. Future *in vitro* analysis on Elp3 proteins should be focused on the expression and tandem affinity purification of the Elongator complex from the *Saccharomyces cerevisiae* to isolate native Elongator. The use of native Elp3 mutated proteins for UV-VIS analyses would resolve the presence of a 2nd [4Fe-S4] cluster. Based on the sensitivity of Elp3 to oxygen, all analyses should be conducted under strict anaerobic conditions to prevent [Fe-S] cluster oxidation and isolation of native Elp3 proteins containing properly inserted [Fe-S] clusters. The results accumulated from the ScElp3C₃-A₃ (triple) and ScElp3C₅-A₅ (quintuple) cysteine mutated variants coupled with the ⁵⁵Fe binding experiment demonstrated the insertion of a 2nd [4Fe-4S] in ScElp3. Further experiments would be imperative to elucidate the presence and function of the 2nd [4Fe-4S] cluster in Elp3. Additional mutations of the ScElp3C₅-A₅ (quintuple) cysteine mutated variant by substituting the conserved cysteine residues to alanine (C249 and C277) would be able to shed more light on the [4Fe-4S] peak at 420 nm observed for the ScElp3C₅-A₅ (quintuple) cysteine mutant. Further experiments to study the influence of Kti11 on the radical SAM domain of ScElp3 should be conducted. If the Kti11/Dph3 protein could act as a reducing agent for the Fe-S cluster of ScElp3, this could be monitored in a reaction cocktail containing S-adenosylmethionine (SAM or AdoMet) and Elongator tRNA substrates. The degradation product of SAM (5'-deoxyadenosine) obtained upon generation of the 5'-deoxyadenosyl radical resulting from the cleavage of SAM by reduced [4Fe-4S]⁺¹ as observed in all radical SAM enzymes, could then be monitored by HPLC. Other studies to elucidate the mechanism of action involved in the formation of the Elongator-dependent side chains on the wobble uridine (U₃₄) in certain tRNAs (Huang *et al.*, 2005, Lu *et al.*, 2005) would be needed. Although proteins contributing to the mcm⁵s²U modification have been detected in a genome-wide screen (Huang *et al.*, 2008), the mechanism involved in this modification is still unknown. The reactions may follow a carbon-based radical mechanism, where the radical SAM domain of ScElp3 generate the highly reactive 5'-deoxyadenosyl radical upon reduction of its [4Fe-4S] cluster by the Kti11 protein.

6.0 References

- Agris, P. F. (1991).** Wobble position modified nucleosides evolved to select transfer RNA codon recognition: a modified-wobble hypothesis. *Biochimie*. **73**: 1345-1349
- Akada, R., Kawahata, M and Nishizawa, Y. (2000).** Elevated temperature greatly improves transformation of fresh and frozen competent cells in yeast. *BioTechniques* **28**: 854-856
- Anderson, S. L., Coli, R., Daly, I. W., Kichula, E. A., Rork, M. J., Volpi, S. A., Ekstein, J., and Rubin, B. Y. (2001).** Familial dysautonomia is caused by mutations of the *IKAP* gene. *Am J. Hum. Genet.* **68**: 753-758
- Arragain, S., Garcia-Serres, R., Blondin, G., Douki, T., Clemancey, M., Latour, J. M., Forouhar, F., Neely, H., Montelione, G. T., Hunt, J. F., Mulliez, E., Fontecave, M., and Atta M. (2010).** Post-translational modification of ribosomal proteins: Structural and functional characterization of RimO from *Thermotoga maritima*, a radical S-adenosylmethionine methylthiotransferase. *J. Biol. Chem.* **285**: 5792-5801
- Atta, M., Fontecave, M., and Mulliez, E. (2009).** RNA-modifying metalloenzymes. In DNA and RNA Modification Enzymes: Structure, Mechanism, Function and Evolution (Molecular Biology Intelligence Unit). Grosjean, H. (ed.), Austin, TX: Landes Bioscience, pp. 347-361
- Atta, M., Mulliez, E., Arragain, S., Forouhar, F., Hunt, J. F., and Marc Fontecave (2010).** S-Adenosylmethionine-dependent radical-based modification of biological macromolecules. *Curr. Opin. Stru. Biol.* **20**: 684-692
- Ausubel, F. M., Brent, R., Kingston, R. E., Moore, D. D., Seidman, J. G., Smith, J. A., and Struhl, K. (1998).** *Current Protocols in Molecular Biology*. John Wiley and Sons., New York
- Banerjee, R. (2003).** Radical carbon skeleton rearrangements: Introduction: Radical Enzymology. *Chem Rev* **103**: 2083-2094
- Bär, C., Zabel, R., Liu, S., Stark, M. J. R., and Schaffrath, R. (2008).** A versatile partner of eukaryotic protein complexes that is involved in multiple biological processes: Kti11/Dph3. *Mol. Microbiol.* **69**: 1221-1233
- Beinert, H., Kennedy, M. C., and Stout, C. D. (1996).** Aconitase as Iron-Sulfur Protein, Enzyme, and Iron-Regulatory Protein. *Chem. Rev.* **96**: 2335-2374

- Beinert, H., Holm, R. H., and Münck, E. (1997).** Iron-sulfur clusters: nature's modular, multipurpose structures. *Science*. **277**: 653-659
- Berkovitch, F., Nicolet, Y., Wan, J. T., Jarrett, J. T., and Drennan, C. L. (2004).** Crystal structure of biotin synthase, an S-adenosylmethionine-dependent radical enzyme. *Science*. **303**: 76-79
- Boal, A. K., Grove, T. L., McLaughlin, M. I., Yennawar, N. H., Booker, S. J., and Rosenzweig, A. C. (2011).** Structural Basis for Methyl Transfer by a Radical SAM Enzyme. *Sci*. **332**: 1089-1092
- Böck, A., King, P. W., Blokesch, M., and Posewitz, M. C. (2006).** Maturation of hydrogenases. *Adv. Microb. Physiol*. **51**: 1-71
- Boeke, J., LaCrute, F., Fink, G. R. (1984).** A positive selection for mutants lacking orotidine-5'-phosphate decarboxylase activity in yeast: 5-fluoro-orotic acid resistance. *Mol. Gen. Genet*. **197**: 345-346
- Booker, S. J., Cicchillo, R. M., and Grove, T. L. (2007).** Self-sacrifice in radical S-adenosylmethionine proteins. *Curr. Opin. Chem. Biol*. **11**: 543-552
- Booker, S. J., and Grove, T. L. (2010).** Mechanistic and functional versatility of radical SAM enzymes. *F1000 Biol. Rep*. **2** (52) 14 July 2010
- Bravo, J., Fita, I., Ferrer, J. C., Ens, W., Hillar, A., Switala, J., Loewen, P. C. (1997).** Identification of a novel bond between a Histidine and the essential Tyrosine in Catalase HPII of *Escherichia coli*. *Prot. Sci*. **6**: 1016-1023
- Bradford, M. (1976).** A rapid and sensitive method for the quantitation of microgram quantities of protein utilizing the principle of protein-dye binding. *Anal. Biochem*. **72**: 248-254
- Broach, R. B., and Jarrett, J. T. (2006).** Role of the [2Fe-2S]²⁺ cluster in biotin synthase: mutagenesis of the atypical metal ligand arginine 260. *Biochem*. **45**: 14166-14174
- Broderick, J. B., Henshaw, T. F., Cheek, J., Wojtuszewski, K., Smith, S. R., Trojan, M. R., McGhan, R. M., Kopf, A., Kibbey, M., and Broderick, W. E. (2000).** Pyruvate formate-lyase-activating enzyme: strictly anaerobic isolation yields active enzyme containing a [3Fe-4S]⁺ cluster. *Biochem. Biophys. Res. Commun*. **269**: 451-456
- Brüser, T., Yano, T., Brune, D. C., and Daldal, F. (2003).** Membrane targeting of a folded and cofactor-containing protein. *Eur. J. Biochem*. **270**: 1211-1221

6 REFERENCES

- Buis, J. M., and Broderick, J. B. (2005).** Pyruvate formate-lyase activating enzyme: Elucidation of a novel mechanism for glycyl radical formation. *Arch. Biochem. Biophys.* **433**: 288-296
- Bukau, B., and Horwich, A. L. (1998).** The Hsp70 and Hsp60 chaperone machines. *Cell.* **92**: 351-366
- Bukau, B., Weissman, J., and Horwich, A. L. (2006).** Molecular chaperones and protein quality control. *Cell.* **125**: 443-451
- Butler, A. R., White, J. H., and Stark, M. J. R. (1991a).** Analysis of the response of *Saccharomyces cerevisiae* cell to *Kluyveromyces lactis* toxin. *J. Gen. Microbiol.* **137**: 1749-1757
- Butler, A. R., O'Donnell, R. W., Martin, V. J., Gooday, G. W., and Stark, M. J. R. (1991b).** *Kluyveromyces lactis* toxin has an essential chitinase activity. *Eur. J. Biochem.* **199**: 483-488
- Butler, A. R., White, J. H., Folawiyo, Y., Edlin, A., Gardiner, D., and Stark, M. J. R. (1994).** Two *Saccharomyces cerevisiae* genes which control sensitivity to G1 arrest induced by *Kluyveromyces lactis* toxin. *Mol. Cell. Biol.* **14**: 6306-6316
- Cairo, G., Recalcati, S., Pietrangelo, A., and Minotti, G. (2002).** The iron regulatory proteins: targets and modulators of free radical reactions and oxidative damage. *Free Radic. Biol. Med.* **32**: 1237-1243
- Carlson, B. A., Xu, X-M, Kryukov, G. V., Rao, M., Berry, M. J., Gladyshev, V. N., and Hatfield, D. L. (2004).** Identification and characterization of phosphoseryl-tRNA^{[Ser]^{Sec}} kinase. *Proc. Natl. Acad. Sci. USA.* **101**: 12848-12853
- Casadaban, M. J. (1976).** Transposition and fusion of the *lac* genes to selected promoters in *Escherichia coli* using bacteriophages lamda and Mu. *J. Mol. Biol.* **104**: 541-555
- Chatterjee, A., Li, Y., Zhang, Y., Grove, T. L., Lee, M., Krebs, C., Booker, S. J., Begley, T. P., and Ealick, S. E. (2008).** Reconstitution of ThiC in Thiamine pyrimidine biosynthesis expands the radical SAM superfamily. *Nat. Chem. Biol.* **4**: 758-765
- Chen, Z., Zhang, H., Jablonowski, D., Zhou, X., Ren, X., Hong, X., Schaffrath, R., Zhu, J. K., and Gong, Z. (2006).** Mutations in ABO1/ELO2, a subunit of holo-Elongator, increase abscisic acid sensitivity and drought tolerance in *Arabidopsis thaliana*. *Mol. Cell. Biol.* **26**: 6902-6912

6 REFERENCES

- Chen, C., Tuck, S., and Byström, A. S. (2009).** Defects in tRNA modification associated with neurological and developmental dysfunctions in *Caenorhabditis elegans* elongator mutants. *PLoS Genet.* **5**: e1000561
- Chimnaronk, M., Suzuki, T., Manita, T., Ikeuchi, Y., Yao, M., Suzuki, T. and Tanaka, I. (2009).** RNA helicase module in an acetyltransferase that modifies a specific tRNA anticodon. *EMBO J.* **28**: 1362-1373
- Chin, K-C., Cresswell, P. (2001).** Viperin (cig5), an IFN-inducible antiviral protein directly induced by human cytomegalovirus. *Proc. Natl. Acad. Sci. USA.* **98**: 15125-15130
- Chinenov, Y. (2002).** A second catalytic domain in the Elp3 histone acetyltransferases: a candidate for histone demethylase activity? *Trends Biochem. Sci.* **27**: 115-117
- Ching, Y. P., Qi, Z., and Wang, J. H. (2000).** Cloning of the three novel neuronal Cdk5 activator binding proteins. *Gene.* **242**: 285-294
- Cicchillo R. M., Iwig, D. F., Jones, A. D., Nesbitt, N. M., Baleanu-Gogonea, C., Souder, M. G., Tu, L., and Booker, S. J. (2004).** Lipoyl synthase requires two equivalents of S-adenosyl-L-methionine to synthesize one equivalent of lipoic acid. *Biochem.* **43**: 6378-6386
- Cicchillo, R. M., Lee, K-H, Baleanu-Gogonea, C., Nesbitt, N.M., Krebs, C., and Booker, S. J. (2004).** *Escherichia coli* lipoyl synthase binds two distinct [4Fe-4S] clusters per polypeptide. *Biochem.* **43**: 11770-11781
- Cline, J. D. (1969).** Spectrophotometric determination of hydrogen sulfide. *Limnol. Oceanogr.* **14**: 454-458
- Close, P., Hawkes, N., Cornez, I., Creppe, C., Lambert, C. A., Rogister, B., Siebenlist, U., Merville, M. P., Slaugenhaupt, S. A., Bours, V., Svejstrup, J. Q., and Charlot, A. (2006).** Transcription impairment and cell migration defects in elongator-depleted cells: implication for familial dysautonomia. *Mol. Cell.* **22**: 521-531
- Cohen, L., Henzel, W. J., and Baeuerle, P. A. (1998).** IKAP is a scaffold protein of the I κ B kinase complex. *Nature.* **395**:292-296
- Collier, R. J. (2001).** Understanding the mode of action of diphtheria toxin: a perspective on progress during the 20th century. *Toxicon.* **39**: 1793-1803

- Collum, R. G., Brutsaert, S., Lee, G., and Schindler, C. (2000).** A Stat3-interacting protein (StIP1) regulates cytokines signal transduction. *Proc. Natl. Acad. Sci. USA.* **97:** 10120-10125
- Creppe, C., Malinouskaya, L., Volvert, M. L., Gillard, M., Close, P., Malaise, O., Laguesse, S., Cornez, I., Rahmouni, S., Ormenese, S., Belachew, S., Malgrange, B., Chappelle, J. P., Siebenlist, U., Moonen, G., Chariot, A., and Nguyen, L. (2009).** Elongator controls the migration and differentiation of cortical neurons through acetylation of alpha-tubulin. *Cell.* **136:** 551-564
- Daley, C. J. A and Holm, R. H. (2001).** Reactivity of $[\text{Fe}_4\text{S}_4(\text{SR})_4]^{2-,3-}$ clusters with sulfonium cations: analogue reaction systems for the initial step in biotin synthase catalysis. *Inorg. Chem.* **40:** 2785-2793
- Daley, C. J. A and Holm, R. H. (2003).** Reactions of the site-differentiated $[\text{Fe}_4\text{S}_4]^{2,+}$ clusters with sulfonium cations: reactivity analogues of biotin synthase and other members of the S-adenosylmethionine enzyme family. *J. Inorg. Biochem.* **97:** 287-298
- Davis, R. W., Thomas, M., Cameron, J., John, T. P., Scherer, S., and Padgett, R. A. (1980).** Rapid DNA isolations for enzymatic and hybridisation analysis. *Methods. Enzymol.* **65:** 404-411
- DeFraia, C. T., Zhang, X., and Mou, Z. (2010).** Elongator subunit 2 is an accelerator of immune responses in *Arabidopsis thaliana*. *The Plant J.* **64:** 511-523
- De Marco, A., Vigh, L., Diamant, S., and Goloubinoff, P. (2005).** Native folding of aggregation-prone recombinant proteins in *Escherichia coli* by osmolytes, plasmid- or benzyl alcohol-overexpressed molecular chaperones. *Cell Stress & Chaperones.* **10:** 329-339
- Demple, B., Ding, H., and Jorgensen, M. (2002).** *Escherichia coli* SoxR protein: sensor/transducer of oxidative stress and nitric oxide. *Methods Enzymol.* **348:** 355-364
- Ding, H. and Demple, B. (2000).** Direct nitric oxide signal transduction via nitrosylation of iron-sulfur centers in the SoxR transcription activator. *PNAS USA.* **97:** 5146-5150
- Duboc-Toia, C., Hassan, A. K., Mulliez, E., Ollagnier-de-Choudens, S., Fontecave, M., Leutwein, C., and Heider, J. (2003).** Very high-field EPR study of glycyl radical enzymes. *J. Am. Chem. Soc.* **125:** 38-39

- Duin, E. C., Lafferty, M. E., Crouse, B. R., Allen, R. M., Sanyal, I., Flint, D. H., and Johnson, M. K. (1997). [2Fe-2S] to [4Fe-4S] cluster conversion in *Escherichia coli* biotin synthase. *Biochem.* **36**: 11811-11820
- Duschene, K. S., Veneziano, S. E., Silver, S. C., and Broderick, J. B. (2009). Control of radical chemistry in the AdoMet radical enzymes. *Curr. Opin. Chem. Biol.* **13**: 74-83
- Duschene, K. S., and Broderick, J. B. (2010). The antiviral protein viperin is a radical SAM enzyme. *FEBS Lett.* **584**: 1263-1267
- Dutnall, R. N., Tafrov, S. T., Sternglanz, R., and Ramakrishnan, V. (1998). Structure of the histone acetyltransferase Hat1: a paradigm for the GCN5-related N-acetyltransferase superfamily. *Cell.* **94**: 427-438
- Eisenstein, R. S. (2000). Iron regulatory proteins and the molecular control of mammalian iron metabolism. *Annu. Rev. Nutr.* **20**: 627-662
- Erman, J. E., and Vitello, L. B. (2002). Yeast cytochrome c peroxidase: mechanistic studies via protein engineering. *Biochim. Biophys. Acta* **1597**: 193-220
- Esberg, B., Leung, H-C. E., Tsui, H-C, T., Björk, G. R., and Winkler, M. E. (1999). Identification of the miaB gene, involved in the methylthiolation of isopentenylated A37 derivatives in the tRNA of *Salmonella typhimurium* and *Escherichia coli*. *J. Bacteriol.* **181**: 7256-7265
- Esberg, A., Huang, B., Johansson, M. J., and Bystrom, A. S. (2006). Elevated levels of two tRNA species bypass the requirement for elongator complex in transcription and exocytosis. *Mol. Cell.* **24**: 139-148
- Falcone, A., Nelissen, H., Fleury, D., Van Lijsebettens, M., and Bitoni, M. B. (2007). Cytological Investigation of the *Arabidopsis thaliana elo1* Mutant Give New Insights into Leaf Lateral Growth and Elongator Function. *Annals Bot.* **100**: 261-270
- Fellows, J., Erdjument-Bromage, H., Tempst, P., and Svejstrup, J. (2000). The Elp2 subunit of Elongator and elongating RNA polymerase II holoenzyme is a WD40 protein. *J. Biol. Chem.* **275**: 12896-12899
- Fichtner, L. (2000). Funktionelle Analyse des *Saccharomyces cerevisiae* Gens *KT112* und dessen Rolle im *Kluyveromyces lactis* Toxin vermittelten Zellzyklusarrest. Diplomarbeit. Martin-Luther-Universität, Halle-Wittenberg.

6 REFERENCES

- Fichtner, L., and Schaffrath, R. (2002).** *KTI11* and *KTI13*, *Saccharomyces cerevisiae* genes controlling sensitivity to G1 arrest induced by *Kluyveromyces lactis* zymocin. *Mol. Microbiol.* **44**: 865-875
- Fichtner, L., Frohloff, F., Bürkner, K., Larsen, M., Breunig, K. D., and Schaffrath, R. (2002a).** Molecular analysis of *KTI12/TOT4*, a *Saccharomyces cerevisiae* gene required for *Kluyveromyces lactis* zymocin action. *Mol. Microbiol.* **43**: 783-791
- Fichtner, L., Jablonowski, D., Stark, M. J. R., and Schaffrath, R. (2002b).** Protein interactions within *Saccharomyces cerevisiae* Elongator, a complex essential for *Kluyveromyces lactis* zymocinicity. *Mol. Microbiol.* **45**: 817-826
- Fink, A. L. (1999).** Chaperone-mediated protein folding. *Physiol. Rev.* **79**: 425-449
- Fish, W. W. (1988).** Rapid colorimetric micromethod for the quantification of complexed iron in biological samples. *Methods Enzymol.* **158**: 357-364
- Fitzpatrick, P. F., Orville, A. M., Nagpal, A. and Valley, M. P. (2005).** Nitroalkane oxidase, a carbanion-forming flavoprotein homologous to Acyl-CoA dehydrogenase. *Arch Biochem. Biophys.* **433**: 157-165
- Flint, D. H., and Allen, R. M. (1996).** Iron-Sulfur Proteins with Nonredox Functions. *Chem. Rev.* **96**: 2315-2334
- Francois, F., Chapeland-Leclerc, F., Villard, J., Noël, T. (2004).** Development of an integrative transformation system for the opportunistic pathogenic yeast *Candida lusitanae* using *URA3* as a selection marker. *Yeast.* **21**: 95-106
- Frazzon, J., and Dean, D. R. (2002).** Biosynthesis of the nitrogenase iron-molybdenum-cofactor from *Azotobacter vinelandii*. *Metal Ion Biol. Syst.* **39**: 163-186
- Frey, P. A., Ballinger, M. D., and Reed, G. H. (1998).** S-adenosylmethionine: a 'poor man's coenzyme B12' in the reaction of lysine 2,3-aminomutase. *Biochem. Soc. Trans.* **26**: 304-310
- Frey, P. A., and Reed, G. H. (2000).** Radical mechanisms in adenosylmethionine- and adenosylcobalamin-dependent enzymatic reactions. *Arch. Biochem. Biophys.* **382**: 6-14
- Frey, P. A. (2001).** Radical mechanisms of enzymatic catalysis. *Annu. Rev. Biochem.* **70**: 121-148
- Frey, P. A., and Booker, S. J. (2001).** Radical mechanisms of S-adenosylmethionine-dependent enzymes. *Adv. Prot. Chem.* **58**: 1-45

6 REFERENCES

- Frey, P. A., and Magnusson, O. Th. (2003).** S-Adenosylmethionine: A Wolf in Sheep's Clothing, or a Rich Man's Adenosylcobalamin? *Chem. Rev.* **103**: 2129-2148
- Frey, P. A., Hegeman, A. D., and Reed, G. H. (2006).** Free radical mechanisms in enzymology. *Chem. Rev.* **106**: 3302-3316
- Frey, P. A., Hegeman, A. D., and Ruzicka, F. J. (2008).** The radical SAM superfamily. *Crit. Rev. Biochem. Mol. Biol.* **43**: 63-88
- Fridovich, I. (1997).** Superoxide Anion Radical (O_2^-), Superoxide Dismutases, and Related Matters. *J. Biol. Chem.* **272**: 18515-18517
- Frohloff, F., Fichtner, L., Jablonowski, D., Breunig, K. D., and Schaffrath, R. (2001).** *Saccharomyces cerevisiae* Elongator mutations confer resistance to the *Kluyveromyces lactis* zymocin. *EMBO J.* **20**: 1993-2003
- Frohloff, F., Jablonowski, D., Fichtner, L., and Schaffrath, R. (2003).** Subunit Communications Crucial for the Functional Integrity of the Yeast RNA Polymerase II Elongator (γ -toxin target (TOT)) Complex. *J. Biol. Chem.* **278**: 956-961
- Frohloff, F. (2005).** Zur Rolle des RNA-Polymerase-II Elongators aus *Saccharomyces cerevisiae* für die Wirkung des *Kluyveromyces lactis* toxin. Dissertation. Martin-Luther-Universität Halle - Wittenberg.
- Georgiou, G., and Valax, P. (1996).** Expression of correctly folded proteins in *Escherichia coli*. *Curr. Opin. Biotechnol.* **7**: 190-197
- Giel, J. L., Rodionov, D., Liu, M., Blattner, F. R., and Kiley, P. J. (2006).** IscR-dependent gene expression links iron-sulphur cluster assembly to the control of O_2 -regulated genes in *Escherichia coli*. *Mol. Microbiol.* **60**: 1058-1075
- Giessing, A. M., Jensen, S. S., Rasmussen, A., Hansen, L. H., Gondela, A., Long, K., Vester, B., and Kirpekar, F. (2009).** Identification of 8-methyladenosine as the modification catalyzed by the radical SAM methyltransferase Cfr that confers antibiotic resistance in bacteria. *RNA.* **15**: 327-336
- Gietz, D., and Sugino, A. (1988).** New Yeast - *Escherichia coli* shuttle vectors constructed with *in vitro* mutagenized yeast genes lacking six base pair restriction sites. *Gene.* **74**: 527-534

- Gilbert, C., Kristjuhan, A., Winkler, G. S., and Svejstrup, J. Q. (2004).** Elongator interactions with nascent mRNA revealed by RNA immunoprecipitation. *Mol. Cell.* **14**: 457-464
- Gomez-Lorenzo, M. G., Spahn, C. M. T., Agrawal, R. K., Grassucci, R. A., Penczek, P., Chakraborty, K., Ballesta, J. P. G., Lavandera, J. L., Gracia-Bustos, J. F., and Frank, J. (2000).** Three-dimensional cryo-electron microscopy localization of EF2 in the *Saccharomyces cerevisiae* 80S ribosome at 17.5Å resolution. *The EMBO J.* **19**: 2710-2718
- Grant, P. A., Duggan, L., Cote, J., Roberts, S. M., Brownell, J. E., Candau, R., Ohba, R., Owen-Hughes, T., Allis, C. D., Winston, F., Berger, S. L., and Workman, J. L. (1997).** Yeast Gcn5 functions in two multisubunit complexes to acetylate nucleosomal histones: characterization of an Ada complex and the SAGA (Spt/Ada) complex. *Genes Dev.* **11**: 1640-1650
- Green, J., Bennett, B., Jordan, P., Ralph, E. T., Thomson, A. J. and Guest, J. R. (1996).** Reconstitution of the [4Fe-4S] cluster in FNR and demonstration of the aerobic -anaerobic transcription switch *in vitro*. *Biochem. J.* **316**: 887-892
- Greenwood, C., Selth, L. A., Dirac-Svejstrup, A. B., and Svejstrup, J. Q. (2009).** An iron-sulfur cluster domain in Elp3 important for the structural integrity of elongator. *J. Biol. Chem.* **284**: 141-149
- Grodberg, J. and Dunn, J. J. (1988).** ompT encodes the *Escherichia coli* outer membrane protease that cleaves T7 RNA polymerase during purification. *J. Bacteriol.* **170**: 1245–1253
- Grove, T. L., Lee, K-H., Clair, J. St., Krebs, C., and Booker, S. J. (2008).** *In vitro* characterization of AtsB, a radical SAM formylglycine-generating enzyme that contains three [4Fe-4S] clusters. *Biochem.* **47**: 7523-7538
- Grove, T. L., Benner, J. S., Radle, M. I., Ahlum, J. H., Landgraf, B. J., Krebs, C., and Booker, S. J. (2011).** A Radically Different Mechanism for S-Adenosylmethionine-Dependent Methyltransferases. *Sci.* **332**: 604-607
- Guan, Z. W., Kamatani, D., Kimura, S. and Iyanagi, T. (2003).** Mechanistic studies on the intramolecular one-electron transfer between the two flavins in the human neuronal nitric-oxide synthase and inducible nitric-oxidase synthase flavin domains. *J. Biol. Chem.* **278**: 30859-30868

- Gunge, N., Tamaru, A., Ozawa, F., and Sakaguchi, K. (1981).** Isolation and characterization of linear deoxyribonucleic acid plasmids from *Kluyveromyces lactis* and the plasmid-associated killer character. *J. Bacteriol.* **145**: 382-390
- Guzman, L. M., Belin, D., Carson, M. J. and Beckwith, J. S. (1995).** Tight regulation, modulation, and high-level expression by vectors containing the arabinose P_{BAD} promoter. *J. Bacteriol.* **177**: 4121-4130
- Hall, D. O., Cammack, R., Rao, K. K. (1971).** Role for ferredoxins in origin of life and biological evolution. *Nature.* **233**: 136-138
- Hanahan, D. (1983).** Studies on transformation of *Escherichia coli* with plasmids. *J. Mol. Biol.* **166**: 557-580
- Hänzelmann, P., Hernández, H. L., Menzel, C., Garcia-Serres, R., Huynh, B. H., Johnson, M. K., Mendel, R. R., and Schindelin, H. (2004).** Characterization of MOCS1A, an Oxygen-sensitive Iron-Sulfur Protein Involved in Human Molybdenum Cofactor Biosynthesis. *J. Biol. Chem.* **279**: 34721-34732
- Hänzelmann, P., and Schindelin, H. (2004).** Crystal structure of the S-adenosylmethionine-dependent enzyme MoaA and its implications for molybdenum cofactor deficiency in humans. *Proc. Natl. Acad. Sci. USA.* **101**: 12870-12875
- Hänzelmann, P., and Schindelin, H. (2006).** Binding of 5'-GTP to the C-terminal FeS cluster of the radical S-adenosylmethionine enzyme MoaA provides insights into its mechanism. *PNAS.* **103**: 6829-6834
- Hawkes, N. A., Otero, G., Winkler, G. S., Marshall, N., Dahmus, M. E., Krappmann, D., Scheiderei, C., Thomas, C. L., Schiavo, G., Erdjument-Bromage, H., Tempst, P., and Svejstrup, J. Q. (2002).** Purification and characterization of the human elongator complex. *J. Biol. Chem.* **277**: 3047-3052
- Hentze, M. W., and Kühn, L. C. (1996).** Molecular control of vertebrate iron metabolism: mRNA-based regulatory circuits operated by iron, nitric oxide, and oxidative stress. *PNAS (USA).* **93**: 8175-8182
- Hernández, H.L., Pierrel, F., Elleingand, E. Garcia-Serres, R., Huynh, B. H., Johnson, M. K., Fontacave, M., Atta, M. (2007).** MiaB, a bifunctional radical - S-adenosylmethionine enzyme involved in the thiolation and methylation of tRNA, contains two essential [4Fe-4S] clusters. *Biochem.* **46**: 5140-5147

- Hinckley, G. T., and Frey, P. A. (2006).** Cofactor dependence of reduction potentials for [4Fe-4S]^{2+/1+} in lysine 2,3-aminomutase. *Biochem.***45**: 3219-3225
- Hirling, H., Henderson, B. R., and Kühn, L. C. (1994).** Mutational analysis of the [4Fe-4S]-cluster converting iron regulatory factor from its RNA-binding form to cytoplasmic aconitase. *EMBO J.* **13**: 453-461
- Holmberg, C., Katz, S., Lerdrup, M., Herdegen, T., Jaattela, M., Aronheim, A., and Kallunki, T. (2002).** A novel specific role for IκB kinase complex-associated protein in cytosolic stress signaling. *J. Biol. Chem.* **277**: 31918-31928
- Hopper, A. K., Schultz, L. D., and Shapiro, R. A. (1980).** Processing of intervening sequences: A new yeast mutant which fails to excise intervening sequences from precursor tRNAs. *Cell* **19**: 741-751
- Huang, B., Johansson, M. J., and Bystrom, A. S. (2005).** The early step in wobble uridine tRNA modification requires the Elongator complex. *RNA.* **11**: 424-436
- Huang, B., Lu, J., and Byström, A. S. (2008).** A genome-wide screen identifies genes required for formation of the wobble nucleoside 5-methoxycarbonylmethyl-2-thiouridine in *Saccharomyces cerevisiae*. *RNA.* **14**: 2183-2194
- Imlay, J. A. (2006).** Iron-sulphur clusters and the problem with oxygen. *Mol. Microbiol.* **59**: 1073-1082
- Jablonowski, D., Fichtner, L., Martin, V. J., Klassen, R., Meinhardt, F., Stark, M. J. R., and Schaffrath, R. (2001a).** *Saccharomyces cerevisiae* cell wall chitin, the *Kluyveromyces lactis* zymocin receptor. *Yeast.* **18**: 1285-1299
- Jablonowski, D., Frohloff, F., Fichtner, L., Stark, M. J., and Schaffrath, R. (2001b).** *Kluyveromyces lactis* zymocin mode of action is linked to RNA polymerase II function via Elongator. *Mol. Microbiol.* **42**: 1095-1105
- Jablonowski, D., Fichtner, L., Stark, M. J., and Schaffrath, R. (2004).** The yeast elongator histone acetylase requires Sit4-dependent dephosphorylation for toxin-target capacity. *Mol. Biol. Cell.* **15**: 1459-1469
- Jablonowski, D., Zink, S., Mehlgarten, C., Daum, G., and Schaffrath, R. (2006).** tRNA^{Glu} wobble uridine methylation by Trm9 identifies Elongator's key role for zymocin-induced cell death in yeast. *Mol. Microbiol.* **59**: 677-688

6 REFERENCES

- Jacobson, M. R., Cash, V. L., Weiss, M. C., Laird, N. F., Newton, W. E., and Dean, D. R. (1989). Biochemical and genetic analysis of the *nifUSVWZM* cluster from *Azotobacter vinelandii*. *Mol. Gen. Genet.* **219**: 49-57
- Jarrett, J. T. (2003). The generation of 5'-deoxyadenosyl radicals by adenosylmethionine-dependent radical enzymes. *Curr. Opin. Chem. Biol.* **7**: 174-182
- Johansson, M. J., Esberg, A., Huang, B., Björk, G. R., and Byström, A. S. (2008). Eukaryotic wobble uridine modifications promote a functionally redundant decoding system. *Mol. Cell. Biol.* **28**: 3301-3312
- Johnson, M. K. (1998). Iron-sulfur proteins: new roles for old clusters. *Curr. Opin. Chem. Biol.* **2**: 173-181
- Johnson, D. C., Dean, D. R., Smith, A. D., and Johnson, M. K. (2005). Structure, function, and formation of biological iron-sulfur clusters. *Annu. Rev. Biochem.* **74**: 247-281
- Kagan, R. M., and Clarke, S. (1994). Widespread occurrence of three sequence motifs in diverse S-adenosylmethionine-dependent methyltransferases suggests a common structure for these enzymes. *Arch. Biochem. Biophys.* **310**: 417-427
- Kalhor, H. R., and Clarke, S. (2003). Novel methyltransferase for modified uridine residues at the wobble position of tRNA. *Mol. Cell. Biol.* **23**: 9283-9292
- Kämper, J., Esser, K., Gunge, N., and Meinhardt, F. (1991). Heterologous expression on the linear DNA killer plasmid from *Kluyveromyces lactis*. *Curr. Genet.* **19**: 109-118
- Kappock, T. J. and Caradonna, J. P. (1996). Pterin-Dependent Amino Acid Hydroxylases. *Chem. Rev.* **96**: 2659-2756
- Kay, C. W., Feicht, R., Schulz, K., Sadewater, P., Sancar, A., Bacher, A., Mobius, K., Richter, G. and Weber, S. (1999). EPR, ENDOR, and TRIPLE Resonance Spectroscopy on the Neutral Flavin Radical in *Escherichia coli* DNA Polymerase. *Biochem.* **38**: 16740-16748
- Kennedy, M. C., Kent, T. A., Emptage, M., Merkle, H., Beinert, H., and Münck, E. (1984). Evidence for the formation of a linear [3Fe-4S] cluster in partially unfolded aconitase. *J. Biol. Chem.* **259**: 14463-14471
- Kent, T. A., Emptage, M. H., Merkle, H., Kennedy, M. C., Beinert, H., and Münck, E. (1985). Mössbauer studies of aconitase. Substrate and inhibitor binding,

- reaction intermediates, and hyperfine interactions of reduced 3Fe and 4Fe clusters. *J. Biol. Chem.* **260**: 6871-6881
- Khoroshilova, N., Popescu, C., Münck, E., Beinert, H., and Kiley, P. J. (1997).** Iron-sulfur cluster disassembly in the FNR protein of *Escherichia coli* by O₂: [4Fe-4S] to [2Fe-2S] conversion with loss of biological activity. *PNAS USA.* **94**: 6087-6092
- Kiley, P. J., and Beinert, H. (2003).** The role of Fe-S proteins in sensing and regulation in bacteria. *Curr. Opin. Microbiol.* **6**: 181-185
- Kim, J. H., Lane, W. S., and Reinberg, D. (2002).** Human Elongator facilitates RNA polymerase II transcription through chromatin. *Proc. Natl. Acad. Sci. USA.* **99**: 1241-1246
- King, D. S., and Reichard, P. (1995).** Mass spectrometric determination of the radical scission site in the anaerobic ribonucleotide reductase of *Escherichia coli*. *Biochem. Biophys. Res. Commun.* **206**: 731-735
- Kishida, M., Tokunaga, M., Katayose, Y., Yajima, H., Kawamura-Watabe, A., and Hishinuma, F. (1996).** Isolation and genetic characterization of pGKL killer-insensitive mutants (iki) from *Saccharomyces cerevisiae*. *Biosci. Biotechnol. Biochem.* **60**: 798-801
- Kispal, G., Csere, P., Prohl, C., and Lill, R. (1999).** The mitochondrial proteins Atm1p and Nfs1p are required for biogenesis of cytosolic Fe/S proteins. *EMBO J.* **18**: 3981-3989
- Klausner, R. D., and Rouault, T. A. (1993).** A double life: cytosolic aconitase as a regulatory RNA binding protein. *Mol. Biol. Cell.* **4**: 1-5
- Klekamp, M. S., and Weil, P. A. (1982).** Specific transcription of homologous class III genes in yeast-soluble cell-free extracts. *J. Biol. Chem.* **257**: 8432-8441
- Knappe, J., and Wagner, A. F. (2001).** Stable glyceryl radical from pyruvate formate-lyase and ribonucleotide reductase (III). *Adv. Protein Chem.* **58**: 277-315
- Kouskouti, A., and Taliandi, I. (2005).** Histone modifications defining active genes persist after transcriptional and mitotic inactivation. *EMBO J.* **24**: 347-357
- Krappmann, D., Hatada, E. N., Tegethoff, S., Li, J., Klippel, A., Giese, K., Baeuerle, P. A., and Scheidereit, C. (2000).** The I κ B kinase (IKK) complex is tripartite and contains IKK gamma but not IKAP as a regular component. *J. Biol. Chem.* **275**: 29779-29787

- Krebs, C., Henshaw, T. F., Cheek, J., Huynh, B. H., and Broderick, J. B. (2000).** Conversion of 3Fe-4S to 4Fe-4S clusters in native pyruvate formate-lyase activating enzyme: Mössbauer characterization and implications for mechanism. *J. Am. Chem. Soc.* **122**: 12497-12506
- Krieger, C. J., Roseboom, W., Albracht, S. P. J., and Spormann, A. M. (2001).** A stable organic free radical in anaerobic benzylsuccinate synthase of *Azoarcus* sp. strain T. *J. Biol. Chem.* **276**: 12924-12927
- Kriek, M., Peters, L., Takahashi, Y., Roach, P. L. (2003).** Effect of iron-sulfur cluster assembly proteins on the expression of *Escherichia coli* lipoic acid synthase. *Prot. Expr.Purif.* **28**: 241-245
- Kriek, M., Martins, F., Leonardi, R., Fairhurst, S. A., Lowe, D. J., and Roach, P. L. (2007).** Thiazole synthase from *Escherichia coli*: an investigation of the substrates and purified proteins required for activity *in vitro*. *J. Biol. Chem.* **282**: 17413-17423
- Krogan, N. J., and Greenblatt, J. F. (2001).** Characterization of a six-subunit holo-elongator complex required for the regulated expression of a group of genes in *Saccharomyces cerevisiae*. *Mol. Cell. Biol.* **21**: 8203-8212
- Külzer, R., Pils, T., Kappl, R., Hüttermann, J., and Knappe, J. (1998).** Reconstitution and characterization of the polynuclear iron-sulfur cluster in pyruvate formate-lyase-activating enzyme: Molecular properties of the holoenzyme form. *J. Biol. Chem.* **273**: 4897-4903
- Kuo, M. H., Zhou, J., Jambeck, P., Churchill, M. E., and Allis, C. D. (1998).** Histone acetyltransferase activity of yeast Gcn5p is required for the activation of target genes *in vivo*. *Genes Dev.* **12**: 627-639
- Laemmli, U. K. (1970).** Cleavage of structural proteins during the assembly of the head of bacteriophage T4. *Nature* **227**: 680-685
- Land, T., and Rouault, T. A. (1998).** Targeting of a human iron-sulfur cluster assembly enzyme, nifs, to different subcellular compartments is regulated through alternative AUG utilization. *Mol. Cell.* **2**: 807-815
- Lau, C.-K., Bachorik, J. L., and Dreyfuss, G. (2009).** Gemin5-snRNA interaction reveals an RNA binding function for WD repeat domains. *Nat. Struct. Mol. Biol.* **16**: 486-491

- Layer, G., Verfürth, K., Mahlitz, E., and Jahn, D. (2002).** Oxygen-independent coproporphyrinogen-III oxidase HemN from *Escherichia coli*. *J. Biol. Chem.* **277**: 34136-34142
- Layer, G., Moser, J., Heinz, D. W., Jahn, D., and Schubert, W. D. (2003).** Crystal structure of coproporphyrinogen III oxidase reveals cofactor geometry of radical SAM enzymes. *EMBO J.* **22**: 6214-6224
- Layer, G., Heinz, D.W., Jahn, D., and Schubert, W-D. (2004).** Structure and function of radical SAM enzymes. *Curr. Opin. Chem. Biol.* **8**: 468-476
- Layer, G., Kervio, E., Morlock, G., Heinz, D.W., Jahn, D., Retey, J., and Schubert, W. D. (2005).** Structural and functional comparison of HemN to other radical SAM Enzymes. *Biol. Chem.* **386**: 971-980
- Lee, K-H., Saleh, L., Anton, B. P., Madinger, C. L., Benner, J. S., Iwig, D. F., Roberts, R. J., Krebs, C., and Booker, S. J. (2009).** Characterization of RimO, a new member of the methylthiotransferase subclass of the radical SAM superfamily. *Biochemistry* **48**: 10162-10174
- Li, Y., Takagi, Y., Jiang, Y., Tokunaga, M., Erdjument-Bromage, H., Tempst, P., and Kornberg, R. D. (2001).** A multiprotein complex that interacts with RNA polymerase II elongator. *J. Biol. Chem.* **276**: 29628-29631
- Li, Q., Fazly, A. M., Zhou, H., Huang, S., Zhang, Z. and Stillman, B. (2009).** The Elongator complex interacts with PCNA and modulates transcriptional silencing and sensitivity to DNA damage agents. *PLoS Genetics.* **5**: e1000684
- Lill, R. and Mühlenhoff, U. (2005).** Iron-sulfur protein biogenesis in eukaryotes. *Trends Biochem. Sci.* **30**: 133-141
- Lill, R. and Mühlenhoff, U. (2006).** Iron-Sulfur Protein Biogenesis in Eukaryotes: Components and Mechanisms. *Annu. Rev. Cell Dev. Biol.* **22**: 457-486
- Lill, R. and Mühlenhoff, U. (2008).** Maturation of iron-sulfur proteins in eukaryotes: mechanisms, connected processes, and diseases. *Annu. Rev. Biochem.* **77**: 669-700
- Lim, V. I. (1994).** Analysis of action of wobble nucleoside modifications on codon-anticodon pairing within the ribosome. *J. Mol. Biol.* **240**: 8-19
- Lipardi, C., and Paterson, B. M. (2009).** Identification of an RNA-dependent RNA polymerase in *Drosophila* involved in RNAi and transposon suppression. *PNAS.* **106**: 15645-15650

6 REFERENCES

- Liu, A., and Gräslund, A. (2000).** Electron paramagnetic resonance evidence for a novel interconversion of [3Fe-4S]⁺ and [4Fe-4S]⁺ clusters with endogenous iron and sulfide in anaerobic ribonucleotide reductase activase *in vitro*. *J. Biol. Chem.* **275**: 12367-12373
- Liu, S., Milne, G. T., Kuremsky, J. G., Fink, G. R., and Leppla, S. H. (2004).** Identification of the proteins required for biosynthesis of diphthamide, the target of bacterial ADP-ribosylating toxins on translation elongation factor 2. *Mol. Cell. Biol.* **24**: 9487-9497
- Lu, J., Huang, B., Esberg, A., Johansson, M. J., and Bystrom, A. S. (2005).** The *Kluyveromyces lactis* γ -toxin targets tRNA anticodons. *RNA.* **11**: 1648-1654
- Lundberg, K. S., Shoemaker, D. D., Adams, M. W., Short, J. M., Sorge, J. A., and Mathur, E. J. (1991).** High-fidelity amplification using a thermostable DNA polymerase isolated from *Pyrococcus furiosus*. *Gene.* **180**: 1-6
- Marsh, E. N. G. and Drennan, C. L. (2001).** Adenosylcobalamin-dependent isomerases: new insights into structure and mechanism. *Curr. Opin. Chem. Biol.* **5**: 499-505
- Marsh, E. N. G., Patterson, D. P., and Lei, L. (2010).** Adenosyl Radical: Reagent and Catalyst in Enzyme Reactions. *ChemBioChem* **11**: 604-621
- Martinez-Gomez, N. C., Downs, D. M. (2008).** ThiC is an [Fe-S] cluster protein that requires AdoMet to generate the 4-amino-5-hydroxymethyl-2-methylpyrimidine moiety in thiamin synthesis. *Biochem.* **47** :9054-9056
- Martinez-Gomez, N. C., Poyner, R. R., Mansoorabadi, S. O., Reed, G. H., and Downs, D. M. (2009).** Reaction of AdoMet with ThiC generates a backbone free radical. *Biochem.* **48**: 217-219
- Mattheakis, L. C., Shen, W. H., and Collier, R. J. (1992).** *DPH5*, a methyltransferase gene required for diphthamide biosynthesis in *Saccharomyces cerevisiae*. *Mol. Cell. Biol.* **12**: 4026-4037
- Mehlgarten, C., and Schaffrath, R. (2004).** After chitin-docking, toxicity of *Kluyveromyces lactis* zymocin requires *Saccharomyces cerevisiae* plasma membrane H⁺-ATPase. *Cell. Microbiol.* **6**: 569-580
- Mehlgarten, C., Zink, S., Rutter, J., and Schaffrath, R. (2007).** Dosage suppression of the *Kluyveromyces lactis* zymocin by *Saccharomyces cerevisiae* *ISR1* and *UGP1*. *FEMS Yeast Res.* **7**: 722-730

- Mehlgarten, C. (2009).** Das *Kluyveromyces lactis* Killertoxin: Regulatoren des Zellimports und der intrazellulären Wirkung in *Saccharomyces cerevisiae*. Dissertation; Martin-Luther-Universität, Halle-Wittenberg.
- Mehlgarten, C., Jablonowski, D., Breunig, K. D., Stark, M. J. R., and Schaffrath, R. (2009).** Elongator function depends on antagonistic regulation by casein kinase Hrr25 and protein phosphatase Sit4. *Mol. Microbiol.* **73**: 869-881
- Mehlgarten, C., Jablonowski, D., Wrackmeyer, U., Tschitschmann, S., Sondermann, D., Jäger, G., Gong, Z., Byström, A. S., Schraffrath, R., and Breunig, K. D. (2010).** Elongator function in tRNA wobble uridine modification is conserved between yeast and plants. *Mol. Microbiol.* **76**: 1082-1094
- Merchant, S., and Dreyfuss, B. W. (1998).** Post-translational assembly of photosynthetic metalloproteins. *Annu. Rev. Plant Physiol. Plant Mol. Biol.* **49**: 25-51
- Metivier, R., Penot, G., Hubner, M. R., Reid, G., Brand, H., Kos, M., and Gannon, F. (2003).** Estrogen receptor- α directs ordered, cyclical, and combinatorial recruitment of cofactors on a natural target promoter. *Cell.* **115**: 751-763
- Miller, H. (1987).** Practical aspects of preparing phage and plasmid DNA: Growth, maintenance, and storage of bacteria and bacteriophage. *Methods Enzymol.* **152**: 145-170
- Miller, J. R., Busby, R. W., Jordan, S. W., Cheek, J., Henshaw, T. F., Ashley, G. W., Broderick, J. B., Cronan, J. E. Jr., Marletta, M. A. (2000).** *Escherichia coli* LipA is a lipoyl synthase: in vitro biosynthesis of lipoylated pyruvate dehydrogenase complex from octanoyl-acyl carrier protein. *Biochem.* **39**: 15166-15178
- Moehring, J. M., Moehring, T. J., and Danley, D. E. (1980).** Post-translational modification of elongation factor 2 in diphtheria toxin-resistant mutants of CHO-K1 cells. *Proc. Natl. Acad. Sci. USA.* **77**: 1010-1014
- Moore, L. J., and Kiley, P. J. (2001).** Characterization of the dimerization domain in the FNR transcription factor. *J. Biol. Chem.* **276**: 45744-45750
- Moreno, C., Macedo, A. L., Moura, I., LeGall, J., and Moura, J. J. (1994).** Redox properties of *Desulfovibrio gigas* [Fe₃S₄] and [Fe₄S₄] ferredoxins and heterometal cubane-type clusters formed within the [Fe₃S₄] core. Square wave voltammetric studies. *J. Inorg. Biochem.* **53**: 219-234

6 REFERENCES

- Moura, I., Moura, J. J., Santos, M. H., Xavier, A. V., and LeGall, J. (1979).** Redox studies of rubredoxins from sulphate and sulphur reducing bacteria. *FEBS Lett.* **107**: 419-421
- Mühlenhoff, U., and Lill, R. (2000).** Biogenesis of iron-sulfur proteins in eukaryotes: a novel task of mitochondria that is inherited from bacteria. *Biochim. Biophys. Acta.* **1459**: 370-382
- Mumberg, D., Muller, R., and Funk, M. (1994).** Regulatable promoters of *Saccharomyces cerevisiae*: comparison of transcriptional activity and their use for heterologous expression. *Nucleic Acids Res.*, **22**: 5767-5768
- Mumberg, D., Muller, R., and Funk, M. (1995).** Yeast vectors for the controlled expression of heterologous proteins in different genetic backgrounds. *Gene***156**: 119-122
- Nachin, L., Loiseau, L., Expert, D. and Barras, F. (2003).** SufC, an unorthodox cytoplasmic ABC/ATPase required for [Fe-S] biogenesis under oxidative stress. *EMBO J.* **22**: 427-437
- Nakamura, M., Saeki, K., and Takahashi, Y. (1999).** Hyperproduction of recombinant ferredoxins in *Escherichia coli* by coexpression of the ORF1-ORF2-*iscS-iscU-iscA-hscB-hscA-fdx*-ORF3 gene cluster. *J. Biochem.* **126**: 10-18
- Nelissen, H., Clarke, J. H., De Block, M., De Block, S., Vanderhaeghen, R., Zielinski, R. E., Dyer, T., Lust, S., Inzé, D., and van Lijsebettens, M. (2003).** Tot4/Kti12 protein, has a function in meristem activity and organ growth in plants. *Plant Cell.* **15**: 639-654
- Nelissen, H., Fleury, D., Bruno, L., Robles, P., De Veylder, L., Traas, J., Micol, J. L., Van Montagu, M., Inze, D., and Van Lijsebettens, M. (2005).** The elongata mutants identify a functional Elongator complex in plants with a role in cell proliferation during organ growth. *Proc. Natl. Acad. Sci. USA.* **102**: 7754-7759
- Nelissen, H., De Groeve, S., Fleury, D., Neyt, P., Bruno, L., Bitonti, m. B., Vandenbussche, F., Van der Straeten, D., Yamaguchi, T., Tsukaya, H., Witters, E., De Jaeger, G., Houben, A., and Van Lijsebettens, M. (2010).** Plant Elongator regulates auxin-related genes during RNA polymerase II transcription elongation. *Proc. Natl. Acad. Sci. USA.* **107**: 1678-1683

6 REFERENCES

- Nelson, M., and McClelland, M. (1992).** Use of DNA methyltransferase/endonuclease enzyme combinations for megabase mapping of chromosomes. *Mtds. Enzymol.* **216**: 279-303
- Neuwald, A. F., and Landsman, D. (1997).** GCN5-related histone N-acetyltransferases belong to a diverse superfamily that includes the yeast SPT10 protein. *Trends Biochem. Sci.* **22**: 154-155
- Nicolet, Y., and Drennan, C. L. (2004).** AdoMet radical proteins - from structure to evolution - alignment of divergent protein sequences reveals strong secondary structure element conservation. *Nucleic Acids Res.* **32**: 4015-4025
- Nicolet, Y., Rubach, J. K., Posewitz, M. C., Amara, P., Mathevon, C., Atta, M., Fontecave, M., and Fontecilla-Camps, J. C. (2008).** X-ray Structure of the [Fe-Fe]-Hydrogenase Maturase HydE from *Thermotoga maritima*. *J. Biol. Chem.* **283**: 18861-18872
- Noma, A., Kirino, Y., Ikeuchi, Y., and Suzuki, T. (2006).** Biosynthesis of wybutosine, a hyper-modified nucleoside in eukaryotic phenylalanine tRNA. *EMBO j.* **25**: 2142-2154
- Novy, R., Yaeger, K., Mierendorf, R. (2001).** Overcoming the codon bias of *E. coli* for enhanced protein expression. *InNovations.* **12**: 1-3
- O'Brien, J. R., Raynaud, C., Croux, C., Girbal, L., Soucaille, P., and Lanzilotta, W. N. (2004).** Insight into the mechanism of the B12-independent glycerol dehydratase from *Clostridium butyricum*: preliminary biochemical and structural characterization. *Biochem.* **43**: 4635-4645
- Okada, Y., Yamagata, K., Hong, K., Wakayama, T., and Zhang, Y. I. (2010).** A role for the Elongator complex in zygotic paternal genome demethylation. *Nature.* **463**: 554-558
- Okumura, S., Takai, K., Yokoyama, S., and Takaku, H. (1995).** Codon recognition by tRNA molecules with a modified or unmodified uridine at the first position of the anticodon. *Nucleic Acids. Symp. Ser. No.* **34**: 203-204
- Ollagnier, S, Meier, C., Mulliez, E., Gaillard, J., Schünemann, V., Trautwein, A., Mattioli, T., Lutz, M., and Fontecave, M. (1999).** Assembly of 2Fe-2S and 4Fe-4S clusters in the anaerobic ribonucleotide reductase from *Escherichia coli*. *J. Am. Chem. Soc.* **121**: 6344-6350

- Ortiz, P. A., Ulloque, R., Kihara, G. K., Zheng, H., and Kinzy, T. G. (2006).** Translation elongation factor 2 anticodon mimicry domain mutants affect fidelity and diphtheria toxin resistance. *J. Biol. Chem.* **281**: 32639-32648
- Otero, G., Fellows, J., Li, Y., de Bizemont, T., Dirac, A. M., Gustafsson, C. M., Erdjument-Bromage, H., Tempst, P., and Svejstrup, J. Q. (1999).** Elongator, a multisubunit component of a novel RNA polymerase II holoenzyme for transcriptional elongation. *Mol. Cell.* **3**: 109-118
- Outten, F. W., Djaman, O., and Storz, G. (2004).** A *suf* operon requirement for Fe-S cluster assembly during iron starvation in *Escherichia coli*. *Mol. Microbiol.* **52**: 861-872
- Paraskevopoulou, C., Fairhurst, S. A., Lowe, D. J., Brick, P., and Onesti, S. (2006).** The Elongator subunit Elp3 contains a Fe₄S₄ cluster and binds S-adenosylmethionine. *Mol. Microbiol.* **59**: 795-806
- Petrakis, T. G., Sogaard, T. M., Erdjument-Bromage, H., Tempst, P., and Svejstrup, J. Q. (2005).** Physical and functional interaction between Elongator and the chromatin-associated Kti12 protein. *J. Biol. Chem.* **280**: 19454-19460
- Petrovich, R., Ruzicka, F., Reed, G. and Frey, P. (1992).** Characterization of iron-sulfur clusters lysine 2,3-aminomutase by electron paramagnetic resonance spectroscopy. *Biochem.* **31**: 10774-10781
- Pierrel, F., Bjork, G. R., Fontecave, M., and Attah, M. (2002).** Enzymatic modification of tRNAs: MiaB is an iron-sulfur protein. *J. Biol. Chem.* **277**: 13367-13370
- Pierrel, F., Hernandez, H. L., Johnson, M. K., Fontecave, M. and Atta, M. (2003).** Characterization of an extremely thermophilic tRNA-methylthiotransferase. *J. Biol. Chem.* **278**: 29515-29524
- Pierrel, F., Douki, T., Fontecave, M., and Attah, M. (2004).** MiaB protein is a bifunctional radical-S-adenosylmethionine enzyme involved in thiolation and methylation of tRNA. *J. Biol. Chem.* **279**: 47555-47563
- Pokholok, D. K., Hannett, N. M., and Young, R. A. (2002).** Exchange of RNA polymerase II initiation and elongation factors during gene expression *in vivo*. *Mol. Cell.* **9**: 799-809
- Proudfoot, M., Sanders, S. A., Singer, A., Zhang, R., Brown, G., Binkowski, A., Xu, L., Lukin, J. A., Murzin, A. G., Joachimiak, A., Arrowsmith, C. H., Edwards, A. M., Savchenko, A. V., and Yakunin, A. F. (2008).** Biochemical

- and Structural Characterization of a Novel Family of Cystathionine β -Synthase Domain Proteins Fused to a Zn Ribbon-Like Domain. *J. Mol. Biol.* **375**: 301-315
- Qiao, C., and Marsh, E. N. G. (2005).** Mechanism of Benzylsuccinate Synthase: Stereochemistry of Toluene Addition to Fumarate and Maleate. *J. Am. Chem. Soc.* **127**: 8608-8609
- Rahl, P. B., Chen, C. Z., and Collins, R. N. (2005).** Elp1p, the yeast homolog of the FD disease syndrome protein, negatively regulates exocytosis independently of transcriptional elongation. *Mol. Cell.* **17**: 841-853
- Ralph, E. T., Scott, C., Jordan, P. A., Thomson, A. J., Guest, J. R., and Green, J. (2001).** Anaerobic acquisition of [4Fe-4S] clusters by the inactive FNR(C20S) variant and restoration of activity by second-site amino acid substitutions. *Mol. Microbiol.* **39**: 1199-1211
- Rao, P. V. and Holm, R. H. (2004).** Synthetic analogues of the active sites of iron-sulfur proteins. *Chem. Rev.* **104**: 527-559
- Rees, D. C., and Howard, J. B. (2000).** Nitrogenase: standing at the crossroads. *Curr. Opin. Chem. Biol.* **4**: 559-566
- Rees, D. C., and Howard, J. B. (2003).** The Interface Between the Biological and Inorganic Worlds: Iron-Sulfur Metalloclusters. *Science.* **300**: 929-931
- Roje, S. (2006).** S-Adenosyl-L-methionine: Beyond the universal methyl group donor. *Phytochem.* **67**: 1686-1698
- Rouault, T. A., and Klausner, R. D. (1996).** The impact of oxidative stress on eukaryotic iron metabolism. *EXS.* **77**: 183-197
- Roy, A., Solodovnikova, N., Nicholson, T., Antholine, W. and Walden, W. E. (2003).** A novel eukaryotic factor for Fe-S cluster assembly. *EMBO J.* **22**: 4826-4835
- Rubach, J., Brazzolotto, X., Gaillard, J., and Fontecave, M. (2005).** Biochemical characterization of the HydE and HydG iron-only hydrogenase maturation enzymes from *Thermotoga maritima*. *FEBS Lett.* **579**: 5055-5060
- Sanger, F., Air, G. M., Barrell, B. G., Brown, N. L., Coulson, A. R., Fiddes, C. A., Hutchison, C. A., Slocombe, P. M., and Smith, M. (1977).** Nucleotide sequence of bacteriophage phi X174 DNA. *Nature.* **265**: 687-695
- Santamaria-Araujo, J. A., Fischer, B., Otte, T., Nimtz, M., Mendel, R. R., Wray, V., and Schwarz, G. (2004).** The Tetrahydropyranopterin Structure of the sulfur-

6 REFERENCES

- free and Metal-free Molybdenum Cofactor Precursor. *J. Biol. Chem.* **279**: 15994-15999
- Schaffrath, R., and Meinhardt, F. (2005).** *Kluyveromyces lactis* zymocin and other plasmid-encoded yeast killer toxins. In Schmitt, M. and Schaffrath, R. (eds.), *Microbial protein toxins*. Springer, New York, NY, **11**: 133-155
- Schultz, D. C., Balasara, B. R., Testa, J. R., and Godwin, A. K. (1998).** Cloning and localization of a human diphthamide biosynthesis-like protein-2 gene, *DPH2L2*, *Genomics*. **52**: 186-191
- Schwartz, C. J., Giel, J. L., Patschkowski, T., Luther, C., Ruzicka, F. J., Beinert, H., and Kiley, P. J. (2001).** IscR, an Fe-S cluster-containing transcription factor, represses expression of *Escherichia coli* genes encoding Fe-S cluster assembly proteins. *PNAS USA*. **98**: 14895-14900
- Sherman, F. (1991).** Getting started with yeast. *Mtds. Enzymol.* **194**: 3-21
- Sherrer, R. L., O'Donoghue, P., and Söll, D. (2008).** Characterization and evolutionary history of an archaeal kinase involved in selenocysteinyl-tRNA formation. *Nucl. Acids. Res.* **36**: 1247-1259
- Sieker, L. C., Stenkamp, R. E., and LeGall, J. (1994).** Rubredoxin in crystalline state. *Mtd. Enzymol.* **243**: 203-216
- Singh, N., Lorbeck, M. T., Zervos, A., Zimmerman, J., and Elefant, F. (2010).** The histone acetyltransferase E1p3 plays an active role in the control of synaptic bouton expansion and sleep in *Drosophila*. *J. Neurochem.* **115**: 493-504
- Siu, F. K., Lee, L. T., and Chow, B. K. (2008).** Southwestern blotting in investigating transcriptional regulation. *Nat. Protoc.* **3**: 51-58
- Slaugenhaupt, S. A., Blumenfeld, A., Gill, S. P., Leyne, M., Mull, J., Cuajungco, M. P., Liebert, C. B., Chadwick, B., Idelson, M., Reznik, L., Robbins, C. M., Makalowska, I., Brownstein, M. J., Krappmann, D., Scheidereit, C., Maayan, C., Axelrod, F. B., and Gusella, J. F. (2001).** Tissue-specific expression of a splicing mutation in the *IKBKAP* Gene causes familial dysautonomia. *Am. J. Hum. Genet.* **68**: 598-605
- Slaugenhaupt, S. A., and Gusella, J. F. (2002).** Familial dysautonomia. *Curr. Opin. Genet. Dev.* **12**: 307-311
- Smith, T. F., Gaitatzes, C., Saxena, K., and Neer, E. J. (1999).** The WD repeat: a common architecture for diverse functions. *Trends. Biochem. Sci.* **24**: 181-185

- Sofia, H. J., Chen, G., Hetzler, B. G., Reyes-Spindola, J. F., Miller, N. E. (2001).** Radical SAM, a novel protein superfamily linking unresolved steps in familiar biosynthetic pathways with radical mechanisms: functional characterization using new analysis and information visualization methods. *Nucleic Acids Res.* **29**: 1097-1106
- Solinger, J. A., Paolinelli, R., Klöß, H., Berlanda Scorza, F., Marchesi, S., Sauder, U., Mitsushima, D., Capuani, F., Stürzenbaum, S. R., and Cassata, G. (2010).** The *Caenorhabditis elegans* Elongator complex regulates neuronal α -tubulin acetylation. *PLoS Genet.* **6**: e1000820
- Spahn, C. M. T., Gomez-Lorenzo, M. G., Grassucci, R. A., Jørgensen, R., Andersen, G. R., Beckmann, R., Penczek, P. A., Ballesta, J. P. G., and Frank, J. (2004).** Domain movements of elongation factor eEF2 and the eukaryotic 80S ribosome facilitate tRNA translocation. *EMBO J.* **23**: 1008-1019
- Stark, M. J. R., Boyd, A., Mileham, A. J., and Romanos, M. A. (1990).** The plasmid-encoded killer system of *Kluyveromyces lactis*: a review. *Yeast.* **6**: 1-29
- Stubbe, J., and van der Donk, W. A. (1998).** Protein Radicals in Enzyme Catalysis. *Chem. Rev.* **98**: 705-762
- Studier, F. W. and Moffatt, B. A. (1986).** Use of bacteriophage T7 RNA polymerase to direct selective high-level expression of cloned genes. *J. Mol. Biol.* **189**: 113-130
- Sugisaki, Y., Gunge, N., Sakaguchi, K., Yamasaki, M., and Tamura, G. (1983).** *Kluyveromyces lactis* killer toxin inhibits adenylate cyclase of sensitive yeast cells. *Nature.* **304**: 464-466
- Sun, X., Harder, J., Krook, M., Jörnvall, H., Sjöberg, B-M., and Reichard, P. (1993).** A possible glycine radical in anaerobic ribonucleotide reductase from *Escherichia coli*: Nucleotide sequence of the cloned *nrdD* gene. *Proc. Natl. Acad. Sci. USA.* **90**: 577-581
- Sun, X., Ollagnier, S., Schmidt, P. P., Atta, M., Mulliez, E., Lepape, L., Eliasson, R., Gräslund, A., Fontecave, M., Reichard, P., and Sjöberg, B-M. (1996).** The free radical of the anaerobic ribonucleotide reductase from *Escherichia coli* is at Glycine 681. *J. Biol. Chem.* **271**: 6827-6831

- Svejstrup, J. Q. (2002).** Chromatin elongation factors. *Curr. Opin. Genet. Dev.* **12**: 156-161
- Svejstrup, J. Q. (2007).** Elongator complex: how many roles does it play? *Curr. Opin. Cell. Biol.* **19**: 331-336
- Takahashi, Y., and Nakamura, M. (1999).** Functional assignment of the ORF2-iscS-iscU-iscA-hscB-hscA-fdx-ORF3 gene cluster involved in the assembly of Fe-S clusters in *Escherichia coli*. *J. Biochem.* **126**: 917-926
- Takahashi, Y., and Tokumoto, U. (2002).** A third bacterial system for the assembly of iron-sulfur clusters with homologs in archaea and plastids. *J. Biol. Chem.* **277**: 28380-28383
- Tamarit, J., Mulliez, E., Meier, C., Trautwein, A., and Fontecave, M. (1999).** The anaerobic ribonucleotide reductase from *Escherichia coli*: The small protein is an activating enzyme containing a [4Fe-4S]²⁺ center. *J. Biol. Chem.* **274**: 31291-31296
- Tang, S. (2001).** A modular polycistronic expression system for overexpressing protein complexes in *Escherichia coli*. *Protein Expr. Purif.* **21**: 224-234
- Täubert, J. E. (2007).** Molekularanalyse der Interaktion zwischen Phosphatase Sit4 und Sit4 assoziierenden Proteinen. Diplomarbeit. Martin-Luther-Universität Halle-Wittenberg.
- Thompson, J. D., Higgins, D.G., and Gibson, T. J. (1994).** CLUSTALW: improving the sensitivity of progressive multiple alignment through sequence weighting, position-specific gap penalties and weight matrix choice. *Nucleic Acids Res.* **22**: 4673-4680
- Tittmann, K., Wille, G., Golbik, R., Weidner, A., Ghisla, S. and Hübner, G. (2005).** Radical Phosphate Transfer Mechanism for the Thiamin Diphosphate- and FAD-Dependent Pyruvate Oxidase from *Lactobacillus plantarum*. Kinetic Coupling of Intercofactor Electron Transfer with Phosphate Transfer to Acetylthiamin Diphosphate via a Transient FAD Semiquinone/Hydroxyethyl-ThDP Radical Pair. *Biochem.* **44**: 13291-13303
- Toh, S. M., Xiong, L., Bae, T., and Mankin, A. S. (2008).** The methyltransferase YfgB/RlmN is responsible for modification of adenosine 2503 in 23S rRNA. *RNA.* **14**: 98-106
- Tokumoto, U., Kitamura, S., Fukuyama, K. and Takahashi, Y. (2004).** Interchangeability and distinct properties of bacterial Fe-S cluster assembly

- systems: functional replacement of the *isc* and *suf* operons in *Escherichia coli* with *nifSU*-like operon from *Helicobacter pylori*. *J. Biochem.* **136**: 199-209
- Tokunaga, M., Kawamura, A., and Hishinuma, F. (1989).** Expression of pGKL killer 28K subunit in *Saccharomyces cerevisiae*: identification of 28K subunit as a killer protein. *Nucleic Acids. Res.* **17**: 3435-3446
- Tomoyasu, T., Mogk, A., Langen, H., Goloubinoff, P., Bukau, B. (2001).** Genetic dissection of the roles of chaperones and proteases in protein folding and degradation in the *Escherichia coli* cytosol. *Mol. Microbiol.* **40**: 397-413
- Ugulava, N. B., Gibney, B. and Jarrett, J. (2001).** Biotin synthase contains two distinct iron-sulfur cluster binding sites: chemical and spectroelectrochemical analysis of iron-sulfur cluster interconversions. *Biochem.* **40**: 8343-8351
- Ugulava, N. B., Surerus, K. K., and Jarrett, J. T. (2002).** Evidence from Mössbauer spectroscopy for distinct $[2\text{Fe-2S}]^{2+}$ and $[4\text{Fe-4S}]^{2+}$ cluster binding sites in biotin synthase from *Escherichia coli*. *J. Am. Chem. Soc.* **124**: 9050-9051
- Ugulava, N. B., Frederick, K. K., and Jarrett, J. T. (2003).** Control of adenosylmethionine-dependent radical generation in biotin synthase: a kinetic and thermodynamic analysis of substrate binding to active and inactive forms of BioB. *Biochem.* **42**: 2708-2719
- Urzica, E., Pierik, A. J., Mühlenhoff, U., and Lill, R. (2009).** Crucial role of conserved cysteine residues in the assembly of two iron-sulfur clusters on the CIA protein Nar1. *Biochem.* **48**: 4946-4958
- Verfürth, K., Pierik, A. J., Leutwein, C., Zorn, S., and Heider, J. (2004).** Substrate specificities and electron paramagnetic resonance properties of benzylsuccinate synthases in anaerobic toluene and m-xylene metabolism. *Arch. Microbiol.* **181**: 155-162
- Vey, J. L., Yang, J., Li, M., Broderick, W. E., Broderick, J. B., and Drennan, C. L. (2008).** Structural basis for glycyl radical formation by pyruvate formate-lyase activating enzyme. *Proc. Natl. Acad. Sci. U.S.A.* **105**: 16137-16141
- Vey, J. L., and Drennan, C. L. (2011).** Structural Insights into Radical Generation by the Radical SAM Superfamily. *Chem. Rev.* **111**: 2487-2506
- Wach, A., Brachat, A., Alberti-Segui, C., Rebischung, C., and Philippsen, P. (1997).** Heterologous *HIS3* marker and GFP reporter modules for PCR-targeting in *Saccharomyces cerevisiae*. *Yeast.* **13**: 1065-1075

- Wagner, A. F. V., Frey, M., Neugebauer, F. A., Schäfer, W., and Knappe, J. (1992).** The free radical in pyruvate formate-lyase is located on glycine-734. *Proc. Natl. Acad. Sci. USA.* **89**: 996-1000
- Walker, J., Kwon, S. Y., Badenhorst, P., East, P., McNeill, H., and Svejstrup, J. Q. (2011).** Role of Elongator Subunit Elp3 in *Drosophila melanogaster* Larval Development and Immunity. *Genet.* **187**: 1067-1075
- Wang, S. C. and Frey, P. A. (2007).** S-adenosylmethionine as an oxidant: the radical SAM superfamily. *Trends Biochem. Sci.* **32**: 101-110
- Wang, S. C. and Frey, P. A. (2007).** Binding energy in the one-electron reductive cleavage of S-adenosylmethionine in lysine 2,3-aminomutase, a radical SAM enzyme. *Biochem.* **46**: 12889-12895
- Wei, C-C, Crane, B. R., and Steuhr, D. J. (2003).** Tetrahydrobiopterin Radical Enzymology. *Chem. Rev.* **103**: 2365-2384
- White, J. H., Butler, A. R., and Stark, M. J. R. (1989).** *Kluyveromyces lactis* toxin does not inhibit yeast adenylyl cyclase. *Nature.* **341**: 666-668
- Winkler, G. S., Petrakis, T. G., Ethelberg, S., Tokunaga, m., Erdjument-Bromage, H., Tempst, P., and Svejstrup, J. Q. (2001).** RNA polymerase II elongator holoenzyme is composed of two discrete subcomplexes. *J. Biol. Chem.* **276**: 32743-32749
- Winkler, G. S., Kristjuhan, A., Erdjument-Bromage, H., Tempst, P., and Svejstrup, J. Q. (2002).** Elongator is a histone H3 and H4 acetyltransferase important for normal histone acetylation levels *in vivo*. *Proc. Natl. Acad. Sci. USA.* **99**: 3517-3522
- Wittschieben, B. Ø., Otero, G., de Bizemont, T., Fellows, J., Erdjument-Bromage, H., Ohba, R., Li, Y., Allis, C. D., Tempst, P., and Svejstrup, J. Q. (1999).** A novel histone acetyltransferase is an integral subunit of elongating RNA polymerase II holoenzyme. *Mol. Cell.* **4**: 123-128
- Wittschieben, B. Ø., Fellows, J., Wendy, Du., Stillman, D. J., and Svejstrup, J. Q. (2000).** Overlapping roles for the histone acetyltransferase activities of SAGA and Elongator *in vivo*. *EMBO J.* **19**: 3060-3068
- Wolf, E., Vassilev, A., Makino, Y., Sali, A., Nakatani, Y., and Burley, S. K. (1998).** Crystal structure of a GCN5-related N-acetyltransferase: *Serratia marcescens* aminoglycoside 3-N-acetyltransferase. *Cell.* **94**: 439-449

6 REFERENCES

- Wrackmeyer, U. (2005).** Vergleichende Charakterisierung der Elongatoruntereinheit Elp3 aus *Saccharomyces cerevisiae* and *Arabidopsis thaliana*. Diplomarbeit; Martin-Luther-Universität Halle-Wittenberg.
- Yeo, W. S., Lee, J. H., and Roe, J. H. (2006).** IscR acts as an activator in response to oxidative stress for the suf operon encoding Fe-S assembly proteins. *Mol. Microbiol.* **61**: 206-218
- Yokoyama, S., and Nishimura, S. (1995).** Modified nucleosides and codon recognition. In *tRNA: Structure, biosynthesis, and function* (eds. D. Söll and U. L. RajBhandary), pp. 207-223. ASM Press, Washington, DC.
- Young, P., Öhman, M., Xu, M. Q., Shub, D. A., and Sjöberg, B-M. (1994).** Intron-containing T4 Bacteriophage Gene *sunY* Encodes an Anaerobic Ribonucleotide Reductase. *J. Biol. Chem.* **269**: 20229-20232
- Young, P., Andersson, J., Sahlin, M., and Sjöberg, B-M. (1996).** Bacteriophage T4 anaerobic ribonucleotide reductase contains a stable glycy radical at position 580. *J. Biol. Chem.* **271**: 20770-20775
- Zabel, R., Bär, C., Mehlgarten, C., and Schaffrath, R. (2008).** Yeast alpha-tubulin suppressor *Ats/Kti13* relates to the Elongator complex and interacts with Elongator partner protein *Kti11*. *Mol. Microbiol.* **69**: 175-187
- Zachariae, W., Shin, T. H., Galova, M., Obermaier, B., and Nasmyth, K. (1996).** Identification of subunits of the anaphase-promoting complex of *Saccharomyces cerevisiae*. *Science.* **274**: 1201-1204
- Zhang, Y., Zhu, X., Torelli, A. T., Lee, M., Dzikovski, B., Koralewski, R. M., Wang, E., Freed, J., Krebs, C., Ealick, S. E., and Lin, H. (2010).** Diphthamide biosynthesis requires an organic radical generated by an iron-sulphur enzyme. *Nature.* **465**: 891-896
- Zheng, L., Cash, V. L., Flint, D. H., and Dean, D. R. (1998).** Assembly of iron-sulfur clusters. Identification of an *iscSUA-hscBA-fdx* gene cluster from *Azotobacter vinelandii*. *J. Biol. Chem.* **273**: 13264-13272
- Zheng, M., Wang, X., Templeton, L. J., Smulski, D. R., LaRossa, R. A. and Storz, G. (2001).** DNA microarray-mediated transcriptional profiling of the *Escherichia coli* response to hydrogen peroxide. *J. Bacteriol.* **183**: 4562-4570
- Zhou, X., Hua, D., Chen, Z., Zhou, Z., and Gong, Z. (2009).** Elongator mediates ABA responses, oxidative stress resistance and anthocyanin biosynthesis in *Arabidopsis*. *Plant J.* **60**: 79-90

6 REFERENCES

- Zhu, X., Dzikovski, B., Su, X., Torelli, A. T., Zhang, Y., Ealick, S. E., Freed, J. H., and Lin, H. (2011). Mechanistic understanding of *Pyrococcus hirokoshii* Dph2, a [4Fe-4S] enzyme required for diphthamide biosynthesis. *Mol. BioSys.* **7**: 74-81
- Zink, S., Mehlgarten, C., Kitamoto, H. K., Nagase, J., Jablonowski, D., Dickson, R. C., Stark, M. J. R., and Schaffrath, R. (2005). M(IP)2C, the major yeast plasma membrane sphingolipid, governs toxicity of *Kluyveromyces lactis* zymocin. *Eukaryot. Cell.* **4**: 879-889

DECLARATION

I, Osita Fidelis Onuma, wish to hereby declare that this scientific Dissertation submitted for assessment is independently written by me and is expressed in my own words without assistance from any person(s). Information from other sources or authors have been properly referenced and acknowledged at the point of their use. Collaborative research and discussions have also been duly acknowledged. With this dissertation, I wish to hereby apply for the award of the Doctorate degree.

Halle / Saale, 19.07.2011

Osita Fidelis Onuma

ACKNOWLEDGEMENTS

This PhD Dissertation was completed in the department of Molecular Genetics of the Institute of Biology, Martin-Luther-University (MLU) Halle-Wittenberg and arose out of years of research that has been done since I came to Prof. Dr. Karin Breunig's group. I had the opportunity to work with a great number of people whose contribution in assorted ways to the research and the making of this Dissertation deserve special mention. It is a pleasure to convey my gratitude to them all in my humble acknowledgement. My sincere and wholehearted gratitude goes to Prof. Dr. Karin Breunig for granting me the great opportunity to embark on this interesting and wonderful research work in the Institute of Biology, AG Molecular Genetics. I am indebted and so grateful to Prof. Dr. Karin Breunig for her untiring preparedness, constructive support to surmount practical and theoretical problems, suggestions and discussions during her supervision of this research work. I am so grateful to her for the privilege she gave me to be part of the VAKZiNOVA research team and likewise influencing my life in a positive direction. It is my pleasure to pay tributes to Prof. Raffael Schaffrath (now at the University of Kassel), Dr. Alexander Anders, and Dr. Renate Langhammer for their wonderful assistance, support, discussions and for the immense roles they played during this research work. Many thanks go to Dr. Lars Fichtner for reading through the manuscript over and over again and for discussions and advice and most especially for the great opportunity of sharing the same office with him. I wish to express my warm gratitude to Dr. Constance Mehlgarten and René Zabel for their willingness to assist as well as their constructive criticism and support during the entire research work. I am indebted to Dr. Mathias Strutz for all his support, advice and assistance. Special acknowledgements are deserved by Ulla Klokow, Karin Sorge, Claudia Rackwitz, members of the VAKZiNOVA project and other members of the AG Breunig for their assistance and provision of a pleasant working and social environment. Immense thanks are due to Prof. Dr. Thomas Brüser (now at the University of Hannover) for his assistance, support and discussions during my research work and for making out time to read through the manuscript. All members of his group are also highly acknowledged for their assistance and the creation of a conducive working atmosphere at the Institute of Microbiology at the MLU in Halle. My sincere thanks also go to Prof. Peter Kroneck and members of his group (University of Konstanz) for conducting the EPR

experiments. I extend special acknowledgements to Prof. Gary Sawers for granting me the opportunity to carry out anaerobic Elp3 purification using ÄKTA Purifier and the anaerobic chamber and to Basem Soboh for the supervision, support and discussions. Other members of the AG Prof. Gary Sawers are gratefully acknowledged for their assistance and support. I will always remain grateful to Prof. Roland Lill and members of his group for granting me a research assistant fellowship in the Institute of Cytobiology and Cytopathology at the Philipps-University, Marburg. My acknowledgements are also deserved by Dr. Antonio Pierik and Dr. Daili Aguilar-Netz for their assistance, support and discussions during the anaerobic Elp3 protein purification and also for conducting the ^{55}Fe binding experiments on Elp3 variants in Marburg in the group of Prof. Roland Lill. Immense appreciations go to Mazi Jude Ohuche-Ukwu, Frau Victoria LaPierre, Humphrey Ajonina, Rita Boateng, Tim Luigs and members of the football club Young Boys Seevetal eV., Pastor Sammy & Sister Damaris Egboh and members of the Resurrection Power Ministries International Halle-Saale, for their prayers and moral support. Thanks to the Federal State of Sachsen-Anhalt and the Graduate programme – Protein complexes of plants – structure, function and evolution, for the PhD scholarship and financial support. My warmest regards go to my parents late Mazi Fidelis Onuma and Catherine Onuma, brothers (Anthony, Chukwudi, Oguguo, Kingsley) and sisters (Edith, Grace, Augustina), Mazi Augustine Onuma, Aunties, Uncles, friends and relatives in Nigeria, for their moral support and prayers for the successful completion of my PhD dissertation at the Martin-Luther-University Halle-Saale. I wish to express my depth of gratitude to my dearly beloved wife, Obiageri and daughter Chinyere Favour for their moral support, understanding, assistance and help during the entire period of my PhD programme. Lastly, glory be to the Almighty God for His everlasting loving kindness, invaluable assistance, support, strength and above all mercy, without these, it would not have been possible for me to complete this PhD Dissertation.

CURRICULUM VITAE

PERSONAL DATA

Name: Osita Fidelis Onuma
Address: Reusenweg 4, 06120 Halle - Saale
Date of birth: 16. March, 1971
Place of birth: Nsukka, Nigeria
Nationality: German
Family status: Married with a daughter



EDUCATIONAL TRAINING AND QUALIFICATION

1983 – 1989 Urhobo College Effurun
West African School Certificate / General Certificate of Education

1991 – 1996 University of Nigeria, Nsukka, Department of Biochemistry
Degree awarded: B.Sc, Biochemistry

2001 – 2002 Technical University of Hamburg-Harburg
Biotechnology-Process Engineering

2002 – 2005 Master's degree studies in Biotechnology and Thesis in the
group of Prof. Dr. Garabed Antranikian, Institute of Technical
Microbiology of the Technical University of Hamburg-Harburg
Degree awarded: M.Sc, Biotechnology

2006 – 2009 PhD research and Dissertation in the group of Prof. Dr. Karin
Breunig at the Institute of Biology, AG Molecular Genetics of the
Martin-Luther-University, Halle-Wittenberg
Topic: Characterization of the radical SAM domain of the Elp3
subunit in yeast and plant Elongator complexes

2009 – 2011 Post-doctoral research on the "VAKZiNOVA" Project in the group
of Prof. Dr. Karin Breunig at the Institute of Biology,
AG Molecular Genetics of the Martin-Luther-University,
Halle-Wittenberg